

# Modulation of Mitotic Progression and Cell Cycle Checkpoints by Phosphorylation-Dependent Protein-Protein Interactions

by

Drew M. Lowery

B.S., Biochemistry and Molecular Biology  
Pennsylvania State University, 2001

Submitted to the Department of Biology  
in Partial Fulfillment of the Requirements for the Degree of

Doctor of Philosophy in Biology  
at the  
Massachusetts Institute of Technology

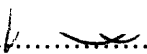
September 2007

© 2007 Drew M. Lowery. All rights reserved.

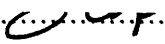
The author hereby grants to MIT permission to reproduce and to distribute publicly  
paper and electronic copies of this thesis document in whole or in part.

Signature of Author.....  .....

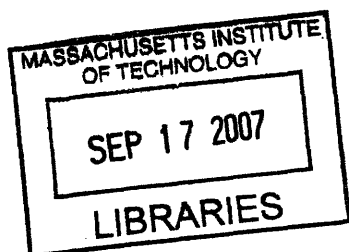
Department of Biology  
August 06, 2007

Certified by.....  .....

Michael B. Yaffe  
Associate Professor of Biology  
Thesis Supervisor

Accepted by.....  .....

Stephen P. Bell  
Professor of Biology  
Chairman, Graduate Student Committee



ARCHIVES

V.1

# **Modulation of Mitotic Progression and Cell Cycle Checkpoints by Phosphorylation-Dependent Protein-Protein Interactions**

By  
Drew M. Lowery

Submitted to the Department of Biology on August 6, 2007 in Partial Fulfillment of the Requirements for the Degree of Doctor of Philosophy in Biology

## **ABSTRACT**

Alteration of mitotic gene function has recently been discovered to play a key role in tumor formation and cancer progression through the induction of chromosomal aberrations and genomic instability. Polo-like-kinase-1 is a critical mitotic regulator, overexpressed in human tumors, that functions in mitotic entry after cellular stress, centrosome maturation, mitotic spindle control, and cytokinesis, which are all dysregulated in cancer cells. To study the role of Polo-like kinases we took advantage of the recent discovery that the polo-box domain of Polo-like kinases is a phosphorylation-dependent binding module that regulates targeting of Polo-like kinases to their substrates. To identify the interactors of Polo-box domains we developed and performed a mitotic-specific yeast two hybrid and a pulldown mass spectrometry screen. This yielded a large number of specific interactors known to be involved in a vast variety of mitotic processes including those previously described to be involved in tumor progression. We demonstrate that Polo-like kinase regulation of cytokinesis-specific guanine-nucleotide exchange factors for the small G-protein Rho is necessary for proper actomyosin ring contraction and cytokinesis. Additionally we demonstrate that Polo-like-kinase-1 directly regulates the activity of the Rho-effector-kinase ROCK2, and thus Polo-like kinases modulate Rho signaling both upstream and downstream of Rho during cytokinesis. In addition to Polo-box domains we also worked on two other phosphorylation-dependent binding domains involved in cell cycle checkpoints that become dysregulated in cancer cells, tandem BRCT domains and WW domains. We examined the molecular basis for phosphorylation-dependent recognition by the tandem BRCT domains of BRCA1 through oriented-peptide-library screening and determination of an X-ray crystal structure of the domain bound to a phosphopeptide. This allowed us to rationalize why inherited mutations within the tandem BRCT domains of BRCA1 promote breast and ovarian cancer in humans. Secondly, we assayed WW domains that were generated from *in silico* determined sequences for natural-like function to more fully understand the folding and binding requirements of this domain class. All three domains (tandem BRCT domains, Polo-box domains, and WW domains) are attractive targets for cancer therapeutics as they participate in control of processes necessary for genomic stability that become dysregulated in cancer.

Thesis Supervisor: Michael B. Yaffe  
Title: Associate Professor of Biology



## Table of Contents

		<u>Page</u>
Abstract		2
Acknowledgements		5
Curriculum Vitae		7
Chapter 1	<b>Polo-like Kinases Control Mitotic Progression</b>	9
	General Roles and Evolution of Polo-like Kinases	10
	Function of the Polo-box Domain	12
	Cancer Connection of Polo-like Kinases	16
	Generation of Polo-box Domain Binding Sites	18
	Activation and Phosphorylation of Polo-like Kinases	27
	Biological Functions of Polo-like Kinases	31
	Polo-like Kinase Structures	38
	Summary and Preview of Thesis	46
	Figures	48
	Table	52
	References	55
Chapter 2	<b>Proteomic Screen Defines the Polo-box Domain Interactome and Identifies Rock2 as a Plk1 Substrate</b>	83
	Abstract	84
	Introduction	85
	Results and Discussion	88
	Experimental Procedures	99
	Figures	108
	Tables	125
	References	139
Chapter 3	<b>Mitotic Specific Yeast Two Hybrid and Chemical Genetic Substrate Trap Reveal Roles for Budding Yeast Polo-like Kinase in Cytokinesis and Nuclear Positioning</b>	145
	Abstract	146
	Introduction	147
	Results and Discussion	149
	Experimental Procedures	162
	Figures	168
	Tables	182
	References	186

Chapter 4	<b>Cytokinesis-Specific Function of RhoGEFs Controlled by Polo-like Kinases in Yeast and Human</b>	192
	Abstract	193
	Introduction	194
	Results and Discussion	195
	Experimental Procedures	204
	Figures	208
	Tables	219
	References	228
Chapter 5	<b>Conclusions, Other Observations, and Future Directions</b>	233
	PBD binding site timing and accessibility:	
	Temporal distribution of Plk substrates	234
	Phospho-dependent binding reactions downstream of Plk phosphorylation events	236
	Suspected Polo-like kinase targets	237
	The Function of Plk1 at the Central Spindle	245
	On the Implications of the Number of Plk Substrates and PBD Binders	247
	Summary and Future Directions	248
	Figures	251
	References	253
Appendix One	<b>Tandem BRCT Domains Function as Phosphopeptide Binding Modules and Control the DNA Damage Responsive Functions of BRCA1</b>	261
	Abstract	262
	Introduction	263
	Results	265
	Discussion	275
	Experimental Procedures	280
	Figures	286
	Tables	302
	References	304
Appendix Two	<b>Natural-like Function in Artificial WW Domains</b>	310
	Abstract	311
	Results and Discussion	312
	Experimental Procedures	319
	Figures	322
	Table	333
	References	334

## Acknowledgments

I would like to thank all members of the Yaffe lab for their encouragement, support, and technical advice over the past five years. My largest debt of gratitude is owed to Isaac Manke who convinced me to join the lab, led the team of us doing the BRCT domain work which was my most exciting time in the Yaffe lab, and became a good friend outside the lab. Majbrit Hjerrild was a visiting graduate student who was an amazing help in getting the data for the PBD pulldown screen. Special thanks to the Graduate Student Club, Sarah Bissonnette, Andrea Tentner, Jes Alexander, and Duaa Mohammad for listening to my latest experimental problems on a weekly basis and sometimes even providing solutions. Duaa has also been a good friend inside and outside the lab as well as being a tremendous asset and partner in many experiments. Thanks to all the postdocs who provided a great learning environment and participated directly in many aspects of my research such as Coky Nguyen, Dan Lim, Kazu Kishi, Erik Wilker, Christian Reinhardt, Marcel van Vugt, Chris Ellson, Jeong-Ho Hong, Alexandra Gardino, Gerry Ostheimer, Scott Floyd for making the Shark Tank the best place to work, and Mary Stewart for keeping the lab running. Many technicians, administrative assistants, and UROPs have also made my life much easier over the years. Lastly, I am grateful to my advisor Michael Yaffe for his ongoing encouragement, boundless enthusiasm, strive for perfection, and continual patience.

Outside of the Yaffe lab there are also a huge number of people who have contributed to my education as a scientist and to the projects described in this thesis. In particular Satoshi Yoshida in David Pellman's lab, Karl Clauser in Steve Carr's lab, and Jen Paulson in Kevan Shokat's lab have been instrumental in certain aspects of my thesis work and have taught me a great deal about their own expertise. In addition I'd like to acknowledge all my other productive collaborations with Bill Russ in Rama Ranganathan's lab, Jaclyn Jansen in Eric Weiss's lab, and Mark Burkard in Prasad Jallepalli's lab. My prelim and thesis committee including Angelika Amon, Frank Solomon, David Sabatini, David Pellman, and Amy Keating have done a tremendous job in steering my research towards meaningful biological questions and pushing me to become a better scientist through insightful and needed critique.

Additionally, I'd like to thank all my former teachers that allowed me to dream about achieving a Ph.D. including my undergraduate research advisor, Frank Pugh, my mentor at Wyeth, Louane Hann, my high school biology teacher, Mr. Towle, my high school math teacher, Mr. McGowan, and my high school coach, Mr. McVeigh.

Most importantly, I need to thank all those people outside the world of science who made my life these past six years fun, rewarding, and meaningful. As throughout my life, my parents and sister, along with my extended family and friends, have supported me completely in all my endeavors. My biggest supporter has been my wife, Laura Anne, whom I met here at MIT in the biology graduate program. Together we have navigated through the many difficult times in graduate school and in life. The past year raising our son Elliot has been a hugely rewarding and challenging experience that has taught me so much more about myself. One of the more powerful connections we have made is with the members of Temple Eitz Chayim whom have been an amazingly supportive community that welcomed our family and provided wonderful friendships and very much-needed time away from science.

## **Drew M. Lowery - Curriculum Vitae**

### **EDUCATION:**

2007: Ph.D. in Biology, Massachusetts Institute of Technology, Cambridge, MA

2001: B.S. Pennsylvania State University, University Park, PA

### **AWARDS:**

2001-2006 Howard Hughes Predoctoral Fellowship in Biological Sciences

2006-2007 David Koch Graduate Fellowship

2001 High Distinction and Honors in Biochemistry and Molecular Biology

### **TEACHING EXPERIENCE:**

Spring 2003: Teaching Assistant, Cell Biology (7.06) Department of Biology, MIT

Spring 2005: Head Teaching Assistant, Biochemistry (7.05) Department of Biology, MIT

### **ORAL PRESENTATIONS:**

**Drew M Lowery.** Screens for Polo-Box Domain Interactors Reveals Role for Polo-Box Domain in Cytokinesis. MIT Center for Cancer Research Retreat. Nov 2004.

**Drew M Lowery** and Michael B. Yaffe. Screens for Polo-Box Domain Interactors Reveals Role for Polo-Box Domain in Cytokinesis. Howard Hughes Medical Institute Fellows Meeting. Sep 2005.

**Drew M Lowery.** Polo-box Domain Interactome Reveals Role of Polo-like Kinases in Cytokinesis. Cold Spring Harbor Laboratory/Wellcome Trust conference on "Interactome Networks". Sep 2006.

**Drew M Lowery.** Polo-box Domain Interactome Reveals Role of Polo-like Kinases in Cytokinesis. MIT Center for Cancer Research Retreat. Oct 2006.

**Drew M Lowery.** Polo-box Domain Interactome Reveals Role of Polo-like Kinases in Cytokinesis. Broad Institute Retreat. Nov 2006.

### **POSTER PRESENTATIONS:**

Isaac A. Manke, **Drew M. Lowery**, Ahnco Nguyen, and Michael B. Yaffe. Tandem BRCT Domains are Phosphoserine/Threonine-Binding Modules that Mediate the DNA Damage Response. Nature Biotechnology Winter Symposium: The Cell Cycle, Chromosomes & Cancer. Miami, FL. Jan 2004.

**Drew M. Lowery**, Duaa H. Mohammad, and Michael B. Yaffe. Polo-box Domain Interactions and Kinase Specificity of Polo-like Kinases. American Society for Biochemistry and Molecular Biology 2004 Conference. Boston, MA. June 2004.

## POSTER PRESENTATIONS CONTINUED:

**Drew M Lowery**, I. A. Manke, I. B. Rangel-Alarcon, and M. B. Yaffe. Structure and Mechanism of BRCA1 BRCT Domain Recognition of Phosphorylated BACH1 with Implications for Cancer. American Society for Microbiology: DNA Damage and Repair Symposium. Bermuda. Nov 2004.

**PUBLICATIONS:** \*these authors contributed equally

Manke, I.A., **Lowery, D.M.\***, Nguyen, A.\*, and Yaffe, M.B. BRCT repeats as phosphopeptide-binding modules involved in protein targeting. *Science* 302, 2003.

**Lowery, D.M.**, Mohammad, D.H., Elia, A.E.H., and Yaffe, M.B. The Polo-Box Domain: A Molecular Integrator of Mitotic Kinase Cascades and Polo-like Kinase Function *Cell Cycle* 3, 2004.

Clapperton, J.A., Manke, I.A., **Lowery, D.M.**, Ho, T., Haire, L.F., Yaffe, M.B., and Smerdon S.J. Structure and mechanism of BRCA1 BRCT domain recognition of phosphorylated BACH1 with implications for cancer. *Nat Struct Mol Biol* 11, 2004.

Alexander, D.E., Kaczorowski, D.J., Jackson-Fisher, A.J., **Lowery, D.M.**, Zanton, S.J., and Pugh, B.F. Inhibition of TBP dimerization by RNA polymerase III transcription initiation factor Brf1. *J Biol Chem* 279, 2004.

**Lowery, D.M.**, Lim, D., and Yaffe, M.B. Structure and Function of Polo-like Kinases. *Oncogene* 24, 2005.

Russ, W.P., **Lowery, D.M.**, Mishra, P., Yaffe, M.B., and Ranganathan, R. Natural-Like Function in Artificial WW Domains. *Nature* 437, 2005.

Yoshida, S., Kono, K., **Lowery, D.M.**, Bartolini, S., Yaffe, M.B., Ohya, Y., and Pellman, D. Polo-like kinase Cdc5 controls the local activation of Rho1 to promote cytokinesis. *Science* 313, 2006.

**Lowery, D.M.\***, Clauser, K.\*, Hjerrild, M.\*, Lim, D., Alexander, J., Kishi, K., Gammeltoft, S., Carr, S.A., and Yaffe, M.B. Proteomic Screen Defines Mitotic Polo-box Domain Interactome and Identifies Rho Kinase as a Plk1 Substrate in Cytokinesis. *EMBO* 26, 2007.

Paulson, J.L., Sullivan, M., **Lowery, D.M.**, Cohen, M.S., Randle, D., Tauton, J., Yaffe, M.B., Morgan, D.O., Shokat, K.M. A coupled chemical genetic and bioinformatic approach to Polo-like kinase pathway exploration. (in preparation)

**Lowery, D.M.**, Yoshida, S., Mohammad, D.H., Paulson, J.L., Shokat, K.M., Pellman, D., Yaffe, M.B. Mitotic Specific Yeast Two Hybrid Reveals Multiple Roles for Budding Yeast Polo-like Kinase Cdc5 in Cytokinesis (in preparation)

# Chapter One

## **Polo-like Kinases Control Mitotic Progression**

Portions Adapted and Expanded From:

Drew M. Lowery, Dan Lim, and Michael B. Yaffe.  
Structure and Function of Polo-like Kinases. *Oncogene* 24, 2005.

### Contributions:

Dan originally wrote the sections on Polo-box structure that are expanded here and made Figure 1.4, and Mike contributed significant input to many sections. I expanded and re-wrote all previously written sections, wrote the new sections, and made the remaining figures.

The primary function of the eukaryotic cell cycle is the complete and accurate transmission of the full genetic material to the two daughter cells. In order to coordinate the multitude of cellular events required, there has to be an over-arching regulatory strategy to provide spatial and temporal control of each step. Part of this order is established through separation of distinct cell cycle phases (G1, S, G2, M) by checkpoints that ensure that the previous series of events has completed before the next series of events begins. Particularly difficult to coordinate is M phase, or mitosis, as an interconnected series of events, including centrosome separation, spindle assembly and disassembly, chromosome segregation, and cytokinesis, need to play out in rapid succession with no room for error. Errors in these processes lead to genetic instability and chromosomal aberrations, which are a hallmark of tumor formation and cancer, that have recently been implicated as being a potential initiating event in some cancers [1-4]. Thus, a full understanding of the mitotic control machinery will enable great insight into the processes of tumor initiation and progression, and hopefully lead to the ability to prevent tumors from forming [5, 6]. This thesis further describes the roles of Polo-like kinase regulation of mitotic processes, particularly cytokinesis, in an attempt to understand the consequences of dysregulation of Polo-like kinases that are seen in human cancers.

### **General Roles and Evolution of Polo-like kinases**

Polo-like kinases (Plk) play key roles during multiple stages of mitosis, including prophase, metaphase, anaphase, and cytokinesis, in addition to less well-understood roles during G1/S and in response to DNA damage [7]. Originally named after the phenotype in flies, polo was found to encode a protein kinase whose mutation resulted in abnormal spindle poles [8, 9]. Flies, budding yeast, and fission yeast contain a single Plk family member (Polo, Cdc5, and Plo1 respectively), while humans, mice, frogs, and worms have 3 Plk family members, denoted Plk1/Plx1/Plc1, Plk2/Plx2/Plc2 (originally known as Snk) and Plk3/Plx3/Plc3 (originally known as Fnk or Prk).

Plks are defined by two conserved features – an N-terminal Ser/Thr kinase domain and a C-terminal duplicated Polo-box region (Figure 1.1). The kinase domains



are very highly conserved among all Plks, and most closely resemble those in Aurora kinases and calcium/calmodulin-dependent kinases. The region that encompasses the two C-terminal Polo-boxes is much less conserved, with only ~70 amino acids considered to form the “core”, which constitutes less than half the full length of the C-terminal domain. This entire region has recently been re-named the Polo-box domain (PBD) due to the fact that it functions as a single unit, as described in detail below.

In humans, Plk1 is expressed primarily during late G2 and M phases, where it appears to regulate much of the machinery involved in mitosis [7, 10]. Plk2 is expressed primarily in early G1, where it may control entry into S phase [11-13]. Plk3 appears to be expressed at constant levels throughout the cell cycle, and plays a role in several stress response pathways, including those activated by DNA damage and spindle disruption [14-17]. Plk2 and Plk3 may also have overlapping roles with Plk1 in several mitotic functions, most notably Golgi fragmentation and cytokinesis [18-22]. In addition, Plk2 and Plk3 have roles in remodeling post-mitotic neurons [23, 24]. Yeast and flies probably accomplish the same set of functions using only their single Plk family members, though the mitotic functions of these kinases have been more extensively studied. Similarly, there has been only limited study of worm Plks, and the data so far suggests that these genes have only limited overlapping functions with other Plk1 orthologs and paralogs [7].

Each of the three Plks in humans, mice, and frogs appear to be orthologous between species and paralogous within a species, since phylogenetic analysis of their sequences reveals that each group clusters separately (Figure 1.2A). Thus, the expansion from one to three Plks must have been an early evolutionary event. However, this expansion appears to have occurred at least twice because the three worm Plk paralogs cluster together separately from the Plks of other organisms. This is consistent with the individual worm Plks having less functional overlap with the other Plk family members. Plk genes from organisms with single family members are slightly more evolutionarily conserved with the Plk1 class than any other, belying their conserved mitotic function (Figure 1.2B).

There are no identified proteins with homology to Plks in bacteria, archae, or plants. This is somewhat surprising for plants because they have cyclin dependent

kinases and much of the same cell cycle machinery as yeast and animals. However, plants also show many novel features of cell cycle control [25]. With several plant genome sequencing projects complete or nearly complete, it seems increasingly unlikely that plant Plks are still awaiting discovery.

A fourth family member has also been characterized in humans and mice, and sequenced in frogs and flies, called Sak or Plk4. Plk4 has a C-terminus that is highly divergent from the other Plk family members, though its kinase domain closely resembles all other Plks. At the extreme C-terminus, Plk4 contains a single “Polo-box” instead of the tandem “Polo-box” repeats seen in all other Plks. This single “Polo-box” is the most divergent in sequence and has been shown to mediate Plk4 dimerization *in vitro* and when overexpressed *in vivo* [26]. Like all other Plks, Plk4 has been implicated in orchestrating cytokinesis [26-28], but its function remains largely unknown. The large (>500 amino acids) region between the kinase and the single Polo-box in Plk4 is a complete mystery as it has no obvious strong homology to any known proteins, and no function has been assigned to it.

### **Function of the Polo-Box Domain**

Plk activity is controlled by intracellular localization, in addition to being regulated at the level of protein abundance. During prophase and metaphase, Plk1 and related family members localize to centrosomes and spindle pole bodies [29-34], where they are required for spindle assembly and centrosome maturation, presumably by phosphorylating largely unknown centrosome-associated targets [35, 36]. Plk1 family members then re-localize to the spindle midzone during late anaphase [10, 30, 33, 37, 38], perhaps facilitating microtubule sliding or some aspect of kinetochore dynamics [39], and eventually come to flank the central portion of the cytokinetic bridge (i.e. the midbody) during telophase and cytokinesis [10, 31, 33, 39, 40]. At least for Cdc5, a portion of the protein is localized at the future site of cytokinesis (the bud neck in budding yeast) from late G2 onward [41] indicating that Plks may be involved in organizing the structures that will eventually result in cytokinesis.

The PBD is critical for both Plk localization and function, since mutations in the conserved residues of human Plk1 result in loss of Plk1 localization to spindle poles and the bud neck and an inability to support mitosis at the restrictive temperature in *cdc5-ts* complementation experiments [29]. Overexpression of the isolated PBD causes a failure to complete cytokinesis in budding yeast [42], and pre-anaphase arrest in mammalian cells [43]. The molecular basis of PBD function was clarified by the recent finding that the entire PBD, including both Polo-boxes, the region between them, and a portion of the linker between the end of the kinase domain and the first Polo-box, function as a single phosphoserine/threonine-binding module that bind proteins after they have been phosphorylated by CDKs [44]. Intriguingly, the optimal sequence motif recognized by the PBD is Ser-[pSer/pThr]-[Pro/X], suggesting that Cdks, MAP kinases, and other mitotic kinases might generate “priming” phosphorylations on substrates or docking proteins to localize Plks in the vicinity of their substrates. An optimal PBD-binding phosphopeptide displaces the PBD from binding to centrosomes in experiments using permeabilized cells [44], and mutations in the PBD that prevent phospho-peptide binding (Fig 1A) also prevent centrosomal localization [45]. The optimal binding motif for all Plks tested (including Plk2, Plk3, Plx1, and Cdc5) was the same as for Plk1, with very strong selection seen for Ser in the position before the phosphorylated residue and very little selection elsewhere [45]. Binding of the Plk1 PBD to a filter array of peptides, based on the optimal binding peptide with one residue mutated in each spot, indicates that the Ser in the -1 position is an absolute requirement for binding phosphopeptides *in vitro* [45]. Other positions showed varying degrees of specificity, with the inability of certain residues at certain positions to bind the PBD, the most obvious feature [45]. Thus, the phosphopeptide-binding function of the PBD is conserved across species and among family members, and is intricately linked to how Plks control cell cycle progression through mitosis.

There are two alternative, though not mutually exclusive, models for how the PBD might function to direct Plk kinase activity (Figure 1.3). In one model, which we refer to as the “processive phosphorylation” model, the PBD first binds to a site on a protein that has been previously phosphorylated by a mitotic priming kinase. This positions the kinase domain of Plk to phosphorylate the same protein at another site. This

type of processive phosphorylation is seen for the Tyr kinase Src, which contains a pTyr-binding SH2 domain [46-48], and for the Ser/Thr kinase GSK-3, whose kinase domain contains a separate pSer/pThr-binding pocket in the substrate binding cleft [49].

Plk1 substrates should contain both PBD-binding sites and kinase phosphorylation motifs if the processive model is correct. Therefore, the model can be examined by looking at known Plk substrates, of which a subset will be discussed here cursorily and many more will be discussed in great detail in the following section (see below and Table 1.1). Verified *in vivo* Plk1 substrates include Cdc25C [50], Brca2 [51], Myt1 [52], cyclin B [53-55], NudC [56], Nlp [57], TCTP [58], MKlp1 [39, 59], MKlp2 [60], Grasp65 [61, 62], and Wee1 [41, 63]. All of these contain potential PBD-binding sites, but only half match the phosphorylation motif of the only known priming kinases for PBD-binding, CDK/MAPK. Also, Cdc25C, MKlp1, MKlp2, TCTP, Grasp65, and NudC have been definitively shown to interact with the Plk1-PBD [44, 45, 56, 58-62]. (Interactions with the other substrate proteins have either not been examined or have only been assessed with full-length Plk1.) In addition, Cdc25C, Brca2, MKlp2, Grasp65, Wee1, and Myt1 are known to be phosphorylated by Cdk1, and NudC, cyclin B and TCTP are similarly phosphorylated by mitotic kinases other than Plk1, although the identity of these kinases and the sites and timing of phosphorylation are not known. Taken together, these data suggest that the processive phosphorylation model may apply to at least some of these substrates.

*In vitro*, however, Plk1 can phosphorylate bacterially-produced (and therefore unprimed) Cdc25C [64], TCTP [58], Myt1 [52], cyclin B [53],[53] and NudC [56], suggesting that priming phosphorylation is not absolutely required under conditions of high substrate and enzyme concentration. The kinetics and efficiency of phosphorylation, before and after a priming phosphorylation, were not investigated for most of these substrates. Phosphorylation of Cyclin B by Erk, however, was found to dramatically enhance its subsequent phosphorylation by Plk1 [55], suggesting a potential role of PBD-binding in Cyclin B phosphorylation by Plk1. Another protein, Emi1, was recently identified as a Plk1 substrate *in vitro* [65]. Emi1 could be phosphorylated by non-physiological concentrations of Plk1 that were ~20-fold higher than those found in mitotic extracts. However, if Emi1 was first phosphorylated by Cdk1, then the amount of

Plk1 that was required was reduced to physiological levels. Quantification of this effect revealed that incubation of Emi1 with Cdk1, prior to incubation with Plk1, increased the phosphorylation of Emi1 by Plk1 by three-fold [65]. Unfortunately, the sites of Cdk1 phosphorylation on Emi1, or the ability of Emi1 to associate with the PBD of Plk1, were not examined. Nevertheless, this data clearly agrees with a processive phosphorylation model. Another recent study demonstrated that Wee1 phosphorylation by Plk1 was stimulated by phosphorylation of Wee1 by Cdk1 [63]. The site of phosphorylation by Cdk1 perfectly matched a consensus site for PBD binding, again indicating a role for the processive model, though this interaction was not directly addressed in the study. A separate study demonstrated that these same events likely occur for the budding yeast homolog of Wee1, Swe1, though the priming kinase was suggested to be Cla4 instead of Cdk1 [41].

A novel substrate of Plx1, claspin, was recently described [66]. Claspin binds to the PBD of Plx1 through a phospho-dependent interaction and is subsequently phosphorylated on a nearby site [67]. The timing of these two events was clearly delineated, and the necessity of PBD binding for the subsequent phosphorylation event was demonstrated. Thus, claspin is the first Plk substrate to definitively use the processive phosphorylation model, though cyclin B, Emi1, and Wee1 are very strong candidates for additional Plk substrates that use this process.

A second alternative model is the “distributed phosphorylation” model, in which the ligand, to which the Polo-box domain binds, is distinct from the substrates, which the Plk kinase domain phosphorylates (Figure 1.3). In this case, Polo-box domain-binding to a phosphorylated scaffold or docking protein localizes the kinase domain to specific sub-cellular structures, proximal to substrates of the kinase domain which could even be bound to the same scaffold molecule. The movement of Plk1, from centrosomes to kinetochores and the spindle midzone, and then to the septin ring as cells progress from G2 through mitosis, is consistent with this model. Most of the putative scaffold molecules have yet to be defined, but there are at least two potential examples of such Plk1 scaffolds. One of the roles of Plk1-related family members is the activation of the Anaphase Promoting Complex (APC), and Cdc23/Cut23 is responsible for localizing Plk/Plx1 to the APC, where additional Plk1/Plx1 substrates are found [68, 69]. The

kinesin-like proteins Mklp1/2, which seem to carry Plk1 to the central spindle during anaphase and telophase [59, 60], may be the scaffolds for Plk1's role in cytokinesis, which presumably requires multiple substrates. Both of the Plk1 scaffolds, Cut23 and Mklp1/2, are themselves substrates of Plk1, suggesting that they function as more than simple docking sites.

Both models will surely turn out to be correct for specific Plk substrates, though which model will predominate is an open question. In either case, the PBD appears to function as an “AND” gate in the lingo of systems biology, by “integrating” the activity of other mitotic kinases with that of Plks. By functioning as a pSer/pThr-binding module, the PBD ensures that Plk-mediated progression through M-phase and sequential activation of discrete mitotic events occurs if, and only if, a prior CDK/MAPK or other mitotic kinase phosphorylation has occurred. In the processive phosphorylation model, the PBD functions as an “integrator” in time – the priming phosphorylation event has to occur at the same time that Plk kinase is present and active, or else the PBD binding site will be lost through the rapid action of phosphatases. In the distributive phosphorylation model, the PBD functions as an “integrator” in space – substrates must be localized in close proximity to the phosphorylated scaffold molecule to which the PBD has bound.

### **Cancer Connection of Polo-like Kinases**

Elevated Plk1 levels have been found in a wide variety of human tumors including non-small-cell-lung cancer [70], esophageal carcinomas [71], breast cancer [72], ovarian cancer [73, 74], pancreatic cancer [75, 76], head/neck squamous cell carcinomas [77], melanomas [78], colorectal cancer [79, 80], prostate carcinomas [81], hepatoblastoma [82], and papillary carcinomas [83]. Even more importantly, Plk1 expression levels have prognostic value in determining the course of some of the cancers listed above, including melanoma, colorectal cancer, and hepatoblastoma [78, 82, 84]. A subset of these studies have also demonstrated that high Plk1 expression is tightly correlated with future metastasis [82, 85]. Thus, Plk1 clearly has a role in oncogenesis, though there is no evidence that Plk1 is an initiating factor in any of these tumors, and mutations or epigenetic changes in Plk1 have not been observed in these human tumor

samples. In transformed cell lines, Plk1 expression is also consistently elevated, and several mutations have been found in the C-terminal region of Plk1 that disrupt its interaction with HSP90 [86].

Data from cell culture systems further supports a role for Plk1 in oncogenic transformation. Overexpression of Plk1 in NIH 3T3 cells produces the classic transformed phenotype of foci formation in soft agar and tumor formation in nude mice [87]. The opposite experiment of inhibiting Plk1 activity in transformed cells, such as U2OS cells, completely eliminates the ability of these cells to form foci [88]. Inhibition of Plk1 in HeLa cells by antibody injection also blocked proliferation [35]. Antisense oligonucleotides that down-regulate Plk1 cause decreased cell proliferation in MDA-MB-435 breast cancer cells and A549 non-small cell lung cancer cells in vitro, and tumor regression when these cells were xenografted onto nude mice [89, 90]. Interestingly, the viability of non-transformed cells such as amniocytes, mesangial cells and skin fibroblasts was unaffected by these types of Plk1 down-regulation [89]. Depletion of Plk1 levels through siRNA, in transformed cell lines derived from tumors, causes apoptosis along with mitotic catastrophe [88, 90, 91]. Strikingly, in primary non-transformed cell lines, depletion of Plk1 causes only minor cell cycle delays [90, 92]. Co-depletion of p53, however, mimics the cell death phenotypes seen in tumor-derived cell lines [92]. In a mouse bladder cancer model, Plk1 knockdown by siRNA was able to shrink tumor size [93].

The recent development of small molecule inhibitors of Plk1 have shed further light on this subject. The first ATP-competitive inhibitors of Plk1 to be described were scytonemin [94, 95] and the previously known PI3K inhibitor, wortmannin [96]. However, both these compounds have significant off-target effects that cause cell cycle phenotypes irrespective of their ability to inhibit Plk1 [94, 96], making them useful solely as starting points for generating Plk1-specific inhibitors. A high-throughput screening program at Boehringer-Ingelheim led to the identification of BI 2356, which inhibits Plk1 activity with an IC<sub>50</sub> of 0.8nM, and is at least 10,000 fold selective for Plk1 compared to the range of kinases studied [97]. In cell culture, this inhibitor prevents the proliferation of a large number of human tumor cell lines by inducing pro-metaphase arrest and subsequent apoptosis [97]. These effects extended to mouse xenograft models where

treatment with BI 2356 inhibited tumor growth and in some cases caused tumor regression [97]. This drug is now in clinical trials. Another ATP-competitive inhibitor of Plk1, LFM-A13, blocked mitosis in breast cancer and glioblastoma cells and delayed toxicity in the MMTV/neu transgenic mouse [98]. A third inhibitor potently inhibits the proliferation of a wide variety of tumor cell lines [99]. Overall, the reports on inhibition of Plk1 through every achievable means point to a critical role for Plk1 in tumor cell maintenance, if not initiation, and demonstrate that Plk1 is an excellent target for anti-cancer therapeutics. Thus, we set out to determine more Plk substrates through identification of PBD binding proteins in order to gain a greater understanding of Plk function in mitosis and its cancer-promoting properties.

### **Generation of Polo-box Domain Binding Sites**

One way to discover the pathways that Plks and the PBD contribute to is to identify the kinases that can generate PBD binding sites. So, what kinases might these be? Any kinase active during a time in the cell cycle when Plk is active, or is active before Plk but has its phosphorylation sites preserved until Plk is active, and which can phosphorylate a Ser or Thr with a Ser in the preceding residue, has the potential to generate PBD binding sites. The initially described PBD binding site-generating kinase is Cdk1/cyclin B [44, 45], as described for many proteins in the previous section. One recent interesting example is that Wee1 phosphorylation by Plk1 was stimulated by phosphorylation of Wee1 by Cdk1 [63, 100]. The site of phosphorylation by Cdk1 perfectly matched a consensus site for PBD binding (Table 1.1). A separate study demonstrated that these same events likely occur for the budding yeast homolog of Wee1, Swe1, though the priming kinase for PBD binding was suggested to be Cla4 instead of Cdk1 [41]. Thus, though the Plk-dependent regulation of Wee1 is conserved between budding yeast and humans, the upstream kinase is different, suggesting that the PBD binding is the critical event, not the mechanism of generation of the phosphorylation site.

There are other CDKs that act at various stages of mitosis. Cdk1/cyclinA is active during G2 and early mitosis and almost certainly generates some PBD binding sites, as many of the known PBD binding sites that are assigned to Cdk1/cyclinB from in



in vitro evidence could just as easily be generated by Cdk1/cyclinA in vivo. As part of the translational shutdown during mitosis, cap-independent translation is increased, and this generates another CDK, known as p58, which is translated from an internal ribosome entry site in Cdk11. Intriguingly, lack of p58 due to siRNA causes centrosome, spindle, and cytokinesis defects, in part because Plk1 is no longer properly recruited to mitotic structures [101-103]. This suggests that during late mitosis, p58 may be generating the PBD binding sites on proteins involved in cytokinesis, when Cdk1/cyclinB activity is no longer present. MAP (mitogen activated protein) kinase cascades have also been implicated in mitosis at least in early development [104-107]. As MAPKs generate a similar pSP motif to CDKs and allow for Ser in the -1 position, they could also be responsible for generating PBD binding sites, though no current evidence for this exists.

Interestingly, Plk1 has been shown to generate its own PBD binding sites on the cytokinesis kinesin MKLP2 [60], the cytokinesis protein PRC1 [108], and the kinetochore scaffold PBIP1 [109] (Table 1.1). There is no strong selection for any residue in the -1 position in the optimal phosphorylation motif of Plks [52] (Jes Alexander – personal communication), so at random, 1 out of 20 Plk phosphorylation sites would make a good PBD binding site. MKLP2 and PRC1 both participate in control of cytokinesis. Thus, during late mitosis, when Cdk1 activity is eliminated through degradation of cyclin B by the APC/C [110], it appears that Plk1 takes over the job of generating PBD binding sites. Why PBIP1 would use a Plk1-generated PBD binding site for its function at kinetochores is unclear, but perhaps the interaction needs to be stable through the metaphase-to-anaphase transition. How Plk1 is recruited to these molecules in order to generate a PBD binding site is a mystery, though the story for PRC1 may be explained by a second kinase and PBD binding site. Two PBD binding sites were identified in PRC1, though the Plk1-generated binding site was found to have a stronger phenotype when mutated in vivo [108]. However, the other binding site was close by, and mutation of it also resulted in cytokinesis defects and improper recruitment of Plk1 to the central spindle [108]. Thus, this site, when phosphorylated by an unknown kinase (though perhaps also Plk1), either regulates the accessibility of the Plk1-generated PBD binding site or, more likely, serves as a signal for initial PBD recruitment to PRC1 where, subsequently, Plk1 can generate its own stronger PBD binding site. PRC1 is also

phosphorylated by Cdk1 [108, 111], but this phosphorylation actually prevented recruitment of Plk1 to PRC1.

The PBD binding ability of Emi1 suggests that Cdk1 and Plk1 can also collaborate to create proteins with strong PBD binding sites. Emi1 is an APC/C inhibitor that is degraded by the SCF ubiquitin ligase, causing Emi1 destruction and allowing progression beyond prometaphase.  $\beta$ -TrCP is the targeting subunit of the SCF for Emi1 and binds Emi1 through the classical phospho-degron motif DpSGXXpS in a Plk1 dependent process [112]. The first phosphorylated Ser in the motif is contained within a standard Plk phosphorylation motif, but both are phosphorylated by Plk1 in vitro (Table 1.1) and respond to Plk1 overexpression in vivo [112]. Emi1 is also a Cdk1 target [65, 112] and interacts with the PBD [112]. Emi1 could be phosphorylated by non-physiological concentrations of Plk1 that were about 20-fold higher than those found in mitotic extracts. When Cdk1 was added to the reaction, it also phosphorylated Emi1 and lowered the amount of Plk1 required for maximum phosphorylation to physiological levels [65]. This clearly suggests that Cdk1 generates a PBD binding site on Emi1, but Emi1 contains no sites that look likely to be phosphorylated by Cdk1 and bind the PBD. Instead, perhaps multiple low affinity PBD sites are generated by the Cdk1 phosphorylation of Emi1, targeting Plk1 to Emi1 and enhancing Plk1's activity towards Emi1. Confusingly, mutation of all of the presumed Cdk1 phosphorylation sites in Emi1 did not eliminate PBD binding, as a Ser-pS motif within the phospho-degron sequence also contributed to PBD binding [112]. Thus, it seems Emi1 is targeted by Plk1 after PBD binding to Emi1 at multiple suboptimal Cdk1 sites and at an optimal site that may be generated by Plk1 itself, after being weakly targeted to Emi1 by Cdk1. This mechanism may be a general one, as it seems quite useful in setting a threshold of Cdk1 activity for PBD binding, but then allowing strong PBD binding after Cdk1 activity has risen high enough for Emi1 to be fully phosphorylated.

Other mitotic kinases might also generate PBD binding sites. Both Aurora A [113] and Aurora B [114] are known to crosstalk with Plk1, though currently the only known information flow is from Plk1 to the Aurora kinases. The phosphorylation motifs for both Aurora kinases consist of an Arg in the -2 position relative to the phosphorylated residue, with no particular selection for the residue in the -1 position [115, 116]. Thus, it

is possible that for certain processes, there might be information flow from Aurora kinases to Plks. Aurora A is localized to the centrosome during G2 and early M [117] at the same time that Plk1 is also localized there [7]. Both kinases are required for proper centrosome maturation and separation [7, 117]. While Aurora A and Plk1 may have distinct substrates at the centrosome, it is possible and logical that they share substrates, though none are currently known. Requiring multiple upstream inputs to create an activity is a common motif in cell cycle processes that can only go in one direction. Aurora B and Plk1 have multiple points of location and functional overlap during mitosis [7, 117] which are conserved all the way back to budding yeast [118]. The kinases co-localize at kinetochores where both are required for proper spindle orientation, and after satisfaction of the spindle attachment checkpoint, Plk1 modifies Aurora B behavior by phosphorylating the Aurora B regulator INCENP [114]. Both kinases then become “chromosome passenger proteins” and stay at the spindle midzone through anaphase and telophase, where they have several shared substrates including vimentin [119, 120] and MKLP1 [39, 59, 121]. Aurora B might generate a PBD binding site on MKLP1, as discussed below. Vimentin is a peculiar case. It has been demonstrated that Cdk1 generates a PBD binding site on vimentin [120], but the Aurora B phosphorylation site in vimentin [119] could also be a PBD binding site (Table 1.1). The Ser immediately preceding the Ser which is phosphorylated by Aurora B, however, is a phosphorylation target for a member of the family of Rho-activated kinases [119], which would render the site unable to bind the PBD. Whether there is some interplay between all these phosphorylation sites in vimentin is unexplored. In summary, further connections between Plk1 and Aurora kinases are likely.

Beyond Aurora kinases, there are yet more mitotic kinases that might generate PBD binding sites. Nek2 is present at the centrosome and required for centrosome maturation [122] like Plk1 and Aurora A. One of the targets of Nek2 is Nlp (ninein-like protein), which is a mother centriole-specific protein that is displaced from the centrosome at the G2/M transition [57, 123]. Nlp appears to be a priming kinase for Plk1 for several reasons: the displacement of Nlp from the centrosome is dependent on both Nek2 and Plk1 phosphorylation of Nlp, phosphorylation of Nlp by Plk1 is disrupted by overexpression of kinase-dead Nek2, and Nlp phosphorylation by Plk1 in vitro is

enhanced by preincubation of Nlp with Nek2 [123]. Plk1 does interact with Nlp, but this has only been shown for full-length kinase-dead Plk1 and not the isolated PBD [57]. Identification of the Nek2-dependent phosphorylation sites on Nlp, and verification that the PBD binds Nlp, will most likely demonstrate that Nek2 can generate PBD binding sites. If this is the case, there will likely be other centrosome targets of Nek2 that are bound by the PBD and phosphorylated by Plk1 to facilitate centrosome separation and maturation. Other Nek family kinases are still being explored. Nek9, like Nek2, localizes to centrosomes and is required for spindle assembly by binding to Ran GTPase [124, 125] and also activates the Nek family kinases Nek6 and Nek7 [126]. Thus, many other Nek family kinases might turn out to be involved in mitotic processes and be PBD binding site-generating kinases.

A less well-known mitotic kinase is LATS2 which, when deleted in mice, results in centrosome fragmentation and cytokinesis defects [127], and when knocked-down by siRNA in human cells, results in impaired centrosomal localization of gamma-tubulin and failure of mitotic spindle formation [128]. LATS2 is a target of Aurora A [129] at the centrosome, where it localizes during early mitosis [128, 129] and contributes to the Mdm2-p53 signaling axis during mitosis [130]. LATS1 also has mitotic roles, as knockdown causes the accumulation of multinucleate cells [131]; it interacts with and modulates Cdk1 activity [132, 133]; and it localizes to mitotic apparatus, including centrosomes, spindle, and the midbody [133]. Thus, both LATS1 and LATS2 could contribute to Plk1 signaling networks. Some other Ser/Thr kinases active in mitosis include LIMK1 [131, 134], GSK3- $\beta$  [135-137], Haspin [138, 139], PBK [140, 141], casein kinase II [142, 143], MEK1 [144-146], PAK [147-149], Kin4 in budding yeast [150, 151]; Bub1, BubR1, and TAO1 in the spindle attachment checkpoint [152, 153]; Cdc15 and Dbf2 in the mitotic exit network in budding yeast [154]; Kic1 and Cbk1 in the regulation of Ace2 and morphogenesis network in budding yeast [155]; Rock1, Rock2, and citron kinase in actomyosin ring contraction [156]. Some of these kinases have highly specialized functions and perhaps only a few substrates, so it is less likely that they generate PBD binding sites than the more generic mitotic kinases, though Plk1 and Cdc5 are required for many of the functions that they perform [7, 154, 157, 158]. Mps1

is another kinase involved in centrosome function and spindle attachment [159, 160] which generates a PBD binding site on the Bloom Syndrome helicase, Blm [161].

Plks contribute to many of the same processes in meiosis as in mitosis, but some differences exist, and other kinases might generate PBD binding sites in meiosis that do not play a role in mitosis. In vertebrate meiosis, unfertilized eggs are arrested in metaphase II, and fertilization triggers a transient increase in cytosolic free  $\text{Ca}^{2+}$ . This activates  $\text{Ca}^{2+}$ /calmodulin-dependent protein kinase II (CaMKII) among other proteins and kinases. One of the targets of CaMKII is Emi2 [162], which is an APC/C inhibitor that contributes to the metaphase arrest in these oocytes and is degraded upon metaphase arrest release [163]. Upon  $\text{Ca}^{2+}$  influx, CaMKII phosphorylates Emi2 at two sites in (R/K)XS(S/T) motifs which make, both, good targets of CaMKII and good binding sites for the PBD after phosphorylation [162] (Table 1.1). At least in vitro, CaMKII phosphorylation of these motifs did induce PBD binding, and in vivo, these motifs were required for proper release of metaphase arrest [162]. Also, Plx1 phosphorylates Emi2 in vitro at a site that targets Emi2 for degradation upon metaphase arrest release [163], and prior phosphorylation of Emi2 by CaMKII makes it a better substrate for Plx1 [164]. Since Plx1 with an intact PBD was also required for proper metaphase arrest release [162, 164], this strongly argues that Plx1 phosphorylates Emi2 in a CaMKII and PBD-dependent manner in vivo. CaMKII does not currently have a known mitotic role, making CaMKII a meiosis-specific PBD binding site-generating kinase. Other meiotic-specific kinases might also generate PBD binding sites

In what may seem to be a completely different process from mitosis and meiosis, Plk1 has found a role in response to DNA damage. However, ultimately, Plk1 is functioning in this process to promote the resolution of the DNA damage response and a return to cell cycle progression by entering mitosis. Thus, this can be seen as the same role which Plk1 is known to play in mitotic entry [7]. In fact, many of the proteins involved are the same, as the DNA damage response inhibits Cdk1, Cdc25B/C, and Plk1 itself, while activating the Cdk1 inhibitory kinase Wee1 [165]. Outside of these pathways already understood from the study of mitosis control by Plk1, Plk1 also plays a role in turning off the pathways that signal the DNA damage response in the first place. This was first discovered in budding yeast, where, after a double strand DNA break, yeast

will arrest in the G2 phase of the cell cycle. When an unrepairable break is engineered, the yeast cell will eventually enter mitosis with the break (so called adaptation), but yeast cells lacking Cdc5 are never able to turn off DNA damage signaling and continue through the cell cycle [166]. A similar phenomenon was seen in *Xenopus* eggs, as the presence of DNA damage did not prevent cell cycle continuation forever [67]. Instead, cell cycle re-entry in the presence of DNA damage was dependent on Plk1 phosphorylation of claspin, and Plk1 was targeted to claspin through PBD binding to an SpTQ motif generated by the DNA damage-responsive protein kinase ATR [67] (Table 1.1). Plk1 control of claspin turned off DNA damage signaling, as claspin is required to continually produce the cell cycle arrest signal [67, 167]. This adaptation response to DNA damage only makes sense, from an evolutionary standpoint, in single-cell organisms and in embryos where the parent does not spend a great deal of time nurturing its progeny. In human cells, an apoptotic response has been commonly observed, but continuation through the cell cycle after DNA damage can occur at prolonged timepoints [168], perhaps to allow cells to die by mitotic catastrophe if the cells fail to apoptose. Plk1 is required for mitotic entry after DNA damage [169], and Plk1 does control claspin [170-172], though the upstream kinase directing PBD binding is probably Cdk1 rather than ATR [171] (Table 1.1). There is another point of contact between DNA damage signaling and Plk1 in human cells, as Plk1 binds Chk2, a DNA damage checkpoint kinase, in a PBD-dependent manner on an SpTQ site generated by ATM [173-175] (Table 1.1). Thus, ATM and ATR can also generate in vivo relevant PBD binding sites. Whether other kinases in these pathways such as Chk1, Chk2, and MAPKAPK2 [175, 176] can also generate PBD binding sites is presently unknown.

There are many PBD interacting proteins with no identified or putative PBD binding sites. One of these proteins is TCTP, translationally controlled tumor protein, which is a Plk1 substrate and PBD binder but for which no clear PBD binding site exists [58]. Two Plk1-dependent phosphorylation sites were identified in TCTP, one of which is Ser<sup>64</sup> which is surrounded by a Glu and a Thr. Perhaps, this site was misidentified, and Plk1 actually phosphorylates the Thr, which would generate a PBD binding site [44, 45] (Table 1.1) as well as position the acidic residue two positions upstream of the phosphorylated residue in an optimal Plk1 phosphorylation site [52]. Thus, TCTP could

have a Plk1-generated PBD binding site like the other proteins described earlier. More likely, since the region of TCTP required for PBD binding does not contain this site [58], TCTP interacts with the PBD in a phospho-independent manner or indirectly.

NudC, nuclear distribution protein C, is also a Plk1 target and PBD binder with no clear PBD binding site [56]. The two mapped Plk1-dependent phosphorylation sites on NudC do not generate PBD binding sites [56]. However, NudC does localize to the spindle midzone and midbody during cytokinesis [177], where Plk1 is present. Since no other kinase has been shown to phosphorylate NudC in mitosis, this suggests that NudC may be a Plk1 target without direct binding to the PBD as described by the distributive phosphorylation model (Figure 1.3). The evidence against this theory is that NudC is required for Plk1 localization to the kinetochores [178] and spindle midzone [177], but this may be due to indirect effects of improper complex formation or mitotic progression without NudC. Oddly, NudC mutated in its Plk1 phosphorylation sites no longer recruits Plk1 to kinetochores despite still being capable of binding Plk1 *in vitro* [178], suggesting that Plk1 phosphorylation of NudC is required for proper kinetochore formation. NudC might also bind the PBD in a phospho-independent way, as it was identified as a PBD binder in a phage display approach where it was unlikely to be phosphorylated [56].

MKLP1 has been a known Plk1 substrate for a long time [39], and it was more recently demonstrated to be a direct PBD binder [59]. Since MKLP1 is involved in cytokinesis and localized to the central spindle [39] like MKLP2, PRC1, and Cyk-4, it seems likely that MKLP1 is also targeted by the PBD through a Plk1-dependent phosphorylation site. This seems plausible since Plk1 can generate a Ser-phosphoserine motif on MKLP1 [59] (Table 1.1). However, this site by sequence analysis appears to be an Aurora-dependent site and not a Plk1-dependent site, and this was subsequently proved [121]. However, this site is well outside the region of MKLP1 required for PBD binding [59]. This suggests that there is a third kinase that generates the initial PBD binding site, after which perhaps Aurora B further contributes to PBD binding to MKLP1.

Cyclin B1 also has a complicated set of phosphorylations. Four phosphorylation sites within cyclin B1 have been known for a long time, and this phosphorylation was thought to direct localization of cyclin B1 to the nucleus [179]. Two of these sites (S133 and S147) were found to be phosphorylated by Plk1, promoting translocation of cyclin

B1 to the nucleus [54] (Table 1.1). Other studies refuted that the S147 site was phosphorylated by Plk1 [53, 55] and suggested that Plk1 phosphorylation is not the critical step that allows cyclin B1 translocation [53]. The other two mapped phosphorylation sites (S126 and S128) were in consensus Cdk1-phosphorylation motifs, and could be phosphorylated in vitro by both Cdk1 and the MAPK Erk2 [55]. When cyclin B1 was pre-phosphorylated by Erk2, this increased Plk1 activity towards cyclin B1 by three to four-fold [55], suggesting that the Erk2 phosphorylation sites created a PBD binding site. Oddly though, Plk1 could phosphorylate unknown sites, in addition to S133 (but not S147), in cyclin B1 after pre-phosphorylation with Erk2 [55], so the additional activity seen could simply be the result of these additional accessible sites. Overall, the issue of how Plk1 targets cyclin B1 is very much unresolved, as perhaps Cdk1 or Erk2 generate PBD binding sites, but it is more likely that cyclin B1 does not directly bind the PBD.

In summary, as more PBD binding sites are identified, the mechanisms of PBD recruitment are further delineated. Single strong PBD binding sites can be generated by Cdk1 as seen with Bub1 [180], Cdc25C [44], Ect2 [181], INCENP [114], Myt1 [52], PICH [182], and TTDN1 [183] (Table 1.1). Multiple weak PBD binding sites can be generated by Cdk1 that collaborate to recruit Plk1 as seen in Emi1 [65, 112] and Nir2 [184] (Table 1.1). Other kinases can generate PBD binding sites such as Nek2 on Nlp [57, 123], CaMKII on Emi2 [162-164], MPS1 on Blm [161], ATM on Chk2 [173], possibly Erk2, and possibly Aurora B (Table 1.1). During late mitosis, Plk1 can generate its own PBD binding sites on PRC1 [108], MKPL2 [60], and maybe PBIP1 [109] (Table 1.1). Also, many Plk1 substrates do not seem likely to directly bind the PBD, or at least not in a phospho-dependent manner such as cohesin [185], NudC [56], and TCTP [58] (Table 1.1). In summation, a large variety of mechanisms exist to generate PBD binding sites and target Plks to their substrates, though most function through direct recruitment of the PBD to a single phosphorylated residue in a target protein.



## Activation and Phosphorylation of Plks

The cell cycle dynamics of Plks has been examined primarily for Cdc5 and Plk1. The levels of these Plks rise dramatically in the G2 phase of the cell cycle, starting from undetectable levels during G1 and beginning their rise in mid S-phase [10, 186, 187]. With this rise in protein levels, there is a concordant increase in kinase activity, but the activity rises much more dramatically than the levels, implicating an activation event [38, 186, 188]. Both the protein levels and the activity peak at the metaphase-anaphase transition, before returning to the interphase baseline at the beginning of the next G1 phase, due to degradation of these Plks by the APC/C [34, 186, 188-190].

Studies of Plk1, Plx1, Polo and Cdc5 have established that activation of these kinases requires their direct phosphorylation [32, 186, 188, 191-193]. Plk1 and Plx1 activation have been the most extensively examined in mechanistic and structural detail, although activation of other family members is believed to occur through the same mechanisms. Several conserved Ser and Thr residues are present within the kinase domains of Plks. Mutation of two of these, T210 and S137 in Plk1 (or the corresponding residues T201 and S128 in Plx1 and T197 and S124 in Plo1), to Asp, as a mimic of phosphorylation, results in the formation of activated Plk1, Plx1, and Plo1 [33, 194-196]. Mutation of these residues results in multiple mitotic phenotypes as discussed below.

T210/201 lies within the T-loop of the Plk kinase domain and has been confirmed to be an *in vivo* phosphorylation site, through phosphopeptide mapping of Plk1, immunoprecipitated from nocodazole-arrested lysates, and Plx1, immunoprecipitated from mitotic *Xenopus* egg extracts [195, 197]. Phosphorylation in T-loops is a common mechanism of activation for many protein kinases, including Aurora A/B, PKA, Cdk1/2, Erk1/2, Rsk1/2, Akt/PKB, and Mek1 [198]. Recent work using multiple phosphospecific antibodies to T210 have demonstrated that this epitope is phosphorylated throughout mitosis, in particular in nocodazole-arrested cells [199, 200]. It is generally believed that phosphorylation at T210 is a requirement for Plk activation, because the phosphomimic mutations mentioned earlier activate the kinase, T210V mutations prevent activation [33, 194, 195], and recognition of Plk1 by the phosphoT210 antibody correlates with Plk1 kinase activity [199, 200]. The corresponding phosphomimic mutation in human Plk2

also activates the kinase [12], suggesting that this is a conserved mechanism of Plk activation.

Production of a T201D mutant form of Plx1, in a *Xenopus* egg extract system, resulted in acceleration of Cdc25C activation during mitotic entry and delayed Cdc25C deactivation during mitotic exit, although T201D expression was not sufficient to induce the first mitotic cell cycle. Additionally, there was a delay in cyclin B2 degradation during anaphase and a corresponding delay in the loss of Cdc2 kinase activity [33]. On the other hand, overexpression of a T210D mutant form of Plk1 in HeLa cells caused an increased G2/M population [195], probably due to accelerated mitotic entry and subsequent mitotic delay [191, 200]. After a prolonged mitotic phase, from nuclear envelope breakdown to anaphase onset, Plk1-T210D expressing cells underwent successful cytokinesis, although it was often accompanied by excessive blebbing of the cell membrane coincident with cleavage furrow ingression [200].

There have been at least two proposals for the upstream kinase that phosphorylates T210/201 – *Xenopus* Plkk1 (equivalent to human SLK or Stk10) and PKA. xPlkk1 was purified as the Plx1 T201-phosphorylating factor in *Xenopus* oocyte extracts [201]. A more recent study demonstrated that xPlkk1 may actually be downstream of Plx1, and the two kinases could function in a positive feedback loop to phosphorylate and activate each other [202]. Immunodepletion of xPlkk1 did not prevent activation of Plx1 or alter the kinetics of mitotic entry in *Xenopus* egg extracts, as monitored by H1 kinase activity, implying that this loop is not required. Activation of Plx1 by phosphorylation was still required, implying that there must be another kinase that can phosphorylate Plx1 T201 in the xPlkk1 depleted extracts. Both human SLK and Stk10 have been shown to phosphorylate human Plk1 at T210 in vitro and are able to stimulate Plk1 activation in vivo [203, 204]. It was previously believed that Stk10 could not be the Plk1-activating kinase because the mouse homolog, LOK, was only expressed in lymphatic tissues. However, more complete expression profiling has shown that Stk10 is expressed in most tissues, so both SLK and Stk10 remain viable candidates or partners for Plk1 T210 phosphorylation. PKA has also been shown to be able to phosphorylate T201 and activate Plx1 activity in vitro [197]. In this same study, xPlkk1 was not able to phosphorylate Plx1 T201, creating a currently unresolved discrepancy in the field.

In contrast to T210/201, there is no mass spectrometry evidence for the *in vivo* phosphorylation of S137/128. At least two studies searched directly for S137/128 phosphorylation, using tryptic phosphopeptide analysis combined with mass-spectrometry in mitotic *Xenopus* extracts [197], and phosphopeptide mapping and phosphoamino acid analysis in mammalian cells [195], but both failed to identify phosphorylated S137. Although these and other studies did identify a number of other phosphoserine residues [188, 197, 201, 205], none of these sites have been shown to have functional significance. A single phosphospecific antibody made to this site has suggested that S137 is phosphorylated during late mitosis, as it recognized Plk1 after a nocodazole release but not in a nocodazole block [199, 200]. Oddly, the antibody only works for immunoprecipitation, so the data really only shows that Plk1 is immunoprecipitated with this antibody, and not that the S137 site is phosphorylated within Plk1 [199, 200]. Furthermore, the S137A mutation failed to prevent activation of Plk1/Plx1 and did not produce any noticeable phenotypes when overexpressed, suggesting that phosphorylation of this site is not critical *in vivo* [33, 195]. Still, the phenotypes seen with an S137D mutant form of Plk1 are striking. When overexpressed in HeLa cells, the S137D mutant Plk1 caused the cells to arrest as a G1/S population rather than the G2/M population seen with T210D or wild type, and the double mutant S137D/T210D also shows the G1/S block [195]. Accelerated mitotic entry is seen in the S137D and S137/T210D-expressing cells, despite their very slow S phase progression [200]. The cells that entered mitosis died at high rates of around 50%, and those that did not die failed in cytokinesis and gave rise to a single multinucleate daughter cell [200]. Mechanistically, it appears that these mutant Plk1 proteins activate the APC in an unregulated manner, leading to the lack of a spindle checkpoint, as shown by the inability of cells expressing these Plk1 mutants to arrest using microtubule poisons [200]. The equivalent S128D/T201D double mutant in Plx1 caused cleavage arrest, resulting in large cells, when injected into a *Xenopus* two cell embryo, and was able to induce the first mitotic cycle in a *Xenopus* egg extract system, unlike wild type or single mutants of Plx1 [33]. Together, this data suggests that if S137/128 is phosphorylated *in vivo*, it is probably only a transient event during late mitosis, with implications for APC activation during anaphase.

The systems that have been used to map phosphorylation sites in Plks have focused primarily on metaphase-arrested or asynchronous cells, and were therefore suited to identify stable phosphorylation sites, perhaps explaining the failure to date to observe Ser-137/128 phosphorylation. Since Plks show striking changes in subcellular localization during late mitosis, and participate in different processes at these times than during earlier stages of mitosis [7], the possibility for additional post-translational modifications of Plks, such as Ser-137 phosphorylation, during the post-metaphase stages remains promising. Demonstration that Ser-137/128 is phosphorylated *in vivo*, and identifying the kinase responsible for this event, would be an advance in the field.

The data for the activation of Cdc5 and Plo1 is somewhat different. Activation of Cdc5, as well as Plk1, is dependent on mitotic CDK activity. This makes sense as Plks are mitotic kinases, and without mitotic CDK activity, there is no mitosis. However, there is no direct evidence that CDKs directly activate Plks through phosphorylation except for one study [193]. Four residues downstream of the Plk1 T210 site is another Thr that is contained within a minimal CDK consensus phosphorylation site. This site is conserved throughout Plks, and was found to be phosphorylated *in vivo* in Cdc5 [193], though the T210 equivalent residue in Cdc5 (T238) was also found phosphorylated [193]. Mutation of the CDK site in Cdc5 to an Ala eliminated kinase activity of Cdc5 *in vitro* [193], however, this only demonstrates that the site cannot be an Ala for proper kinase function. The one piece of data that really suggests that Cdc28 can activate Cdc5 is that Cdc5 treated with a phosphatase *in vitro* has no activity, but after the addition of Cdc28, the activity of Cdc5 is restored [193]. Plo1 may be activated by the same activation loop phosphorylation as the other Plks [196], but it is also activated by a completely different mechanism through phosphorylation of residue S402 by SRP [206], a stress response protein kinase. Phosphorylation of Plo1 on this site promotes its interaction with the spindle pole body [206], probably by eliminating the negative regulation between the kinase domain of Plo1 and its PBD. Future work will clarify which sites are phosphorylated in the various Plks at what times of the cell cycle. These phosphorylation site potentially allow some (as yet unknown) combinatorial control of Plk activity.

## **Biological Functions of Polo-like Kinases**

### **Plk1 and Homologues**

Polo-like-kinase-1, and its characterized homologs (Cdc5 in budding yeast, Plo1 in fission yeast, Polo in *Drosophila*, and Plx1 in *Xenopus*), play key roles during multiple stages of mitosis, including prophase, metaphase, anaphase, and cytokinesis [7, 158]. Plk1 and Plx1 are required for the timely activation of the Cdc25C phosphatase, that initiates mitotic onset through dephosphorylation of cyclin-B/Cdk complexes [32, 33, 64, 207-210]. During prophase and metaphase, Plk1 and related family members localize to centrosomes and spindle pole bodies [29-34], where they are required for proper centrosome maturation and spindle assembly [32, 35, 36], presumably by phosphorylating a critical set of as-yet-unknown molecular targets. Plk1 family members then relocate to the spindle midzone during anaphase [10, 33, 37, 38], perhaps facilitating microtubule sliding or some aspect of kinetochore dynamics [39], and later flank the central portion of the cytokinetic bridge (i.e. the midbody) during telophase and cytokinesis [10, 31, 33, 39]. In *Xenopus* oocytes, Plx1 kinase activity facilitates the bulk of cohesion release from chromosomes during prophase [185], while Cdc5 has been shown to directly phosphorylate the Scc1 cohesin subunit, making it a better substrate for the protease separase that triggers sister chromatid separation in anaphase [211]. Plo1 is required for formation of the actin ring and septum during cytokinesis [212], and loss of Cdc5 results in cytokinetic arrest, while overexpression of the isolated Cdc5 C-terminus causes incomplete cleavage septa and aberrant septin ring structures [42]. Data showing a similar role for Polo-like kinases in cytokinesis in animal cells is beginning to accumulate [39, 43, 177, 194, 213, 214]. Additionally, Plks are both regulators and substrates of the APC, phosphorylating several APC subunits, together with Cyclin B/Cdk1, to activate APC ubiquitin ligase activity towards cyclins, as well as towards Plks themselves [34, 68, 69, 189, 215, 216]. This Plk-regulated destruction process is required for mitotic exit [215], and its own auto-catalytically-triggered ubiquitin-mediated destruction likely explains the observed variation of Plk protein levels during the cell cycle, with maximal levels during late G2 and early M, and nearly non-existent levels during late G1 and throughout S [10, 39].

Activation of Cdc25C, the phosphatase that activates CDK1/CyclinB to drive mitotic entry, results from a series of Cdc25C phosphorylation events mediated by both CDK1/CyclinB and Plks, but the connection between these kinase phosphorylation events has remained mysterious [33, 64, 209, 217-220]. The Plk PBD binding motif rationalizes the synergy between these two kinase pathways, with CDK1/CyclinB providing priming phosphorylations on PBD motifs in Cdc25C, that target Cdc25C to Plks in a timely and efficient manner. Plk1 has also been reported to directly phosphorylate cyclin B [53, 54], inactivating a nuclear export sequence and targeting cyclin-B to the nucleus [54], but this is controversial, as described earlier. A new model for this activation loop has recently been coalescing from the observation that Cdc25B and Plk1 are required for mitotic entry after a DNA damage-mediated G2 cell cycle arrest [169]. Initial activation of Cdc25B by the action of Plk1 and some cyclin-Cdk complex, perhaps CDK2/CyclinA, could start the mitotic entry process. Cdc25B, in turn, would lead to an initial activation of CDK1/CyclinB at the centrosome and translocation of active CDK1/CyclinB into the nucleus, where it provides priming phosphorylation of nuclear Cdc25C. Since Plk1 is both nuclear and cytoplasmic [10], nuclear Plk1 could then provide the final activating phosphorylation events required for Cdc25C activation in this compartment, with subsequent activation of additional CDK1/CyclinB and further priming of additional Cdc25C. This sequence of events generates a positive feedback loop, in which Plk acts as the “trigger kinase” [10, 33, 64] and Cdc25B acts as the “starter motor” [221, 222]. This fits with the observation that elimination of a single Plk PBD binding site results in incomplete activation of Cdc25C in vivo [44]. Additional targets of Plk1 involved in mitotic entry are the CDK1 inhibitory kinases, Wee1 and Myt1, which are both targeted for inactivation by Plk1 [41, 52, 63, 100, 221, 222]. Thus, Plks play a crucial role in nearly all known aspects of generating mitotic kinase activity.

In parallel with and subsequent to mitotic entry, centrosomes have to mature and the mitotic spindle must form. The very first observation of Polo mutants noted a high number of monopolar spindles or bipolar spindles with one of the poles displaying abnormal morphology [9]. Work in other organisms including human confirms that interference with the activity of Plks leads to severe spindle defects [8, 35, 88, 90]. These defects are thought to result from a failure of centrosome separation and maturation, as

Plks regulate both positive and negative regulators of this process. Nlp and OP18 are negative regulators of microtubule nucleation, that are inhibited by Plk1 and Polo, respectively [57, 123, 223]. Plk1 also directly binds gamma-tubulin [224] and recruits it to centrosomes [35], where it can perform its function as the site of spindle nucleation. The microtubule stabilizing proteins, Asp and TCTP, are also regulated by Polo and Plk1, respectively [36, 58]. This might be the central biological role for Plks as spindle defects have been the primary phenotype identified using several recently reported Plk inhibitors [225-227].

Perhaps the critical point in mitosis is the metaphase-to-anaphase transition, where the cell switches from getting chromosomes and other cellular machinery ready, in a state of high CDK activity, to the stage where segregation of chromosomes and other material occurs, in a state of low CDK activity. This transition is delayed, until everything is fully prepared, by the spindle assembly checkpoint, which monitors bipolar orientation of each chromosome through the sensing of tension [153]. The 3F3/2 epitope at kinetochores is correlated with a lack of tension, and was recently shown to be generated by the activity of Plks [228]. Plk activity is also required for the localization of some proteins to the kinetochore [228], though the spindle assembly checkpoint is still active when Plk activity is absent [185, 228, 229]. However, the ultimate target of the spindle assembly checkpoint is the APC/C (anaphase promoting complex or cyclosome), which is under the direct regulation of Plks both through phosphorylation of APC/C subunits [230] and phosphorylation of APC/C inhibitors [65, 112]. Functionally, the APC/C is poised to degrade both securin and cyclin B, which allows activation of separase and cleavage of cohesin, resulting in sister chromosome separation [153]. Plks also play a role in this part of the metaphase-to-anaphase transition, by regulation of separase cleavage of cohesin [185, 211, 231] and regulation of the cohesion protecting protein shugoshin [232].

The role of Plks in anaphase events has been most well-studied in budding yeast, where the FEAR (cdc14 early anaphase release network) and MEN (mitotic exit network) networks have been worked out in great detail [154, 233, 234]. Though the requirement for Cdc5 in these networks is definitive, the exact mechanisms behind Cdc5 control of these processes is not clear. The purpose of these networks is to activate Cdc14, the

phosphatase that dephosphorylates many of the CDK sites generated in early mitosis [233]. Fission yeast have an analogous pathway to MEN, termed SIN, that is also controlled by Plo1, but it has a slightly different biological role [154]. In animal cells, very little is known about these pathways, other than that the role of Cdc14 is highly conserved and required for turning off mitotic CDK signaling. Very recently, a connection between Plk1 and Cdc14 was shown [235], suggesting that the role of Plks in this process is conserved. So, as in mitotic entry, Plks mediate many events (FEAR, MEN, and APC activation) that ultimately impinge on the control of CDK1/CyclinB activity.

At the end of mitosis, Plks still have yet another job to do, which is control of cytokinesis. Cytokinesis failure has been seen in weaker alleles of Polo that get past spindle failure [214], in overexpression studies with Plk1 [191], and in Plk1 inhibition studies, if the spindle defect is circumvented [43, 88]. As mentioned earlier, all Plks studied localize to the spindle midzone, cleavage furrow, and midbody [10, 30, 31, 33, 37-41], where they have multiple substrates [39, 51, 59, 60, 108, 120, 181]. Disruption of Plk signaling through Nir2 [184], NudC [56], Npm1 [236], MKLP1 [59], MKLP2 [60], Cep55 [237], and PRC1 [108], causes cytokinesis defects and, many times, failures. Why there needs to be so many targets of Plks to regulate cytokinesis is unclear, as is the actual function of most of these proteins in cytokinesis. Regulation of MKLP1 by Plk1 has been suggested to modify the microtubule bundling ability of MKLP1 [39, 59], and regulation of Ect2 by Plk1 has been suggested to modify the RhoGEF activity of Ect2 [181]. However, for the most part, the data regarding Plk regulation of cytokinesis proteins has been solely limited to localization control, which, while critically important, does not give any insight into the molecular underpinnings of the physical process of cytokinesis.

Plks also have roles outside mitosis, in meiosis and in the DNA damage response. The general role of Plks in meiosis seems to be similar to their roles in mitosis, particularly, in regulating cohesion during the different meiotic stages, exact details of which continue to be elaborated [238, 239]. Plk1 is itself a target of the DNA damage checkpoint pathway, undergoing phosphorylation and inactivation by Chk2, in response to DNA damage [240]. Furthermore, Plk1 is found in association with Chk2 at



centrosomes, even in the absence of DNA damage, although the interaction appears to be dependent upon ATM activity [174]. This makes sense, as many cell cycle regulators are turned off by the DNA damage pathway. However, in the case of Plks, they are also required to exit the DNA damage response, as detailed earlier for the Plk substrate claspin, and described in detail for Cdc5 in a series of papers [166, 241-243]. How small amounts of Plk activity are generated during a cell cycle arrest, to allow cell cycle re-entry, is currently unclear.

## **Plk2**

Plk2 was first identified as a serum-inducible immediate-early response gene in NIH 3T3 cells [13]. Its mRNA levels and protein levels track together across the cell cycle, with a spike in G1/S and with minimal amounts at other times [12, 13]. In addition, Plk2 is a stress-responsive gene, that is downstream of p53 transcriptional activation after X-ray irradiation, UV, and other DNA damaging agents [18, 244]. However, Plk2 is a nonessential gene that can be fully knocked out in mice [245], and whose knockdown shows no ill effects in common human cell lines [18]. Plk2-knockout MEFs do show a slightly reduced growth rate, and the embryos are slightly growth retarded [245], suggesting that Plk2 does have a general cell cycle role. This cell cycle role is probably related to centriole duplication, as overexpression and depletion of Plk2 lead to an increase and decrease, respectively, of centrosome numbers in cell culture models, in a functional kinase-dependent manner [246]. Oddly, silencing of Plk2 by siRNA in the presence of mitotic inhibitors, such as nocodazole, resulted in apoptosis during mitosis [18], suggesting a requirement for p53 induction of Plk2 in maintaining cell viability during a spindle checkpoint arrest, though this could be a downstream effect of the centriole duplication problem seen in a different study [246]. In adult tissues, Plk2 is found in some non-cycling organs such as the heart, lung, and specific regions of the brain [11, 13], where the Plk2 gene is responsive to stimuli that promote synaptic plasticity [24]. In the brain, the Plk2 PBD has a specific interaction with SPAR (spine-associated RapGAP) [23]. Cell culture models show that Plk2 phosphorylates SPAR, leading to its degradation [23], which has been correlated with the depletion of mature dendritic spines and corresponding increase in the exploratory precursors of spines [23].

The only other known neuronal interactor of Plk2 is CIB (calcium and integrin binding protein) [24], which was shown to inhibit Plk2 activity in a cell culture system [12]. Overall, there is still very little understood about Plk2 function, and in particular there is nothing known about the role of the Plk2 PBD, other than that it targets Plk2 to bind SPAR [23] and that it selects the same phosphopeptides in vitro as Plk1 [45].

### **Plk3**

Some of the reported Plk3 data is similar to that for Plk2, as Plk3 was also first identified as an immediate-early response gene to FGF signaling in NIH 3T3 cells [15]. All the neuronal information for Plk2 is equally true for Plk3, as Plk3 has been shown to bind CIB [24] and SPAR [23] in neuronal cells, where its expression is also responsive to stimuli that promote synaptic plasticity [24]. The need for two Plks to do the same thing is unclear as well as logically baffling. Despite these similarities, Plk3 cell cycle roles have very little functional overlap with Plk2. Instead of the protein amount tracking the mRNA amount, Plk3 protein is nearly completely stable throughout the cell cycle [14, 247] despite the mRNA only being expressed during the G1 phase [15, 248, 249]. Explaining this continual protein level, it appears that Plk3 normally exists in an inactive state [14] in the cytoplasm [250]. since Plk3 protein is rapidly degraded in the nucleus via a ubiquitin-associated pathway [251]. So, what stimuli promote Plk3 activity?

Plk3 kinase activity is activated upon oxidative stress and DNA damage through an ATM-dependent pathway, likely through direct phosphorylation of Plk3 by ATM [16, 252]. This is the exact opposite of the effect of DNA damage and other stressors on Plk1 function, as discussed earlier. The role of Plk3 during the damage response is thought to be two-fold, as Plk3 interacts with, phosphorylates, and enhances the activity of Chk2 [14, 17] along with phosphorylating Ser-20 on p53 [252]. This site on p53 has long been known to be important for p53-mediated cell cycle arrest, and thought to be phosphorylated by Chk1 and Chk2 [253-255]. However, the sequence surrounding the site closely matches the known Plk consensus motif [52], with an acidic residue two positions upstream of the phosphorylated serine. The sequence does not match the known Chk consensus motif [256], which requires a basic residue three positions upstream of the phosphorylated serine. Another Plk3 substrate during stress responses

has been reported to be Cdc25C [257, 258], with a phosphorylation site of Ser-216, which is also thought to be a Chk1 and Chk2 site [259, 260]. In this case, the site conforms to the Chk consensus motif and not the Plk consensus motif, and the belief in the field is that this site is not actually phosphorylated by Plk3. If Plk3 did target Cdc25C directly it should hit the same sites as Plk1, since they have similar kinase domains (see below) and similar PBD binding motifs [45]. Overall, the cases of p53 Ser-20 and Cdc25C Ser-216 suggest that Plk3 has overlapping and intertwining roles with the Chk kinases during the DNA damage response.

Following along with Plk3's opposite function during the DNA damage response as Plk1, Plk3 also has shown to be oppositely correlated with cancers, as compared to Plk1. Many studies have shown a decrease in Plk3 mRNA expression in tumor samples compared to non-tumorigenic tissue [249, 261-263]. Also, ectopic expression of Plk3 slows cell cycle time [262] and results in cell cycle arrest along with apoptosis [19, 22], all in a kinase activity-dependent manner. So, clearly, Plk3 has a tumor suppressor function, as opposed to the oncogenic function of Plk1.

Further confusing the mystery of the relationship of Plk1 and Plk3 is that both these kinases can rescue the *cdc5-1* temperature sensitive allele at the restrictive temperature in budding yeast [194], suggesting overlapping function. At the least, Plk1 and Plk3 must have some overlapping PBD binding specificities [45], and overlapping kinase motifs (personal communication – Jes Alexander). In fact, overexpression of the Plk3 PBD results in the same localization pattern as that seen with Plk1. with clear localization to the centrosome, spindle poles, central spindle, and midbody [264]. Furthermore, overexpression of GFP-tagged full-length Plk3 causes cytokinesis failures, with subsequent rounding up and cell death [19]. In cycling cells, both proteins are present during mitosis, so the separation of Plk1 and Plk3 function must be due to upstream regulation or components in the linker region between the kinase and PBD that do not affect the function in budding yeast. More recently, reports have suggested that endogenous Plk3 localizes to the nucleolus, and plays a role in the G1/S transition [265], so the real cell cycle function of Plk3 remains controversial.

## **Plk4**

Plk4, as described earlier, is by far the most divergent member of the Plk family. It contains only a single polo-box region, and is highly unlikely to bind phosphopeptides (see below). Plk4 expression levels rise in S phase and stays fairly high through mitosis before falling again as cells re-enter G1 [266]. The regulation of the activity of Plk4 and its protein level changes across the cell cycle are not yet known, but it is solely expressed in cycling tissues in adults [267]. Like Plk1, Plk4 is an essential gene, as the mouse knockout is inviable, dying at E7.5 [28]. These embryos display large numbers of mitotic cells with high cyclin B levels, suggesting that Plk4 is absolutely essential for passing through some stage of mitosis [28]. Cells grown from these embryos display a large number of cells arresting as a dumbbell shape, indicative of telophase failure [28]. Thus, Plk4 deficient cells probably are defective in mitotic exit during anaphase, but continue cycling into telophase until the CDK activity arrests the cells. Knockdown of Plk4 in cell culture systems gives similar results, as cells arrest [267] and apoptose [268]. Fascinatingly, cells from Plk4 mouse heterozygotes display slow growth, centrosomal amplification, multipolar spindles, and aneuploidy [269]. This points to a haploinsufficiency of Plk4 activity, and strikingly, these mice develop multifocal liver tumors of high grade with prominent mitotic irregularities [269]. Overall, this suggests that Plk4 could have tumor suppressor functions, though there have not been comprehensive studies correlating Plk4 levels or function with tumor samples. The actual function of Plk4 during mitosis is elusive. Plk4 localizes to the centrosomes and midbody, much like Plk1, dependent on both its polo-box and the linker between the polo-box and the kinase domain [28]. What Plk4 does at the midbody is unclear, but at the centrosome, it probably functions in centriole duplication [270, 271], like Plk2.

## **Polo-like Kinase Structures**

### **Structure of the Plk4 Polo Box**

Structural analysis of the Polo-box first emerged from the crystal structure of the single Polo-box of murine Plk4 (residues 845-919) [26]. The structure revealed that the Polo-box had crystallized as an intermolecular dimer with a clam-like shape, consisting,

in total, of two  $\alpha$ -helices and two six-stranded antiparallel  $\beta$ -sheets. Each  $\beta$ -sheet contained four contiguous strands from one Polo-box ( $\beta$ -strands 6, 1, 2 and 3), with the remaining two strands coming from the other Polo-box. The association of  $\beta$ -strand 3 from both Polo-boxes formed a hinge region, opposite to which was an interfacial cleft and pocket ( $\sim 17 \times 8 \times 12 \text{ \AA}$ ). The presence of 9 of 19 conserved hydrophobic residues lining the interior of the pocket hinted at a possible ligand binding function, although actual ligands of the Plk4 Polo-box dimer remain to be identified.

The dimeric structure of the Plk4 Polo-box seen in the crystals was also shown to occur within cells using coimmunoprecipitation assays of differentially tagged Plk4 Polo-box constructs [26]. Interestingly, a C-terminal construct of Plk4 containing residues 596 to 836 (Plk4<sub>241</sub>) but lacking the Polo-box region was also observed to dimerize, indicating the presence of one or more dimerization domains in addition to the Polo-box within Plk4. The subcellular localization of enhanced green fluorescence protein (EGFP) fusion constructs of the Polo-box region alone, and of full-length Plk4 in NIH 3T3 cells, suggested that the Polo-box may play a role in targeting Plk4 to centrosomes and the cleavage furrow. However, in contrast to loss of localization observed for Polo-box truncations in other members of the Plk family, subcellular localization of Plk4 was not disrupted by deletion of the Polo-box. Significant loss of proper subcellular localization of Plk4 was only observed if both the C-terminal region following the kinase domain, but preceding the Polo-box (residues 596-836), and the Polo-box itself were deleted. Given the ability of the Polo-box and Plk4<sub>241</sub> constructs to dimerize, it is unclear if the observed subcellular localizations of these domains result from their interaction with components of centrosomes and the cleavage furrow or from association with endogenous Plk4.

### **Structure of the Plk1 Polo-box domain**

Crystal structures of the Polo-box domain (PBD) of human Plk1 [45, 272] revealed some similarities and a number of key differences from the structure of the Plk4 Polo-box dimer. Each of the individual Polo-box repeats (PB1 and PB2) in Plk1 consisted of a self-contained six-stranded  $\beta$ -sheet and  $\alpha$ -helix (Figure 1.4A). This was similar to the structure of the single  $\alpha$ -helix/ $\beta$ -sheets seen in the Plk4 Polo-box dimer, however in the Plk4 structure, each of the  $\beta$ -sheets contains contributions from two Polo-boxes. In

contrast, no strand swapping was observed in the Plk1 PBD  $\beta$ -sandwich. Furthermore, the association between the Polo-box repeats in Plk1 differed completely from that of the Plk4 Polo-box dimer. The  $\beta$ -sheets in the Plk1 PBD pack together with the two  $\alpha$ -helices on either side of the  $\beta$ -sandwich, such that residues located at the interface in the Plk4 Polo-box homodimer correspond to residues on the exterior faces of the  $\beta$ -sandwich in the Plk1 PBD. The PBD also contained a Polo cap (Pc) region consisting of an  $\alpha$ -helix connected via a linker (L1) to the first  $\beta$ -strand of PB1 and a second linker (L2) connecting the two Polo-box repeats, helping to hold both Polo-boxes in the correct orientation.

Peptide library screening to determine the optimal phosphopeptide motifs recognized by the PBDs of human Plk1, Plk2 and Plk3, *Xenopus* Plx1 and *Saccharomyces cerevisiae* Cdc5 revealed a strong selection for Ser in the pThr/pSer-1 position and a modest preference for Pro in the pThr/pSer+1 position [44, 45]. Crystal structures of the human Plk1 PBD in complex with its optimal phosphopeptide revealed the structural basis of the phospho-dependent binding and motif recognition. The phosphopeptide binding site is located at one end of a shallow cleft between the two  $\beta$ -sheets within the only highly conserved region on the PBD surface. The phosphate group is bound via eight hydrogen-bonding interactions, involving indirect contacts through a lattice of ordered water molecules and direct contacts arising from the pincer-like arrangement of the His-538 and Lys-540 side chains. The importance of His-538 and Lys-540 in phosphospecific binding was confirmed by mutation of these residues to Ala, which eliminated binding [45]. The strong selection for Ser at the pThr-1 position can be accounted for by three hydrogen bond interactions of the Ser-1 side chain hydroxyl to the main chain atoms of Trp-414 and with the backbone carbonyl of Leu 491 via a water molecule. Van der Waals contacts between the Ser-1 C $\beta$  atom and the C $\delta$ 1 of a strictly conserved Trp-414 side chain reveal that larger hydroxyl-containing side chains such as Thr or Tyr at the pThr/pSer-1 position would result in a steric clash. The importance of Trp-414 is shown by the fact that a W414F mutation results in loss of centrosomal Plk1 localization and failure of this mutant to rescue the *cdc5-1* allele in *S. cerevisiae* [194]. The pThr/pSer+1 Pro residue makes a smaller contribution to the binding surface and likely increases binding affinity by introducing a kink via its trans peptide bond

conformation, to direct the residues C-terminal to it back towards the binding surface, thereby reducing the entropic penalty of binding. Structure-based sequence alignments of the Plk1 PBD with other PBDs suggest that all coordinate phosphate in a similar manner as the His-538, Lys-540, and Trp-414 residues and surrounding regions are completely conserved (Figure 1.4B). Similarly, the inverted structure of the dimeric PLK4 polo-box region suggests that it cannot possibly bind phosphopeptides in the same manner as the other Plk family members [26], and almost definitely does not bind phosphopeptides at all (Andy Elia – personal communication).

Another set of Plk1-PBD structures, complexed with phosphorylated and non-phosphorylated versions of the Plk1-PBD Cdc25C target peptide, were recently published [273]. The structures were nearly identical to each other and the previously published structures, with the only notable exception that the loop connecting to the two polo-boxes (residues 488-507) was unstructured when bound to the non-phosphorylated Cdc25C peptide [273]. This region was also unstructured in the previously described apo structure [272], but is well-structured in the presence of a phosphorylated peptide [45, 272, 273]. These residues flank the bound peptide, and contribute some minor interactions between the backbone of the Plk1-PBD and the peptide, as well as with the ordered water molecules [45]. Whether this loop is floppy until phosphopeptide binding has not been studied, but this crystal structure observation certainly suggests that the stabilization of this loop could be a major contributor to the selectivity of the Plk1-PBD towards phosphopeptides compared to non-phosphopeptides.

A mutually inhibitory interaction between the Plk1 kinase domain and Polo-box domain results in both a ~3-fold reduction in kinase activity and a ~10-fold reduction in phosphopeptide binding by the PBD, with significantly reduced phosphospecificity [45, 191, 194, 274]. Conversely, binding of the optimal phosphopeptide to full-length Plk1 stimulated kinase activity by ~2.6 fold, and suggests that binding of the PBD to substrates with primed phosphorylation sites simultaneously targets Plk1 to its substrates and activates the kinase domain. The structural basis for regulatory interaction between the kinase and Polo-box domains remains unclear. In the Src family of protein tyrosine kinases, intramolecular binding of the SH2 domain to a C-terminal phosphotyrosine motif positions the N-terminal SH3 domain for binding to a linker connecting the SH2 and

kinase domains [275, 276]. The SH3 domain and the linker interact with the kinase domain to stabilize it in an inactive conformation. This mechanism of intramolecular regulation does not appear to be applicable to Plk1, due to the absence of an internal optimal PBD motif. Additionally, mutations of the His-538/Lys-540 pincer residues, that disrupt phosphospecific binding by the PBD, do not abrogate binding of the PBD to the isolated kinase domain in trans. These observations indicate that the sites of interaction on the PBD with phosphopeptide ligands and with the kinase domain are distinct. Partial overlap of these sites, such that binding at one site sterically occludes binding to the other site, however, would provide one possible mechanism of the mutually inhibitory interaction.

An alternative mechanism to regulate catalytic activity via an intramolecular phosphopeptide binding domain is illustrated by the SHP family of phosphatases, in which binding of the N-terminal SH2 domain to the phosphatase domain partially occludes the catalytic cleft and distorts the conformation of the SH2 domain, reducing its phospholigand affinity [277]. Conversely, phospholigand binding to the SH2 domain results in activation by stabilizing an alternate conformation of the SH2 domain, with reduced affinity for the phosphatase domain. A similar “molecular switch” mechanism may be applicable to the Polo-box domain and would be consistent with its reduced phospho-dependent binding in full-length Plk1 and the increased activity of full-length Plk1, upon addition of optimal phosphopeptide. Crystal structures of the PBD in the apo state and in complex with its optimal phosphopeptide reveal that phosphopeptide binding does not induce significant conformational changes in the PBD [272], except for the previously described observation that the linking region between the two polo-boxes is ordered, when bound to a phosphopeptide, and unstructured, when not [273]. Thus, the linking loop could be the location of influence by the kinase domain to control phosphobinding affinity. Additionally it is not known if the kinase active site is simply occluded as in the SHP phosphatases, or if the kinase domain adopts a distinct inactive conformation when bound to the PBD. A crystal structure of full-length Plk1 or a complex of the isolated kinase domain with the PBD will be needed to observe the kinase domain and the PBD in their mutually inhibited states.



### **Structure of the Plk1 kinase domain**

Very recently, a structure of the isolated Plk1 kinase domain was published [278], but no other structures of Plk family member kinase domains have been solved. The structure was determined with a T210V mutation, in order to lock in an inactive conformation, and with ATP analogs, to help order the substrate binding cleft. Unsurprisingly, the Plk1 kinase domain adopts a typical kinase fold, with the ATP binding cleft between an N-terminal  $\beta$ -sheet containing lobe and a C-terminal  $\alpha$ -helical containing lobe [278]. Oddly, the activation loop assumed an extended conformation typical of active kinase structures [278], despite the attempt to generate an inactive form by prevention of activation loop phosphorylation by mutation of the phosphorylated residue. However, this extended activation loop conformation is stabilized by a zinc ion not previously seen in kinase structures that is coordinated by residues from several different molecules of kinase domain. Furthermore, the absolutely conserved interaction between the activation loop and the catalytic lysine seen in structures of active Ser/Thr kinases is not present [198] due to zinc ion coordination. Thus, the activation loop's conformation is controlled by crystal contacts, and not by its intrinsic structure, making interpretation of this region and its impact on Plk1 activation unwarranted and prone to artifact.

Ser-137 of Plk1 shares a similar surrounding sequence context as Thr-210 and has been proposed to be a second site of phosphorylation [195], although this remains controversial as discussed above. In the Plk1 kinase structure, Ser-137 is solvent-exposed and located within the presumed peptide binding cleft, near the predicted substrate Ser/Thr-3 position. However, gross conformational changes and/or movements of the two lobes of the kinase domain would be required to make Ser-137 accessible to a kinase, suggesting that it is never phosphorylated *in vivo* [278]. Phosphorylation of Ser-137 would be expected to introduce a strong negative charge and increase selectivity for a positively charged residue, such as Arg or Lys in the substrate at the -3 position. Interestingly, the crystal structure of Akt/PKB in complex with GSK3-peptide shows a negatively charged residue at this position (Glu 236) forming a bi-dentate salt bridge to the -3 Arg of GSK3-peptide [279]. A similar interaction is also observed in the structure of a PKA-peptide complex [280]. Thus, phosphorylation of Ser-137, if it occurs, might

be expected to alter Plk substrate specificity, leading to phosphorylation of alternative targets than those selected when Ser-137 is not phosphorylated. Intriguingly, Ser-137 of Plk1 is conserved in Plk2 (Ser 166) and Plk3 (Ser 107) but is replaced with glutamate in Plk4 (Glu 96).

### **Prospects for structure-based drug design**

As discussed earlier, Plk1 is likely to be a highly effective target for anti-cancer drug design. The Plk1 kinase domain is an obvious target for drug development, and high-throughput screening and structure-based approaches used in the discovery and optimization of inhibitors of other protein kinases can be applied [281-283]. The deep cavity of the ATP binding pocket of kinases provides an excellent binding site for small molecules, and consequently the majority of available kinase inhibitors are ATP analogs. The lack of specificity of many such inhibitors is a significant problem, however, owing to the highly conserved nature of the ATP-binding pocket. In some cases, selectivity can be achieved by exploiting unique structural features. For example, deschloro-flavopiridol utilizes an additional less-conserved pocket within the ATP-binding site of CDK2 [284]. The diaryl urea, and quinazolinone and pyridol-pyrimidine classes of p38 MAP kinase inhibitors, also exploit novel binding sites within the ATP-binding pocket, some of which are created by inducing subtle conformational changes [285, 286]. High specificity is also achieved by targeting a distinct inactive conformation of a kinase, as shown by the inhibition of Abelson tyrosine kinase by STI571/Gleevec [287]. Crystal structures of the Plk1 kinase domain in the true active and inactive conformations will be extremely valuable for the optimization of lead compounds.

The recent Plk1 kinase domain structure [278] allows identification of areas of the Plk1 active site that can be exploited to generate specific inhibitors. The striking differences of the Plk1 ATP binding pocket, compared to other kinases, are the presence of a Cys at the roof of the pocket and a Phe at the bottom of the pocket which are much more commonly Val and Leu. This creates a larger-than-average space at the roof and a smaller-than-average space at the bottom of Plk1's ATP binding pocket. There is also a cluster of three arginines in a solvent-exposed region of the Plk1 ATP binding pocket that contains no positively charged residues and a highly conserved glycine in most kinases.

All these residues are well conserved in Plk2 and Plk3, but not Plk4. One potential method of creating specificity towards Plk1, and at the expense of Plk2, is to target binding in the site created by Leu132 in Plk1, which is a tyrosine in Plk2 and in most other kinases. The Plk1 inhibitor BI 2536 was recently demonstrated to be highly selective towards Plk1, though it also inhibits other Plk family members [97]. Docking of this inhibitor into the Plk kinase domain structure suggests that it utilizes the anomalous Cys67 and Leu132 to form its specific binding pocket [278]. Structural models of the other recent inhibitors with the Plk1 kinase domain structure have not been reported. Now that several Plk1 inhibitors and the kinase domain structure are known, structures of the inhibitors bound to the kinase domain will be necessary to understand exactly how specificity is generated by these compounds. These structures can then be readily utilized for structure-based drug design, by modification of the current inhibitors at appropriate places.

The Polo-box domain presents an additional unique target for the development of novel and specific Plk inhibitors, since it is essential for normal Plk function. To date, disruption of protein-protein interactions have been looked upon unfavourably as targets for drug design, primarily because such interactions often involve burial of large amounts of hydrophobic surface. However, the identification of a relatively polar, small optimal phosphopeptide ligand for the PBD, capable of disrupting Plk-substrate interactions [44], suggests that small molecules should be sufficient to accomplish this task. Furthermore, the availability of Plk PBD optimal phosphopeptides should facilitate development of high throughput assays for small molecule inhibitors that will disrupt PBD function, while the availability of crystal structures of the PBD-phosphopeptide complex will facilitate structure-based optimization of any lead compounds identified in these screens. And, as there are no other proteins with structure known to be similar to the polo-box domain, off target effects should be minimal. Specificity among the different Plk family members would be very difficult to achieve, as they all appear to have the same phosphopeptide selectivity [45]. There is one potential PBD inhibitor currently in the literature, HMN-214, which has broad spectrum antitumor activity in mouse xenograft models [288]. This drug has passed through phase I clinical trials [289], and supposedly

inhibits Plk1 subcellular localization but not kinase activity [289]. This makes it appear that HMN-214 is a PBD inhibitor, but as this data is all unpublished, it is hard to know.

### **Summary and Preview of Thesis**

A role for Plk1 as an oncogene in a variety of human tumors is becoming increasingly clear. Identifying the biological mechanisms of Plk1 function and substrates of Plks will be critical to understanding and subsequently modulating Plk function. The large amount of conservation between the roles of Plks in different organisms allows a variety of systems to be used for addressing Plk function. What is known is that Plks play critical roles during multiple stages of cell cycle, and in particular mitotic, progression. All Plks contain an N-terminal Ser/Thr kinase catalytic domain and a C-terminal region that contains one or two Polo-boxes. For Plks 1, 2, and 3, and their homologs, the entire C-terminal region, including both Polo-boxes, functions as a single modular phosphoserine/threonine-binding domain known as the Polo-box domain. In the absence of a bound substrate, the PBD inhibits the basal activity of the kinase domain. Phosphorylation-dependent binding of the PBD to its ligands releases the kinase domain while simultaneously localizing Plks to specific subcellular structures. These observations suggest that the PBD integrates signals arising from other mitotic kinases to target the activated kinase towards distinct substrates. Thus, identification of PBD targets is one mechanism to identify Plk substrates and to gain a greater understanding of the roles of Plks in the regulation of mitotic processes.

In this thesis, we set out to identify the PBD interactors of Plk1 through a pull-down mass spectrometry approach (Chapter Two) and the PBD interactors of Cdc5 through a novel mitotic-specific yeast two hybrid screen (Chapter Three). The recent X-ray crystal structures of the PBD provided insights into the structural basis for PBD function, and allow us to create and use optimal negative controls to identify the phosphorylation-specific interactors of the PBD. The results from both these screens led us to explore the role of Plk1 and Cdc5 in cytokinesis, where we demonstrate that both Plks modulate members of the Rho signalling network during cytokinesis, including proteins downstream of RhoA (Chapter Two) and upstream of Rho1/A (Chapter Four). Our extensive data sets lead us to a number of hypotheses on the mitotic roles of Plks,

and on various specific proteins that might be regulated by Plks, which are explored in Chapter Five. In addition to the work on Plks, we describe the identification of tandem BRCT domains as phosphorylation-dependent binding domains involved in DNA damage-dependent signalling (Appendix One), and the functional characterization of designed WW domains (Appendix Two), which are another class of phosphorylation-dependent binding domains involved in cell cycle control and cancer susceptibility.

**Figure 1.1: Domain structure and key residues of Polo-like kinases.**

Polo-like kinases contain an amino-terminal kinase domain and a carboxy-terminal Polo-box domain connected by a short linker. Plks are activated by phosphorylation of a conserved Thr residue within the T-loop (Thr-210), and bind phosphopeptides through a pocket in the Polo-box domain containing the key residues Trp-414, His-538, and Lys-540. Numbering is for human Plk1.

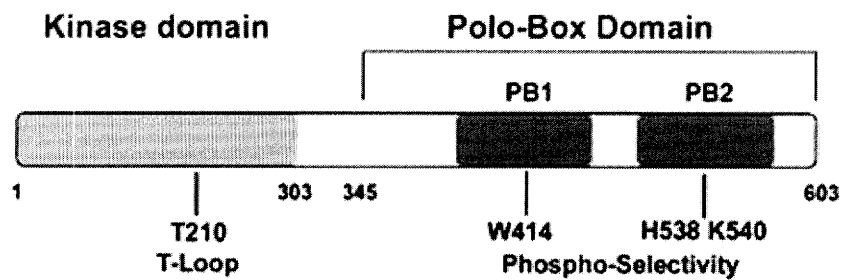


**Figure 1.2: Phylogenetic analysis of Polo-like kinase family members.**

(A) Full length sequences of known Plk family members were aligned using ClustalW [290]. A rooted tree was constructed using PHYLIP [291] showing one model of evolutionary descent.

(B) An unrooted tree shows the distance relationship between Polo-like kinases from organisms containing only a single Plk family member (Polo, Plo1, Cdc5) from other members of the Plk family.

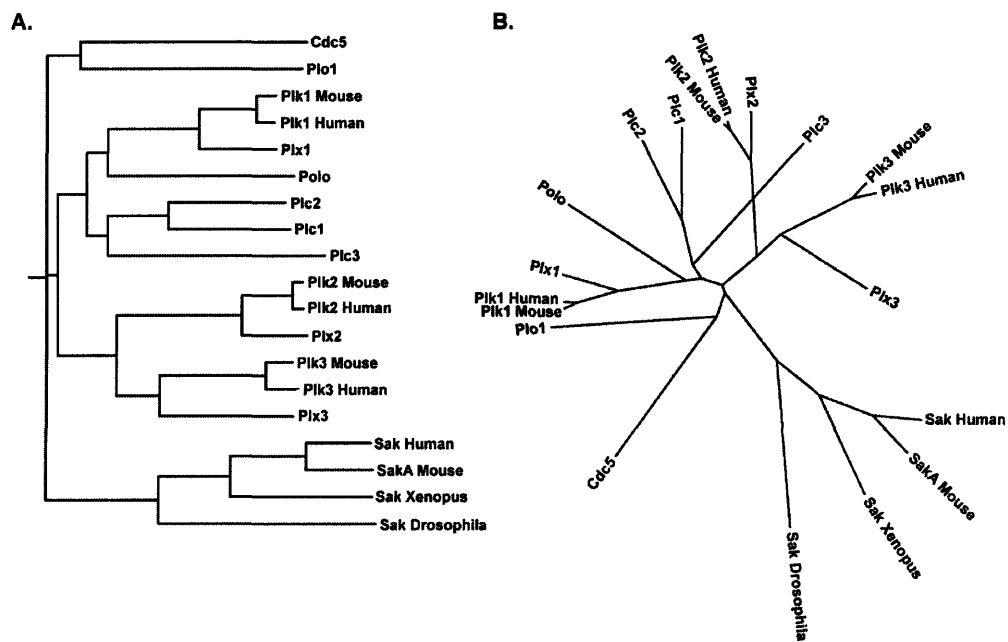


**Figure 1.3: Two proposed models for Polo-box Domain-mediated substrate targeting.**

In the distributive model (upper), Plks are targeted to specific subcellular locales through binding of the PBD to a single protein. Additional substrates of the kinase domain are then encountered in these locations. In this model, Plks function as spatial integrators of mitotic signalling. In the processive model (lower), PBD binding to a protein targets that protein for subsequent phosphorylation by Plks. In this model, Plks function as temporal integrators of mitotic phosphorylation events.

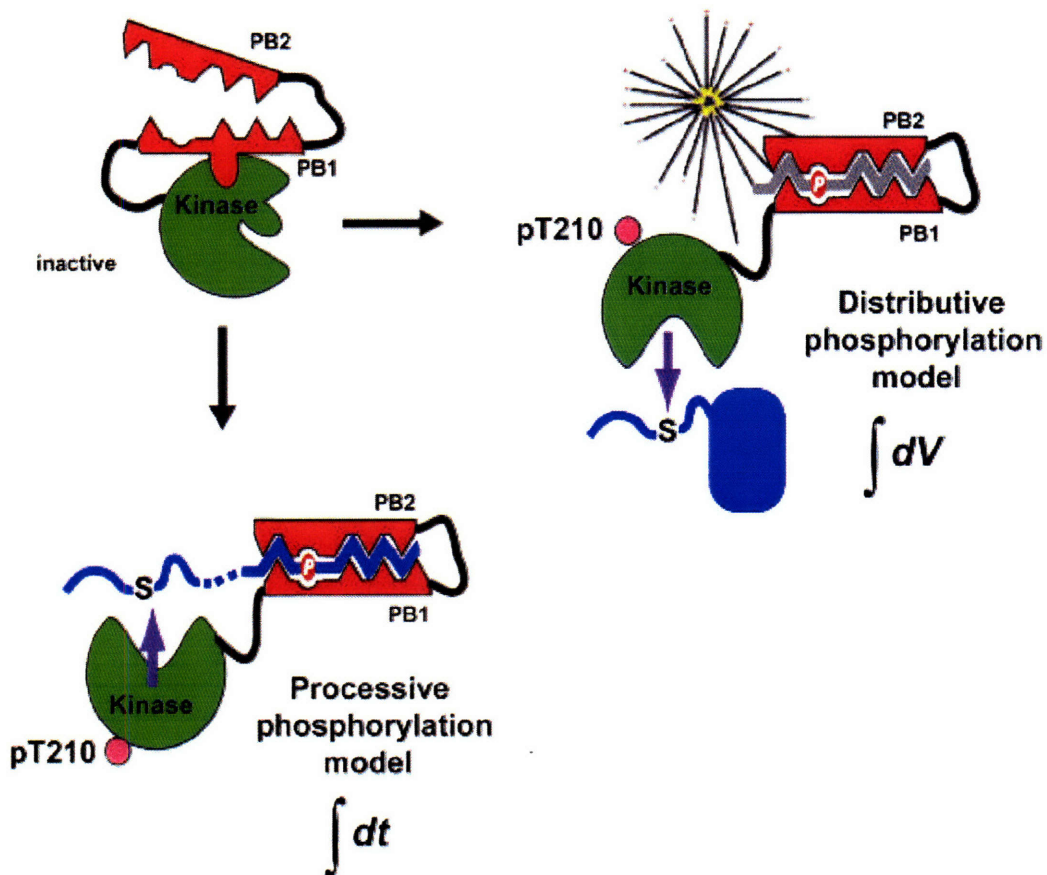






**Table 1.1: Polo-like Kinase Substrate and Polo-box Domain Binders**

Protein	Mapped Plk1 Phosphorylation Site(s)	Potential Polobox Domain Binding Site <sup>1</sup>	Interacts With Plk1 Polobox Domain	Presumed Kinase that Generates PBD binding site	Reference
Asp1 <sup>2</sup>	ND	many (S/T)P sites	ND	CDK1	[36]
Bfal <sup>3</sup>	ETS <sup>17</sup> F, NTT <sup>24</sup> L	SS <sup>454</sup> P	ND	CDK1	[294-296]
Blm	ND	SS <sup>144</sup> P, SS <sup>1296</sup> P	+	MPS1	[161]
Brca2	DMS <sup>193</sup> W, DES <sup>239</sup> L	ST <sup>77</sup> P, SS <sup>1818</sup> P, ST <sup>2310</sup> P, ST <sup>3193</sup> P, SS <sup>3219</sup> P, ST <sup>3242</sup> P	ND	CDK1	[51]
Bub1	ND	ST <sup>609</sup> P	+	CDK1	[180]
BubR1	ELT <sup>792</sup> V, EAT <sup>1008</sup> V	ST <sup>620</sup> P	+	CDK1	[180, 297]
Cdc25C	EFS <sup>198</sup> L	ST <sup>130</sup> P	+	CDK1	[44, 50]
Cdc27 <sup>4</sup>	QDT <sup>209</sup> I, NDS <sup>427</sup> L, DSS <sup>435</sup> I	many (S/T)P sites	Not tested	CDK1	[230]
Centrin	Not tested	SS <sup>796</sup> P	+	CDK1	[298]
Cep170	ND	ST <sup>288</sup> P, SS <sup>313</sup> P, ST <sup>765</sup> P, SS <sup>1398</sup> P	ND	CDK1	[299]
Cep55	NES <sup>436</sup> L	AS <sup>425</sup> P, KS <sup>428</sup> P	+	CDK1, Erk2	[237]
Chk2	ND	ST <sup>68</sup> Q	+	ATM	[173, 174]
Claspin <sup>5</sup>	SDS <sup>30</sup> GQGS <sup>34</sup> Y one or both	ST <sup>955</sup> P	ND	CDK1	[171]
Cohesin SCC1 <sup>6</sup>	ND	ESS <sup>40</sup> V, VST <sup>186</sup> T, QST <sup>199</sup> S	Not tested	Plk1? Indirect binder?	[185]
Cyclin B <sup>7</sup>	ETS <sup>133</sup> G, AFS <sup>147</sup> D	AS <sup>126</sup> PS <sup>128</sup> P, ST <sup>414</sup> LP	ND	CDK1? ERK2? Indirect binder?	[53-55]
Ect2	ND	ST <sup>413</sup> P	+	CDK1	[181]
Emi1	EDS <sup>145</sup> G, YSS <sup>149</sup> F	AS <sup>20</sup> P, YT <sup>75</sup> P, GS <sup>98</sup> P, VS <sup>102</sup> P, QS <sup>182</sup> P, EDS <sup>145</sup> GYSS <sup>149</sup> F	+	CDK1 and Plk1	[65, 112]
Emi2 <sup>8</sup>	QDS <sup>33</sup> GYSDS <sup>38</sup> L one or both	RSST <sup>195</sup> , RLST <sup>336</sup>	+	CaMKII	[162-164]
Grasp65	ND	SS <sup>122</sup> P	+	CDK1	[61, 62]
INCENP	Not tested	ST <sup>388</sup> P	+	CDK1	[114]
Kizuna	DLT <sup>379</sup> I	SS <sup>13</sup> P, SS <sup>436</sup> P	+	CDK1	[300]
Mcm2	Not tested	SS <sup>13</sup> P, SS <sup>27</sup> P, SS <sup>41</sup> P	+	CDK1	[301]
MKLP1 <sup>9</sup>	RRS <sup>911</sup> S, RSS <sup>912</sup> T	RSS <sup>912</sup> T	+	Aurora?	[39, 59, 121]
MKLP2	EHS <sup>528</sup> L	EHS <sup>528</sup> L	+	Plk1	[60]
Myt1 <sup>10</sup>	DSS <sup>426</sup> L, DDS <sup>435</sup> L, DLS <sup>469</sup> D, EDT <sup>495</sup> L	ST <sup>455</sup> P	ND	CDK1	[52, 302]
Ndd1 <sup>11</sup>	ESS <sup>85</sup> L	SS <sup>357</sup> P	ND	CDK1	[303]
Net1 <sup>12</sup>	ESS <sup>31</sup> Q, DAS <sup>48</sup> L, NVS <sup>60</sup> F, ERS <sup>242</sup> F, and many more	ST <sup>212</sup> P	Not tested	CDK1	[304-307]

**Table 1.1: Continued**

Protein	Mapped Plk1 Phosphorylation Site(s)	Potential Polobox Domain Binding Site <sup>1</sup>	Interacts With Plk1 Polobox Domain	Presumed Kinase that Generates PBD binding site	Reference
Nir2	Not tested	ST <sup>794</sup> P, many (S/T)P sites	+	CDK1	[184]
Nlp	EDS <sup>87</sup> S <sup>88</sup> S, EST <sup>167</sup> K EKS <sup>686</sup> Q	LCSS <sup>308</sup> L, LFSS <sup>314</sup> , Several others	ND	Nek2	[57, 123]
Npm1	EDS <sup>4</sup> M	ST <sup>219</sup> P	+	CDK1	[236]
NudC	ENS <sup>274</sup> K, DFS <sup>326</sup> K	SS <sup>232</sup> WL, SS <sup>260</sup> DP	+	Phospho-independent?	[56]
OP18 <sup>13</sup>	ND	LS <sup>23</sup> P, LS <sup>38</sup> P	ND	CDK1	[223]
Orc2	ND	Many (S/T)P sites	+	CDK1?	[301]
PBIP1	DVS <sup>53</sup> S, HSTT <sup>78</sup> A, EFS <sup>88</sup> K, DTS <sup>111</sup> G, EAS <sup>116</sup> E, DDS <sup>139</sup> E, QPS <sup>194</sup> V, EKT <sup>261</sup> H, DYS <sup>369</sup> D, KET <sup>381</sup> Y	HST <sup>78</sup> A	+	Plk1	[109]
PICH	ND	ST <sup>1063</sup> P	+	CDK1	[182]
Pin1	KHS <sup>63</sup> Q	NSS <sup>42</sup> S, several others	+	Plk1?	[308]
PRC1	NST <sup>602</sup> N	AST <sup>578</sup> Y, NST <sup>602</sup> N	+	Plk1	[108]
Ran	AKS <sup>135</sup> I	none	ND	Indirect binder?	[309]
RGC32	ND	ST <sup>82</sup> P	+	CDK1	[310, 311]
Shugoshin <sup>14</sup>	ND	ST <sup>331</sup> P	+	CDK1	[232]
TCTP	DDS <sup>46</sup> L, TES <sup>64</sup> T	none	+	Phospho-independent?	[58]
TTDN1	Not tested	ST <sup>120</sup> P	+	CDK1	[183]
vimentin	QDS <sup>82</sup> V	SS <sup>53</sup> P	+	CDK1	[120]
Wee1	EDS <sup>53</sup> A	SS <sup>123</sup> P	+	CDK1	[41, 63, 100]

ND = not determined but does interact with full length Plk and is a substrate of Plk.

Not tested = not tested as a Plk1 substrate

None = no clear potential PBD binding sites

### Table 1.1: Notes

- <sup>1</sup> Proteins are labeled as interacting with the PBD if an interaction with full length Plk was demonstrated to be phosphorylation dependent in addition to if an interaction is observed with the isolated PBD. The Polo-box domain binding sites for Blm, Bub1, Cdc25C, Chk2, Cyk4, Ect2, Emi2, INCENP, Myt1, Nir2, PICH, PRC1, TTDN1, vimentin, and Wee1 have been identified in the indicated references.
- <sup>2</sup> Asp has only been shown to be a Plk substrate and binder in drosophila.
- <sup>3</sup> All data on Bfa1 are from budding yeast.
- <sup>4</sup> Only the subset of the in vitro mapped phosphorylation sites that were also seen in vivo are listed [230]. The APC subunits APC1, APC4, and AP7 were also shown to be phosphorylated by Plk1 in vitro though none of the mapped sites were seen in vivo.
- <sup>5</sup> Xenopus claspin contains an ST<sup>906</sup>Q motif instead of an STP motif at the potential PBD binding site. This site was proven to be the PBD binding site and is generated by the DNA damage responsive protein kinase, ATR [67]. A different site was described to be phosphorylated by Plx1 in xenopus claspin, SSS<sup>934</sup>F [67], then in human claspin.
- <sup>6</sup> Cohesin, SCC1, phosphorylation sites have been identified in budding yeast [211, 231], but the human data suggests a slightly different mode of regulation though it is still Plk1 dependent [185].
- <sup>7</sup> The S147 site in cyclin B1 is probably not phosphorylated by Plk1 [53, 55].
- <sup>8</sup> Emi2 data is from xenopus oocytes, but all relevant sites are completely conserved in human Emi2.
- <sup>9</sup> The sites ascribed to Plk1 in MKLP1 are probably generated by Aurora B, and this has been proved for the latter site [121].
- <sup>10</sup> The PBD binding site in Myt1 is confirmed in the xenopus system [302], but only suggested in the mammalian system.
- <sup>11</sup> All data on Ndd1 are from budding yeast.
- <sup>12</sup> All data on Net1 are from budding yeast.
- <sup>13</sup> OP18 has only been demonstrated to be a Plk substrate and binder in Xenopus.
- <sup>14</sup> Shugoshin sites are from drosophila data though the sites are conserved in human shugoshin and the data that has been published indicates the same regulation is occurring.

## References

1. Kops, G.J., Weaver, B.A., and Cleveland, D.W. (2005). On the road to cancer: aneuploidy and the mitotic checkpoint. *Nat Rev Cancer* 5, 773-785.
2. Jallepalli, P.V., and Lengauer, C. (2001). Chromosome segregation and cancer: cutting through the mystery. *Nat Rev Cancer* 1, 109-117.
3. Li, J.J., and Li, S.A. (2006). Mitotic kinases: the key to duplication, segregation, and cytokinesis errors, chromosomal instability, and oncogenesis. *Pharmacol Ther* 111, 974-984.
4. Perez de Castro, I., de Carcer, G., and Malumbres, M. (2007). A census of mitotic cancer genes: new insights into tumor cell biology and cancer therapy. *Carcinogenesis* 28, 899-912.
5. Jackson, J.R., Patrick, D.R., Dar, M.M., and Huang, P.S. (2007). Targeted anti-mitotic therapies: can we improve on tubulin agents? *Nat Rev Cancer* 7, 107-117.
6. Miglarese, M.R., and Carlson, R.O. (2006). Development of new cancer therapeutic agents targeting mitosis. *Expert Opin Investig Drugs* 15, 1411-1425.
7. Barr, F.A., Sillje, H.H., and Nigg, E.A. (2004). Polo-like kinases and the orchestration of cell division. *Nat Rev Mol Cell Biol* 5, 429-440.
8. Llamazares, S., Moreira, A., Tavares, A., Girdham, C., Spruce, B.A., Gonzalez, C., Karess, R.E., Glover, D.M., and Sunkel, C.E. (1991). polo encodes a protein kinase homolog required for mitosis in *Drosophila*. *Genes Dev* 5, 2153-2165.
9. Sunkel, C.E., and Glover, D.M. (1988). polo, a mitotic mutant of *Drosophila* displaying abnormal spindle poles. *J Cell Sci* 89 ( Pt 1), 25-38.
10. Golsteyn, R.M., Schultz, S.J., Bartek, J., Ziemiecki, A., Ried, T., and Nigg, E.A. (1994). Cell cycle analysis and chromosomal localization of human Plk1, a putative homologue of the mitotic kinases *Drosophila* polo and *Saccharomyces cerevisiae* Cdc5. *J Cell Sci* 107 ( Pt 6), 1509-1517.
11. Liby, K., Wu, H., Ouyang, B., Wu, S., Chen, J., and Dai, W. (2001). Identification of the human homologue of the early-growth response gene Snk, encoding a serum-inducible kinase. *DNA Seq* 11, 527-533.
12. Ma, S., Liu, M.A., Yuan, Y.L., and Erikson, R.L. (2003). The Serum-Inducible Protein Kinase Snk Is a G(1) Phase Polo-Like Kinase That Is Inhibited by the Calcium- and Integrin-Binding Protein CIB. *Mol Cancer Res* 1, 376-384.

13. Simmons, D.L., Neel, B.G., Stevens, R., Evett, G., and Erikson, R.L. (1992). Identification of an early-growth-response gene encoding a novel putative protein kinase. *Mol Cell Biol* 12, 4164-4169.
14. Bahassi el, M., Conn, C.W., Myer, D.L., Hennigan, R.F., McGowan, C.H., Sanchez, Y., and Stambrook, P.J. (2002). Mammalian Polo-like kinase 3 (Plk3) is a multifunctional protein involved in stress response pathways. *Oncogene* 21, 6633-6640.
15. Donohue, P.J., Alberts, G.F., Guo, Y., and Winkles, J.A. (1995). Identification by targeted differential display of an immediate early gene encoding a putative serine/threonine kinase. *J Biol Chem* 270, 10351-10357.
16. Xie, S., Wu, H., Wang, Q., Cogswell, J.P., Husain, I., Conn, C., Stambrook, P., Jhanwar-Uniyal, M., and Dai, W. (2001). Plk3 functionally links DNA damage to cell cycle arrest and apoptosis at least in part via the p53 pathway. *J Biol Chem* 276, 43305-43312.
17. Xie, S., Wu, H., Wang, Q., Kunicki, J., Thomas, R.O., Hollingsworth, R.E., Cogswell, J., and Dai, W. (2002). Genotoxic stress-induced activation of Plk3 is partly mediated by Chk2. *Cell Cycle* 1, 424-429.
18. Burns, T.F., Fei, P., Scata, K.A., Dicker, D.T., and El-Deiry, W.S. (2003). Silencing of the novel p53 target gene Snk/Plk2 leads to mitotic catastrophe in paclitaxel (taxol)-exposed cells. *Mol Cell Biol* 23, 5556-5571.
19. Conn, C.W., Hennigan, R.F., Dai, W., Sanchez, Y., and Stambrook, P.J. (2000). Incomplete cytokinesis and induction of apoptosis by overexpression of the mammalian polo-like kinase, Plk3. *Cancer Res* 60, 6826-6831.
20. Xie, S., Wang, Q., Ruan, Q., Liu, T., Jhanwar-Uniyal, M., Guan, K., and Dai, W. (2004). MEK1-induced Golgi dynamics during cell cycle progression is partly mediated by Polo-like kinase-3. *Oncogene* 23, 3822-3829.
21. Ruan, Q., Wang, Q., Xie, S., Fang, Y., Darzynkiewicz, Z., Guan, K., Jhanwar-Uniyal, M., and Dai, W. (2004). Polo-like kinase 3 is Golgi localized and involved in regulating Golgi fragmentation during the cell cycle. *Exp Cell Res* 294, 51-59.
22. Wang, Q., Xie, S., Chen, J., Fukasawa, K., Naik, U., Traganos, F., Darzynkiewicz, Z., Jhanwar-Uniyal, M., and Dai, W. (2002). Cell cycle arrest and apoptosis induced by human Polo-like kinase 3 is mediated through perturbation of microtubule integrity. *Mol Cell Biol* 22, 3450-3459.
23. Pak, D.T., and Sheng, M. (2003). Targeted protein degradation and synapse remodeling by an inducible protein kinase. *Science* 302, 1368-1373.

24. Kauselmann, G., Weiler, M., Wulff, P., Jessberger, S., Konietzko, U., Scafidi, J., Staubli, U., Bereiter-Hahn, J., Strebhardt, K., and Kuhl, D. (1999). The polo-like protein kinases Fnk and Snk associate with a Ca(2+)- and integrin-binding protein and are regulated dynamically with synaptic plasticity. *Embo J* 18, 5528-5539.
25. Dewitte, W., and Murray, J.A. (2003). The plant cell cycle. *Annu Rev Plant Biol* 54, 235-264.
26. Leung, G.C., Hudson, J.W., Kozarova, A., Davidson, A., Dennis, J.W., and Sicheri, F. (2002). The Sak polo-box comprises a structural domain sufficient for mitotic subcellular localization. *Nat Struct Biol* 9, 719-724.
27. Hudson, J.W., Chen, L., Fode, C., Binkert, C., and Dennis, J.W. (2000). Sak kinase gene structure and transcriptional regulation. *Gene* 241, 65-73.
28. Hudson, J.W., Kozarova, A., Cheung, P., Macmillan, J.C., Swallow, C.J., Cross, J.C., and Dennis, J.W. (2001). Late mitotic failure in mice lacking Sak, a polo-like kinase. *Curr Biol* 11, 441-446.
29. Lee, K.S., Grenfell, T.Z., Yarm, F.R., and Erikson, R.L. (1998). Mutation of the polo-box disrupts localization and mitotic functions of the mammalian polo kinase Plk. *Proc Natl Acad Sci U S A* 95, 9301-9306.
30. Logarinho, E., and Sunkel, C.E. (1998). The Drosophila POLO kinase localises to multiple compartments of the mitotic apparatus and is required for the phosphorylation of MPM2 reactive epitopes. *J Cell Sci* 111 ( Pt 19), 2897-2909.
31. Moutinho-Santos, T., Sampaio, P., Amorim, I., Costa, M., and Sunkel, C.E. (1999). In vivo localisation of the mitotic POLO kinase shows a highly dynamic association with the mitotic apparatus during early embryogenesis in Drosophila. *Biol Cell* 91, 585-596.
32. Qian, Y.W., Erikson, E., Li, C., and Maller, J.L. (1998). Activated polo-like kinase Plx1 is required at multiple points during mitosis in *Xenopus laevis*. *Mol Cell Biol* 18, 4262-4271.
33. Qian, Y.W., Erikson, E., and Maller, J.L. (1999). Mitotic effects of a constitutively active mutant of the *Xenopus* polo-like kinase Plx1. *Mol Cell Biol* 19, 8625-8632.
34. Shirayama, M., Zachariae, W., Ciosk, R., and Nasmyth, K. (1998). The Polo-like kinase Cdc5p and the WD-repeat protein Cdc20p/fizzy are regulators and substrates of the anaphase promoting complex in *Saccharomyces cerevisiae*. *Embo J* 17, 1336-1349.

35. Lane, H.A., and Nigg, E.A. (1996). Antibody microinjection reveals an essential role for human polo-like kinase 1 (Plk1) in the functional maturation of mitotic centrosomes. *J Cell Biol* *135*, 1701-1713.
36. do Carmo Avides, M., Tavares, A., and Glover, D.M. (2001). Polo kinase and Asp are needed to promote the mitotic organizing activity of centrosomes. *Nat Cell Biol* *3*, 421-424.
37. Glover, D.M., Hagan, I.M., and Tavares, A.A. (1998). Polo-like kinases: a team that plays throughout mitosis. *Genes Dev* *12*, 3777-3787.
38. Golsteyn, R.M., Mundt, K.E., Fry, A.M., and Nigg, E.A. (1995). Cell cycle regulation of the activity and subcellular localization of Plk1, a human protein kinase implicated in mitotic spindle function. *J Cell Biol* *129*, 1617-1628.
39. Lee, K.S., Yuan, Y.L., Kuriyama, R., and Erikson, R.L. (1995). Plk is an M-phase-specific protein kinase and interacts with a kinesin-like protein, CHO1/MKLP-1. *Mol Cell Biol* *15*, 7143-7151.
40. Song, S., Grenfell, T.Z., Garfield, S., Erikson, R.L., and Lee, K.S. (2000). Essential function of the polo box of Cdc5 in subcellular localization and induction of cytokinetic structures. *Mol Cell Biol* *20*, 286-298.
41. Sakchaisri, K., Asano, S., Yu, L.R., Shulewitz, M.J., Park, C.J., Park, J.E., Cho, Y.W., Veenstra, T.D., Thorner, J., and Lee, K.S. (2004). Coupling morphogenesis to mitotic entry. *Proc Natl Acad Sci U S A* *101*, 4124-4129.
42. Song, S., and Lee, K.S. (2001). A novel function of *Saccharomyces cerevisiae* CDC5 in cytokinesis. *J Cell Biol* *152*, 451-469.
43. Seong, Y.S., Kamijo, K., Lee, J.S., Fernandez, E., Kuriyama, R., Miki, T., and Lee, K.S. (2002). A spindle checkpoint arrest and a cytokinesis failure by the dominant-negative polo-box domain of Plk1 in U-2 OS cells. *J Biol Chem* *277*, 32282-32293.
44. Elia, A.E., Cantley, L.C., and Yaffe, M.B. (2003). Proteomic screen finds pSer/pThr-binding domain localizing Plk1 to mitotic substrates. *Science* *299*, 1228-1231.
45. Elia, A.E., Rellos, P., Haire, L.F., Chao, J.W., Ivins, F.J., Hoepker, K., Mohammad, D., Cantley, L.C., Smerdon, S.J., and Yaffe, M.B. (2003). The molecular basis for phosphodependent substrate targeting and regulation of Plks by the Polo-box domain. *Cell* *115*, 83-95.
46. Scott, M.P., and Miller, W.T. (2000). A peptide model system for processive phosphorylation by Src family kinases. *Biochemistry* *39*, 14531-14537.



47. Mayer, B.J., Hirai, H., and Sakai, R. (1995). Evidence that SH2 domains promote processive phosphorylation by protein-tyrosine kinases. *Curr Biol* 5, 296-305.
48. Pellicena, P., and Miller, W.T. (2002). Coupling kinase activation to substrate recognition in SRC-family tyrosine kinases. *Front Biosci* 7, d256-267.
49. Frame, S., and Cohen, P. (2001). GSK3 takes centre stage more than 20 years after its discovery. *Biochem J* 359, 1-16.
50. Toyoshima-Morimoto, F., Taniguchi, E., and Nishida, E. (2002). Plk1 promotes nuclear translocation of human Cdc25C during prophase. *EMBO Rep* 3, 341-348.
51. Lin, H.R., Ting, N.S., Qin, J., and Lee, W.H. (2003). M phase-specific phosphorylation of BRCA2 by Polo-like kinase 1 correlates with the dissociation of the BRCA2-P/CAF complex. *J Biol Chem* 278, 35979-35987.
52. Nakajima, H., Toyoshima-Morimoto, F., Taniguchi, E., and Nishida, E. (2003). Identification of a consensus motif for Plk (Polo-like kinase) phosphorylation reveals Myt1 as a Plk1 substrate. *J Biol Chem* 278, 25277-25280.
53. Jackman, M., Lindon, C., Nigg, E.A., and Pines, J. (2003). Active cyclin B1-Cdk1 first appears on centrosomes in prophase. *Nat Cell Biol* 5, 143-148.
54. Toyoshima-Morimoto, F., Taniguchi, E., Shinya, N., Iwamatsu, A., and Nishida, E. (2001). Polo-like kinase 1 phosphorylates cyclin B1 and targets it to the nucleus during prophase. *Nature* 410, 215-220.
55. Yuan, J., Eckerdt, F., Bereiter-Hahn, J., Kurunci-Csacsco, E., Kaufmann, M., and Strebhardt, K. (2002). Cooperative phosphorylation including the activity of polo-like kinase 1 regulates the subcellular localization of cyclin B1. *Oncogene* 21, 8282-8292.
56. Zhou, T., Aumais, J.P., Liu, X., Yu-Lee, L.Y., and Erikson, R.L. (2003). A role for Plk1 phosphorylation of NudC in cytokinesis. *Dev Cell* 5, 127-138.
57. Casenghi, M., Meraldi, P., Weinhart, U., Duncan, P.I., Korner, R., and Nigg, E.A. (2003). Polo-like kinase 1 regulates Nlp, a centrosome protein involved in microtubule nucleation. *Dev Cell* 5, 113-125.
58. Yarm, F.R. (2002). Plk phosphorylation regulates the microtubule-stabilizing protein TCTP. *Mol Cell Biol* 22, 6209-6221.
59. Liu, X., Zhou, T., Kuriyama, R., and Erikson, R.L. (2004). Molecular interactions of Polo-like-kinase 1 with the mitotic kinesin-like protein CHO1/MKLP-1. *J Cell Sci* 117, 3233-3246.

60. Neef, R., Preisinger, C., Sutcliffe, J., Kopajtich, R., Nigg, E.A., Mayer, T.U., and Barr, F.A. (2003). Phosphorylation of mitotic kinesin-like protein 2 by polo-like kinase 1 is required for cytokinesis. *J Cell Biol* *162*, 863-875.
61. Lin, C.Y., Madsen, M.L., Yarm, F.R., Jang, Y.J., Liu, X., and Erikson, R.L. (2000). Peripheral Golgi protein GRASP65 is a target of mitotic polo-like kinase (Plk) and Cdc2. *Proc Natl Acad Sci U S A* *97*, 12589-12594.
62. Sutterlin, C., Lin, C.Y., Feng, Y., Ferris, D.K., Erikson, R.L., and Malhotra, V. (2001). Polo-like kinase is required for the fragmentation of pericentriolar Golgi stacks during mitosis. *Proc Natl Acad Sci U S A* *98*, 9128-9132.
63. Watanabe, N., Arai, H., Nishihara, Y., Taniguchi, M., Hunter, T., and Osada, H. (2004). M-phase kinases induce phospho-dependent ubiquitination of somatic Wee1 by SCFbeta-TrCP. *Proc Natl Acad Sci U S A* *101*, 4419-4424.
64. Kumagai, A., and Dunphy, W.G. (1996). Purification and molecular cloning of Plx1, a Cdc25-regulatory kinase from *Xenopus* egg extracts. *Science* *273*, 1377-1380.
65. Moshe, Y., Boulaire, J., Pagano, M., and Hershko, A. (2004). Role of Polo-like kinase in the degradation of early mitotic inhibitor 1, a regulator of the anaphase promoting complex/cyclosome. *Proc Natl Acad Sci U S A* *101*, 7937-7942.
66. Kumagai, A., and Dunphy, W.G. (2000). Claspin, a novel protein required for the activation of Chk1 during a DNA replication checkpoint response in *Xenopus* egg extracts. *Mol Cell* *6*, 839-849.
67. Yoo, H.Y., Kumagai, A., Shevchenko, A., and Dunphy, W.G. (2004). Adaptation of a DNA replication checkpoint response depends upon inactivation of Claspin by the Polo-like kinase. *Cell* *117*, 575-588.
68. Golan, A., Yudkovsky, Y., and Hershko, A. (2002). The cyclin-ubiquitin ligase activity of cyclosome/APC is jointly activated by protein kinases Cdk1-cyclin B and Plk. *J Biol Chem* *277*, 15552-15557.
69. May, K.M., Reynolds, N., Cullen, C.F., Yanagida, M., and Ohkura, H. (2002). Polo boxes and Cut23 (Apc8) mediate an interaction between polo kinase and the anaphase-promoting complex for fission yeast mitosis. *J Cell Biol* *156*, 23-28.
70. Wolf, G., Elez, R., Doermer, A., Holtrich, U., Ackermann, H., Stutte, H.J., Altmannsberger, H.M., Rubsamen-Waigmann, H., and Strebhardt, K. (1997). Prognostic significance of polo-like kinase (PLK) expression in non-small cell lung cancer. *Oncogene* *14*, 543-549.

71. Tokumitsu, Y., Mori, M., Tanaka, S., Akazawa, K., Nakano, S., and Niho, Y. (1999). Prognostic significance of polo-like kinase expression in esophageal carcinoma. *Int J Oncol* 15, 687-692.
72. Wolf, G., Hildenbrand, R., Schwar, C., Grobholz, R., Kaufmann, M., Stutte, H.J., Strebhardt, K., and Bleyl, U. (2000). Polo-like kinase: a novel marker of proliferation: correlation with estrogen-receptor expression in human breast cancer. *Pathol Res Pract* 196, 753-759.
73. Takai, N., Miyazaki, T., Fujisawa, K., Nasu, K., Hamanaka, R., and Miyakawa, I. (2001). Expression of polo-like kinase in ovarian cancer is associated with histological grade and clinical stage. *Cancer Lett* 164, 41-49.
74. Weichert, W., Denkert, C., Schmidt, M., Gekeler, V., Wolf, G., Kobel, M., Dietel, M., and Hauptmann, S. (2004). Polo-like kinase isoform expression is a prognostic factor in ovarian carcinoma. *Br J Cancer* 90, 815-821.
75. Weichert, W., Schmidt, M., Jacob, J., Gekeler, V., Langrehr, J., Neuhaus, P., Bahra, M., Denkert, C., Dietel, M., and Kristiansen, G. (2005). Overexpression of Polo-like kinase 1 is a common and early event in pancreatic cancer. *Pancreatology* 5, 259-265.
76. Gray, P.J., Jr., Bearss, D.J., Han, H., Nagle, R., Tsao, M.S., Dean, N., and Von Hoff, D.D. (2004). Identification of human polo-like kinase 1 as a potential therapeutic target in pancreatic cancer. *Mol Cancer Ther* 3, 641-646.
77. Knecht, R., Elez, R., Oechler, M., Solbach, C., von Ilberg, C., and Strebhardt, K. (1999). Prognostic significance of polo-like kinase (PLK) expression in squamous cell carcinomas of the head and neck. *Cancer Res* 59, 2794-2797.
78. Strebhardt, K., Kneisel, L., Linhart, C., Bernd, A., and Kaufmann, R. (2000). Prognostic value of pololike kinase expression in melanomas. *Jama* 283, 479-480.
79. Macmillan, J.C., Hudson, J.W., Bull, S., Dennis, J.W., and Swallow, C.J. (2001). Comparative expression of the mitotic regulators SAK and PLK in colorectal cancer. *Ann Surg Oncol* 8, 729-740.
80. Takahashi, T., Sano, B., Nagata, T., Kato, H., Sugiyama, Y., Kunieda, K., Kimura, M., Okano, Y., and Saji, S. (2003). Polo-like kinase 1 (PLK1) is overexpressed in primary colorectal cancers. *Cancer Sci* 94, 148-152.
81. Weichert, W., Schmidt, M., Gekeler, V., Denkert, C., Stephan, C., Jung, K., Loening, S., Dietel, M., and Kristiansen, G. (2004). Polo-like kinase 1 is overexpressed in prostate cancer and linked to higher tumor grades. *Prostate* 60, 240-245.

82. Yamada, S., Ohira, M., Horie, H., Ando, K., Takayasu, H., Suzuki, Y., Sugano, S., Hirata, T., Goto, T., Matsunaga, T., Hiyama, E., Hayashi, Y., Ando, H., Suita, S., Kaneko, M., Sasaki, F., Hashizume, K., Ohnuma, N., and Nakagawara, A. (2004). Expression profiling and differential screening between hepatoblastomas and the corresponding normal livers: identification of high expression of the PLK1 oncogene as a poor-prognostic indicator of hepatoblastomas. *Oncogene* *23*, 5901-5911.
83. Ito, Y., Miyoshi, E., Sasaki, N., Kakudo, K., Yoshida, H., Tomoda, C., Uruno, T., Takamura, Y., Miya, A., Kobayashi, K., Matsuzuka, F., Matsuura, N., Kuma, K., and Miyauchi, A. (2004). Polo-like kinase 1 overexpression is an early event in the progression of papillary carcinoma. *Br J Cancer* *90*, 414-418.
84. Weichert, W., Kristiansen, G., Schmidt, M., Gekeler, V., Noske, A., Niesporek, S., Dietel, M., and Denkert, C. (2005). Polo-like kinase 1 expression is a prognostic factor in human colon cancer. *World J Gastroenterol* *11*, 5644-5650.
85. Kneisel, L., Strebhardt, K., Bernd, A., Wolter, M., Binder, A., and Kaufmann, R. (2002). Expression of polo-like kinase (PLK1) in thin melanomas: a novel marker of metastatic disease. *J Cutan Pathol* *29*, 354-358.
86. Simizu, S., and Osada, H. (2000). Mutations in the Plk gene lead to instability of Plk protein in human tumour cell lines. *Nat Cell Biol* *2*, 852-854.
87. Smith, M.R., Wilson, M.L., Hamanaka, R., Chase, D., Kung, H., Longo, D.L., and Ferris, D.K. (1997). Malignant transformation of mammalian cells initiated by constitutive expression of the polo-like kinase. *Biochem Biophys Res Commun* *234*, 397-405.
88. van Vugt, M.A., van de Weerd, B.C., Vader, G., Janssen, H., Calafat, J., Klompmaaker, R., Wolthuis, R.M., and Medema, R.H. (2004). Polo-like kinase-1 is required for bipolar spindle formation but is dispensable for anaphase promoting complex/Cdc20 activation and initiation of cytokinesis. *J Biol Chem* *279*, 36841-36854.
89. Elez, R., Piiper, A., Kronenberger, B., Kock, M., Brendel, M., Hermann, E., Pliquett, U., Neumann, E., and Zeuzem, S. (2003). Tumor regression by combination antisense therapy against Plk1 and Bcl-2. *Oncogene* *22*, 69-80.
90. Spankuch-Schmitt, B., Wolf, G., Solbach, C., Loibl, S., Knecht, R., Stegmüller, M., von Minckwitz, G., Kaufmann, M., and Strebhardt, K. (2002). Downregulation of human polo-like kinase activity by antisense oligonucleotides induces growth inhibition in cancer cells. *Oncogene* *21*, 3162-3171.
91. Liu, X., and Erikson, R.L. (2003). Polo-like kinase (Plk)1 depletion induces apoptosis in cancer cells. *Proc Natl Acad Sci U S A* *100*, 5789-5794.

92. Liu, X., Lei, M., and Erikson, R.L. (2006). Normal cells, but not cancer cells, survive severe Plk1 depletion. *Mol Cell Biol* *26*, 2093-2108.
93. Nogawa, M., Yuasa, T., Kimura, S., Tanaka, M., Kuroda, J., Sato, K., Yokota, A., Segawa, H., Toda, Y., Kageyama, S., Yoshiki, T., Okada, Y., and Maekawa, T. (2005). Intravesical administration of small interfering RNA targeting PLK-1 successfully prevents the growth of bladder cancer. *J Clin Invest* *115*, 978-985.
94. Stevenson, C.S., Capper, E.A., Roshak, A.K., Marquez, B., Eichman, C., Jackson, J.R., Mattern, M., Gerwick, W.H., Jacobs, R.S., and Marshall, L.A. (2002). The identification and characterization of the marine natural product scytonemin as a novel antiproliferative pharmacophore. *J Pharmacol Exp Ther* *303*, 858-866.
95. Stevenson, C.S., Capper, E.A., Roshak, A.K., Marquez, B., Grace, K., Gerwick, W.H., Jacobs, R.S., and Marshall, L.A. (2002). Scytonemin--a marine natural product inhibitor of kinases key in hyperproliferative inflammatory diseases. *Inflamm Res* *51*, 112-114.
96. Liu, Y., Shreder, K.R., Gai, W., Corral, S., Ferris, D.K., and Rosenblum, J.S. (2005). Wortmannin, a widely used phosphoinositide 3-kinase inhibitor, also potently inhibits mammalian polo-like kinase. *Chem Biol* *12*, 99-107.
97. Steegmaier, M., Hoffmann, M., Baum, A., Lenart, P., Petronczki, M., Krssak, M., Gurtler, U., Garin-Chesa, P., Lieb, S., Quant, J., Grauert, M., Adolf, G.R., Kraut, N., Peters, J.M., and Rettig, W.J. (2007). BI 2536, a potent and selective inhibitor of polo-like kinase 1, inhibits tumor growth in vivo. *Curr Biol* *17*, 316-322.
98. Uckun, F.M., Dibirdik, I., Qazi, S., Vassilev, A., Ma, H., Mao, C., Benyumov, A., and Emami, K.H. (2007). Anti-breast cancer activity of LFM-A13, a potent inhibitor of Polo-like kinase (PLK). *Bioorg Med Chem* *15*, 800-814.
99. Lansing, T.J., McConnell, R.T., Duckett, D.R., Spehar, G.M., Knick, V.B., Hassler, D.F., Noro, N., Furuta, M., Emmitte, K.A., Gilmer, T.M., Mook, R.A., Jr., and Cheung, M. (2007). In vitro biological activity of a novel small-molecule inhibitor of polo-like kinase 1. *Mol Cancer Ther* *6*, 450-459.
100. Watanabe, N., Arai, H., Iwasaki, J., Shiina, M., Ogata, K., Hunter, T., and Osada, H. (2005). Cyclin-dependent kinase (CDK) phosphorylation destabilizes somatic Wee1 via multiple pathways. *Proc Natl Acad Sci U S A* *102*, 11663-11668.
101. Petretti, C., Savoian, M., Montembault, E., Glover, D.M., Prigent, C., and Giet, R. (2006). The PITSLRE/CDK11p58 protein kinase promotes centrosome maturation and bipolar spindle formation. *EMBO Rep* *7*, 418-424.

102. Wilker, E.W., van Vugt, M.A., Artim, S.A., Huang, P.H., Petersen, C.P., Reinhardt, H.C., Feng, Y., Sharp, P.A., Sonenberg, N., White, F.M., and Yaffe, M.B. (2007). 14-3-3sigma controls mitotic translation to facilitate cytokinesis. *Nature* *446*, 329-332.
103. Hu, D., Valentine, M., Kidd, V.J., and Lahti, J.M. (2007). CDK11p58 is required for the maintenance of sister chromatid cohesion. *J Cell Sci* *120*, 2424-2434.
104. Borysov, S.I., Cheng, A.W., and Guadagno, T.M. (2006). B-Raf is critical for MAPK activation during mitosis and is regulated in an M phase-dependent manner in *Xenopus* egg extracts. *J Biol Chem* *281*, 22586-22596.
105. Zhang, W.L., Huitorel, P., Glass, R., Fernandez-Serra, M., Arnone, M.I., Chiri, S., Picard, A., and Ciapa, B. (2005). A MAPK pathway is involved in the control of mitosis after fertilization of the sea urchin egg. *Dev Biol* *282*, 192-206.
106. Zhang, W.L., Huitorel, P., Geneviere, A.M., Chiri, S., and Ciapa, B. (2006). Inactivation of MAPK in mature oocytes triggers progression into mitosis via a Ca<sup>2+</sup>-dependent pathway but without completion of S phase. *J Cell Sci* *119*, 3491-3501.
107. MacCorkle, R.A., and Tan, T.H. (2004). Inhibition of JNK2 disrupts anaphase and produces aneuploidy in mammalian cells. *J Biol Chem* *279*, 40112-40121.
108. Neef, R., Gruneberg, U., Kopajtich, R., Li, X., Nigg, E.A., Sillje, H., and Barr, F.A. (2007). Choice of Plk1 docking partners during mitosis and cytokinesis is controlled by the activation state of Cdk1. *Nat Cell Biol* *9*, 436-444.
109. Kang, Y.H., Park, J.E., Yu, L.R., Soung, N.K., Yun, S.M., Bang, J.K., Seong, Y.S., Yu, H., Garfield, S., Veenstra, T.D., and Lee, K.S. (2006). Self-regulated Plk1 recruitment to kinetochores by the Plk1-PBIP1 interaction is critical for proper chromosome segregation. *Mol Cell* *24*, 409-422.
110. Irniger, S. (2002). Cyclin destruction in mitosis: a crucial task of Cdc20. *FEBS Lett* *532*, 7-11.
111. Fu, C., Yan, F., Wu, F., Wu, Q., Whittaker, J., Hu, H., Hu, R., and Yao, X. (2007). Mitotic phosphorylation of PRC1 at Thr470 is required for PRC1 oligomerization and proper central spindle organization. *Cell Res* *17*, 449-457.
112. Hansen, D.V., Loktev, A.V., Ban, K.H., and Jackson, P.K. (2004). Plk1 regulates activation of the anaphase promoting complex by phosphorylating and triggering SCFbetaTrCP-dependent destruction of the APC Inhibitor Emi1. *Mol Biol Cell* *15*, 5623-5634.

113. De Luca, M., Lavia, P., and Guarguaglini, G. (2006). A functional interplay between Aurora-A, Plk1 and TPX2 at spindle poles: Plk1 controls centrosomal localization of Aurora-A and TPX2 spindle association. *Cell Cycle* 5, 296-303.
114. Goto, H., Kiyono, T., Tomono, Y., Kawajiri, A., Urano, T., Furukawa, K., Nigg, E.A., and Inagaki, M. (2006). Complex formation of Plk1 and INCENP required for metaphase-anaphase transition. *Nat Cell Biol* 8, 180-187.
115. Cheeseman, I.M., Anderson, S., Jwa, M., Green, E.M., Kang, J., Yates, J.R., 3rd, Chan, C.S., Drubin, D.G., and Barnes, G. (2002). Phospho-regulation of kinetochore-microtubule attachments by the Aurora kinase Ipl1p. *Cell* 111, 163-172.
116. Honda, R., Korner, R., and Nigg, E.A. (2003). Exploring the functional interactions between Aurora B, INCENP, and survivin in mitosis. *Mol Biol Cell* 14, 3325-3341.
117. Fu, J., Bian, M., Jiang, Q., and Zhang, C. (2007). Roles of Aurora kinases in mitosis and tumorigenesis. *Mol Cancer Res* 5, 1-10.
118. Rancati, G., Crispo, V., Lucchini, G., and Piatti, S. (2005). Mad3/BubR1 phosphorylation during spindle checkpoint activation depends on both Polo and Aurora kinases in budding yeast. *Cell Cycle* 4, 972-980.
119. Goto, H., Yasui, Y., Kawajiri, A., Nigg, E.A., Terada, Y., Tatsuka, M., Nagata, K., and Inagaki, M. (2003). Aurora-B regulates the cleavage furrow-specific vimentin phosphorylation in the cytokinetic process. *J Biol Chem* 278, 8526-8530.
120. Yamaguchi, T., Goto, H., Yokoyama, T., Sillje, H., Hanisch, A., Uldschmid, A., Takai, Y., Oguri, T., Nigg, E.A., and Inagaki, M. (2005). Phosphorylation by Cdk1 induces Plk1-mediated vimentin phosphorylation during mitosis. *J Cell Biol* 171, 431-436.
121. Guse, A., Mishima, M., and Glotzer, M. (2005). Phosphorylation of ZEN-4/MKLP1 by aurora B regulates completion of cytokinesis. *Curr Biol* 15, 778-786.
122. O'Connell, M.J., Krien, M.J., and Hunter, T. (2003). Never say never. The NIMA-related protein kinases in mitotic control. *Trends Cell Biol* 13, 221-228.
123. Rapley, J., Baxter, J.E., Blot, J., Wattam, S.L., Casenghi, M., Meraldi, P., Nigg, E.A., and Fry, A.M. (2005). Coordinate regulation of the mother centriole component nlp by nek2 and plk1 protein kinases. *Mol Cell Biol* 25, 1309-1324.
124. Roig, J., Groen, A., Caldwell, J., and Avruch, J. (2005). Active Nerccl1 protein kinase concentrates at centrosomes early in mitosis and is necessary for proper spindle assembly. *Mol Biol Cell* 16, 4827-4840.

125. Roig, J., Mikhailov, A., Belham, C., and Avruch, J. (2002). Nercc1, a mammalian NIMA-family kinase, binds the Ran GTPase and regulates mitotic progression. *Genes Dev* 16, 1640-1658.
126. Belham, C., Roig, J., Caldwell, J.A., Aoyama, Y., Kemp, B.E., Comb, M., and Avruch, J. (2003). A mitotic cascade of NIMA family kinases. Nercc1/Nek9 activates the Nek6 and Nek7 kinases. *J Biol Chem* 278, 34897-34909.
127. Yabuta, N., Okada, N., Ito, A., Hosomi, T., Nishihara, S., Sasayama, Y., Fujimori, A., Okuzaki, D., Zhao, H., Ikawa, M., Okabe, M., and Nojima, H. (2007). Lats2 is an essential mitotic regulator required for the coordination of cell division. *J Biol Chem*.
128. Abe, Y., Ohsugi, M., Haraguchi, K., Fujimoto, J., and Yamamoto, T. (2006). LATS2-Ajuba complex regulates gamma-tubulin recruitment to centrosomes and spindle organization during mitosis. *FEBS Lett* 580, 782-788.
129. Toji, S., Yabuta, N., Hosomi, T., Nishihara, S., Kobayashi, T., Suzuki, S., Tamai, K., and Nojima, H. (2004). The centrosomal protein Lats2 is a phosphorylation target of Aurora-A kinase. *Genes Cells* 9, 383-397.
130. Aylon, Y., Michael, D., Shmueli, A., Yabuta, N., Nojima, H., and Oren, M. (2006). A positive feedback loop between the p53 and Lats2 tumor suppressors prevents tetraploidization. *Genes Dev* 20, 2687-2700.
131. Yang, X., Yu, K., Hao, Y., Li, D.M., Stewart, R., Insogna, K.L., and Xu, T. (2004). LATS1 tumour suppressor affects cytokinesis by inhibiting LIMK1. *Nat Cell Biol* 6, 609-617.
132. Morisaki, T., Hirota, T., Iida, S., Marumoto, T., Hara, T., Nishiyama, Y., Kawasuzi, M., Hiraoka, T., Mimori, T., Araki, N., Izawa, I., Inagaki, M., and Saya, H. (2002). WARTS tumor suppressor is phosphorylated by Cdc2/cyclin B at spindle poles during mitosis. *FEBS Lett* 529, 319-324.
133. Nishiyama, Y., Hirota, T., Morisaki, T., Hara, T., Marumoto, T., Iida, S., Makino, K., Yamamoto, H., Hiraoka, T., Kitamura, N., and Saya, H. (1999). A human homolog of Drosophila warts tumor suppressor, h-warts, localized to mitotic apparatus and specifically phosphorylated during mitosis. *FEBS Lett* 459, 159-165.
134. Sumi, T., Matsumoto, K., and Nakamura, T. (2002). Mitosis-dependent phosphorylation and activation of LIM-kinase 1. *Biochem Biophys Res Commun* 290, 1315-1320.



135. Wakefield, J.G., Stephens, D.J., and Tavaré, J.M. (2003). A role for glycogen synthase kinase-3 in mitotic spindle dynamics and chromosome alignment. *J Cell Sci* *116*, 637-646.
136. Acevedo, N., Wang, X., Dunn, R.L., and Smith, G.D. (2007). Glycogen synthase kinase-3 regulation of chromatin segregation and cytokinesis in mouse preimplantation embryos. *Mol Reprod Dev* *74*, 178-188.
137. Yeh, T.Y., Sbodio, J.I., and Chi, N.W. (2006). Mitotic phosphorylation of tankyrase, a PARP that promotes spindle assembly, by GSK3. *Biochem Biophys Res Commun* *350*, 574-579.
138. Dai, J., Sultan, S., Taylor, S.S., and Higgins, J.M. (2005). The kinase haspin is required for mitotic histone H3 Thr 3 phosphorylation and normal metaphase chromosome alignment. *Genes Dev* *19*, 472-488.
139. Dai, J., Sullivan, B.A., and Higgins, J.M. (2006). Regulation of mitotic chromosome cohesion by Haspin and Aurora B. *Dev Cell* *11*, 741-750.
140. Nandi, A.K., Ford, T., Fleksher, D., Neuman, B., and Rapoport, A.P. (2007). Attenuation of DNA damage checkpoint by PBK, a novel mitotic kinase, involves protein-protein interaction with tumor suppressor p53. *Biochem Biophys Res Commun* *358*, 181-188.
141. Abe, Y., Takeuchi, T., Kagawa-Miki, L., Ueda, N., Shigemoto, K., Yasukawa, M., and Kito, K. (2007). A Mitotic Kinase TOPK Enhances Cdk1/cyclin B1-dependent Phosphorylation of PRC1 and Promotes Cytokinesis. *J Mol Biol* *370*, 231-245.
142. Cardenas, M.E., Dang, Q., Glover, C.V., and Gasser, S.M. (1992). Casein kinase II phosphorylates the eukaryote-specific C-terminal domain of topoisomerase II in vivo. *Embo J* *11*, 1785-1796.
143. Escargueil, A.E., Plisov, S.Y., Filhol, O., Cochet, C., and Larsen, A.K. (2000). Mitotic phosphorylation of DNA topoisomerase II alpha by protein kinase CK2 creates the MPM-2 phosphoepitope on Ser-1469. *J Biol Chem* *275*, 34710-34718.
144. Chung, E., and Chen, R.H. (2003). Phosphorylation of Cdc20 is required for its inhibition by the spindle checkpoint. *Nat Cell Biol* *5*, 748-753.
145. Horne, M.M., and Guadagno, T.M. (2003). A requirement for MAP kinase in the assembly and maintenance of the mitotic spindle. *J Cell Biol* *161*, 1021-1028.

146. Roberts, E.C., Shapiro, P.S., Nahreini, T.S., Pages, G., Pouyssegur, J., and Ahn, N.G. (2002). Distinct cell cycle timing requirements for extracellular signal-regulated kinase and phosphoinositide 3-kinase signaling pathways in somatic cell mitosis. *Mol Cell Biol* 22, 7226-7241.
147. Zhao, Z.S., Lim, J.P., Ng, Y.W., Lim, L., and Manser, E. (2005). The GIT-associated kinase PAK targets to the centrosome and regulates Aurora-A. *Mol Cell* 20, 237-249.
148. Thiel, D.A., Reeder, M.K., Pfaff, A., Coleman, T.R., Sells, M.A., and Chernoff, J. (2002). Cell cycle-regulated phosphorylation of p21-activated kinase 1. *Curr Biol* 12, 1227-1232.
149. Banerjee, M., Worth, D., Prowse, D.M., and Nikolic, M. (2002). Pak1 phosphorylation on t212 affects microtubules in cells undergoing mitosis. *Curr Biol* 12, 1233-1239.
150. D'Aquino, K.E., Monje-Casas, F., Paulson, J., Reiser, V., Charles, G.M., Lai, L., Shokat, K.M., and Amon, A. (2005). The protein kinase Kin4 inhibits exit from mitosis in response to spindle position defects. *Mol Cell* 19, 223-234.
151. Pereira, G., and Schiebel, E. (2005). Kin4 kinase delays mitotic exit in response to spindle alignment defects. *Mol Cell* 19, 209-221.
152. Draviam, V.M., Stegmeier, F., Nalepa, G., Sowa, M.E., Chen, J., Liang, A., Hannon, G.J., Sorger, P.K., Harper, J.W., and Elledge, S.J. (2007). A functional genomic screen identifies a role for TAO1 kinase in spindle-checkpoint signalling. *Nat Cell Biol* 9, 556-564.
153. Musacchio, A., and Salmon, E.D. (2007). The spindle-assembly checkpoint in space and time. *Nat Rev Mol Cell Biol* 8, 379-393.
154. Bardin, A.J., and Amon, A. (2001). Men and sin: what's the difference? *Nat Rev Mol Cell Biol* 2, 815-826.
155. Nelson, B., Kurischko, C., Horecka, J., Mody, M., Nair, P., Pratt, L., Zougman, A., McBroom, L.D., Hughes, T.R., Boone, C., and Luca, F.C. (2003). RAM: a conserved signaling network that regulates Ace2p transcriptional activity and polarized morphogenesis. *Mol Biol Cell* 14, 3782-3803.
156. Matsumura, F. (2005). Regulation of myosin II during cytokinesis in higher eukaryotes. *Trends Cell Biol* 15, 371-377.
157. Lee, K.S., Park, J.E., Asano, S., and Park, C.J. (2005). Yeast polo-like kinases: functionally conserved multitask mitotic regulators. *Oncogene* 24, 217-229.

158. van de Weerd, B.C., and Medema, R.H. (2006). Polo-like kinases: a team in control of the division. *Cell Cycle* *5*, 853-864.
159. Fisk, H.A., Mattison, C.P., and Winey, M. (2003). Human Mps1 protein kinase is required for centrosome duplication and normal mitotic progression. *Proc Natl Acad Sci U S A* *100*, 14875-14880.
160. Stucke, V.M., Sillje, H.H., Arnaud, L., and Nigg, E.A. (2002). Human Mps1 kinase is required for the spindle assembly checkpoint but not for centrosome duplication. *Embo J* *21*, 1723-1732.
161. Leng, M., Chan, D.W., Luo, H., Zhu, C., Qin, J., and Wang, Y. (2006). MPS1-dependent mitotic BLM phosphorylation is important for chromosome stability. *Proc Natl Acad Sci U S A* *103*, 11485-11490.
162. Hansen, D.V., Tung, J.J., and Jackson, P.K. (2006). CaMKII and polo-like kinase 1 sequentially phosphorylate the cytostatic factor Emi2/XErp1 to trigger its destruction and meiotic exit. *Proc Natl Acad Sci U S A* *103*, 608-613.
163. Schmidt, A., Duncan, P.I., Rauh, N.R., Sauer, G., Fry, A.M., Nigg, E.A., and Mayer, T.U. (2005). *Xenopus* polo-like kinase Plx1 regulates XErp1, a novel inhibitor of APC/C activity. *Genes Dev* *19*, 502-513.
164. Liu, J., and Maller, J.L. (2005). Calcium elevation at fertilization coordinates phosphorylation of XErp1/Emi2 by Plx1 and CaMK II to release metaphase arrest by cytostatic factor. *Curr Biol* *15*, 1458-1468.
165. Bartek, J., and Lukas, J. (2007). DNA damage checkpoints: from initiation to recovery or adaptation. *Curr Opin Cell Biol* *19*, 238-245.
166. Toczyski, D.P., Galgoczy, D.J., and Hartwell, L.H. (1997). CDC5 and CKII control adaptation to the yeast DNA damage checkpoint. *Cell* *90*, 1097-1106.
167. Gewurz, B.E., and Harper, J.W. (2006). DNA-damage control: Claspin destruction turns off the checkpoint. *Curr Biol* *16*, R932-934.
168. Syljuasen, R.G., Jensen, S., Bartek, J., and Lukas, J. (2006). Adaptation to the ionizing radiation-induced G2 checkpoint occurs in human cells and depends on checkpoint kinase 1 and Polo-like kinase 1 kinases. *Cancer Res* *66*, 10253-10257.
169. van Vugt, M.A., Bras, A., and Medema, R.H. (2004). Polo-like kinase-1 controls recovery from a G2 DNA damage-induced arrest in mammalian cells. *Mol Cell* *15*, 799-811.

170. Mailand, N., Bekker-Jensen, S., Bartek, J., and Lukas, J. (2006). Destruction of Claspin by SCFbetaTrCP restrains Chk1 activation and facilitates recovery from genotoxic stress. *Mol Cell* 23, 307-318.
171. Peschiaroli, A., Dorrello, N.V., Guardavaccaro, D., Venere, M., Halazonetis, T., Sherman, N.E., and Pagano, M. (2006). SCFbetaTrCP-mediated degradation of Claspin regulates recovery from the DNA replication checkpoint response. *Mol Cell* 23, 319-329.
172. Mamely, I., van Vugt, M.A., Smits, V.A., Semple, J.I., Lemmens, B., Perrakis, A., Medema, R.H., and Freire, R. (2006). Polo-like kinase-1 controls proteasome-dependent degradation of Claspin during checkpoint recovery. *Curr Biol* 16, 1950-1955.
173. Tsvetkov, L.M., Tsekova, R.T., Xu, X., and Stern, D.F. (2005). The Plk1 Polo box domain mediates a cell cycle and DNA damage regulated interaction with Chk2. *Cell Cycle* 4, 609-617.
174. Tsvetkov, L., Xu, X., Li, J., and Stern, D.F. (2003). Polo-like kinase 1 and Chk2 interact and co-localize to centrosomes and the midbody. *J Biol Chem* 278, 8468-8475.
175. Zhou, B.B., and Elledge, S.J. (2000). The DNA damage response: putting checkpoints in perspective. *Nature* 408, 433-439.
176. Reinhardt, H.C., Aslanian, A.S., Lees, J.A., and Yaffe, M.B. (2007). p53-deficient cells rely on ATM- and ATR-mediated checkpoint signaling through the p38MAPK/MK2 pathway for survival after DNA damage. *Cancer Cell* 11, 175-189.
177. Aumais, J.P., Williams, S.N., Luo, W., Nishino, M., Caldwell, K.A., Caldwell, G.A., Lin, S.H., and Yu-Lee, L.Y. (2003). Role for NudC, a dynein-associated nuclear movement protein, in mitosis and cytokinesis. *J Cell Sci* 116, 1991-2003.
178. Nishino, M., Kurasawa, Y., Evans, R., Lin, S.H., Brinkley, B.R., and Yu-Lee, L.Y. (2006). NudC is required for Plk1 targeting to the kinetochore and chromosome congression. *Curr Biol* 16, 1414-1421.
179. Li, J., Meyer, A.N., and Donoghue, D.J. (1995). Requirement for phosphorylation of cyclin B1 for *Xenopus* oocyte maturation. *Mol Biol Cell* 6, 1111-1124.
180. Qi, W., Tang, Z., and Yu, H. (2006). Phosphorylation- and polo-box-dependent binding of Plk1 to Bub1 is required for the kinetochore localization of Plk1. *Mol Biol Cell* 17, 3705-3716.

181. Niiya, F., Tatsumoto, T., Lee, K.S., and Miki, T. (2006). Phosphorylation of the cytokinesis regulator ECT2 at G2/M phase stimulates association of the mitotic kinase Plk1 and accumulation of GTP-bound RhoA. *Oncogene* 25, 827-837.
182. Baumann, C., Korner, R., Hofmann, K., and Nigg, E.A. (2007). PICH, a centromere-associated SNF2 family ATPase, is regulated by Plk1 and required for the spindle checkpoint. *Cell* 128, 101-114.
183. Zhang, Y., Tian, Y., Chen, Q., Chen, D., Zhai, Z., and Shu, H.B. (2007). TTDN1 is a Plk1-interacting protein involved in maintenance of cell cycle integrity. *Cell Mol Life Sci* 64, 632-640.
184. Litvak, V., Argov, R., Dahan, N., Ramachandran, S., Amarilio, R., Shainskaya, A., and Lev, S. (2004). Mitotic phosphorylation of the peripheral Golgi protein Nir2 by Cdk1 provides a docking mechanism for Plk1 and affects cytokinesis completion. *Mol Cell* 14, 319-330.
185. Sumara, I., Vorlaufer, E., Stukenberg, P.T., Kelm, O., Redemann, N., Nigg, E.A., and Peters, J.M. (2002). The dissociation of cohesin from chromosomes in prophase is regulated by Polo-like kinase. *Mol Cell* 9, 515-525.
186. Cheng, L., Hunke, L., and Hardy, C.F. (1998). Cell cycle regulation of the *Saccharomyces cerevisiae* polo-like kinase *cdc5p*. *Mol Cell Biol* 18, 7360-7370.
187. Hardy, C.F., and Pautz, A. (1996). A novel role for *Cdc5p* in DNA replication. *Mol Cell Biol* 16, 6775-6782.
188. Hamanaka, R., Smith, M.R., O'Connor, P.M., Maloid, S., Mihalic, K., Spivak, J.L., Longo, D.L., and Ferris, D.K. (1995). Polo-like kinase is a cell cycle-regulated kinase activated during mitosis. *J Biol Chem* 270, 21086-21091.
189. Charles, J.F., Jaspersen, S.L., Tinker-Kulberg, R.L., Hwang, L., Szidon, A., and Morgan, D.O. (1998). The Polo-related kinase *Cdc5* activates and is destroyed by the mitotic cyclin destruction machinery in *S. cerevisiae*. *Curr Biol* 8, 497-507.
190. Lindon, C., and Pines, J. (2004). Ordered proteolysis in anaphase inactivates Plk1 to contribute to proper mitotic exit in human cells. *J Cell Biol* 164, 233-241.
191. Mundt, K.E., Golsteyn, R.M., Lane, H.A., and Nigg, E.A. (1997). On the regulation and function of human polo-like kinase 1 (PLK1): effects of overexpression on cell cycle progression. *Biochem Biophys Res Commun* 239, 377-385.
192. Tavares, A.A., Glover, D.M., and Sunkel, C.E. (1996). The conserved mitotic kinase polo is regulated by phosphorylation and has preferred microtubule-associated substrates in *Drosophila* embryo extracts. *Embo J* 15, 4873-4883.

193. Mortensen, E.M., Haas, W., Gygi, M., Gygi, S.P., and Kellogg, D.R. (2005). Cdc28-dependent regulation of the Cdc5/Polo kinase. *Curr Biol* *15*, 2033-2037.
194. Lee, K.S., and Erikson, R.L. (1997). Plk is a functional homolog of *Saccharomyces cerevisiae* Cdc5, and elevated Plk activity induces multiple septation structures. *Mol Cell Biol* *17*, 3408-3417.
195. Jang, Y.J., Ma, S., Terada, Y., and Erikson, R.L. (2002). Phosphorylation of threonine 210 and the role of serine 137 in the regulation of mammalian polo-like kinase. *J Biol Chem* *277*, 44115-44120.
196. MacIver, F.H., Tanaka, K., Robertson, A.M., and Hagan, I.M. (2003). Physical and functional interactions between polo kinase and the spindle pole component Cut12 regulate mitotic commitment in *S. pombe*. *Genes Dev* *17*, 1507-1523.
197. Kelm, O., Wind, M., Lehmann, W.D., and Nigg, E.A. (2002). Cell cycle-regulated phosphorylation of the *Xenopus* polo-like kinase Plx1. *J Biol Chem* *277*, 25247-25256.
198. Johnson, L.N., Noble, M.E., and Owen, D.J. (1996). Active and inactive protein kinases: structural basis for regulation. *Cell* *85*, 149-158.
199. Tsvetkov, L., and Stern, D.F. (2005). Phosphorylation of Plk1 at S137 and T210 is inhibited in response to DNA damage. *Cell Cycle* *4*, 166-171.
200. van de Weerd, B.C., van Vugt, M.A., Lindon, C., Kauw, J.J., Rozendaal, M.J., Klompmaker, R., Wolthuis, R.M., and Medema, R.H. (2005). Uncoupling anaphase-promoting complex/cyclosome activity from spindle assembly checkpoint control by deregulating polo-like kinase 1. *Mol Cell Biol* *25*, 2031-2044.
201. Qian, Y.W., Erikson, E., and Maller, J.L. (1998). Purification and cloning of a protein kinase that phosphorylates and activates the polo-like kinase Plx1. *Science* *282*, 1701-1704.
202. Erikson, E., Haystead, T.A., Qian, Y.W., and Maller, J.L. (2004). A feedback loop in the polo-like kinase activation pathway. *J Biol Chem*.
203. Ellinger-Ziegelbauer, H., Karasuyama, H., Yamada, E., Tsujikawa, K., Todokoro, K., and Nishida, E. (2000). Ste20-like kinase (SLK), a regulatory kinase for polo-like kinase (Plk) during the G2/M transition in somatic cells. *Genes Cells* *5*, 491-498.
204. Walter, S.A., Cutler, R.E., Jr., Martinez, R., Gishizky, M., and Hill, R.J. (2003). Stk10, a new member of the polo-like kinase kinase family highly expressed in hematopoietic tissue. *J Biol Chem* *278*, 18221-18228.

205. Wind, M., Kelm, O., Nigg, E.A., and Lehmann, W.D. (2002). Identification of phosphorylation sites in the polo-like kinases Plx1 and Plk1 by a novel strategy based on element and electrospray high resolution mass spectrometry. *Proteomics* 2, 1516-1523.
206. Petersen, J., and Hagan, I.M. (2005). Polo kinase links the stress pathway to cell cycle control and tip growth in fission yeast. *Nature* 435, 507-512.
207. Karaiskou, A., Cayla, X., Haccard, O., Jesus, C., and Ozon, R. (1998). MPF amplification in *Xenopus* oocyte extracts depends on a two-step activation of cdc25 phosphatase. *Exp Cell Res* 244, 491-500.
208. Karaiskou, A., Jesus, C., Brassac, T., and Ozon, R. (1999). Phosphatase 2A and polo kinase, two antagonistic regulators of cdc25 activation and MPF auto-amplification. *J Cell Sci* 112 (Pt 21), 3747-3756.
209. Qian, Y.W., Erikson, E., Taieb, F.E., and Maller, J.L. (2001). The polo-like kinase Plx1 is required for activation of the phosphatase Cdc25C and cyclin B-Cdc2 in *Xenopus* oocytes. *Mol Biol Cell* 12, 1791-1799.
210. Abrieu, A., Brassac, T., Galas, S., Fisher, D., Labbe, J.C., and Doree, M. (1998). The Polo-like kinase Plx1 is a component of the MPF amplification loop at the G2/M-phase transition of the cell cycle in *Xenopus* eggs. *J Cell Sci* 111 (Pt 12), 1751-1757.
211. Alexandru, G., Uhlmann, F., Mechtler, K., Poupart, M.A., and Nasmyth, K. (2001). Phosphorylation of the cohesin subunit Scc1 by Polo/Cdc5 kinase regulates sister chromatid separation in yeast. *Cell* 105, 459-472.
212. Ohkura, H., Hagan, I.M., and Glover, D.M. (1995). The conserved *Schizosaccharomyces pombe* kinase plo1, required to form a bipolar spindle, the actin ring, and septum, can drive septum formation in G1 and G2 cells. *Genes Dev* 9, 1059-1073.
213. Adams, R.R., Tavares, A.A., Salzberg, A., Bellen, H.J., and Glover, D.M. (1998). pavarotti encodes a kinesin-like protein required to organize the central spindle and contractile ring for cytokinesis. *Genes Dev* 12, 1483-1494.
214. Carmena, M., Riparbelli, M.G., Minestrini, G., Tavares, A.M., Adams, R., Callaini, G., and Glover, D.M. (1998). *Drosophila* polo kinase is required for cytokinesis. *J Cell Biol* 143, 659-671.
215. Descombes, P., and Nigg, E.A. (1998). The polo-like kinase Plx1 is required for M phase exit and destruction of mitotic regulators in *Xenopus* egg extracts. *Embo J* 17, 1328-1335.

216. Kotani, S., Tugendreich, S., Fujii, M., Jorgensen, P.M., Watanabe, N., Hoog, C., Hieter, P., and Todokoro, K. (1998). PKA and MPF-activated polo-like kinase regulate anaphase-promoting complex activity and mitosis progression. *Mol Cell* *1*, 371-380.
217. Kumagai, A., and Dunphy, W.G. (1992). Regulation of the cdc25 protein during the cell cycle in *Xenopus* extracts. *Cell* *70*, 139-151.
218. Hoffmann, I., Clarke, P.R., Marcote, M.J., Karsenti, E., and Draetta, G. (1993). Phosphorylation and activation of human cdc25-C by cdc2--cyclin B and its involvement in the self-amplification of MPF at mitosis. *Embo J* *12*, 53-63.
219. Izumi, T., and Maller, J.L. (1995). Phosphorylation and activation of the *Xenopus* Cdc25 phosphatase in the absence of Cdc2 and Cdk2 kinase activity. *Mol Biol Cell* *6*, 215-226.
220. Izumi, T., and Maller, J.L. (1993). Elimination of cdc2 phosphorylation sites in the cdc25 phosphatase blocks initiation of M-phase. *Mol Biol Cell* *4*, 1337-1350.
221. Gabrielli, B.G., De Souza, C.P., Tonks, I.D., Clark, J.M., Hayward, N.K., and Ellem, K.A. (1996). Cytoplasmic accumulation of cdc25B phosphatase in mitosis triggers centrosomal microtubule nucleation in HeLa cells. *J Cell Sci* *109 (Pt 5)*, 1081-1093.
222. Lammer, C., Wagerer, S., Saffrich, R., Mertens, D., Ansorge, W., and Hoffmann, I. (1998). The cdc25B phosphatase is essential for the G2/M phase transition in human cells. *J Cell Sci* *111 (Pt 16)*, 2445-2453.
223. Budde, P.P., Kumagai, A., Dunphy, W.G., and Heald, R. (2001). Regulation of Op18 during spindle assembly in *Xenopus* egg extracts. *J Cell Biol* *153*, 149-158.
224. Feng, Y., Hodge, D.R., Palmieri, G., Chase, D.L., Longo, D.L., and Ferris, D.K. (1999). Association of polo-like kinase with alpha-, beta- and gamma-tubulins in a stable complex. *Biochem J* *339 (Pt 2)*, 435-442.
225. Lenart, P., Petronczki, M., Steegmaier, M., Di Fiore, B., Lipp, J.J., Hoffmann, M., Rettig, W.J., Kraut, N., and Peters, J.M. (2007). The small-molecule inhibitor BI 2536 reveals novel insights into mitotic roles of polo-like kinase 1. *Curr Biol* *17*, 304-315.
226. McInnes, C., Mazumdar, A., Mezna, M., Meades, C., Midgley, C., Scaerou, F., Carpenter, L., Mackenzie, M., Taylor, P., Walkinshaw, M., Fischer, P.M., and Glover, D. (2006). Inhibitors of Polo-like kinase reveal roles in spindle-pole maintenance. *Nat Chem Biol* *2*, 608-617.



227. Peters, U., Cherian, J., Kim, J.H., Kwok, B.H., and Kapoor, T.M. (2006). Probing cell-division phenotype space and Polo-like kinase function using small molecules. *Nat Chem Biol* 2, 618-626.
228. Ahonen, L.J., Kallio, M.J., Daum, J.R., Bolton, M., Manke, I.A., Yaffe, M.B., Stukenberg, P.T., and Gorbsky, G.J. (2005). Polo-like kinase 1 creates the tension-sensing 3F3/2 phosphoepitope and modulates the association of spindle-checkpoint proteins at kinetochores. *Curr Biol* 15, 1078-1089.
229. van Vugt, M.A., Smits, V.A., Klompmaker, R., and Medema, R.H. (2001). Inhibition of Polo-like kinase-1 by DNA damage occurs in an ATM- or ATR-dependent fashion. *J Biol Chem* 276, 41656-41660.
230. Kraft, C., Herzog, F., Gieffers, C., Mechtler, K., Hagting, A., Pines, J., and Peters, J.M. (2003). Mitotic regulation of the human anaphase-promoting complex by phosphorylation. *Embo J* 22, 6598-6609.
231. Hornig, N.C., and Uhlmann, F. (2004). Preferential cleavage of chromatin-bound cohesin after targeted phosphorylation by Polo-like kinase. *Embo J* 23, 3144-3153.
232. Clarke, A.S., Tang, T.T., Ooi, D.L., and Orr-Weaver, T.L. (2005). POLO kinase regulates the Drosophila centromere cohesion protein MEI-S332. *Dev Cell* 8, 53-64.
233. Stegmeier, F., and Amon, A. (2004). Closing mitosis: the functions of the Cdc14 phosphatase and its regulation. *Annu Rev Genet* 38, 203-232.
234. Stegmeier, F., Visintin, R., and Amon, A. (2002). Separase, polo kinase, the kinetochore protein Slk19, and Spo12 function in a network that controls Cdc14 localization during early anaphase. *Cell* 108, 207-220.
235. Yuan, K., Hu, H., Guo, Z., Fu, G., Shaw, A.P., Hu, R., and Yao, X. (2007). Phospho-regulation of HSCDC14A by polo-like kinase 1 is essential for mitotic progression. *J Biol Chem*.
236. Zhang, H., Shi, X., Paddon, H., Hampong, M., Dai, W., and Pelech, S. (2004). B23/nucleophosmin serine 4 phosphorylation mediates mitotic functions of polo-like kinase 1. *J Biol Chem* 279, 35726-35734.
237. Fabbro, M., Zhou, B.B., Takahashi, M., Sarcevic, B., Lal, P., Graham, M.E., Gabrielli, B.G., Robinson, P.J., Nigg, E.A., Ono, Y., and Khanna, K.K. (2005). Cdk1/Erk2- and Plk1-dependent phosphorylation of a centrosome protein, Cep55, is required for its recruitment to midbody and cytokinesis. *Dev Cell* 9, 477-488.
238. Lee, B.H., and Amon, A. (2003). Role of Polo-like kinase CDC5 in programming meiosis I chromosome segregation. *Science* 300, 482-486.

239. Brar, G.A., Kiburz, B.M., Zhang, Y., Kim, J.E., White, F., and Amon, A. (2006). Rec8 phosphorylation and recombination promote the step-wise loss of cohesins in meiosis. *Nature* 441, 532-536.
240. Smits, V.A., Klompmaker, R., Arnaud, L., Rijksen, G., Nigg, E.A., and Medema, R.H. (2000). Polo-like kinase-1 is a target of the DNA damage checkpoint. *Nat Cell Biol* 2, 672-676.
241. Lee, S.E., Moore, J.K., Holmes, A., Umezumi, K., Kolodner, R.D., and Haber, J.E. (1998). *Saccharomyces* Ku70, mre11/rad50 and RPA proteins regulate adaptation to G2/M arrest after DNA damage. *Cell* 94, 399-409.
242. Pellicioli, A., Lee, S.E., Lucca, C., Foiani, M., and Haber, J.E. (2001). Regulation of *Saccharomyces* Rad53 checkpoint kinase during adaptation from DNA damage-induced G2/M arrest. *Mol Cell* 7, 293-300.
243. Lee, S.E., Pellicioli, A., Malkova, A., Foiani, M., and Haber, J.E. (2001). The *Saccharomyces* recombination protein Tid1p is required for adaptation from G2/M arrest induced by a double-strand break. *Curr Biol* 11, 1053-1057.
244. Shimizu-Yoshida, Y., Sugiyama, K., Rogounovitch, T., Ohtsuru, A., Namba, H., Saenko, V., and Yamashita, S. (2001). Radiation-inducible hSNK gene is transcriptionally regulated by p53 binding homology element in human thyroid cells. *Biochem Biophys Res Commun* 289, 491-498.
245. Ma, S., Charron, J., and Erikson, R.L. (2003). Role of Plk2 (Snk) in mouse development and cell proliferation. *Mol Cell Biol* 23, 6936-6943.
246. Warnke, S., Kemmler, S., Hames, R.S., Tsai, H.L., Hoffmann-Rohrer, U., Fry, A.M., and Hoffmann, I. (2004). Polo-like kinase-2 is required for centriole duplication in mammalian cells. *Curr Biol* 14, 1200-1207.
247. Chase, D., Feng, Y., Hanshew, B., Winkles, J.A., Longo, D.L., and Ferris, D.K. (1998). Expression and phosphorylation of fibroblast-growth-factor-inducible kinase (Fnk) during cell-cycle progression. *Biochem J* 333 ( Pt 3), 655-660.
248. Anger, M., Kues, W.A., Klima, J., Mielenz, M., Kubelka, M., Motlik, J., Esner, M., Dvorak, P., Carnwath, J.W., and Niemann, H. (2003). Cell cycle dependent expression of Plk1 in synchronized porcine fetal fibroblasts. *Mol Reprod Dev* 65, 245-253.
249. Li, B., Ouyang, B., Pan, H., Reissmann, P.T., Slamon, D.J., Arceci, R., Lu, L., and Dai, W. (1996). Prk, a cytokine-inducible human protein serine/threonine kinase whose expression appears to be down-regulated in lung carcinomas. *J Biol Chem* 271, 19402-19408.

250. Winkles, J.A., and Alberts, G.F. (2005). Differential regulation of polo-like kinase 1, 2, 3, and 4 gene expression in mammalian cells and tissues. *Oncogene* 24, 260-266.
251. Alberts, G.F., and Winkles, J.A. (2004). Murine FGF-inducible kinase is rapidly degraded via the nuclear ubiquitin-proteasome system when overexpressed in NIH 3T3 cells. *Cell Cycle* 3, 678-684.
252. Xie, S., Wang, Q., Wu, H., Cogswell, J., Lu, L., Jhanwar-Uniyal, M., and Dai, W. (2001). Reactive oxygen species-induced phosphorylation of p53 on serine 20 is mediated in part by polo-like kinase-3. *J Biol Chem* 276, 36194-36199.
253. Hirao, A., Kong, Y.Y., Matsuoka, S., Wakeham, A., Ruland, J., Yoshida, H., Liu, D., Elledge, S.J., and Mak, T.W. (2000). DNA damage-induced activation of p53 by the checkpoint kinase Chk2. *Science* 287, 1824-1827.
254. Shieh, S.Y., Ahn, J., Tamai, K., Taya, Y., and Prives, C. (2000). The human homologs of checkpoint kinases Chk1 and Cds1 (Chk2) phosphorylate p53 at multiple DNA damage-inducible sites. *Genes Dev* 14, 289-300.
255. Chehab, N.H., Malikzay, A., Appel, M., and Halazonetis, T.D. (2000). Chk2/hCds1 functions as a DNA damage checkpoint in G(1) by stabilizing p53. *Genes Dev* 14, 278-288.
256. O'Neill, T., Giarratani, L., Chen, P., Iyer, L., Lee, C.H., Bobiak, M., Kanai, F., Zhou, B.B., Chung, J.H., and Rathbun, G.A. (2002). Determination of substrate motifs for human Chk1 and hCds1/Chk2 by the oriented peptide library approach. *J Biol Chem* 277, 16102-16115.
257. Bahassi el, M., Hennigan, R.F., Myer, D.L., and Stambrook, P.J. (2004). Cdc25C phosphorylation on serine 191 by Plk3 promotes its nuclear translocation. *Oncogene* 23, 2658-2663.
258. Ouyang, B., Li, W., Pan, H., Meadows, J., Hoffmann, I., and Dai, W. (1999). The physical association and phosphorylation of Cdc25C protein phosphatase by Prk. *Oncogene* 18, 6029-6036.
259. Matsuoka, S., Huang, M., and Elledge, S.J. (1998). Linkage of ATM to cell cycle regulation by the Chk2 protein kinase. *Science* 282, 1893-1897.
260. Sanchez, Y., Wong, C., Thoma, R.S., Richman, R., Wu, Z., Piwnicka-Worms, H., and Elledge, S.J. (1997). Conservation of the Chk1 checkpoint pathway in mammals: linkage of DNA damage to Cdk regulation through Cdc25. *Science* 277, 1497-1501.

261. Holtrich, U., Wolf, G., Yuan, J., Bereiter-Hahn, J., Karn, T., Weiler, M., Kauselmann, G., Rehli, M., Andreesen, R., Kaufmann, M., Kuhl, D., and Strebhardt, K. (2000). Adhesion induced expression of the serine/threonine kinase Fnk in human macrophages. *Oncogene* 19, 4832-4839.
262. Dai, W., Li, Y., Ouyang, B., Pan, H., Reissmann, P., Li, J., Wiest, J., Stambrook, P., Gluckman, J.L., Noffsinger, A., and Bejarano, P. (2000). PRK, a cell cycle gene localized to 8p21, is downregulated in head and neck cancer. *Genes Chromosomes Cancer* 27, 332-336.
263. Ando, K., Ozaki, T., Yamamoto, H., Furuya, K., Hosoda, M., Hayashi, S., Fukuzawa, M., and Nakagawara, A. (2004). Polo-like kinase 1 (Plk1) inhibits p53 function by physical interaction and phosphorylation. *J Biol Chem* 279, 25549-25561.
264. Jiang, N., Wang, X., Jhanwar-Uniyal, M., Darzynkiewicz, Z., and Dai, W. (2006). Polo box domain of Plk3 functions as a centrosome localization signal, overexpression of which causes mitotic arrest, cytokinesis defects, and apoptosis. *J Biol Chem* 281, 10577-10582.
265. Zimmerman, W.C., and Erikson, R.L. (2007). Polo-like kinase 3 is required for entry into S phase. *Proc Natl Acad Sci U S A* 104, 1847-1852.
266. Fode, C., Binkert, C., and Dennis, J.W. (1996). Constitutive expression of murine Sak-a suppresses cell growth and induces multinucleation. *Mol Cell Biol* 16, 4665-4672.
267. Fode, C., Motro, B., Yousefi, S., Heffernan, M., and Dennis, J.W. (1994). Sak, a murine protein-serine/threonine kinase that is related to the Drosophila polo kinase and involved in cell proliferation. *Proc Natl Acad Sci U S A* 91, 6388-6392.
268. Li, J., Tan, M., Li, L., Pamarthy, D., Lawrence, T.S., and Sun, Y. (2005). SAK, a new polo-like kinase, is transcriptionally repressed by p53 and induces apoptosis upon RNAi silencing. *Neoplasia* 7, 312-323.
269. Ko, M.A., Rosario, C.O., Hudson, J.W., Kulkarni, S., Pollett, A., Dennis, J.W., and Swallow, C.J. (2005). Plk4 haploinsufficiency causes mitotic infidelity and carcinogenesis. *Nat Genet* 37, 883-888.
270. Bettencourt-Dias, M., Rodrigues-Martins, A., Carpenter, L., Riparbelli, M., Lehmann, L., Gatt, M.K., Carmo, N., Balloux, F., Callaini, G., and Glover, D.M. (2005). SAK/PLK4 is required for centriole duplication and flagella development. *Curr Biol* 15, 2199-2207.
271. Habedanck, R., Stierhof, Y.D., Wilkinson, C.J., and Nigg, E.A. (2005). The Polo kinase Plk4 functions in centriole duplication. *Nat Cell Biol* 7, 1140-1146.

272. Cheng, K.Y., Lowe, E.D., Sinclair, J., Nigg, E.A., and Johnson, L.N. (2003). The crystal structure of the human polo-like kinase-1 polo box domain and its phospho-peptide complex. *Embo J* 22, 5757-5768.
273. Garcia-Alvarez, B., de Carcer, G., Ibanez, S., Bragado-Nilsson, E., and Montoya, G. (2007). Molecular and structural basis of polo-like kinase 1 substrate recognition: Implications in centrosomal localization. *Proc Natl Acad Sci U S A* 104, 3107-3112.
274. Jang, Y.J., Lin, C.Y., Ma, S., and Erikson, R.L. (2002). Functional studies on the role of the C-terminal domain of mammalian polo-like kinase. *Proc Natl Acad Sci U S A* 99, 1984-1989.
275. Sicheri, F., Moarefi, I., and Kuriyan, J. (1997). Crystal structure of the Src family tyrosine kinase Hck. *Nature* 385, 602-609.
276. Xu, W., Doshi, A., Lei, M., Eck, M.J., and Harrison, S.C. (1999). Crystal structures of c-Src reveal features of its autoinhibitory mechanism. *Mol Cell* 3, 629-638.
277. Hof, P., Pluskey, S., Dhe-Paganon, S., Eck, M.J., and Shoelson, S.E. (1998). Crystal structure of the tyrosine phosphatase SHP-2. *Cell* 92, 441-450.
278. Kothe, M., Kohls, D., Low, S., Coli, R., Cheng, A.C., Jacques, S.L., Johnson, T.L., Lewis, C., Loh, C., Nonomiya, J., Sheils, A.L., Verdries, K.A., Wynn, T.A., Kuhn, C., and Ding, Y.H. (2007). Structure of the catalytic domain of human polo-like kinase 1. *Biochemistry* 46, 5960-5971.
279. Yang, J., Cron, P., Good, V.M., Thompson, V., Hemmings, B.A., and Barford, D. (2002). Crystal structure of an activated Akt/protein kinase B ternary complex with GSK3-peptide and AMP-PNP. *Nat Struct Biol* 9, 940-944.
280. Bossemeyer, D., Engh, R.A., Kinzel, V., Ponstingl, H., and Huber, R. (1993). Phosphotransferase and substrate binding mechanism of the cAMP-dependent protein kinase catalytic subunit from porcine heart as deduced from the 2.0 Å structure of the complex with Mn<sup>2+</sup> adenylyl imidodiphosphate and inhibitor peptide PKI(5-24). *Embo J* 12, 849-859.
281. Fabbro, D., Ruetz, S., Buchdunger, E., Cowan-Jacob, S.W., Fendrich, G., Liebetanz, J., Mestan, J., O'Reilly, T., Traxler, P., Chaudhuri, B., Fretz, H., Zimmermann, J., Meyer, T., Caravatti, G., Furet, P., and Manley, P.W. (2002). Protein kinases as targets for anticancer agents: from inhibitors to useful drugs. *Pharmacol Ther* 93, 79-98.
282. Noble, M.E., Endicott, J.A., and Johnson, L.N. (2004). Protein kinase inhibitors: insights into drug design from structure. *Science* 303, 1800-1805.

283. Stout, T.J., Foster, P.G., and Matthews, D.J. (2004). High-throughput structural biology in drug discovery: protein kinases. *Curr Pharm Des* 10, 1069-1082.
284. De Azevedo, W.F., Jr., Mueller-Dieckmann, H.J., Schulze-Gahmen, U., Worland, P.J., Sausville, E., and Kim, S.H. (1996). Structural basis for specificity and potency of a flavonoid inhibitor of human CDK2, a cell cycle kinase. *Proc Natl Acad Sci U S A* 93, 2735-2740.
285. Pargellis, C., Tong, L., Churchill, L., Cirillo, P.F., Gilmore, T., Graham, A.G., Grob, P.M., Hickey, E.R., Moss, N., Pav, S., and Regan, J. (2002). Inhibition of p38 MAP kinase by utilizing a novel allosteric binding site. *Nat Struct Biol* 9, 268-272.
286. Tong, L., Pav, S., White, D.M., Rogers, S., Crane, K.M., Cywin, C.L., Brown, M.L., and Pargellis, C.A. (1997). A highly specific inhibitor of human p38 MAP kinase binds in the ATP pocket. *Nat Struct Biol* 4, 311-316.
287. Schindler, T., Bornmann, W., Pellicena, P., Miller, W.T., Clarkson, B., and Kuriyan, J. (2000). Structural mechanism for STI-571 inhibition of abelson tyrosine kinase. *Science* 289, 1938-1942.
288. Takagi, M., Honmura, T., Watanabe, S., Yamaguchi, R., Nogawa, M., Nishimura, I., Katoh, F., Matsuda, M., and Hidaka, H. (2003). In vivo antitumor activity of a novel sulfonamide, HMN-214, against human tumor xenografts in mice and the spectrum of cytotoxicity of its active metabolite, HMN-176. *Invest New Drugs* 21, 387-399.
289. Garland, L.L., Taylor, C., Pilkington, D.L., Cohen, J.L., and Von Hoff, D.D. (2006). A phase I pharmacokinetic study of HMN-214, a novel oral stilbene derivative with polo-like kinase-1-interacting properties, in patients with advanced solid tumors. *Clin Cancer Res* 12, 5182-5189.
290. Thompson, J.D., Higgins, D.G., and Gibson, T.J. (1994). CLUSTAL W: improving the sensitivity of progressive multiple sequence alignment through sequence weighting, position-specific gap penalties and weight matrix choice. *Nucleic Acids Res* 22, 4673-4680.
291. Felsenstein, J. (1997). An alternating least squares approach to inferring phylogenies from pairwise distances. *Syst Biol* 46, 101-111.
292. Esnouf, R.M. (1997). An extensively modified version of MolScript that includes greatly enhanced coloring capabilities. *J Mol Graph Model* 15, 132-134, 112-133.
293. Merritt, E.A., and Murphy, M.E. (1994). Raster3D Version 2.0. A program for photorealistic molecular graphics. *Acta Crystallogr D Biol Crystallogr* 50, 869-873.

294. Hu, F., Wang, Y., Liu, D., Li, Y., Qin, J., and Elledge, S.J. (2001). Regulation of the Bub2/Bfa1 GAP complex by Cdc5 and cell cycle checkpoints. *Cell* *107*, 655-665.
295. Geymonat, M., Spanos, A., Walker, P.A., Johnston, L.H., and Sedgwick, S.G. (2003). In vitro regulation of budding yeast Bfa1/Bub2 GAP activity by Cdc5. *J Biol Chem* *278*, 14591-14594.
296. Lee, S.E., Jensen, S., Frenz, L.M., Johnson, A.L., Fesquet, D., and Johnston, L.H. (2001). The Bub2-dependent mitotic pathway in yeast acts every cell cycle and regulates cytokinesis. *J Cell Sci* *114*, 2345-2354.
297. Matsumura, S., Toyoshima, F., and Nishida, E. (2007). Polo-like kinase 1 facilitates chromosome alignment during prometaphase through BubR1. *J Biol Chem* *282*, 15217-15227.
298. Soung, N.K., Kang, Y.H., Kim, K., Kamijo, K., Yoon, H., Seong, Y.S., Kuo, Y.L., Miki, T., Kim, S.R., Kuriyama, R., Giam, C.Z., Ahn, C.H., and Lee, K.S. (2006). Requirement of hCenexin for proper mitotic functions of polo-like kinase 1 at the centrosomes. *Mol Cell Biol* *26*, 8316-8335.
299. Guarguaglini, G., Duncan, P.I., Stierhof, Y.D., Holmstrom, T., Duensing, S., and Nigg, E.A. (2005). The forkhead-associated domain protein Cep170 interacts with Polo-like kinase 1 and serves as a marker for mature centrioles. *Mol Biol Cell* *16*, 1095-1107.
300. Oshimori, N., Ohsugi, M., and Yamamoto, T. (2006). The Plk1 target Kizuna stabilizes mitotic centrosomes to ensure spindle bipolarity. *Nat Cell Biol* *8*, 1095-1101.
301. Stuermer, A., Hoehn, K., Faul, T., Auth, T., Brand, N., Kneissl, M., Putter, V., and Grummt, F. (2007). Mouse pre-replicative complex proteins colocalise and interact with the centrosome. *Eur J Cell Biol* *86*, 37-50.
302. Inoue, D., and Sagata, N. (2005). The Polo-like kinase Plx1 interacts with and inhibits Myt1 after fertilization of *Xenopus* eggs. *Embo J* *24*, 1057-1067.
303. Darieva, Z., Bulmer, R., Pic-Taylor, A., Doris, K.S., Geymonat, M., Sedgwick, S.G., Morgan, B.A., and Sharrocks, A.D. (2006). Polo kinase controls cell-cycle-dependent transcription by targeting a coactivator protein. *Nature* *444*, 494-498.
304. Azzam, R., Chen, S.L., Shou, W., Mah, A.S., Alexandru, G., Nasmyth, K., Annan, R.S., Carr, S.A., and Deshaies, R.J. (2004). Phosphorylation by cyclin B-Cdk underlies release of mitotic exit activator Cdc14 from the nucleolus. *Science* *305*, 516-519.

305. Visintin, R., Stegmeier, F., and Amon, A. (2003). The role of the polo kinase Cdc5 in controlling Cdc14 localization. *Mol Biol Cell* *14*, 4486-4498.
306. Shou, W., Azzam, R., Chen, S.L., Huddleston, M.J., Baskerville, C., Charbonneau, H., Annan, R.S., Carr, S.A., and Deshaies, R.J. (2002). Cdc5 influences phosphorylation of Net1 and disassembly of the RENT complex. *BMC Mol Biol* *3*, 3.
307. Loughrey Chen, S., Huddleston, M.J., Shou, W., Deshaies, R.J., Annan, R.S., and Carr, S.A. (2002). Mass spectrometry-based methods for phosphorylation site mapping of hyperphosphorylated proteins applied to Net1, a regulator of exit from mitosis in yeast. *Mol Cell Proteomics* *1*, 186-196.
308. Eckerdt, F., Yuan, J., Saxena, K., Martin, B., Kappel, S., Lindenau, C., Kramer, A., Naumann, S., Daum, S., Fischer, G., Dikic, I., Kaufmann, M., and Strebhardt, K. (2005). Polo-like kinase 1-mediated phosphorylation stabilizes Pin1 by inhibiting its ubiquitination in human cells. *J Biol Chem* *280*, 36575-36583.
309. Feng, Y., Yuan, J.H., Maloid, S.C., Fisher, R., Copeland, T.D., Longo, D.L., Conrads, T.P., Veenstra, T.D., Ferris, A., Hughes, S., Dimitrov, D.S., and Ferris, D.K. (2006). Polo-like kinase 1-mediated phosphorylation of the GTP-binding protein Ran is important for bipolar spindle formation. *Biochem Biophys Res Commun* *349*, 144-152.
310. Saigusa, K., Imoto, I., Tanikawa, C., Aoyagi, M., Ohno, K., Nakamura, Y., and Inazawa, J. (2007). RGC32, a novel p53-inducible gene, is located on centrosomes during mitosis and results in G2/M arrest. *Oncogene* *26*, 1110-1121.
311. Badea, T., Niculescu, F., Soane, L., Fosbrink, M., Sorana, H., Rus, V., Shin, M.L., and Rus, H. (2002). RGC-32 increases p34CDC2 kinase activity and entry of aortic smooth muscle cells into S-phase. *J Biol Chem* *277*, 502-508.



# Chapter Two

## **Proteomic Screen Defines the Polo-box Domain Interactome and Identifies Rock2 as a Plk1 Substrate**

Published: Drew M. Lowery, Karl Clauser, Majbrit Hjerrild, Dan Lim, Jes Alexander, Kazu Kishi, Steen Gammeltoft, Steven A. Carr, and Michael B. Yaffe.  
Proteomic Screen Defines Mitotic Polo-box Domain Interactome and Identifies Rho Kinase as a Plk1 Substrate in Cytokinesis. *EMBO* 26, 2007.

### Contributions:

Karl Clauser performed all mass spectrometry analysis and generated Tables 2.1 and 2.2 and figure 2.10 along with writing the appropriate methods sections. Majbrit Hjerrild and I performed the experiments in figures 2.1C-E, 2.2, 2.3, 2.8F, and 2.9 and wrote the initial draft of the manuscript. Dan Lim contributed to the initial experimental design as outlined in figure 2.1B and assisted in protein purification. Jes Alexander assisted with bioinformatic analysis and generated the random protein datasets that allowed the construction of figure 2.5. Kazu Kishi performed the localization experiment shown in figure 2.8E. Steven Carr provided intellectual support, helped design experiments, and provided mass spectrometry facilities. Mike helped design and analyze most of the experiments, re-wrote the manuscript with me, and provided intellectual support. All other work was performed by myself.

## **Abstract**

Polo-like kinase-1 (Plk1) phosphorylates a number of mitotic substrates, but the diversity of Plk1-dependent processes suggests the existence of additional targets. Plk1 contains a specialized phosphoserine-threonine binding domain, the Polo-box domain (PBD), postulated to target the kinase to its substrates. Using the specialized phosphoserine-threonine binding domain, the Polo-box domain (PBD), of Polo-like kinase-1 (Plk1) as an affinity capture agent, we performed a screen to define the mitotic Plk1-PBD interactome by mass spectrometry. We identified 622 proteins that showed phosphorylation-dependent mitosis-specific interactions, including proteins involved in well-established Plk1-regulated processes, and in processes not previously linked to Plk1 such as translational control, RNA processing, and vesicle transport. Many proteins identified in our screen play important roles in cytokinesis, where, in mammalian cells, the detailed mechanistic role of Plk1 remains poorly defined. We go on to characterize the mitosis-specific interaction of the Plk1-PBD with the cytokinesis effector kinase Rho-associated coiled-coiled domain-containing protein kinase 2 (Rock2), demonstrate that Rock2 is a Plk1 substrate, and show that Rock2 co-localizes with Plk1 during cytokinesis. Finally, we show that Plk1 and RhoA function together to maximally enhance Rock2 kinase activity in vitro and within cells, and implicate Plk1 as a central regulator of multiple pathways that synergistically converge to regulate actomyosin ring contraction during cleavage furrow ingression.

## Introduction

In eukaryotic cells, Polo-like kinase-1 (Plk1) and related orthologues perform a wide variety of essential functions during mitosis [1-3]. Levels of Plk1 peak in late G2 and early M, accompanied by dramatic changes in subcellular localization as cells transit through various mitotic stages [4]. During interphase and early prophase Plk1 resides primarily at the centrosome, where it facilitates centrosome maturation, separation, and microtubule nucleation during late prophase and prometaphase [5-7]. By metaphase, a fraction of Plk1 has relocated to the kinetochores, where it seems to be involved in regulating aspects of spindle checkpoint function and the metaphase-anaphase transition [8, 9]. During anaphase, Plk1 is concentrated in the spindle midzone, where it probably facilitates microtubule sliding, while following chromosome segregation, Plk1 remains in the central spindle and midbody, where it participates in ingression of the cleavage furrow [10, 11]. Particularly prominent cytokinetic phenotypes are observed in budding and fission yeast where mutations in the respective Plk1 orthologues, Cdc5 and Plo1, result in incomplete assembly of actomyosin and septin ring structures along with delayed and improper deposition of septal material [12, 13].

Although these and related mutational studies have provided many insights into Cdc5/Plo1 function in simple model organisms, the diversity of Plk1 functions in higher eukaryotes makes it difficult to comprehensively identify Plk1-regulated pathways or define the bulk of the Plk1 interactome using standard molecular genetics techniques. Separation of function alleles are hard to identify due to the presence of a single common binding pocket and substrate phosphorylation cleft shared by most, if not all substrates [14, 15]. Full genetic disruption of the drosophila Plk1 orthologue, polo, causes embryonic lethality [16], while full depletion of the Xenopus Plk1 orthologue, Plx1, prevents mitotic entry [17].

More recently, RNA interference has been used to examine the effect of Plk1 depletion in human cell lines, revealing a marked dependence of phenotype on the particular genetic background of the cell. In tumor derived cell lines depletion of Plk1 causes apoptosis along with mitotic catastrophe, making the delineation of specific Plk1 functions difficult [18, 19]. In other immortalized cell lines, depletion of Plk1 causes a

delay in mitotic entry with subsequent arrest at prometaphase, preventing analysis of later phenotypes without sensitization strategies to avoid activation of various mitotic checkpoints. If both the DNA damage and spindle checkpoints are bypassed, Plk1-depleted cells can complete an apparently normal mitosis, however chromosome segregation fails [20, 21]. In non-transformed cell lines, depletion of Plk1 causes only very minor cell cycle defects, although co-depletion of p53 mimics the cell death phenotypes seen in tumor derived cell lines [18]. The various Plk1-depletion phenotypes are complicated by varying degrees of Plk1 knockdown, since a 90% knockdown of Plk1 in HeLa cells can allow normal mitotic processes whereas a ~100% depletion completely blocks cell cycle progression [18, 22].

In an effort to more comprehensively elucidate the substrates and interacting proteins of Plk1, we pursued a biochemical/proteomic approach. All Polo-like kinases have a similar protein architecture including a N-terminal Ser/Thr kinase domain and a conserved C-terminal Polo-box domain (PBD) (Figure 2.1A). The PBD of Plks was previously identified in our lab as a pSer/pThr-binding module that specifically recognizes Ser-[pSer/pThr]-Pro/X motifs on peptides with low micromolar affinity (Elia et al., 2003a). Phospho-dependent ligand recognition by the PBD is necessary for targeting of Plk1 to specific substrates (i.e. processive phosphorylation) as well as for the dynamic re-localization of Plk1 to specific subcellular structures during mitosis where other Plk1 targets reside (i.e. distributive phosphorylation) [23]. We therefore performed affinity purification and mass spectrometry studies to identify Plk1 PBD-interacting proteins from U2OS cells at different stages of the cell cycle.

Our strategy was to define all putative interacting partners, and then select one particular sub-network to investigate in more detail at the molecular level. We identified approximately six hundred proteins that were members of phosphorylation-dependent Plk1 PBD interacting complexes. These proteins are known to be involved in a wide variety of mitotic processes, including processes not previously thought to be regulated by Plk1. We chose to focus on the roles of Plk1 in regulating cytokinesis. The requirement for Plk1 and its orthologues for proper initiation and completion of cytokinesis has been well established in unicellular organisms [24, 25] and drosophila [26], and several previously described PBD-associated proteins are known to play roles

in this process in mammalian cells [10, 11, 27], although exactly how Plk1 fits into the complete cytokinesis network is unclear. One of the major upstream regulators of cytokinesis is RhoA, which, together with its downstream targets, controls the formation and constriction of the actomyosin ring at the cleavage furrow [28]. The functions of Plk1 and Rho GTPases may be linked, since cytokinesis-specific GEFs for Rho were recently identified as Plk targets both in mammalian cells [29] and by our recent work in budding yeast [13].

We now report that Plk1 functions in multiple parallel overlapping pathways with RhoA, and directly interacts with a subset of critical effectors of RhoA. We demonstrate that Plk1 and RhoA synergize to maximally activate the cytokinetic protein kinase Rock2 *in vitro* and within cells, and that Plk1 and Rock2 interact directly *in vivo* in a phosphorylation-dependent mitosis-specific manner, with maximal co-localization at the midbody during cytokinesis.

## Results and Discussion

### **The Plk1 Polo-box domain shows mitosis-specific interactions with many proteins involved in diverse aspects of cell division.**

To identify potential targets of Plk1, we examined the ability of the isolated PBD to bind to proteins in a cell cycle-dependent manner. Recombinant Plk1 PBD was expressed in bacteria and purified to homogeneity (Figure 2.1C). We also purified a His-538 Ala/Lys-540 Met double mutant form of the PBD which does not bind to phosphorylated ligands [15] and therefore serves as an optimal negative control to reveal sticky non-specific interactions or phospho-independent protein-PBD interactions that might arise from high abundance. The wild type and mutant PBD proteins were cross-linked to sepharose CN-4B beads and used as an affinity matrix. Human osteosarcoma U2OS cells were arrested at the G1/S transition by a double thymidine block or arrested in mitosis by treatment with nocodazole. Cell cycle synchronization was verified by FACS (Figure 2.1D). Lysates from these two cell populations were prepared and equal amounts of total protein were applied to columns containing either the wild type or mutant PBD column. After extensive washing with a near neutral pH medium-salt buffer that is not expected to disrupt complexes, PBD-interacting proteins were eluted off the columns by competition with an optimal PBD binding phospho-peptide (YMQS-pT-PK) [30]. The recovered proteins were then separated by SDS-PAGE and visualized by SYPRO Ruby staining (Figure 2.1B top).

Both the wild type and mutant PBD bound very weakly, and with similar affinity, to a variety of proteins in the G1/S cell lysate. In marked contrast, the wild type PBD, but not the mutant PBD, showed very strong binding to a large number of proteins in the mitotic cell lysates (Figure 2.1E). The darkest band at 25kd is the PBD itself indicating that there is some leeching of the PBD from the column. These observations suggest that the Plk1 PBD can specifically interact with many mitotic proteins in a phospho-dependent manner. Furthermore, because Plk1 has been reported to interact with microtubules [31], we used nocodazole treatment to obtain the mitotically arrested cells, as this drug depolymerizes microtubules and should therefore minimize potential indirect interactions of the PBD with other microtubule-interacting proteins. The affinity-based

purification assay shown in Figure 2.1E could either isolate mitotic proteins that bound directly to the PBD, or proteins that were not themselves direct PBD-interactors but instead were components of larger PBD-associated complexes. The specificity of PBD binding was therefore investigated by Far-Western blotting. Many of the mitotic proteins captured with the wild type PBD were capable of direct interaction. In contrast, none of the proteins that were retained by the mutant PBD showed a strong detectable interaction with the wild type PBD in this assay (Figure 2.2A).

To examine the extent to which the binding of mitotic ligands to the PBD is dependent upon phosphorylation, nocodazole-arrested cell lysates were dephosphorylated with  $\lambda$ -phosphatase prior to the PBD pull down. As shown in Figure 2.2B, both the number of recovered ligands and intensity of ligand binding was greatly reduced after phosphatase treatment of the mitotic cell lysates. Next, to investigate if any of the Plk1 PBD-interacting proteins were also potential Plk1 substrates; the affinity purified proteins were incubated with a constitutively active mutant of full-length Plk1, Plk1-T210D, in the presence of  $^{32}\text{P}$ - $\gamma$ -ATP. As shown in Figure 2.2C, incubation with Plk1-T210D resulted in the direct phosphorylation of many of these PBD-interacting proteins. Taken together, the data in Figures 2.1 and 2.2 strongly support a model where the PBD facilitates the interaction of Plk1 with a wide range of mitotic targets that have undergone prior priming phosphorylation during mitosis, and indicates that a subset of the interacting proteins are themselves Plk1 substrates.

Liquid chromatography tandem mass spectrometry (LC/MS/MS) was used to identify the mitotic PBD-interacting proteins. Each lane of the gel from the nocodazole arrested cell lysates in Figure 2.1E was excised, cut into 12 pieces as indicated (Figure 2.1E), and subjected to in-gel digestion with trypsin. The extracted peptide mixtures were then separated using reverse phase HPLC, which was coupled to an LTQ-FT hybrid ion trap Fourier transform mass spectrometer for peptide identification (Figure 2.1B bottom), and the corresponding proteins identified by database searching. For each protein, the relative ratio of wild-type/mutant PBD-bound abundances was determined using the sum of the extracted ion current measured for each sequenced peptide precursor ion in the intervening MS scans of the LC/MS/MS chromatogram. Proteins were then categorized as being wild-type specific (peptide ions only present in the wild-type PBD eluents),

wild-type enriched (peptide ions present at >20-fold intensity in the wild-type PBD eluents compared to the mutant PBD eluents), and non-specific (peptide ions present at  $\leq$ 20-fold intensity in the wild-type versus mutant PBD eluents). In total, we identified 622 distinct proteins that were at least 20-fold more abundant in the wild type PBD pull down compared to the mutant H538A/K540M PBD pull down and were considered to be potential PBD interaction partners (Table 2.1). All proteins were characterized according to GO categories defining their molecular function [32] (Figure 2.4A).

We selected a small random subset of proteins identified in the mass spectrometry-based screen for further validation based on the availability of antibodies: Lamin A, Cofilin, MCMs, the protein kinase CK2 alpha, myosin phosphatase targeting subunit 1 (MYPT) and Rock2. Pull downs from mitotic lysates followed by immunoblotting confirmed that all these proteins preferentially interacted with wild type PBD compared to the mutant PBD (Figure 2.3A). The cell cycle-dependent interaction of the selected proteins with the PBD was investigated by performing in vitro pulldown assays with lysates from double thymidine blocked (G1) and nocodazole-treated (M) cells. As shown in Figure 2.3B, interactions between the PBD and all of these proteins were mitotic specific. To investigate the requirement for phosphorylation, mitotic lysates were treated with  $\lambda$ -protein phosphatase prior to PBD pull-downs and immunoblotting for. In each case, interaction of these proteins with the PBD was either eliminated or substantially reduced following phosphatase treatment (Figure 2.3C). Thus, all six of the interactions tested were mitotic phosphorylation-dependent interactions.

The complete set of proteins identified in our PBD interactome included proteins previously demonstrated to associate with Plk1 such as MCMs [33], septins [25], anillin, (shown to be a Plk1 substrate in vitro; [34]), and members of the 20S proteasome complex [35]. Some other known endogenous Plk1 interacting proteins, such as Cdc25C, were not identified in this screen, likely as a result of our nocodazole treatment/spindle checkpoint arrest strategy, which appeared to enrich for late mitotic targets. Plk1 targets such as Cdc25C and Wee1 are thought to play a role in entry into mitosis, and thus might not bind to Plk1 once mitosis is underway. Additional Plk1 interactors such as Bub3 are only expected to be engaged after the spindle checkpoint is extinguished.



Most of the PBD interacting proteins identified in this study have not been previously reported. Many of those proteins participate in a broad range of cellular functions that show distinct changes during mitosis; transcription, translation, splicing and metabolism (Figure 2.4A). Intriguingly, although protein synthesis is necessary for mitotic entry and progression, the overall rate of protein synthesis in mitotic cells has been reported to be markedly decreased to 25-30% of the rate seen in interphase cells [36]. At the same time the synthesis of a number of proteins including c-myc is enhanced during mitosis [37]. Transcription and mRNA splicing has also been shown to be inhibited during mitosis [38]. The metabolic state of mitotic cells also undergoes significant alterations in order to accommodate disruption and distribution of membrane compartments and components [39]. Recently a transcriptional co-activator protein, Ndd1, has been discovered to be a direct substrate of Cdc5, the yeast Plk1 orthologue. Cdc5 was recruited to specific promoters where it phosphorylated Ndd1 to activate transcription of cell cycle regulated genes involved in mitotic progression [40]. Plk1 has also been shown to regulate the nuclear translocation of the transcription factor HSF1 [41]. Thus we can anticipate further roles for Plk1 in these processes.

**Bioinformatic analysis reveals that Plk1 Polo-box domain ligands are enriched in Ser-[Ser/Thr]-Pro motifs and are potential Plk1 substrates.**

In order to help distinguish between indirect and direct interactors, each of the PBD-interacting proteins identified by mass spectrometry was evaluated for the presence of an optimal PBD recognition motif. Isolated phosphopeptides bind to the Plk1 PBD through the optimal consensus motif S-[pS/pT]-[P/X], where the Ser residue preceding the pSer/pThr makes 3 hydrogen bonding interactions with the PBD (one through a bound water molecule) and contributes significantly to ligand affinity [15]. As seen in Figure 2.4B, PBD recognition motifs were identified in 47.3% of the wild-type-specific PBD-interacting proteins and 41.3% of the wild-type-enriched interactions. In contrast, only 16.2% of the non-specific PBD-interacting proteins contained this motif. To determine whether these values were statistically significant, we generated 2000 'mock' protein datasets by randomly selecting either 622 (the total number of combined wild-type PBD-specific or -enriched interactions: Fig 2.4B, column 1, red boxes) or 277

proteins (the total number of non-specific interactions: Fig 2.4B, column 1, gray box) from the current human NCBI RefSeq collection, and examined these datasets of randomly selected proteins for the percentage of proteins containing S-[S/T]-P motifs. As shown in Figure 2.5A and B, the distribution of the number of protein in each of the random datasets containing S-[S/T]-P motifs was roughly normally distributed, with the same average value of 31.4%. The percentage of PBD-specific or -enriched interacting proteins containing S-[S/T]-P motifs that we identified in our mass spectrometry-based screen (average value 45.3%) was over 7 standard deviations above the mean from that expected for a similar sized collection of random proteins (Figure 2.5B). Likewise, the percentage of PBD non-specific interacting proteins containing S-[S/T]-P motifs was over 5 standard deviations below that expected (Figure 2.5A). Thus, our non-biased method for identifying PBD interactors greatly enriched for proteins that contained the optimal motifs necessary for PBD binding suggesting that the optimal PBD binding motif for isolated phosphopeptides likely functions in an analogous way for many full-length phosphoprotein ligands.

The wild-type PBD -specific or -enriched interacting proteins were also evaluated for the presence of potential Plk1 phosphorylation sites [E/D]-X-[S/T]-[F/L/I/Y/W/V/M] [42]. Among the 282 proteins that contain a PBD recognition motif, this motif was found in 88% of the proteins. In contrast, among the 340 proteins that do not contain a PBD recognition motif this phosphorylation motif was present in 75% of the proteins (Figure 2.4B). We performed a similar statistical analysis for putative Plk1 phosphorylation sites in random proteins datasets containing either 282 proteins (the number of wild-type PBD -specific or -enriched interactions containing S-[S/T]-P motifs: Figure 2.4B, blue boxes, column 2) or 340 proteins (the number of wild-type PBD -specific or -enriched interactions not containing S-[S/T]-P motifs: Figure 2.4B, white boxes, column 2). This revealed a similar mean value of 74.4% (Figure 2.5C, D). The co-occurrence of a Plk1 phosphorylation motif in the S-[S/T]-P motif-containing PBD-specific or -enriched proteins found in our mass spectrometry-based screen was nearly 5 standard deviations greater than that expected by chance alone in a randomly selected set of proteins (Figure 2.5D). In contrast, for the PBD-specific or -enriched proteins found in our mass spectrometry-based screen that lacked S-[S/T]-P motifs, the occurrence of a Plk1

phosphorylation motif was the same as that expected by random chance (Figure 2.5C). We interpret these findings as evidence that Plk1 interactors capable of binding directly to the PBD are likely to also be Plk1 substrates, while proteins in complexes with direct PBD interactors may be less likely to be Plk1 substrates than the PBD interactors themselves.

The mass spectrometry analysis of the PBD interacting proteins also resulted in the mapping of 247 phosphorylation sites (Figure 2.4C, Table 2.2), although this was not the primary intent of our study. The majority of mapped phosphorylation sites were derived from the gel band tryptic digests of our PBD pulldowns with a few from a TiO<sub>2</sub> IMAC using a tryptic digest of an aliquot of the PBD pulldowns. Within the tryptic peptides, many of the phosphorylation motifs are present in a sequence context that is not readily amenable to binding and elution from a reversed-phase column and ionization/fragmentation by MS/MS (i.e. too short, long, hydrophobic, hydrophilic, or contain too many nearby basic residues). Therefore, we expect to observe only a portion of phosphopeptides actually present. In 282 proteins that were identified as wild-type PBD -specific or -enriched interacting proteins (Fig 2.4B, column 2, blue boxes), we were able to map 49 phosphorylation sites in 43 proteins that exactly matched the Ser-(pSer/pThr)-Pro PBD recognition motif (Table 2.2). An additional 4 mapped sites contained the motif Ser-pSer, which would also be expected to bind strongly to the PBD [15]. Amongst the entire 899 proteins identified in our study we were able to map an additional 168 phosphorylation sites matching the minimal consensus [pS/pT]P motif for CDKs. Thus 90% of our mapped sites match the minimal CDK motif.

### **A large network of proteins involved in cytokinesis is connected by Plk1 Polo-box domain ligands.**

In order to examine one part of the PBD interactome in more detail, we chose to focus on a mitotic process in which Plk1 was thought to be involved, but where many of the details of Plk1-dependent regulation were unclear. At the end of mitosis, the parent cell is cleaved into two daughter cells by a mechanical process known as cytokinesis. During early cytokinesis the cell elongates and a cleavage furrow is created under the plasma membrane by an actomyosin-based structure known as the contractile ring. The

spatial orientation of this ring is controlled by both the central spindle and septins. Later in cytokinesis the two daughter cells remain connected by a cytoplasmic bridge called the midbody, until abscission, when the two cells separate [28]. Cells lacking or inappropriately overexpressing certain components for many of these processes fail to complete cytokinesis, resulting in either cells arrested at the midbody stage, or as binucleated cells. In budding and fission yeast, cytokinesis seems to be highly dependent on the fungal homologue of Plk1 [12]. In mammalian cells, there is data implicating Plk1 in the cytokinetic process, but exactly how Plk1 is connected to the network of core cytokinesis components is unknown. In addition to the incompletely understood role of Plk1, regulation of cytokinesis is under the direct control of several other protein kinases including CDK1, AuroraB, and the Rho-regulated protein kinases; Rock1, Rock2, and Citron kinase.

To evaluate additional roles of Plk1 in regulating cytokinesis, we examined protein-protein interactions known to be involved in this process. First, we constructed models of cytokinesis sub-networks for core protein-protein interactions controlling central spindle organization, myosin activation, and actin dynamics based on recent summaries and reviews [28, 43] with interaction data taken from the Human Protein Reference Database [44] (Figure 2.6B-D). We then constructed a similar model of the subset of Plk1-interacting proteins relevant to cytokinesis by searching for proteins with described cytokinesis phenotypes that were also known to interact with Plk1 from published literature (Figure 2.6A) [10, 11, 27, 45-49]. As seen in Figure 2.6E, published data allows only one direct link to be constructed between Plk1 and the core cytokinesis processes of actin dynamics and myosin activation, through the Rho-GEF Ect2. Plk1 can bind to and phosphorylate Ect2, and Ect2 depletion results in cytokinesis defects [29], but the likely direct connection between Plk1 and cytokinesis through Ect2 has not yet been definitively shown. In budding yeast, however, we recently showed that the yeast Plk1 orthologue Cdc5 directs the localization of the RhoGEFs, Tus1 and Rom2, to the bud neck (the budding yeast equivalent of the mammalian furrow/midbody) and that Cdc5 phosphorylation of Tus1 is necessary for cells to complete cytokinesis [13]. The only other published link connecting Plk1 to core components of the cytokinesis network is

through the intermediate filament protein vimentin, which appears to be a critical substrate of both Rock and Plk1 [48, 50] necessary for completion of cytokinesis.

We next examined which of the core cytokinesis proteins in panels B-D showed mitosis-dependent interactions with the Plk1 PBD in our screen (Figure 2.6F, yellow circles). This revealed a total of 11 new putative Plk1-modulated core cytokinesis interactions, including potential roles for Plk1 in the direct regulation of several Rho-dependent kinases (Figure 2.6F, circled red). To identify additional links between Plk1 and these core cytokinetic sub-networks, we expanded the network to include Plk1 PBD-interacting proteins identified in our screen that had previously been experimentally validated to make direct protein-protein interactions with components of these core sub-networks (Figure 2.6G, green circles). This resulted in creation of a more extended Plk1 PBD-annotated cytokinesis network that contained 27 new PBD-binding proteins that touch the core cytokinesis components to form another 33 potential Plk1-regulated links (Figure 2.6G, thick black lines, and Figure 2.7).

#### **Plk1 co-localizes with Rock2 during cytokinesis and works synergistically with RhoA to stimulate Rock2 kinase activity.**

The large set of potential Plk1-regulated cytokinesis proteins revealed by this mass spectrometry/proteomics approach exceeded our capacity to directly investigate in an experimentally tractable manner. We therefore focused our attention on the subset of Rho-regulated protein kinases and phosphatases in the core cytokinesis network that control myosin activation (Figure 2.6F, circled red). We confirmed that each of these proteins - Rock1, Rock2, Citron kinase, and MYPT1 - bound to the Plk1 PBD in a phospho-dependent manner (Figure 2.6H), and proceeded to investigate Rock2 in detail.

Rock2 contains an N-terminal kinase domain and a C-terminal Rho-binding domain and PH domain (Figure 2.8A), and phosphorylates myosin regulatory light chain and myosin phosphatase targeting subunit in manner that is enhanced upon RhoA binding [51]. To demonstrate an interaction between full-length Rock2 and Plk1 within cells, myc-tagged Rock2 and Flag-tagged Plk1 containing either a wild-type or mutant PBD, were co-expressed in U2OS cells. Lysates were collected from asynchronous and mitotically arrested cells. Immunoprecipitation of the lysates using anti-Flag M2 beads

revealed a strong mitosis-dependent interaction of full-length Plk1 containing a wild-type PBD, but not a mutant PBD, with Rock2 (Figure 2.8B, C). Furthermore, this Plk1-Rock2 interaction was lost when the lysates were treated with  $\lambda$ -phosphatase, confirming that the interaction between the full length proteins was phospho-dependent (Figure 2.8D). We also observed significant co-localization of the endogenous proteins during cytokinesis, most prominently at the midbody (Figure 2.8E), consistent with previously published localization data for each of these proteins individually [11, 52].

To investigate whether Rock2 could serve as a substrate for Plk1, full length bovine Rock2 (Rock2-FL) as well as N-terminal kinase domain- (Rock2-CAT) and C-terminal RBD and PH domain-containing fragments (Rock2-RBD/PH) of Rock2 were phosphorylated by the Plk1 kinase domain in vitro in the presence of [ $^{32}$ P]- $\gamma$ -ATP (Figure 2.9). Radioactivity was incorporated into all three fragments of Rock2. When in vitro phosphorylated full-length Rock2 was analyzed by mass spectrometry, phosphorylated peptides from only the C-terminal part of the molecule were detected, corresponding to residues Thr-967 (*DApTI*), Ser-1099 (*EEpSQ*), a mono-phosphorylated species phosphorylated on one of three consecutive serines from Ser-1132 to Ser-1134 (Figs. 2.8A, 2.9 and 2.10), and Ser-1374 (*NQpSI*). Three of these mapped sites conform to the general Plk1 kinase consensus motif [E/D]X[S/T] assuming that the third site is actually Ser-1133 (*DSpSSI*), while the fourth site at Ser-1374 contains an N in the -2 position. This pSer-2 Asn has been recently been reported in several mapped phosphorylation sites targeted by Cdc5 [53], and fits with our unpublished data on the in vitro Plk1 phosphorylation consensus motif (J. Alexander and M.B. Yaffe unpublished). In addition, Ser-1374 phosphorylation was reported in a high-throughput phospho-proteomics screen [54] indicating that it is phosphorylated in vivo. All four of these motifs are conserved in bovine, mouse, rat, and human Rock2. The most likely candidate Plk1 N-terminal site in Rock2 based on consensus motif matching is Thr-489, which is contained in a very acidic stretch of sequence, and peptides containing that site were not recovered in either a phosphorylated or non-phosphorylated form.

To assess the functional significance of Rock2 phosphorylation by Plk1, myc-tagged bovine Rock2 was immunoprecipitated from 293T cells and its kinase activity assayed using a substrate peptide from its physiological substrate, myosin regulatory light

chain (Figure 2.8F). Following phosphorylation, the myosin regulatory light chain peptide substrate was recovered from solution by spotting onto P81 paper and the incorporated radioactivity measured by scintillation counting. The addition of GTP-loaded RhoA increased the basal activity of Rock2 by ~3-fold, similar to the 2-fold increase reported previously [55]. Intriguingly, phosphorylation of Rock2 by Plk1 resulted in a similar 2-fold elevation of Rock2 kinase activity even in the absence of RhoA-GTP, while Plk1 phosphorylation in combination with RhoA resulted in an even more dramatic 6-fold enhancement. Control reactions containing RhoA-GTP, Plk1, and myosin regulatory light chain substrate peptide did not result in detectable peptide phosphorylation in the absence of Rock2, nor did additional control reactions containing RhoA-GTP, Plk1 and Rock2 but no peptide substrate. Therefore, the data in panels 5B-F, taken together, suggests that both Plk1 phosphorylation of Rock2 and RhoA-GTP binding may act synergistically to maximize the kinase activity of Rock2.

To further verify that Plk1 phosphorylation directly activated Rock2, we constructed a mutant version of Rock2 lacking all four Plk1 phosphorylation sites (Rock2-4A). Both wild-type Rock2 and Rock2-4A had similar basal RhoA-activated kinase activity in vitro towards myosin regulatory light chain in the absence of Plk1 (Figure 2.12A, lanes 1 and 2). Following pre-incubation of the wild-type and 4A mutant of Rock2 with Plk1, only the wild-type Rock2, but not the Rock2-4A mutant, showed enhanced protein kinase activity (Figure 2.12A, lanes 3 and 4).

In order to investigate the potential relevance of Plk1 phosphorylation of Rock2 within cells, it was necessary to devise an assay in which Rock2 activity resulted in a specific cellular phenotype. Because the pathways controlling acto-myosin ring contraction during cytokinesis are highly redundant, with at least three kinases other than Rock2 able to phosphorylate myosin regulatory light chain [51], simple knock-downs or knock-outs of several of these kinases results in very mild or absent phenotypes. For example, elimination of Rock2 alone, or even both Rock2 and Rock1 by siRNA causes only a slight increase in the population of multinucleated cells [56] (and data not shown). We therefore took advantage of the fact that completion of cytokinesis requires that the activity of RhoA and Rock2 be shut off in order to allow disassembly of the acto-myosin

ring [57]. Overexpression of Rock2 prevented this disassembly and resulted in delay or failure of cells at the midbody stage to complete cytokinesis (Figure 2.12B).

We used siRNA to deplete endogenous Rock2 while simultaneously overexpressing either the wild-type or 4A mutant forms of Rock2, and examined an asynchronous population of Rock2-overexpressing cells for failure of cytokinesis exit. As seen in Figure 2.12C, by 24 hrs after transfection over one-third of the cells that overexpressed wild-type Rock2 and were in mitosis appeared to be in cytokinesis, compared to ~15% of the control cells. In contrast, overexpression of the Rock2-4A mutant that cannot undergo Plk activation reduced the percentage of mitotic cells that were in cytokinesis by about 50% compared to the wild-type Rock2. By 72 hrs following transfection, overexpression of wild-type Rock2 resulted in a marked increase in the population of cells with = 4N DNA content (Figure 2.12D, E), consistent with the emergence of binucleated cells capable of undergoing additional rounds of DNA replication, similar to what is seen in cells with persistently active RhoA [58]. This phenotype was significantly diminished in the cells overexpressing the Rock2-4A mutant in which Plk1 cannot enhance Rock2 kinase activity. Together, this data suggests that Plk1 can phosphorylate Rock2 in vivo to regulate its activity.

In summary, our study has identified over 600 new mitotic phosphorylation-dependent PBD ligands, and suggests an additional function for Plk1 in regulating the kinase activity of the RhoA effector kinases, Rock2, at specific subcellular mitotic structures, in a manner that synergizes with RhoA-GTP binding as part of a novel mechanism for Rock2 activation (Figure 2.12F). These findings suggest that Plk1 may participate in two distinct but synergistic processes to maximally activate Rock2, first by facilitating the localized exchange of RhoA-GTP for RhoA-GDP via Ect2 or other GTP-exchange factors, and second, by directly activating the RhoA-GTP effector kinase itself. The experimental analysis of the Plk1 PBD interactome places Plk1 at the center of a large network of mitotic protein-protein interactions, and suggests that Plk1 may play a much larger role than previously appreciated in regulating diverse aspects of mitosis.



## **Experimental Procedures**

### **Cloning, Expression and Protein Purification**

Nucleotides encoding the C-terminal Polo-box domain of human Plk1 (residues 371-603) were cloned into the expression vector pET28a (Novagen). The fusion protein contains an N-terminal His<sub>6</sub>-tag followed by MBP and a recognition site of Tev protease between MBP and the PBD. Point mutations of His-538 and Lys-540 to Ala and Met, respectively were introduced using the QuickChange mutagenesis kit (Stratagene) and verified by sequencing. Proteins were expressed in *E. coli* BL21(DE3) cells and purified by Ni-NTA affinity chromatography. The PBD was further purified by affinity chromatography on amylose beads, cleaved with Tev protease, re-passaged through Ni-NTA to remove the cleaved His<sub>6</sub>-MBP tag, and finally purified by gel filtration on a Superose 12 column. GST-tagged Plk1 and RhoA were expressed in bacteria and purified by glutathione-affinity chromatography. Plasmids encoding Myc-tagged full length or the C- and N-terminal fragment of Rock2 were kindly provided by K. Kaibuchi [59] and point mutations were introduced as described above. The plasmids encoding Flag-tagged Plk1 were subcloned from previously described vectors [30, 60]. A hairpin shRNA construct based on a previously described siRNA oligonucleotide that efficiently knocked-down Rock2 [56] was cloned into a PolIII driven miR-30 based expression vector [61]. Constructs were transfected into U2OS cells using Fugene (Roche) according to manufacture's instructions with minor modifications. Myc-tagged protein was immunoprecipitated as previously described [62], and Flag-tagged protein was immunoprecipitated with M2 agarose (Sigma) according to manufacture's instructions.

### **Isolation of PBD-interacting proteins.**

Wild-type and mutant PBD protein was coupled to CNBr activated sepharose 4B beads (Amersham Biosciences) according to manufacturer's instructions. The beads were transferred to a column and excess PBD washed away with Wash Buffer I (0.1 M Tris pH 8, 0.5 M NaCl and 1 mM DTT). The column was equilibrated with Wash Buffer II (50 mM Tris pH 8, 0.2 M NaCl, 2 mM DTT and 10 mM NaF), and the beads then incubated with U2OS cell lysate overnight. Unbound proteins were washed away with ten column

volumes Wash Buffer II. PBD interacting proteins were eluted by incubating the beads with 2 mL of 1 mM phosphopeptide (YMQS-pT-PK) in Wash Buffer II for 1 hour at 4°C. The beads were washed with additional 2 mL of the phosphopeptide containing buffer.

### **Preparation of G<sub>1</sub>/S and Mitotic Cell lysates**

Human osteosarcoma U2OS cells were maintained in Dulbecco's modified Eagle's medium supplemented with 10% fetal calf serum, 100 U/mL penicillin and 100 µg/mL streptomycin at 37°C in a humidified atmosphere containing 5% CO<sub>2</sub>. Cells were grown to 50% confluence, arrested in G<sub>2</sub>/M by treatment with 50 ng/mL nocodazole for 14 hours, and collected by a "mitotic shake-off". U2OS cells were synchronized at the G<sub>1</sub>/S transition by a double thymidine block. Cells were treated with 2.5 mM thymidine for 16 hours and released from the thymidine block by washing twice with PBS followed by incubation in fresh medium. Ten hours after release, thymidine was added for another 16 hours. Ten 15 cm plates were used for each pull down experiment. Cells were lysed in lysis buffer (50 mM Tris-HCl, pH 7.5, 150 mM NaCl, 1% (v/v) NP-40, 5 mM EDTA, 2 mM DTT, 1 mM AEBSF, 1 µg/mL aprotinin, 1 µg/mL leupeptin, 10 µM E64, 1 µg/mL pepstatin A, 1.6 µg/mL benzamidine, 2 mM Na<sub>3</sub>VO<sub>4</sub>, 10 mM NaF, 20 nM microcystin LR, 5 nM okadaic acid, 2 µM canthardin, 0.00073% p-bromotetramisole, 0.4 nM cypermethrin, 100 µM dephostatin, 100 nM bestatin, 100 ng/mL TPCK) at 4°C for 15 minutes. The lysates were cleared by centrifugation at 4°C at 10,000xg for 15 minutes. Alternatively, the lysis buffer contained 50 mM Tris-HCl, pH 7.5, 150 mM NaCl, 1% (v/v) NP-40, 1 mM EDTA, 2 mM DTT, 2 mM AEBSF, 2 µg/mL aprotinin, 2 µg/mL leupeptin, 20 µM E64, 2 µg/mL pepstatin A, 3.2 µg/mL benzamidine, 3 mM MnCl<sub>2</sub> and 6000 U λ-protein phosphatase (New England Biolabs) and dephosphorylation was obtained by incubation at 30°C for two hours.

### **Flow cytometry**

FACS analysis was performed on U2OS cells fixed in ice-cold ethanol and incubated at 37°C for 30 minutes in PBS containing 1% BSA, 2 mg/mL RNase (previously boiled for 5 minutes) and 125 µg/mL propidium iodide. For live cell FACS experiments used in Figure 2.12, U2OS cells were incubated with the cell permeable

DNA dye DRAQ5 (Biostatus Limited ) according to manufacture's instructions and examined within two hours. Fluorescent signals were quantified on a FAC Star Plus (Becton Dickinson) cell-sorting machine using Cell Quest software. Further analysis of cell cycle distribution was performed using FlowJo software.

#### **Far-Western analysis.**

For Far-Western analysis, proteins eluted from wild type or mutant PBD columns were separated by SDS-PAGE, and transferred onto a PVDF membrane. The membrane was blocked in 5% skim milk in TBS-T and subsequently incubated with 6  $\mu\text{g/ml}$  of PBD at 4°C for 6 hours. After washing with TBS-T, the PBD was detected with a  $\alpha$ -Plk cocktail (Zymed Laboratories) as above.

#### **Phosphorylation of substrates by Plk1**

Proteins that were affinity purified with the wild type PBD were eluted and phosphorylated in vitro by full-length Plk1-T210D. Samples were first incubated in kinase buffer containing 50 mM Tris-HCl pH 8, 200 mM NaCl, 2 mM DTT, 5 mM NaF, 200  $\mu\text{M}$  ATP, 500  $\mu\text{M}$   $\text{MgCl}_2$  at 30°C in the absence of radioactive ATP or Plk1 for 2 hr to allow saturation of Plk1-independent phosphorylation sites by any kinases that were present in the reactions. 20  $\mu\text{Ci}$  of [ $^{32}\text{P}$ ]- $\gamma$ -ATP and 7 ng/ml Plk1 was then added, and the reaction incubated for an additional 20 min at 30°C, and products analyzed by SDS-PAGE and autoradiography. To examine Plk1 phosphorylation of Rock2, Myc-tagged full-length or the C- or N-terminal part of Rock2 was expressed in 293T cells by transfection using calcium phosphate. Anti-Myc immunoprecipitates were phosphorylated in vitro using Plk1 and analyzed as above.

#### **Mass spectrometry**

Concentrated eluates from the wild-type and mutant PBD columns were boiled in reducing sample buffer containing  $\beta$ -mercaptoethanol, separated by SDS-PAGE, and visualized by SYPRO Ruby staining (Bio-Rad). Lanes from the gel were excised, cut into 12 fields as shown in Fig 2.1E and digested overnight at 37°C with an excess of sequencing grade trypsin. Peptides were extracted from the gel with 50% acetonitrile/

0.1% formic acid and concentrated in a Speed-Vac. Tryptic digests were analyzed with an automated nano LC/MS/MS system, using an 1100 series autosampler and nano pump (Agilent Technologies, Wilmington, DE) coupled to an LTQ-FT hybrid ion trap Fourier transform mass spectrometer (Thermo Electron, San Jose, CA) equipped with a nanoflow ionization source (James A. Hill Instrument Services, Arlington, MA). Peptides were eluted from a (75  $\mu\text{m}$  x 10 cm) PicoFrit (New Objective, Woburn, MA) column packed with (5  $\mu\text{m}$  x 200 Å) Magic C-18AQ reversed-phase beads (Michrom Bioresources, Inc., Auburn, CA) using a 70 min acetonitrile/0.1% formic acid gradient at a flow rate of 250 nl/min to yield ~25 sec peak widths. Data-dependent LC/MS/MS spectra were acquired in ~3 sec cycles; each cycle was of the form: 1 full FT MS scan followed by 8 MS/MS scans in the ion trap on the most abundant precursor ions excluding charges 1 and unknown charge, subject to accurate-mass, dynamic exclusion for a period of 45 sec. Some of the phosphorylation sites were established with additional LC/MS/MS experiments performed on aliquots of the gel band digests with the instrument operated in a targeted mode where MS/MS of 5-17 precursor  $m/z$ 's were repetitively taken in 3-9 sec cycles throughout the acetonitrile gradient. These precursor masses were selected because they correspond to the phosphorylated form of expected tryptic peptides containing S[ST]P motifs derived from proteins confidently identified in aliquots of sample used for the data-dependent experiments. For Rock2 phosphopeptide mapping both trypsin and chymotrypsin were used to maximize coverage.

### **TiO<sub>2</sub> Immobilized Metal Affinity Capture (IMAC) of phosphopeptides**

An aliquot of the protein mixture eluted from the wild-type PBD column was put through a Microcon 10kD filter to remove the eluting phosphopeptide, reduced with DTT, alkylated with iodoacetamide, and digested with trypsin. Phosphopeptides were enriched by TiO<sub>2</sub> IMAC essentially as described previously [63]. Briefly, 2  $\mu\text{L}$  of Titansphere material (GL Science, Japan) was placed above a plug of Empore C8 packed into a 200  $\mu\text{L}$  StageTip [64]. The TiO<sub>2</sub> column was washed with 30  $\mu\text{L}$  of 1% NH<sub>4</sub>OH in 10% acetonitrile/water, equilibrated with 30  $\mu\text{L}$  0.1% TFA. The peptide sample was loaded to the TiO<sub>2</sub> StageTip and first washed with 30  $\mu\text{L}$  of 10% acetonitrile/0.1% TFA followed by 2 x 30  $\mu\text{L}$  80% acetonitrile/0.1% TFA. Phosphopeptides were eluted directly into

autosampler vials, first with 30  $\mu\text{L}$  of 1%  $\text{NH}_4\text{OH}$  in 10% acetonitrile/water ( $\sim\text{pH}$  10.5) and followed by 30  $\mu\text{L}$  of 1%  $\text{NH}_4\text{OH}$  in 80% acetonitrile/water ( $\sim\text{pH}$  10.5). The eluates were dried in a vacuum centrifuge and analyzed by data-dependent LC/MS/MS as described above.

### **Protein identification, quantitation, and phosphosite determination.**

MS/MS spectra passing the quality filter by having a sequence tag length  $> 0$  (i.e., minimum of two masses separated by the in-chain mass of an amino acid) were interpreted to determine protein identities and relative abundances using the SpectrumMill v3.03b software package (Agilent Technologies Inc.; Santa Clara, CA). Peptide sequences were interpreted from the MS/MS spectra by searching the human subset of the NCBI non-redundant protein database supplemented with expected contaminant proteins (October 2005,  $\sim 125,000$  entries). Initial search parameters included  $\beta$ -mercaptoethanol modification of cysteines, 30% minimum matched peak intensity,  $\pm 0.05$  Da and  $\pm 0.75$  Da tolerance on precursor and product ion masses respectively, 2 missed tryptic cleavages, ESI linear ion trap scoring parameters, and allowed variable modifications included oxidized Met, deamidation of Asn and Gln, and pyro-glutamic acid modification at N-terminal glutamines with a precursor  $\text{MH}^+$  shift range of -18 to 65 Da. Identities interpreted for individual spectra were automatically designated as valid by applying the following scoring threshold criteria to all spectra derived from both lanes on the gel: protein details mode: protein score  $> 25$ , peptide (score, Scored Percent Intensity, delta rank1 – rank2 ) peptide charge +2: ( $> 8$ ,  $> 65\%$ ,  $> 2$ ) peptide charge +3: ( $> 9$ ,  $> 65\%$ ,  $> 2$ ) peptide charge +4: ( $> 9$ ,  $> 70\%$ ,  $> 2$ ) peptide charge +2: ( $> 6$ ,  $> 90\%$ ,  $> 1$ ). These threshold parameters result in 899 proteins being considered identified only when 2 or more non-phosphorylated unique peptides are identified in 16,293 spectra of moderate quality or better. The false positive rate for automated interpretation of the MS/MS spectra using the above criteria was estimated by searching all spectra passing the quality filter against the same database with all of the protein sequences reversed. After applying the above criteria to the search results from the reversed database 22 spectra passed the thresholds yielding 7 proteins (all large, 80kDa-

3.8MDa, with 2 or 3 unique peptides, protein scores 25-36). Thus the estimated overall false-positive identification rates are spectra: 0.1% (22/16,293) and protein: 0.8% (7/899).

In calculating scores at the protein level and reporting the identified proteins, redundancy is addressed in the following manner: the protein score is the sum of the scores of unique peptides. A unique peptide is the single highest scoring instance of a peptide detected through an MS/MS spectrum. MS/MS spectra for a particular peptide may have been recorded multiple times, (i.e. as different precursor charge states, isolated from adjacent gel bands, modified by deamidation at Asn or oxidation of Met) but are still counted as a single unique peptide. When a peptide sequence >8 residues long is contained in multiple protein entries in the sequence database, the proteins are grouped together and the highest scoring one and its accession number are reported. In some cases when the protein sequences are grouped in this manner there are distinct peptides which uniquely represent a lower scoring member of the group (isoforms and family members). In these instances more than one member of the group is reported and counted towards the total number of proteins and in Table 2.1 they are given related protein subgroup numbers (i.e. 7 members of the 14-3-3 proteins were identified: YWHAB, YWHAE, YWHAG, YWHAH, YWHAQ, YWHAZ, SFN and are listed as subgroup numbers 550.1 – 550.7). Overall 899 distinct proteins were identified in the samples from 784 protein groups. In a few instances 2 distinct proteins have been found yet they currently share the same NCBI official symbol (i.e. both shared and distinct peptides were found for the related proteins 14286186, 34365273 which are currently both designated as ZNF185).

MS/MS spectra of phosphopeptides obtained during LC/MS/MS of the TiO<sub>2</sub> IMAC elutions, as well as the data-dependent and targeted analysis of the gel bands, were interpreted in a second round of searches against only the subset of proteins confidently identified from the unphosphorylated peptides observed during the data-dependent LC/MS/MS of the gel band tryptic digests of the PBD pulldowns. The allowed variable modifications were expanded to include phosphoserine and phosphothreonine, with a precursor MH<sup>+</sup> shift range of -18 to 177 Da. The spectrum of each phosphopeptide was manually inspected by an expert. For ~10% of phosphosites observed the MS/MS spectra lack sufficient information to assign the site of phosphorylation to a particular Ser or Thr residue. In those cases that ambiguity is noted in Table 2.2 and the motif chosen to list in

Table 2.1 and count in Figure 2.4B is preferentially chosen in the following order (the optimal PBD-binding motif S-[*pS/pT*]-P, the minimal Cyclin-dependent kinase phosphorylation motif ([*pS/pT*]-P), or none of the above ([*pS/pT*]).

Relative abundance of proteins in the wild-type and mutant PBD bound protein pull-downs were determined using the ion current measured for each peptide precursor ion in the intervening 100K resolution FT-MS scans of the data-dependent LC/MS/MS analyses of the gel band tryptic digests from the PBD pulldowns. The chromatographic peak area of each precursor ion was calculated in the region +/- 30 secs with +/- 0.04 m/z windows around each individual member of the isotope cluster. An individual protein's abundance was calculated as the total ion current measured for all peptide precursor ions with MS/MS spectra confidently assigned to that protein. The determined protein ratios are semi-quantitative, and are generally reliable to within a factor of 2-3-fold of the actual ratio. Numerous experimental factors contribute to the variability in the determined abundance for a protein, including incomplete digestion of the protein; widely varying response of individual peptides due to inherent variability in ionization efficiency as well as interference/suppression by other components eluting at the same time as the peptide of interest (the matrix effect); differences in instrument sensitivity over the mass range analyzed, and inadequate sampling of the chromatographic peak between MS/MS scans.

### **Immunoblotting**

Proteins were separated by SDS-PAGE, transferred to a PVDF membrane and immunoblotting was performed according to standard techniques. Proteins were detected with 0.25 µg/mL α-Cofilin (Cytoskeleton), 1 µg/mL α-Lamin A/C (Upstate), α-MCM2-7 clone AS1.1 (diluted 1:200; generous gift from Stephen Bell, Howard Hughes Medical Institute, M.I.T.), 0.25 µg/mL α-Rock2 (BD transduction laboratories), 0.5 µg/mL α-MYPT1 (BD transduction laboratories), 4 µg/mL α-Actinin α1 (Upstate), 10 µg/mL α-CKIIα (Calbiochem), 2 µg/mL α-Anillin (Abcam), 0.5 µg/mL α-Citron (BD transduction laboratories), 1 µg/mL α-Rock1 (BD transduction laboratories), 0.8 µg/mL α-Plk1 cocktail (Zymed Laboratories), 0.5 µg/mL α-Myc-Tag (Cell Signaling), 5µg/mL M2 α-Flag (Sigma), or a 1:5000 dilution of α-actin (Sigma). Following incubation with

appropriate secondary antibodies, immuno-reactive proteins were visualized by enhanced chemiluminescence (Amersham).

### **Rock2 kinase assays**

Myc-tagged Rock2 was pre-incubated in kinase buffer (50 mM Tris pH 8, 200 mM NaCl, 2 mM DTT, 5 mM NaF, 200  $\mu$ M ATP and 500  $\mu$ M MgCl<sub>2</sub>) containing 1 mM GTP with or without 5  $\mu$ g RhoA and/or 7 ng/ $\mu$ L Plk1 kinase domain for 30 minutes at 30°C. Reactions were then supplemented with 20  $\mu$ Ci [<sup>32</sup>P]- $\gamma$ -ATP and 50  $\mu$ M substrate peptide (Myosin Light Chain Kinase Substrate; AKRPQRATSNVFS; Sigma-Aldrich), and aliquots of the reaction spotted onto squares of Whatman P81 paper after an additional 0, 5, 10 or 20 minutes. The P81 paper was washed with 0.5% phosphoric acid five times, and incorporation of <sup>32</sup>P into the substrate peptide was assessed by scintillation counting. For comparison of wild-type and 4A mutant ROCK2, full length myosin light chain (Sigma) was used as a substrate, and the radiolabeled phosphate incorporation was assessed by autoradiography following SDS-PAGE.

### **Immunofluorescence microscopy**

Rock2 and Plk1 co-localization was examined in sub-confluent U2OS cells transfected with the indicated plasmids and treated with 100 ng/ml nocodazole for 19 hours. Mitotic cells were collected and resuspended into Dulbecco's modified Eagle medium supplemented with 10 % fetal calf serum and penicillin-streptomycin. The cells were then re-seeded onto 18 mm<sup>2</sup> glass coverslips and incubated for 75min at 37°C. The cells were washed with cold phosphate-buffered saline (PBS) and fixed with 3% paraformaldehyde/2% sucrose in PBS for 15 min at room temperature. The fixed cells were washed with PBS and permeablized with 0.5% Triton X-100 in buffer (30 mM Tris buffer (pH 7.8), 75 mM NaCl, 0.3 M sucrose, 3 mM MgCl<sub>2</sub>) for 15 min at room temperature. Coverslips were blocked with 1% bovine serum albumin/1% sucrose in PBS for 1 hour, and stained with mouse monoclonal anti-Rock2 antibody (Clontech Laboratories) at 4°C overnight. After washing, coverslips were stained with Alexa Fluor 488-labeled anti-mouse IgG antibody (Invitrogen, Carlsbad, CA) secondary antibody for 1 hour at room temperature. The coverslips were washed and then incubated with



Rhodamine-labeled mouse monoclonal anti-Plk1 antibody for 3 hours at room temperature. Rhodamine-labeled mouse monoclonal anti-Plk1 antibody was made using mouse monoclonal anti-Plk1 antibody (Zymed Laboratories) and EZ-Label Rhodamine Protein Labeling Kit (PIERCE) according to the manufacturer's protocol. The coverslips were then mounted onto slides with Fluoromount-G (Southern Biotechnologies) containing 4',6'-diamidino-2-phenylindole (DAPI) for DNA staining. Images were collected on a Deltavision (Carl Zeiss) and the Rock2:Plk1 co-localization images were digitally deconvolved using Softworx graphic processing software (SGI).

Mitotic phenotypes of Rock2-overexpressing cells were examined in sub-confluent U2OS cells seeded on coverslips and transfected with the indicated plasmids. After 24-72hrs cells were fixed, washed, permeabilized blocked and stained with mouse monoclonal anti- $\beta$ -tubulin antibody (Sigma) for 1hr at room temperature, washed with PBS, and stained with secondary antibody as above.. Transfected cells were scored by eye for mitotic hallmarks (condensed DAPI and rounded shape) and for presence of a tubulin bridge connecting two cell bodies each with a distinct DAPI signal. We are grateful to the MIT CCR Microscopy and Imaging Core Facility for help with all microscopy work.

### **Random Protein Dataset Generation and Analysis**

The NCBI RefSeq protein collection (version 18 – released July 17, 2006) was filtered to include only human proteins. Strictly computationally predicted proteins were then removed from the collection. The resulting sequences (24314 proteins) were used to generate 2000 random protein datasets of either 622, 277, 282, or 340 proteins using a pseudo-random number generator. The proteins in these sets were then searched for the presence of either a S-[S/T]-P motif for the sets with 622 and 277 proteins or a [E/D]-X-[S/T]-[F/L/I/Y/W/M] motif for the sets with 282 and 340 proteins. The percent of proteins containing the searched for motif was recorded, and a histogram generated indicating the results for all 2000 sets.

**Figure 2.1: The Polo-box domain of Plk1 preferentially binds ligands in mitosis.**

- (A) Domain structure of Plk1. Residues His-538 and Lys-540 are required for phosphopeptide binding by the Polo-box domain (PBD).
- (B) Experimental strategy for identifying cell cycle-dependent PBD ligands.
- (C) Purity and equivalence of recombinant wild-type and mutant PBDs used for interaction screening. Samples were analyzed by SDS-PAGE and stained with Coomassie blue.
- (D) U2OS cells were synchronized at the G1/S transition by a double thymidine block or in M-phase by nocodazole treatment, and DNA content analyzed by flow cytometry.
- (E) Wild type (WT) and mutant (MUT) PBD was used to pull down interaction partners from double thymidine blocked or the nocodazole-arrested U2OS cell lysates. Bound proteins were separated by SDS-PAGE and visualized by SYPRO Ruby staining. Lines on right of gel indicate where gel was cut prior to subsequent mass spectrometry analysis with each labeled section correlated with Table 2.1.

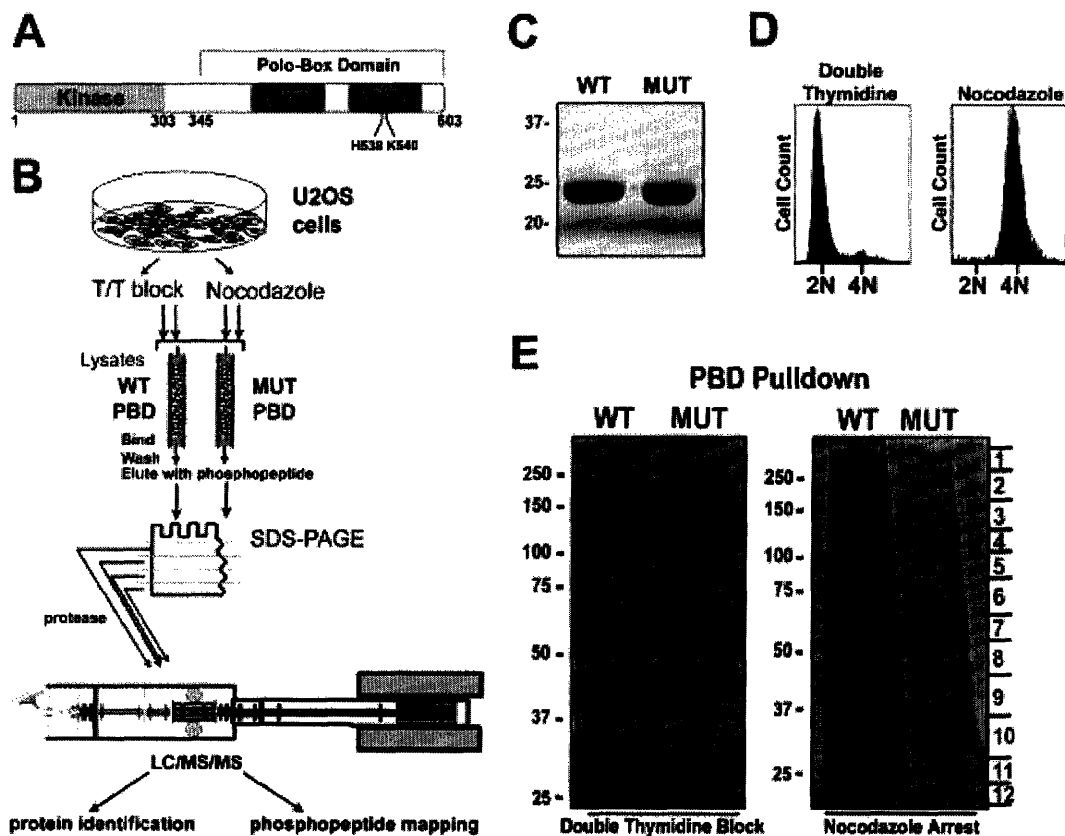


**Figure 2.2: Mitotic proteins bind to the Polo-box domain in a phospho-dependent manner and are substrates of Plk1.**

(A) Direct binding of PBD-interacting proteins. Proteins interacting with the WT and MUT PBD from nocodazole arrested U2OS cell lysates (Figure 2.1B) were transferred to PVDF membrane and analyzed for direct binding by Far-Western analysis using the wild-type PBD as a probe.

(B) Phosphorylation-dependent PBD interactions. Nocodazole arrested U2OS cell lysates were incubated with (+) or without (-)  $\lambda$ -protein phosphatase prior to WT-PBD pull down. The bound proteins were separated by SDS-PAGE and visualized by SYPRO Ruby staining.

(C) Plk1 phosphorylation of PBD-interacting proteins. Wild type PBD was used to pull-down interacting proteins from nocodazole arrested U2OS cell lysates. The proteins were incubated with or without active Plk1 and  $^{32}\text{P}$ - $\gamma$ -ATP, separated by SDS-PAGE, and visualized by autoradiography.

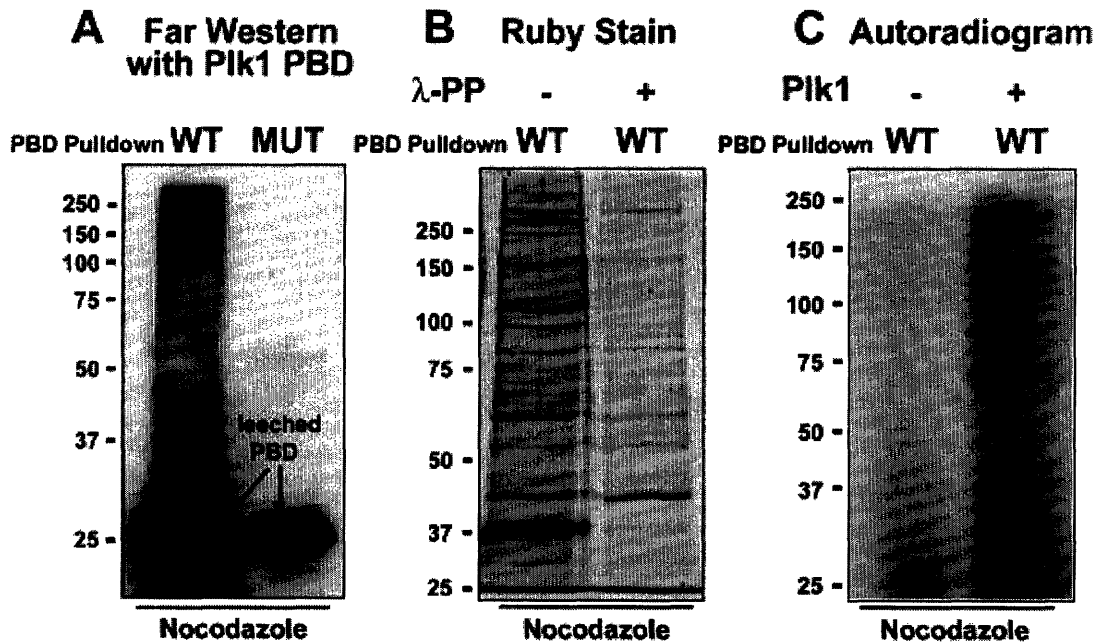


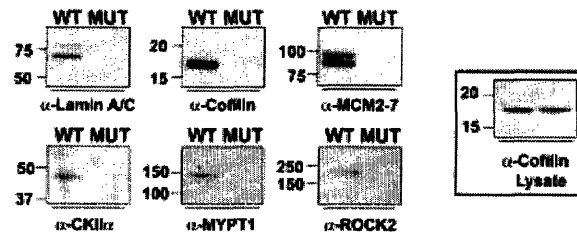
**Figure 2.3: Verification of mitosis-specific, phosphorylation-dependent, Polo-box domain interacting proteins identified by mass spectrometry.**

(A) WT and MUT PBD was used to affinity purify interaction partners from nocodazole arrested U2OS cell lysate. Proteins were separated by SDS-PAGE and analyzed by immunoblotting with the indicated antibodies.

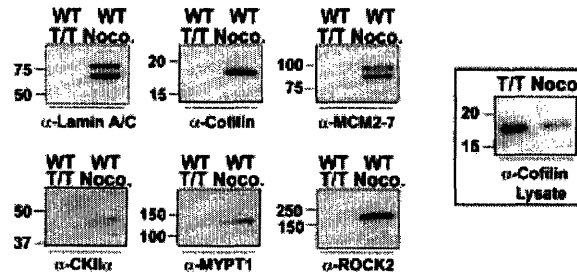
(B) U2OS cells were arrested at G<sub>1</sub>/S by a double thymidine block (T/T) or in M-phase by nocodazole arrest (Noco.). Lysates were incubated with WT PBD and bound proteins separated by SDS-PAGE and analyzed by immunoblotting with the indicated antibodies.

(C) Lysates from nocodazole-arrested U2OS cells were incubated with (+) or without (-) λ-protein phosphatase at 30°C for 2 hours prior to WT-PBD pull down. Bound proteins were separated by SDS-PAGE and analyzed by immunoblotting with the indicated antibodies.

**A PBD Interactions are Specific to the WT PBD**



**B PBD Interactions are Specific to Mitosis**



**C PBD Interactions are Phosphorylation Specific**

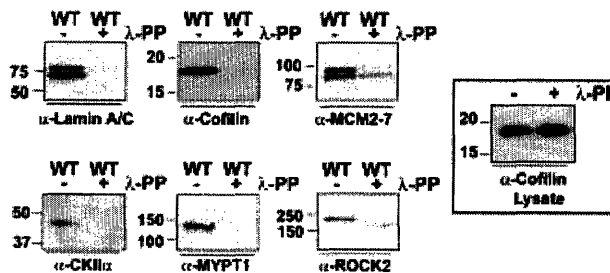


**Figure 2.4: The Polo-Box Domain Interactome .**

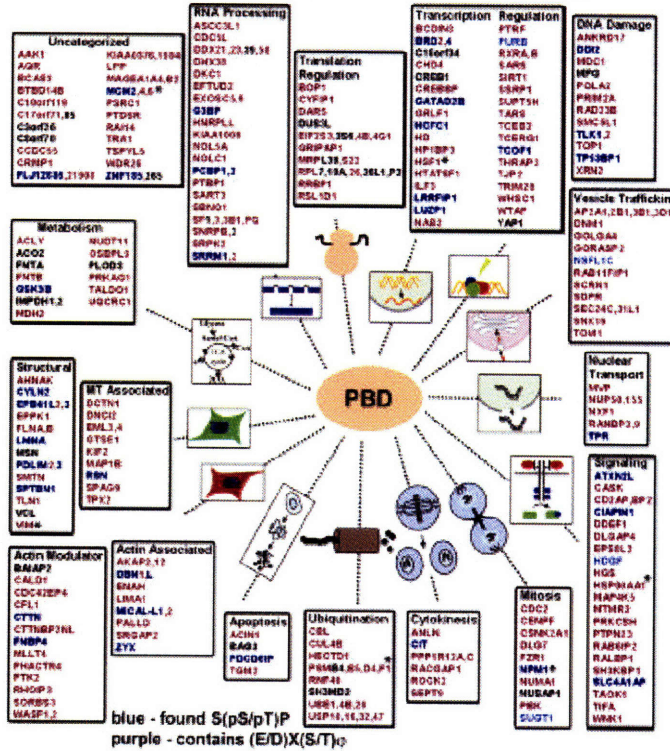
(A) Only WT PBD -specific or -enriched interacting proteins that contain at least one match to the optimal PBD binding motif (S-[S/T]-P) are shown (Figure 2.4B, blue boxes, column 2). Proteins were categorized according to their known biological function by GO terms. Blue text indicates those proteins in which we were able to map at least one S-[pS/pT]-P site; dark blue indicates those that also contain an optimal Plk1 phosphorylation site, while light blue indicates those that do not. For the remaining proteins, those shown in purple contain an optimal Plk1 (E/D)X(S/T)φ phosphorylation site while those shown in black do not. Previously known Plk1 interactors are indicated with an asterisk.

(B) Summary statistics of proteins identified by mass spectrometry from Plk1 PBD-pulldown assays in nocodazole -arrested U2OS cells. Proteins were divided into three categories based on specificity for the wild type versus mutant PBD. Dark red denotes proteins that only bound to the wild-type PBD; light red, proteins with  $\geq 20$ -fold enhanced binding to WT PBD; dark grey, proteins with  $<20$ -fold enhanced binding to WT PBD. The presence of optimal PBD-binding S-[S/T]-P motifs are shown by dark and light blue and grey filled bars in the 2nd column. White boxes in the second column correspond to identified interacting proteins that do not contain the optimal PBD-binding motif. Potential Plk1 (E/D)X(S/T)φ phosphorylation sites are indicated by purple and gray wedges in pie charts.

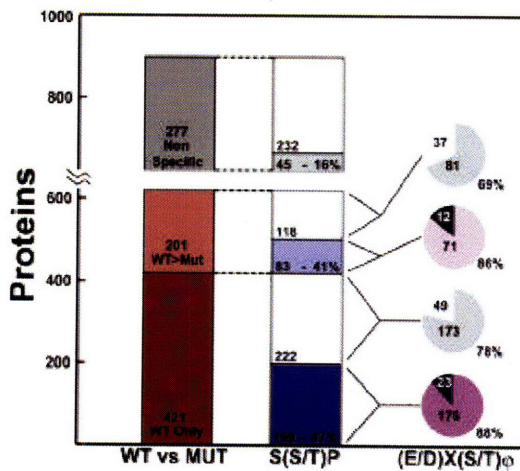
(C) A subset of phosphorylation sites in the WT specific/enriched versus non-specific PBD-interacting proteins were mapped by mass spectrometry. Mapped sites were categorized into those that matched the optimal PBD-binding motif (S-[pS/pT]-P, the minimal peptide PBD-binding motif (S-[pS/pT]), the minimal Cyclin-dependent kinase phosphorylation motif ([pS/pT]-P), or none of the above ([pS/pT]).

Figure 2.4 Continued

## A Polo-Box Domain Binders



## B Mass Spec Results



## C Mapped Phosphosites

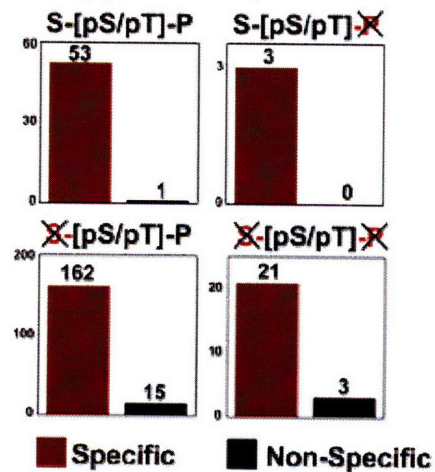


**Figure 2.5: Bioinformatic Analysis of the Polo-Box Domain Interactome.**

(A, B) Distribution of (S-[S/T]-P) motif occurrence in 2000 random protein datasets. In panel B each dataset contained 622 proteins while in panel A each dataset contained 277 proteins. The means and standard deviations of the distributions are shown. Thick vertical arrows indicate the percentage of WT PBD-specific/enriched proteins (B) and WT PBD non-specific proteins (A) that were observed to contain the S-[S/T]-P motif.

(C, D) Distribution of potential Plk1 phosphorylation motifs (E/D)-X-(S/T)-□ in 2000 random protein datasets. In panel D each dataset contained 282 proteins while in panel C each dataset contained 340 proteins. Thick vertical arrow in (D) indicates the percentage of WT PBD-specific/enriched interacting proteins containing both S-[S/T]-P motifs and potential Plk1 phosphorylation motifs. The arrow in (C) indicates the percentage of WT PBD-specific/enriched interacting proteins that lack S-[S/T]-P motifs but contain potential Plk1 phosphorylation motifs.

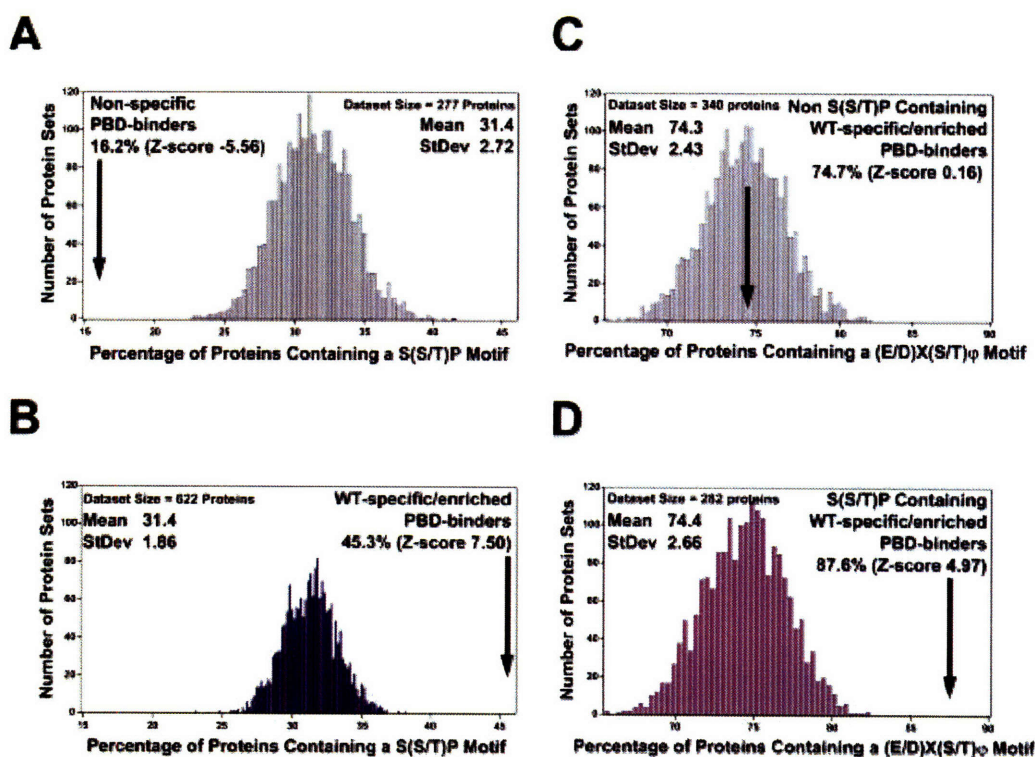




**Figure 2.6: A data-driven Plk1-related cytokinesis network.**

Circle color coding: orange, Plk1; red, myosin activation network; blue, actin dynamics network; light purple, proteins bridging the actin and myosin networks; dark purple, central spindle organization network; green, proteins not known to function as part of any core cytokinesis network. Proteins are labeled using HUGO gene nomenclature except for actin, tubulin, myosin, and myosin light chains. Myosin phosphatase is shown generically as a node labeled MYPT (official gene symbol for the protein we identified is PPP1R12A). Lines indicate direct protein-protein interactions, arrows indicate a kinase-substrate relationship, and the filled circle between MYPT and myosin RLC indicates a phosphatase-substrate relationship.

(A) The known Plk1 network of proteins that participate in cytokinesis.

(B) The core cytokinesis network of central spindle organization.

(C) The core cytokinesis network of myosin activation.

(D) The core cytokinesis network of actin dynamics.

(E) Core cytokinesis network. The networks from panels A-D are shown connected by all of the direct, experimentally verified, protein-protein interactions. The thick line between Ect2 and RhoA represents the only mechanistic connection between previously known Plk1-interacting proteins and the actomyosin cytokinesis subnetworks.

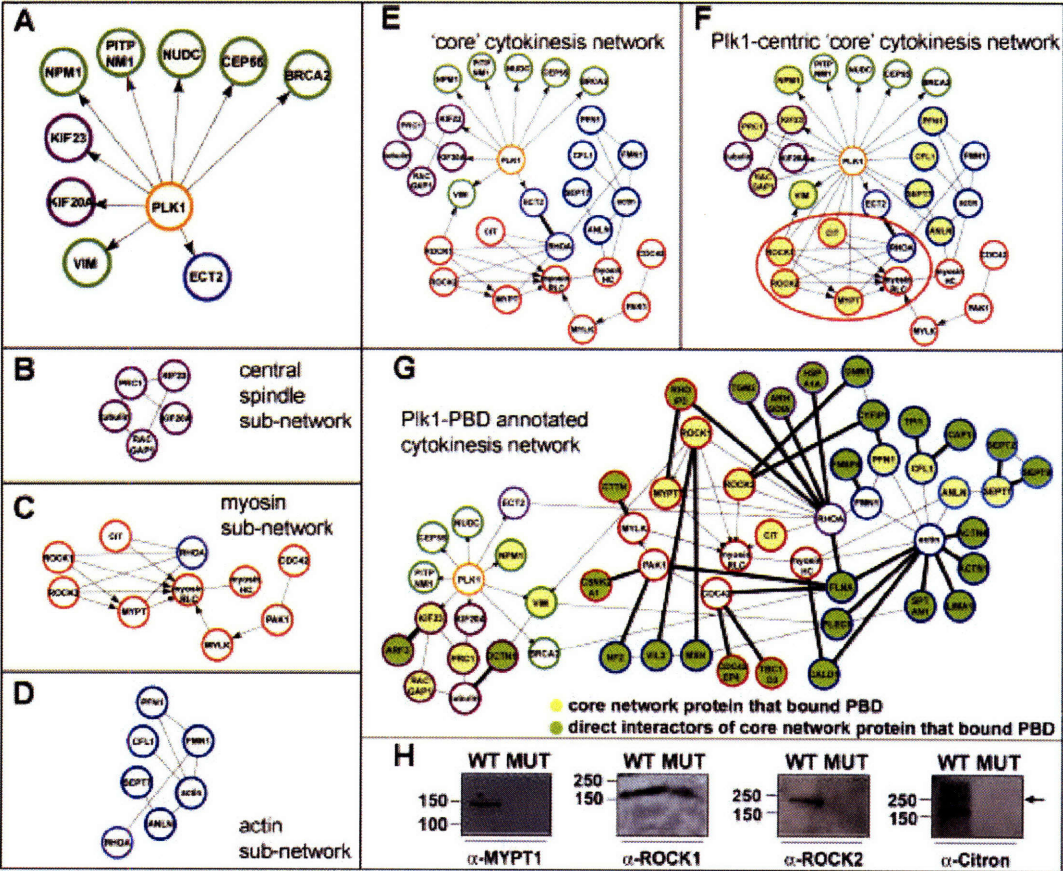
(F) Plk1-centric core cytokinesis network. The network in panel E redrawn with additional interactions between Plk1 and core network components as revealed by the Plk1 PBD interactome screen. Core cytokinesis network components detected in the Plk1 PBD interaction screen are shaded yellow. Red circle indicates the section of the network selected for further study.

(G) A Plk1-PBD annotated cytokinesis network. A view of the core cytokinesis network expanded to include additional Plk1 PBD-interacting proteins that were detected in our screen and are known to participate in protein-protein interactions with one or more of the core cytokinesis components. Yellow shading indicates PBD-interacting proteins in the core network; green shading indicates PBD-interacting proteins that also interact with proteins in the core network; thick black lines denote interactions between core network proteins and the additional Plk1 PBD-interacting proteins in the expanded network.

(H) Proteins within the red circled region from panel F were investigated as in Figure 2.3.

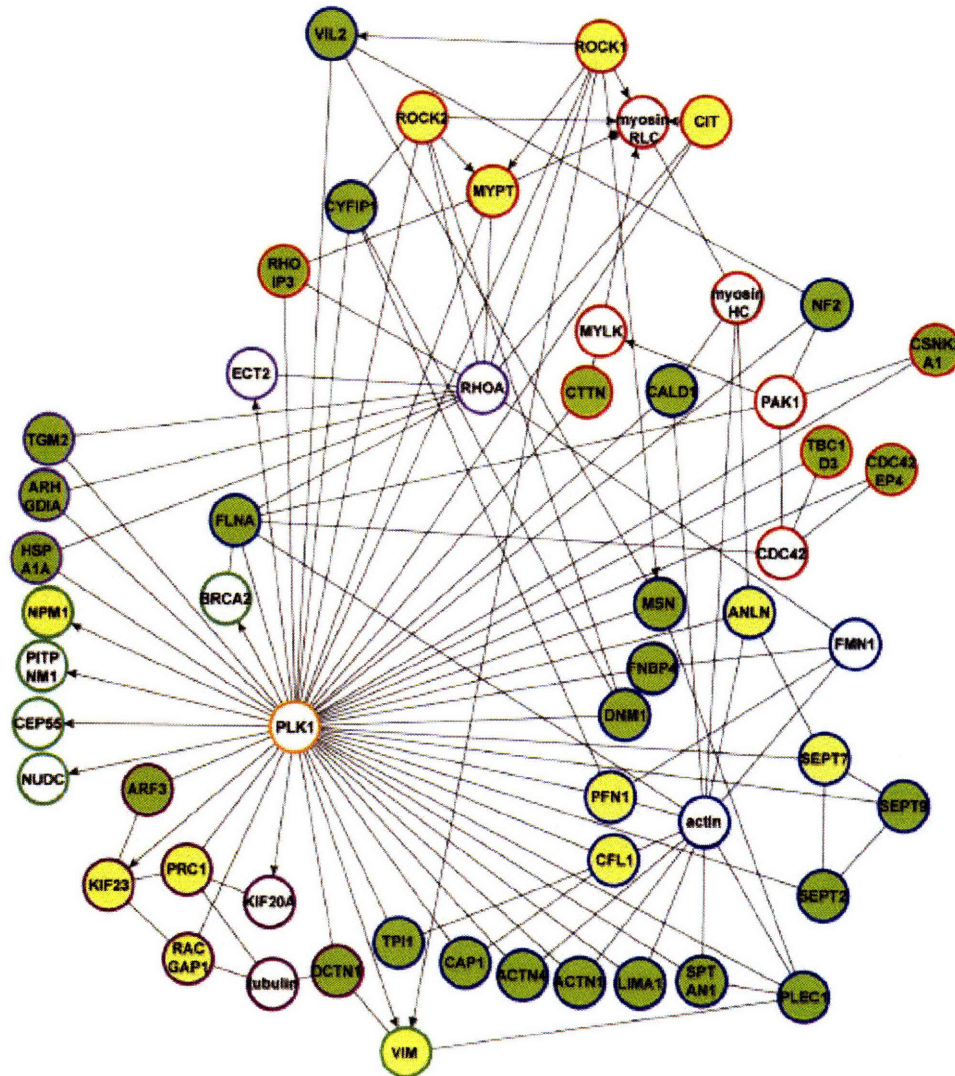


Figure 2.6 Continued



**Figure 2.7: Plk1-centric Plk1-PBD annotated cytokinesis network**

An alternative view of the data shown in Figure 2.6G with Plk1 placed at the center. Yellow shading indicates PBD-interacting proteins in the core network; green shading indicates PBD-interacting proteins that also interact with proteins in the core network. Lines indicate direct protein-protein interactions, arrows indicate a kinase-substrate relationship, and the filled circle between MYPT and myosin RLC indicates a phosphatase-substrate relationship.



**Figure 2.8: Plk1 and RhoA synergistically activate Rock2.**

(A) Domain structure of Rock2, with amino acid sequence indicated below. Plk1-dependent phosphorylation sites were mapped by mass spectrometry and are indicated by filled red circles.

(B) Plk1 and Rock2 interact in cells during mitosis. Full length myc-tagged Rock2 and Flag-tagged Plk1 (containing WT or MUT PBD) were expressed in U2OS cells. Lysates from asynchronous cells or following mitotic arrest with nocodazole were immunoprecipitated using M2  $\alpha$ -Flag beads, and immunoblotted for myc as shown. Note that expression of the mutant Plk1 was much higher than the wild type Plk1 as expected since overexpression of wild type Plk1 is somewhat toxic to cells [65, 66].

(C) The amount of Rock2 co-precipitating with Plk1 in panel B was quantified by normalization relative to the level of Rock2 expression.

(D) Rock2-binding to Plk1 in mitosis is phosphorylation-dependent. Myc-tagged Rock2 and Flag-tagged Plk1 were co-expressed in U2OS cells. Mitotic lysates were prepared from nocodazole-arrested cells, treated for 2h with  $\lambda$  protein-phosphatase or mock treated, then immunoprecipitated using M2  $\alpha$ -Flag beads and immunoblotted for myc.

(E) Rock2 and Plk1 co-localize at the midbody during cytokinesis. U2OS cells were released from a nocodazole block, and fixed and 1 hr later stained for endogenous Plk1 and Rock2. DNA was stained with DAPI. Deconvolution images are shown. Scale bars = 5 $\mu$ m.

(F) Plk1 and RhoA synergize to amplify Rock2 kinase activity. Myc-Rock2 was immunoprecipitated from asynchronous cells and kinase activity against a myosin light chain peptide assayed in the presence or absence of RhoA and/or in response to Rock2 phosphorylation by Plk1. Error bars represent the standard deviation of 3 independent experiments.

Figure 2.8 Continued

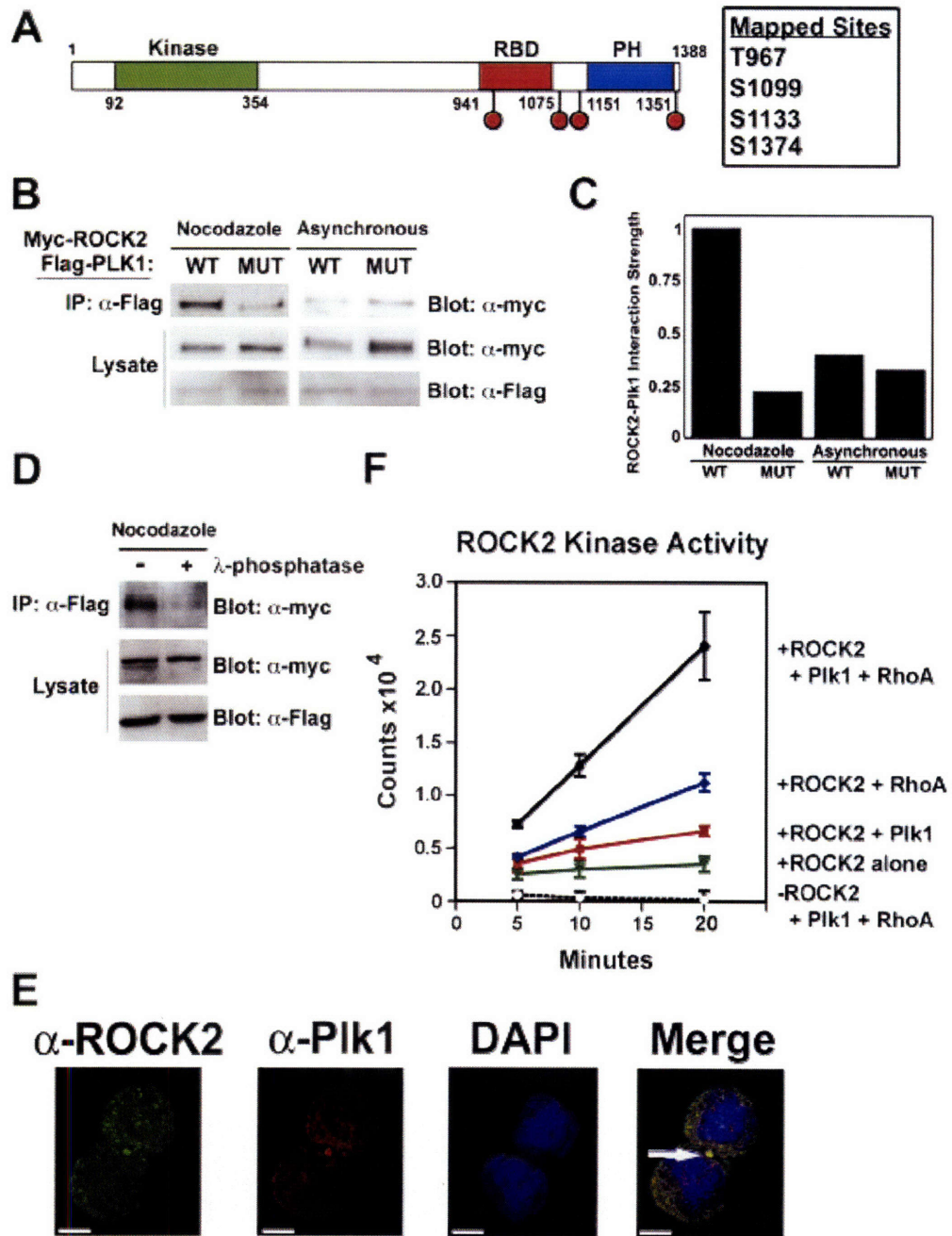




**Figure 2.9: Plk1 phosphorylates ROCK2 in vitro**

(A) Domain structure of Rock2 constructs, with amino acid sequence boundaries shown.

Plk1-dependent phosphorylation sites were mapped by mass spectrometry as indicated.

(B) The indicated Rock2 constructs were immunoprecipitated from 293T cells. The

proteins were then incubated with or without active Plk1 and  $^{32}\text{P}$ - $\gamma$ -ATP, separated by

SDS-PAGE, and visualized by autoradiography.

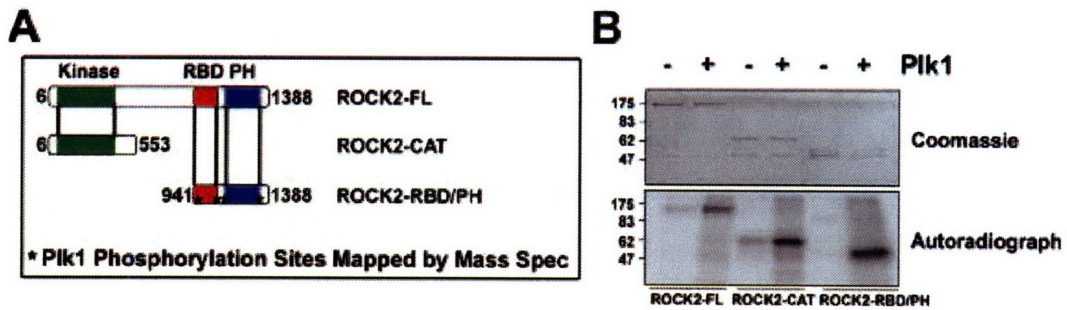


**Figure 2.10: Mass spectrometry spectra identifying Plk1 phosphorylation sites in ROCK2**

(A-D) MS/MS spectra of peptides containing the indicated sites are shown with b-ions in blue and y-ions in red. Ions indicating neutral loss of phosphate from the precursor are shown in green. The phosphorylation site in C could be any of the three consecutive serines centered on S1133.

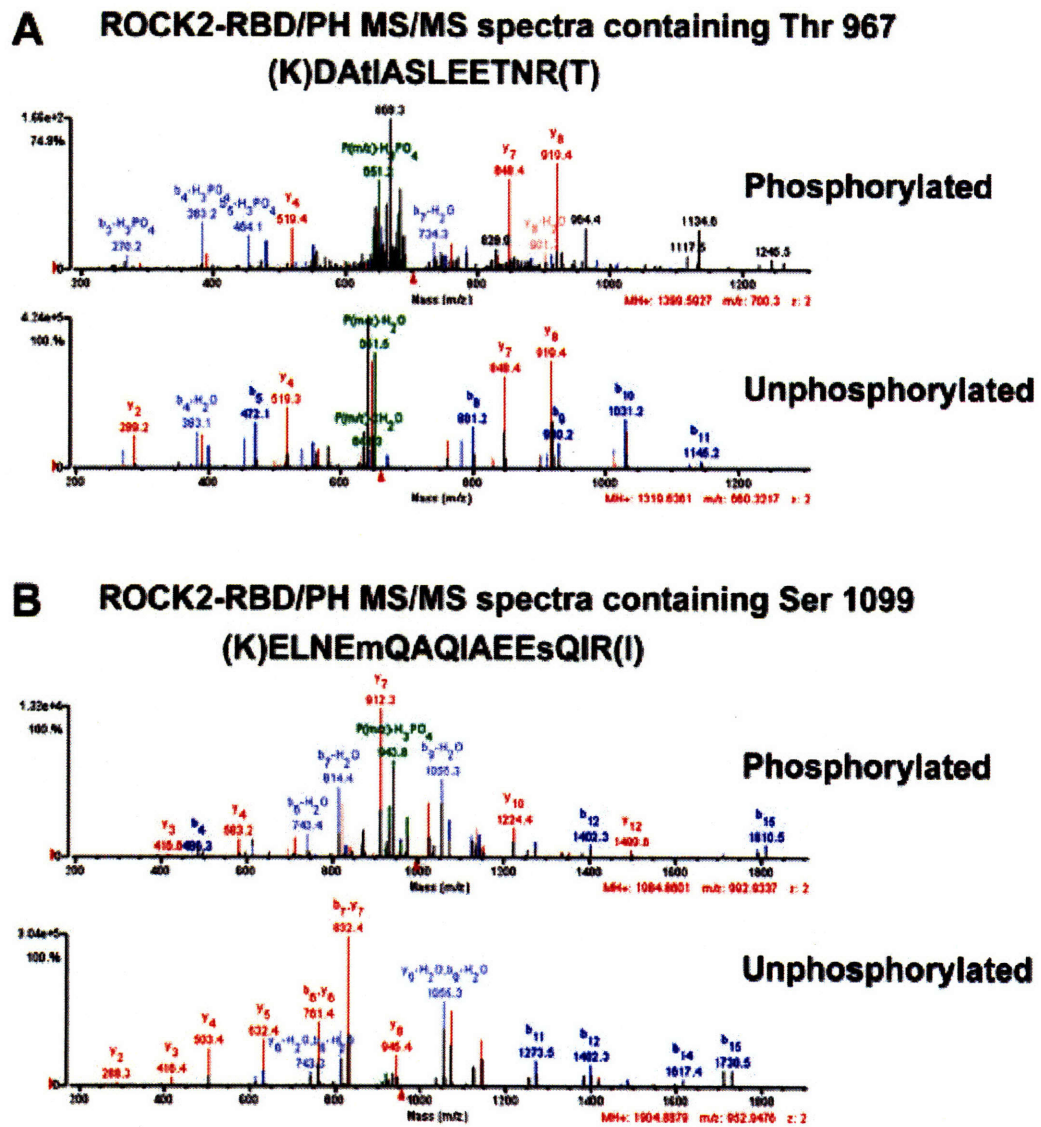
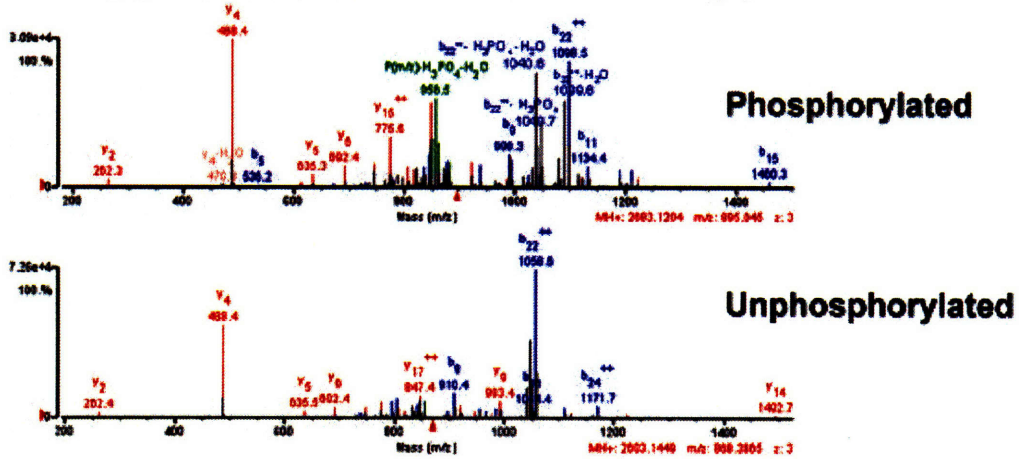
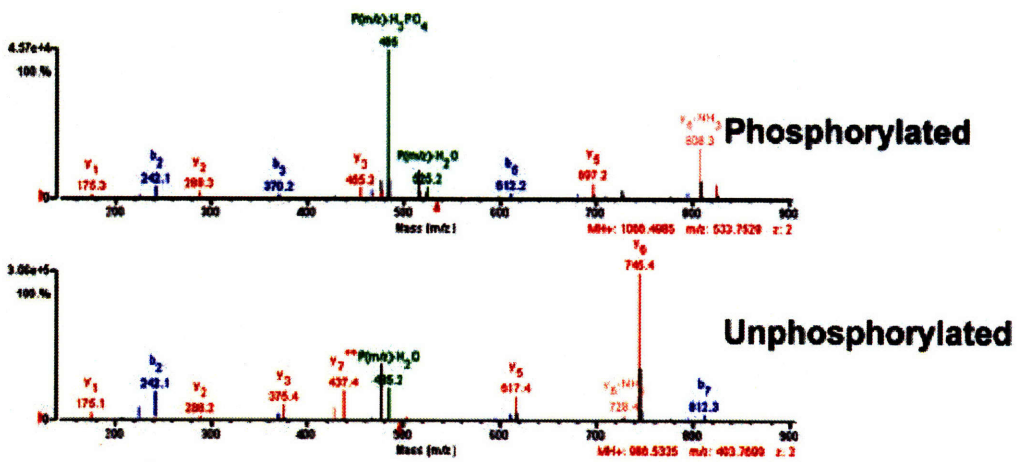


Figure 2.10 Continued

**C ROCK2-RBD/PH MS/MS spectra containing Ser 1133  
(L)HIGLDSsSIGSGPGDTEADDGFESR(L)**



**D ROCK2-RBD/PH MS/MS spectra containing Ser 1374  
(K)IQQNQsIR(R)**



**Figure 2.11: Expression of exogenous myc-tagged ROCK2.**

Western blots with indicated antibodies are shown.

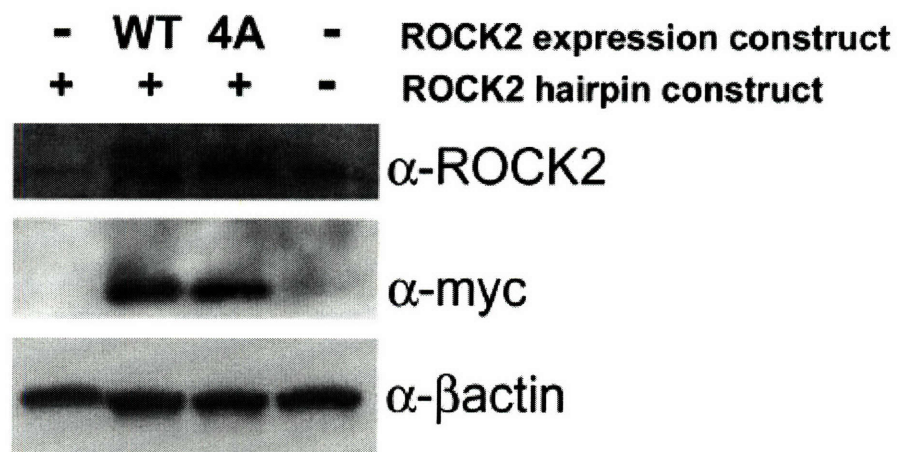




**Figure 2.12: Plk1 activates Rock2 in cells.**

(A) Myc-Rock2 or myc-Rock2-4A was immunoprecipitated from asynchronous cells. Each I.P. was split in half, and one-half pre-incubated with Plk1 for 60 min in the presence of cold ATP. Following additional washing, Rock2 kinase activity against myosin regulatory light chain was assayed in the presence of RhoA and  $^{32}\text{P}$ - $\gamma$ -ATP, and analyzed by SDS-PAGE/autoradiography. A strong Rock2 autophosphorylation band is also present. Lanes 1 and 2 in the left panel and lanes 3 and 4 in the right panel are each from the same gel and autoradiograph allowing direct comparison.

(B) Overexpression of Rock2 causes accumulation of cells in terminal cytokinesis. Asynchronous U2OS cells were transfected with pEF-BOS (control) or pEF-BOS expressing wild-type Rock2. Mitotic cells from the control transfections displayed a normal rounded-up morphology, while many of the mitotic cells overexpressing Rock2 appeared to be in the terminal midbody stage of cytokinesis. Scale bars = 10 $\mu\text{m}$ .

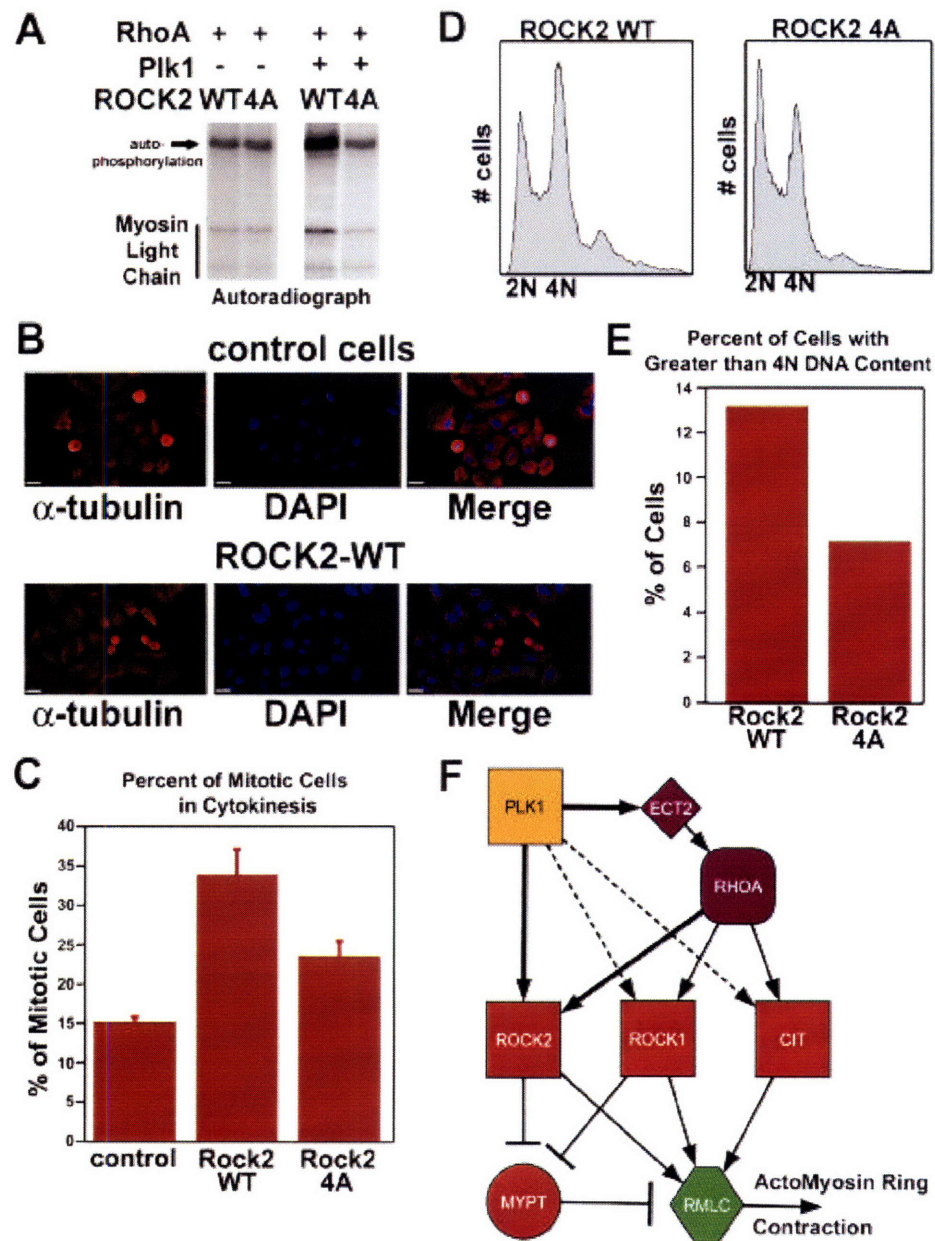
(C) Percentage of mitotic cells in cytokinesis 24 hrs after transfection with myc-Rock2, myc-Rock2-4A, or control vectors. Mean values and S.D. from n=3 experiments.

(D) FACS profiles of cells 72 hrs after transfection with myc-Rock2 or myc-Rock2-4A.

(E) Percentage of cells containing greater than 4N DNA content from FACS profiles above. These results are representative of n=3 independent experiments.

(F) A model of Plk1 control of regulatory myosin light chain (RMLC) phosphorylation during cytokinesis. Arrows indicate activation events and bars indicate inhibition events. Kinases are indicated as squares, phosphatases as circles, GEFs as diamonds, and small G-proteins as rounded squares.

Figure 2.12 Continued



## Terms and color coding used in Table 2.1 and Table 2.2

Table 2.1 - Proteins that were Pulled-down with the Plk1 Polo-box Domain

5Column	Columns used to sort the table
Rows	Wt-PBD specific proteins that contain both S[ST]P (PBD binding) and [ED]X[ST]F[LYVWMM] (PLK phosphorylation) motifs.
Rows	Wt-PBD specific proteins that contain an S[ST]P but not an [ED]X[ST]F[LYVWMM] motif.
Rows	Wt-PBD specific proteins that lack an S[ST]P motif.
Rows	Non-specifically bound proteins.
[st] (#)	The number of phospho-Ser/Thr sites mapped in the protein.
S[st]P (#)	The number of phospho-Ser/Thr sites mapped in the protein with the 3 residue motif.
S[st]P (#)	The number of phospho-Ser/Thr sites mapped in the protein with the 3 residue motif (not Pro in position 3).
^S[st]P (#)	The number of phospho-Ser/Thr sites mapped in the protein with the 3 residue motif (not Ser in position 1 & not Pro in position 3).
^S[st]P (#)	The number of phospho-Ser/Thr sites mapped in the protein with the 3 residue motif (not Ser in position 1).
Primary Band	The main area on the gel in Fig 1e in which the protein was identified.

Table 2.2 - Phosphorylation Sites Mapped in Proteins that were Pulled-down with the Plk1 Polo-box Domain

Columns	Columns used to sort the table
WT-dd	Peptide was observed in the data-dependent LC/MS/MS experiments performed on the in-gel digests of the Wt-PBD lane of Fig 1e.
Mut-dd	Peptide was observed in the data-dependent LC/MS/MS experiments performed on the in-gel digests of the Mut-PBD lane of Fig 1e.
WT-Targeted	Peptide was observed in the targeted LC/MS/MS experiments performed on the in-gel digests of the Wt-PBD lane of Fig 1e.
WT-IMAC	Peptide was observed in the data-dependent LC/MS/MS experiments performed on IMAC eluates from the Wt-PBD pulldown.
Z	Precursor charge of the peptide.
Score	Score from the interpretation of the peptide's MS/MS spectrum.
SPI	Scored percent intensity from the interpretation of the peptide's MS/MS spectrum.
MH+ Shift (Da)	Mass shift from the modified residues in the peptide.
Site Ambiguity	Possible indistinguishable positions of the phosphorylated residue(s) if the fragment ion series observed in the MS/MS spectrum are incomplete.
Sequence	s: phospho Ser t: phospho Thr m: oxidized Met n: deamidated Asn q: pyro Glu from Gln

When a phosphorylated peptide was observed in multiple precursor charge states or multiple forms due to missed cleavage by the enzyme, only the highest scoring spectrum or the one with the least ambiguity in phosphosite assignment is listed in the table.































**Table 2.2 - Phosphorylation Sites Mapped in Proteins that were Pulled-down with the Plk1 Polo-box Domain**

WT-4d	z Score	SPI	Mut-4d	z Score	WT-Targeted	z Score	WT-MAC	z Score	WT-Res	z Score	WT-Res	Other (D)	m/z	Shift (D)	MH+	Site	Modif	Site	Site	Position	Sequence	NCBI	HUGO	Symbol	#	Protein	
2	9.62	76.7											594.75	80.0	Ssp	OK	OK			S3296	(R)EIESRGR(L)			45751604	ATXN2L	5	31.1
2	15.49	70.9										864.93	80.0	GSP	OK	OK			S8176	(R)EDVGLLTPMGRVSS(KT)			46751604	ATXN2L	5	31.1	
2	14.77	78.8										897.86	80.0	Ssp	OK	OK			S4146	(R)GPHHLDMSRFRGSEAR(G)			45751604	ATXN2L	5	31.1	
2	16.26	90.3										568.25	80.0	Ssp	OK	591.82			S6825	(K)LCRSSRFRSISLDPPR(K)			45751604	ATXN2L	5	31.1	
3	15.09	85.9										790.72	80.0	Ssp	OK				S4475	(N)TLSPSRPSSGSEITPPAVGR(M)			55690000	TPR	4	31.1	
2	14.41	91.1										861.91	80.0	Vsl	OK				S11856	(K)EGVQGRLVVALEEGR(S)			55690000	TPR	4	31.1	
2	20.75	96.2										1063.51	96.0	MsP	OK				S3795	(K)GALSEEELAAKMTAAVA(K)			55690000	TPR	7	7	
3	12.06	82.0										815.75	80.0	Ssp	OK	1672.76	77.79		T1677	(R)GALSTEDPTAAKMTAAVA(K)			55690000	TPR	7	7	
3	16.33	86.6										992.18	80.0	Ssp	OK				T8411	(R)ILLSTQTGVAIVVAASSLDVLSASPK(R)			55690000	TPR	7	7	
2	16.44	90.9										226.15	80.0	Hsp	OK				S21556	(R)TDGFAHAPVQAVGPR(F)			55690000	TPR	7	7	
2	7.84	35.2										776.92	175.9	KsIP	OK				T16921	(K)YVTAAMKQKIKR(A)			55690000	TPR	7	7	
2	17.83	95.3			2	11.99	75.8					849.93	80.0	Ssp	OK	OK			S16915	(R)MGRGSRFLSLRGR(G)			12062736		2	78.1	
2	16.02	91.5			2	12.03	79.0					1208.10	80.0	Ssp	OK	OK			T1181	(K)GPAVATGASRPEGRAPPAPAPK(G)			12062736		2	78.1	
2	10.13	63.9										1077.98	80.0	Ssp	OK	214.15			T2161	(R)GGGDFPAPVAPGAPAPSPR(Q)			14286186	ZNF185	3	89.1	
2	17.89	96.6										677.81	80.0	GSP	OK	68.69	71		S716	(K)KSTGPTQETGAPFAK(R)			14286186	ZNF185	3	89.1	
2	16.61	92.2										991.99	80.0	Ssp	OK				S2215	(R)QSPGSSGELVY(R)			42988842	SPYBN1	4	6.1	
2	16.61	92.2			2	13.17	78.7					991.99	80.0	Ssp	OK				S22915	(R)AAQTLPTSAVITTSRSPGK(R)			42988842	SPYBN1	4	6.1	
2	10.54	77.1										817.90	81.0	Ssp	OK				S20886	(K)GEGVSNQGLPAECGGR(M)			62988842	SPYBN1	4	6.1	
2	10.54	77.1										817.90	80.0	Ssp	OK				T22707	(K)HEVASLTSQSRASR(A)			62988842	SPYBN1	4	6.1	
2	10.54	77.1										898.27	80.0	Psp	OK				S20926	(R)RPPPEPSTK(V)			62988842	SPYBN1	4	6.1	
2	14.21	86.8										897.42	80.0	Dsd	OK				S1496	(R)XLLVDPDEDEERPAK(K)			434793	MCM2	3	39.1	
2	14.21	86.8										890.79	80.0	Ssp	OK				S375	(R)RNDPITSPGR(S)			434793	MCM2	3	39.1	
3	15.92	85.1										830.75	80.0	Ssp	OK				S515	(R)RNDPITSPGR(S)			434793	MCM2	3	39.1	
3	16.15	79.7			4	15.84	67.2					837.10	80.0	Ssp	OK	187.88	89		S1895	(R)RNDPITSPGR(S)			14141168	PCBP2	2	105.1	
3	15.99	93.2										707.05	80.0	Ssp	OK				S2725	(K)LLHPTMRPSSPMFRAGDGR(V)			14141168	PCBP2	2	105.1	
3	17.84	96.8										923.40	80.0	APF	OK				T9221	(K)LLHPTMRPSSPMFRAGDGR(V)			14141168	PCBP2	2	105.1	
2	11.96	64.0										827.89	81.0	VIP	OK				T16094	(R)EGVGLQPEVAVLTK(A)			50321186	TP53BP1	5	11.1	
2	10.86	79.3										566.77	80.0	APF	OK				S10286	(R)KINDSTVAASVAPGDK(T)			50321186	TP53BP1	5	11.1	
2	16.57	85.6										906.42	80.0	TIP	OK				T10568	(R)SEDPPTPR(G)			50321186	TP53BP1	5	11.1	
2	11.10	82.4			2	13.64	85.3					458.24	80.0	Ssp	OK	S379	80.82		S3806	(R)STFVPSRFTGDSR(Q)			50321186	TP53BP1	5	11.1	
2	10.28	74.8			2	10.08	65.5					188.92	80.0	Ssp	OK				S11175	(K)IHPRIK(S)			19718731	BRD4	2	16.1	
2	14.44	80.9										188.92	80.0	Hsp	OK				S4705	(K)MPRDEEFAVVAISPAAPPTK(V)			19718731	BRD4	2	16.1	
2	8.14	56.9										596.80	80.0	Ssp	OK				S9008	(R)MALAPAKERPK(N)			40368833	TCOF1	8	17.1	
2	12.26	81.1										502.25	80.0	Psp	OK				T9141	(R)KGMAPPRPK(T)			40368833	TCOF1	8	17.1	
2	11.80	62.0										861.77	80.0	Lsg	OK				S13505	(R)KLLGDDPAAR(T)			40368833	TCOF1	8	17.1	
2	14.98	89.7										721.84	80.0	Ssp	OK				S12285	(K)LLDSRFSVSTLA(KD)			40368833	TCOF1	8	17.1	
2	11.92	70.2										734.32	80.0	VSP	OK				S13785	(K)LLDSRFSVSTLA(KD)			40368833	TCOF1	8	17.1	
2	11.92	70.2										840.40	96.0	Lsp	OK				S112675	(K)LLGAGEGGEASVPER(KT)			40368833	TCOF1	8	17.1	
2	16.06	90.2										818.89	80.0	ESP	OK				S3815	(K)QELKQQAQMLSPR(KT)			40368833	TCOF1	8	17.1	
2	16.57	85.6										661.95	80.0	KSP	OK				S1666	(K)TSCVGAASAPAEPR(K)			40368833	TCOF1	8	17.1	
2	10.28	74.8										661.95	80.0	KSP	OK				S1666	(K)TSCVGAASAPAEPR(K)			40368833	TCOF1	8	17.1	
2	10.28	74.8										721.32	159.9	Psp	APF	OK			S3975	(R)HRPFPAPAPPK(T)			55665396	SRRM1	22	37.1	
2	9.96	77.9										644.28	159.9	Asp	APF	OK			S7475	(K)KAAPFPOSVR(R)			55665396	SRRM1	22	37.1	
2	13.14	66.9										461.21	159.9	Esp	APF	OK			S7496	(K)REPRPAPAPPK(N)			55665396	SRRM1	22	37.1	
3	13.89	75.3										398.97	80.0	Hsp	OK				S4475	(R)RLLPSAPPR(R)			55665396	SRRM1	22	37.1	
2	14.87	85.8										764.32	80.0	Ssp	OK				S3885	(R)RLLPSAPPR(R)			55665396	SRRM1	22	37.1	
2	12.22	66.4										652.31	80.0	Ssp	OK				S7225	(R)ALPSTSSAPPK(R)			55665396	SRRM1	22	37.1	
2	8.29	72.6										717.35	80.0	KFP	OK				T2201	(K)EKDELPEPSV(K)			55665396	SRRM1	22	37.1	
2	9.65	76.7										721.32	159.9	Psp	APF	OK			T4011	(R)HRPFPAPAPPK(T)			55665396	SRRM1	22	37.1	
2	9.96	77.9										619.29	159.9	Rfp	APF	OK			S5925	(K)KAAPFPOSVR(R)			55665396	SRRM1	22	37.1	
3	10.41	84.9										514.57	159.9	Lsp	Asp	OK			S4475	(R)RLLPSAPPR(R)			55665396	SRRM1	22	37.1	
3	10.76	48.1										408.52	159.9	Qsp	APF	OK			S3885	(R)RLLPSAPPR(R)			55665396	SRRM1	22	37.1	
2	8.97	55.1										619.29	159.9	Rfp	APF	OK			S5925	(K)KAAPFPOSVR(R)			55665396	SRRM1	22	37.1	
2	10.07	82.6										548.77	80.0	Vsp	OK				S9008	(R)RYVAPPQGR(R)			55665396	SRRM1	22	37.1	
2	11.21	85.2										894.75	159.9	Vsp	APF	OK			S6145	(R)RYVAPPQGR(R)			55665396	SRRM1	22	37.1	
2	8.55	48.9										532.73	159.9	Vsp	APF	OK			S8185	(K)SRVAVAPGK(T)			55665396	SRRM1	22	37.1	
2	11.77	75.9										568.28	80.0	Asp	OK				S4285	(R)TAPPAPPK(R)			55665396	SRRM1	22	37.1	
3																											

WT-Add	z Score	SPI	Mut-add	z Score	SPI	WT-Targeted	z Score	SPI	WT-INAC	z Score	SPI	WT-RNAi	z Score	SPI	WT-RNAi	z Score	SPI	m/z	Shift (Da)	MH+	Site	Site	Position	Sequence	NCBI	HUGO	Symbol	#	Protein	
2	14.38	87.9																1032.50		159.9	Ssp	729.30	729.30	(R)EPAASPIPTAYGSFAGSHPPTPAPR(K)	56202825	Z207538	PDC038P	2	44.1	
3	15.82	84.6																704.16		80.0	Ssp	399.90	91.1	S2306	(K)KIPAPIPSSAPGPDSDR(Q)	56202825			4	46.1
2	12.36	74.6																919.47		80.0	Asp	ok	ok	S2306	(K)ICELAPAPGAPRPA(R)	56202825			4	46.1
3	21.38	93.1																1166.90		80.0	Asp	ok	ok	S2306	(K)SSSEPAHHPGAPRPSLSLSSLSASSGEVPR(K)	56202825			4	46.1
2	11.80	50.1																788.96		86.0	Asp	ok	ok	S5786	(R)VEGMQAPAPQLP(R)	66302825	TLKI	4	46.1	
2	17.62	90.2																1032.53		80.0	Lsp	ok	ok	S1946	(R)SDVTCVGGGSGSHP(R)	21216428	GATAD2B	3	49.1	
2	15.00	82.4																1099.00		96.0	Lsp	ok	ok	S4886	(R)LQQCALPTTAPAVSVM(K)	21216428	GATAD2B	3	75.1	
2	7.81	65.4																1099.00		96.0	Ssp	ok	ok	S3346	(R)VSAPLPSAPMTDAVSSAA(K)	14041996	GATAD2B	3	75.1	
2	19.24	91.7																744.33		96.0	Ssp	ok	ok	S2346	(R)YMSSTLSPPQPK(L)	21961340	GSN3B	1	91.1	
2	12.16	85.8																1092.48		80.0	Ssp	ok	ok	T4031	(R)IOAAASMTATASDANTGDR(G)	33186798	DDX2	1	93.1	
2	9.38	76.1																807.99		80.0	Ssp	ok	ok	S1096	(R)IDPFSAAVPTSPR(L)	34991767	SLUGT1	1	98.1	
2	11.75	74.5																882.80		80.0	Ssp	ok	ok	S2816	(K)NLYPSKPYTR(N)	10092873	CAPN1	1	102.1	
3	16.22	78.8																816.92		80.0	Ssp	169.70	169.70	S1706	(K)KLSAPKAPERTASIPEDVYR(M)	20579876	POLM13	1	114.1	
2	12.07	62.6																1280.63		80.1	Ssp	169.70	169.70	S1706	(R)SLDCEASPTTAVSHPGAP(A)	71043497	SLC1A1AP	1	55.1	
2	17.11	96.6																744.96		80.0	Ssp	143.44	143.44	S1446	(R)TTLTVKHSVFGSALSLG(K)	1708183	HCTC1	2	12.1	
2	12.07	62.6																1166.66		96.0	Ksp	ok	ok	S5986	(K)VASAPVAVSNPATR(M)	49168854	HCTC1	2	12.1	
2	17.37	86.5																982.96		96.0	Ssp	ok	ok	S2326	(K)SSAPADIAQVGEDLR(T)	3804412	RSN	1	14.1	
2	8.92	48.0																1065.25		79.6	Ssp	43.44	45.1	T431	(K)ASSPSETDEEVDR(V)	32889888	CIT	2	9.1	
2	13.36	67.2																617.90		80.0	Ksp	ok	ok	S1940S	(R)VASAPAPGSPSHR(E)	62998243	NSFL1C	2	98.1	
3	11.70	65.8																534.27		80.0	Ksp	ok	ok	S1146	(R)KKGEMLVDFR(G)	62998243	NSFL1C	2	98.1	
2	15.90	90.0																1197.50		79.8	Ssp	ok	ok	S2726	(K)LGSTAPQVSTSPAPQDAENLAK(A)	4786218	HDCP	2	119.1	
2	16.17	81.9																584.74		80.0	Ssp	ok	ok	T2001	(K)NIGSPGSGR(G)	4786218	HDCP	2	119.1	
2	15.80	93.4																640.80		80.0	Dsp	ok	ok	S1856	(R)RAGDLEDPR(K)	66530846	ZYX	6	77.1	
2	12.91	75.2																1267.90		96.0	Ssp	142.43	142.43	S2816	(R)EVSADLEDSLSLDMDTK(N)	66530846	ZYX	6	77.1	
2	12.46	76.8																838.33		159.9	Fsp	Gsg	Gsg	S2816	(K)FAPGAPGSGSPQDK(L)	66530846	ZYX	6	77.1	
2	12.97	68.5																578.77		80.0	Ssp	ok	ok	S2886	(R)GPPASAPAPK(F)	66530846	ZYX	6	77.1	
2	16.34	70.0																893.09		80.0	Gsp	306.308	306.308	S3086	(K)LGPEALVAGTGPQSFYTAQDR(E)	66530846	ZYX	6	77.1	
2	9.00	70.0																660.29		80.0	Rsp	ok	ok	S3446	(R)PAGAPR(L)T(LK)	4786890	LRRFP1	6	57.1	
2	8.04	55.2																863.96		80.0	Ksp	ok	ok	S6906	(K)IDGATGSPAPAP(S)	4786890	LRRFP1	6	57.1	
3	17.94	93.6																863.96		80.0	Ksp	ok	ok	S9576	(K)KKEPPEYEL(K)	4786890	LRRFP1	6	57.1	
3	23.80	83.2																180.94		80.0	ESE	ok	ok	S1726	(K)CGSGVAVHGQALVAVNEDEAEDEEEDV(K)	33684244	NPM1	4	18.1	
2	11.05	72.0																747.67		96.0	Gsp	ok	ok	S705	(K)DELHVEHMANTEGHP(V)	33684244	NPM1	4	18.1	
2	18.62	83.1																527.73		80.0	Ssp	217.218	219.1	T2191	(K)DSPSSPR(S)	33684244	NPM1	4	18.1	
3	18.62	83.1																506.22		80.0	SAV	ok	ok	S2436	(K)DSEVDE(K)	33684244	NPM1	4	18.1	
3	18.62	83.1																527.73		80.0	Ssp	217.218	219.1	T2191	(K)DSPSSPR(S)	33684244	NPM1	4	18.1	
2	11.05	72.0																506.22		80.0	SAV	ok	ok	S2436	(K)DSEVDE(K)	33684244	NPM1	4	18.1	
2	11.56	74.0																1112.51		80.0	Ssp	ok	ok	S1016	(R)DLSGPFIEVAVQLGSPSPQLAAGAEEGGGR(R)	15147219	PURB	4	116.1	
2	19.10	78.2																795.86		80.0	Ssp	ok	ok	S4186	(R)LPSPVVEEASFR(K)	20357542	CTTN	1	116.1	
2	16.91	89.7																1102.55		80.0	Ssp	ok	ok	T661	(R)AQAQVPEPEEQCALAEQAAAHSR(VR)	13544008	EPB41L3	5	45.1	
2	14.35	88.2																841.43		80.0	Vip	ok	ok	T4871	(K)GSGTNUVLTVEPK(K)	13544008	EPB41L3	5	45.1	
2	17.37	71.6																690.35		80.0	Vip	ok	ok	T5104	(R)KGEVPSISAR(H)	13544008	EPB41L3	5	45.1	
2	13.11	79.0																961.90		96.0	Rel	ok	ok	S4436	(R)ILDGASVNEHEMK(D)	13544008	EPB41L3	5	45.1	
2	11.68	81.4																773.97		80.0	Vsp	ok	ok	S7406	(K)TETFSGVAPGQV(K)	13544008	EPB41L3	5	45.1	
2	10.24	72.1																701.32		159.9	Lsp	ok	ok	S3906	(R)LRLSPPTSR(S)	27436946	LNMA	4	61.1	
2	16.47	80.8																720.33		80.0	Lsp	ok	ok	S3926	(R)ISGAKSSTPLPFR(I)	27436946	LNMA	4	61.1	
2	10.46	70.1																760.31		159.9	Ssp	Lsp	ok	S191	(R)SAGKASSTPLPFR(I)	27436946	LNMA	4	61.1	
3	15.92	67.6																901.04		94.9	Ssp	262.63	64.1	S2646	(R)YQSHAPMmHGQFAGIDSSPEVK(Q)	6463804	PCBP1	1	110.1	
2	17.74	89.5																962.94		80.0	Ssp	ok	ok	T371	(K)LSLEGDHSPSAYGSK(A)	60046388	ANKK2	1	100.1	
2	9.54	75.6																539.27		79.9	Ksa	ok	ok	S1746S	(K)VSCHIKAK(L)	19823466	SRINM2	1	3.1	
2	9.47	71.6																558.29		80.0	Csp	ok	ok	T14921	(K)ALLPCRPR(S)	19823466	SRINM2	1	3.1	
2	9.23	72.8																560.29		80.0	Psp	ok	ok	S2881S	(K)RVPPTPAPK(E)	19823466	SRINM2	4	4.1	
2	14.22	83.6																550.26		159.9	Rsp	ok	ok	T03431	(R)MHP(L)PAPK(E)	19823466	SRINM2	4	4.1	
3	13.41	84.3																817.04		96.0	Esp	ok	ok	S2032S	(R)AIRGQHPSEAVMTFmGDR(Q)	40788894	MDC1	7	10.1	
3	19.11</																													





WT-dd	WT-dd z Score	Mut-dd	Mut-dd z Score	WT-Targeted	WT-Targeted z Score	WT-IMAC	WT-IMAC z Score	WT/IMAC Intensity	Obs. (Da)	m/z	Shift (Da)	MH+	Site	Site	Ambiguity	Position	Sequence	NCBI	HLGO	[a1]	[a2]	Symbol	#	slqdp	Protein	Group #
2	17.04	88.1	2	13.74	73.2	2	14.70	86.0	92.9	967.99	81.0	ASP	OK	OK	S182s	(K)KASPRLSLNATPTVR(R)		9489881	ANLN	3	0	0	25.2			
2	14.82	94.7	2	15.62	89.5	2	13.36	70.8	92.9	773.83	96.0	ASP	OK	OK	S793s	(K)NKAPQSEFMPK(G)		9489881	ANLN	3	0	0	25.2			
3	10.79	56.9	2	13.76	89.6	2	13.56	83.6	92.9	820.91	80.0	TIP	OK	OK	T366t	(K)STPFGTKFLEK(F)		9489881	ANLN	1	0	0	25.2			
2	17.83	91.1	2	15.62	84.3	2	13.56	83.6	70.6	735.71	80.0	TIP	OK	OK	T227t	(K)STIPPAPVLSIQEPPK(RV)		3098601		3	0	0	88.1			
2	19.83	97.6	2	15.62	84.3	2	13.56	83.6	68.4	1081.96	112.0	LSP	OK	OK	S317s	(R)MNTLPCDEEAAGQASSR(S)		5739810	TACC3	2	0	0	50.1			
2	14.81	78.9	2	15.62	84.3	2	13.56	83.6	68.4	1124.00	80.0	GSP	OK	OK	S177s	(K)VSGPEQAVENLSSVSDRR(R)		5739810	TACC3	2	0	0	50.1			
2	14.16	88.0	2	15.62	84.3	2	13.56	83.6	61.6	755.35	80.0	GSP	OK	OK	S1084s	(K)MFGQLQGGSAQPAR(F)		57294201	FLNA	1	0	0	3.1			
2	14.70	86.0	2	15.62	84.3	2	13.56	83.6	50.5	970.48	80.0	EIP	OK	OK	I62t	(K)LDGLVVGTVESLPK(V)		21327708	TRIM28	1	0	0	96.1			
2	14.70	86.0	2	15.62	84.3	2	13.56	83.6	40.8	979.49	80.1	LSP	OK	OK	S752s	(K)LAPPVSPQCFADQVGR(M)		5032179	TRIM28	2	0	0	96.1			
2	14.70	86.0	2	15.62	84.3	2	13.56	83.6	40.8	609.25	96.0	RSG	OK	OK	S473s	(R)SGEEVLSQMLK(K)		5032179	TRIM28	2	0	0	96.1			
2	14.70	86.0	2	15.62	84.3	2	13.56	83.6	36.7	682.29	96.0	RSP	OK	OK	S33s	(R)PPPGMLQNDNR(G)		4826998	SFPQ	1	1	0	63.1			
2	14.70	86.0	2	15.62	84.3	2	13.56	83.6	24.5	566.75	159.9	PSR	OK	OK	S440s	(K)LKERPSR(E)		13634076	TLP2	2	0	0	20.1			
2	12.29	89.0	2	15.62	84.3	2	13.56	83.6	23.4	999.01	80.0	GAY	OK	OK	S415	(R)GKVGDLGGRTITQVTPK(D)		62088704	HNRPK	2	0	0	87.1			
2	19.65	94.7	2	15.62	84.3	2	13.56	83.6	23.4	710.89	80.0	ESP	OK	OK	S357s	(K)LDLSEPK(G)		62088704	HNRPK	2	0	0	87.1			
2	14.52	82.1	2	15.62	84.3	2	13.56	83.6	23.3	481.26	80.0	LSP	OK	OK	S196s	(K)LDLSEPK(G)		4506897	RPL12	1	0	0	94.1			
4	20.25	83.6	2	15.62	84.3	2	13.56	83.6	23.3	925.14	112.0	DG	OK	OK	S38s	(K)MFLPAPQVQVQAFEDAHED*GQEDGEDPDK(R)		56961192	HIDAC2	1	0	0	76.1			
2	11.83	70.6	2	15.62	84.3	2	13.56	83.6	23.1	611.81	80.0	TIP	OK	OK	S394s	(R)MLPAPQVQVQAFEDAHED*GQEDGEDPDK(R)		5174525	MAP1B	2	0	0	7.1			
2	10.31	65.7	2	15.62	84.3	2	13.56	83.6	23.1	722.90	80.0	ASP	OK	OK	T230t	(K)KAPRTTPEV(K)		5174525	MAP1B	2	0	0	7.1			
2	12.62	83.5	2	15.62	84.3	2	13.56	83.6	21.5	703.87	80.0	ASP	OK	OK	S2271s	(R)KAPPLAASPRAQ(LK)		4885377	HIST1H1D	1	0	0	123.1			
2	10.73	82.8	2	15.62	84.3	2	13.56	83.6	17.8	489.77	80.0	ASP	OK	OK	S375s	(K)KALLKAPK(K)		62897783	RPL14	1	0	0	117.1			
2	11.49	86.3	2	15.62	84.3	2	13.56	83.6	16.4	579.31	80.0	LSP	OK	OK	S135s	(R)GRLSPVPR(A)		8051631	RALY	1	0	0	62.1			
2	12.77	82.5	2	15.62	84.3	2	13.56	83.6	16.1	482.76	80.0	ASP	OK	OK	T121t	(K)ALVAPGK(G)		55956788	NCL	2	0	0	62.1			
2	13.10	88.9	2	15.62	84.3	2	13.56	83.6	14.2	601.80	80.0	VSP	OK	OK	S67s	(K)KVVVSPFK(K)		20127499	SFRS6	1	0	0	104.1			
3	15.88	84.6	2	15.62	84.3	2	13.56	83.6	14.1	1131.53	97.0	NSP	OK	OK	S303s	(R)SNAPLPVPSK(A)		19923181	PDUM4	2	0	0	112.1			
2	17.29	91.6	2	15.62	84.3	2	13.56	83.6	14.1	523.42	80.0	VSP	OK	OK	S166s	(R)PVPVHNGSEATLPAQSTLHV*PPSAQPAR(G)		19923181	PDUM4	2	0	0	112.1			
2	15.48	91.1	2	15.62	84.3	2	13.56	83.6	14.0	780.34	96.0	GSP	OK	OK	S112s	(R)HHPEDDGGFTSR(R)		19923181	PDUM4	2	0	0	112.1			
2	12.75	74.3	2	15.62	84.3	2	13.56	83.6	10.3	844.83	96.0	VSP	OK	OK	S499s	(R)HTAPQTQVPR(K)		14043783	EBF1D	1	0	0	67.1			
2	16.24	86.9	2	15.62	84.3	2	13.56	83.6	9.9	1130.03	96.0	HSM	OK	OK	S293s	(R)YHGHMSIDPQSTRT(I)		4503665	PDHA1	1	0	0	96.1			
2	18.61	95.9	2	15.62	84.3	2	13.56	83.6	9.9	978.92	80.0	GIP	OK	OK	T450t	(R)FGQALMEIGALGAPAFNR(A)		2809511	NONO	1	0	0	85.1			
2	13.11	75.3	2	15.62	84.3	2	13.56	83.6	7.8	921.44	80.0	TSP	OK	OK	S62s	(R)WVSSFFDDATFRLGDR(N)		45709422	KPNQ2	1	0	0	80.1			
2	13.56	83.6	2	15.62	84.3	2	13.56	83.6	7.8	902.93	80.0	VIP	OK	OK	T316t	(K)YVGGALNSGRMPFR(T)		46249376	PPP1CB	1	1	0	111.1			
2	7.89	51.5	2	15.62	84.3	2	13.56	83.6	6.0	712.31	80.0	OSP	OK	OK	S74s	(R)RADLNGGDFPSPSR(R)		20148675	EFHD2	1	0	0	122.1			
2	11.38	64.4	2	15.62	84.3	2	13.56	83.6	5.8	712.31	159.9	VSA.PSP	OK	OK	S240s	(K)LDQVAVAPPR(D)		633870	CCDC6	2	0	0	73.1			
2	11.38	64.4	2	15.62	84.3	2	13.56	83.6	3.6	690.31	80.0	ESP	OK	OK	S244s	(K)SEAPEPELRI(K)		133254	HNRPA1	1	1	0	107.1			
2	10.96	70.8	2	15.62	84.3	2	13.56	83.6	3.0	995.89	80.0	GSP	OK	OK	S356s	(R)SSGAPVGGGQVGGSSGGVGR(R)		34740929	HNRPA3	1	1	0	103.1			
2	10.96	70.8	2	15.62	84.3	2	13.56	83.6	1.5	809.39	80.0	GSA	OK	OK	S215s	(R)SSGGFSSGALGINKYR(R)		17318569	KRT1	1	0	0	72.1			



## References

1. Barr, F.A., Sillje, H.H., and Nigg, E.A. (2004). Polo-like kinases and the orchestration of cell division. *Nat Rev Mol Cell Biol* 5, 429-440.
2. Glover, D.M. (2005). Polo kinase and progression through M phase in *Drosophila*: a perspective from the spindle poles. *Oncogene* 24, 230-237.
3. van de Weerd, B.C., and Medema, R.H. (2006). Polo-like kinases: a team in control of the division. *Cell Cycle* 5, 853-864.
4. Golsteyn, R.M., Schultz, S.J., Bartek, J., Ziemiecki, A., Ried, T., and Nigg, E.A. (1994). Cell cycle analysis and chromosomal localization of human Plk1, a putative homologue of the mitotic kinases *Drosophila* polo and *Saccharomyces cerevisiae* Cdc5. *J Cell Sci* 107 (Pt 6), 1509-1517.
5. De Luca, M., Lavia, P., and Guarguaglini, G. (2006). A functional interplay between Aurora-A, Plk1 and TPX2 at spindle poles: Plk1 controls centrosomal localization of Aurora-A and TPX2 spindle association. *Cell Cycle* 5, 296-303.
6. Lane, H.A., and Nigg, E.A. (1996). Antibody microinjection reveals an essential role for human polo-like kinase 1 (Plk1) in the functional maturation of mitotic centrosomes. *J Cell Biol* 135, 1701-1713.
7. Rapley, J., Baxter, J.E., Blot, J., Wattam, S.L., Casenghi, M., Meraldi, P., Nigg, E.A., and Fry, A.M. (2005). Coordinate regulation of the mother centriole component nlp by nek2 and plk1 protein kinases. *Mol Cell Biol* 25, 1309-1324.
8. Ahonen, L.J., Kallio, M.J., Daum, J.R., Bolton, M., Manke, I.A., Yaffe, M.B., Stukenberg, P.T., and Gorbsky, G.J. (2005). Polo-like kinase 1 creates the tension-sensing 3F3/2 phosphoepitope and modulates the association of spindle-checkpoint proteins at kinetochores. *Curr Biol* 15, 1078-1089.
9. Goto, H., Kiyono, T., Tomono, Y., Kawajiri, A., Urano, T., Furukawa, K., Nigg, E.A., and Inagaki, M. (2006). Complex formation of Plk1 and INCENP required for metaphase-anaphase transition. *Nat Cell Biol* 8, 180-187.
10. Liu, X., Zhou, T., Kuriyama, R., and Erikson, R.L. (2004). Molecular interactions of Polo-like-kinase 1 with the mitotic kinesin-like protein CHO1/MKLP-1. *J Cell Sci* 117, 3233-3246.
11. Neef, R., Preisinger, C., Sutcliffe, J., Kopajtich, R., Nigg, E.A., Mayer, T.U., and Barr, F.A. (2003). Phosphorylation of mitotic kinesin-like protein 2 by polo-like kinase 1 is required for cytokinesis. *J Cell Biol* 162, 863-876.
12. Lee, K.S., Park, J.E., Asano, S., and Park, C.J. (2005). Yeast polo-like kinases: functionally conserved multitask mitotic regulators. *Oncogene* 24, 217-229.

13. Yoshida, S., Kono, K., Lowery, D.M., Bartolini, S., Yaffe, M.B., Ohya, Y., and Pellman, D. (2006). Polo-like kinase Cdc5 controls the local activation of Rho1 to promote cytokinesis. *Science* 313, 108-111.
14. Cheng, K.Y., Lowe, E.D., Sinclair, J., Nigg, E.A., and Johnson, L.N. (2003). The crystal structure of the human polo-like kinase-1 polo box domain and its phospho-peptide complex. *Embo J* 22, 5757-5768.
15. Elia, A.E., Rellos, P., Haire, L.F., Chao, J.W., Ivins, F.J., Hoepker, K., Mohammad, D., Cantley, L.C., Smerdon, S.J., and Yaffe, M.B. (2003). The molecular basis for phosphodependent substrate targeting and regulation of plks by the polo-box domain. *Cell* 115, 83-95.
16. Donaldson, M.M., Tavares, A.A., Ohkura, H., Deak, P., and Glover, D.M. (2001). Metaphase arrest with centromere separation in polo mutants of *Drosophila*. *J Cell Biol* 153, 663-676.
17. Qian, Y.W., Erikson, E., Taieb, F.E., and Maller, J.L. (2001). The polo-like kinase Plx1 is required for activation of the phosphatase Cdc25C and cyclin B-Cdc2 in *Xenopus* oocytes. *Mol Biol Cell* 12, 1791-1799.
18. Liu, X., Lei, M., and Erikson, R.L. (2006). Normal cells, but not cancer cells, survive severe Plk1 depletion. *Mol Cell Biol* 26, 2093-2108.
19. Spankuch-Schmitt, B., Wolf, G., Solbach, C., Loibl, S., Knecht, R., Stegmüller, M., von Minckwitz, G., Kaufmann, M., and Strebhardt, K. (2002). Downregulation of human polo-like kinase activity by antisense oligonucleotides induces growth inhibition in cancer cells. *Oncogene* 21, 3162-3171.
20. van Vugt, M.A., Bras, A., and Medema, R.H. (2004). Polo-like kinase-1 controls recovery from a G2 DNA damage-induced arrest in mammalian cells. *Mol Cell* 15, 799-811.
21. van Vugt, M.A., van de Weerd, B.C., Vader, G., Janssen, H., Calafat, J., Klompaker, R., Wolthuis, R.M., and Medema, R.H. (2004). Polo-like kinase-1 is required for bipolar spindle formation but is dispensable for anaphase promoting complex/Cdc20 activation and initiation of cytokinesis. *J Biol Chem* 279, 36841-36854.
22. Liu, X., Lin, C.Y., Lei, M., Yan, S., Zhou, T., and Erikson, R.L. (2005). CCT chaperonin complex is required for the biogenesis of functional Plk1. *Mol Cell Biol* 25, 4993-5010.
23. Lowery, D.M., Lim, D., and Yaffe, M.B. (2005). Structure and function of Polo-like kinases. *Oncogene* 24, 248-259.

24. Ohkura, H., Hagan, I.M., and Glover, D.M. (1995). The conserved *Schizosaccharomyces pombe* kinase *plp1*, required to form a bipolar spindle, the actin ring, and septum, can drive septum formation in G1 and G2 cells. *Genes Dev* 9, 1059-1073.
25. Song, S., and Lee, K.S. (2001). A novel function of *Saccharomyces cerevisiae* CDC5 in cytokinesis. *J Cell Biol* 152, 451-469.
26. Carmena, M., Riparbelli, M.G., Minestrini, G., Tavares, A.M., Adams, R., Callaini, G., and Glover, D.M. (1998). *Drosophila* polo kinase is required for cytokinesis. *J Cell Biol* 143, 659-671.
27. Zhou, T., Aumais, J.P., Liu, X., Yu-Lee, L.Y., and Erikson, R.L. (2003). A role for Plk1 phosphorylation of NudC in cytokinesis. *Dev Cell* 5, 127-138.
28. Glotzer, M. (2005). The molecular requirements for cytokinesis. *Science* 307, 1735-1739.
29. Niiya, F., Tatsumoto, T., Lee, K.S., and Miki, T. (2006). Phosphorylation of the cytokinesis regulator ECT2 at G2/M phase stimulates association of the mitotic kinase Plk1 and accumulation of GTP-bound RhoA. *Oncogene* 25, 827-837.
30. Elia, A.E., Cantley, L.C., and Yaffe, M.B. (2003). Proteomic screen finds pSer/pThr-binding domain localizing Plk1 to mitotic substrates. *Science* 299, 1228-1231.
31. Feng, Y., Hodge, D.R., Palmieri, G., Chase, D.L., Longo, D.L., and Ferris, D.K. (1999). Association of polo-like kinase with alpha-, beta- and gamma-tubulins in a stable complex. *Biochem J* 339 ( Pt 2), 435-442.
32. GO Consortium. (2001). Creating the gene ontology resource: design and implementation. *Genome Res* 11, 1425-1433.
33. Tsvetkov, L., and Stern, D.F. (2005). Interaction of chromatin-associated Plk1 and Mcm7. *J Biol Chem* 280, 11943-11947.
34. Straight, A.F., Field, C.M., and Mitchison, T.J. (2005). Anillin binds nonmuscle myosin II and regulates the contractile ring. *Mol Biol Cell* 16, 193-201.
35. Feng, Y., Longo, D.L., and Ferris, D.K. (2001). Polo-like kinase interacts with proteasomes and regulates their activity. *Cell Growth Differ* 12, 29-37.
36. Tarnowka, M.A., and Baglioni, C. (1979). Regulation of protein synthesis in mitotic HeLa cells. *J Cell Physiol* 99, 359-367.

37. Kim, J.H., Paek, K.Y., Choi, K., Kim, T.D., Hahm, B., Kim, K.T., and Jang, S.K. (2003). Heterogeneous nuclear ribonucleoprotein C modulates translation of c-myc mRNA in a cell cycle phase-dependent manner. *Mol Cell Biol* 23, 708-720.
38. Shin, C., and Manley, J.L. (2002). The SR protein SRp38 represses splicing in M phase cells. *Cell* 111, 407-417.
39. Warren, G. (1993). Membrane partitioning during cell division. *Annu Rev Biochem* 62, 323-348.
40. Darieva, Z., Bulmer, R., Pic-Taylor, A., Doris, K.S., Geymonat, M., Sedgwick, S.G., Morgan, B.A., and Sharrocks, A.D. (2006). Polo kinase controls cell-cycle-dependent transcription by targeting a coactivator protein. *Nature* 444, 494-498.
41. Kim, S.A., Yoon, J.H., Lee, S.H., and Ahn, S.G. (2005). Polo-like kinase 1 phosphorylates heat shock transcription factor 1 and mediates its nuclear translocation during heat stress. *J Biol Chem* 280, 12653-12657.
42. Nakajima, H., Toyoshima-Morimoto, F., Taniguchi, E., and Nishida, E. (2003). Identification of a consensus motif for Plk (Polo-like kinase) phosphorylation reveals Myt1 as a Plk1 substrate. *J Biol Chem* 278, 25277-25280.
43. Robinson, D.N., and Spudich, J.A. (2004). Mechanics and regulation of cytokinesis. *Curr Opin Cell Biol* 16, 182-188.
44. Mishra, G.R., Suresh, M., Kumaran, K., Kannabiran, N., Suresh, S., Bala, P., Shivakumar, K., Anuradha, N., Reddy, R., Raghavan, T.M., Menon, S., Hanumanthu, G., Gupta, M., Upendran, S., Gupta, S., Mahesh, M., Jacob, B., Mathew, P., Chatterjee, P., Arun, K.S., Sharma, S., Chandrika, K.N., Deshpande, N., Palvankar, K., Raghavnath, R., Krishnakanth, R., Karathia, H., Rekha, B., Nayak, R., Vishnupriya, G., Kumar, H.G., Nagini, M., Kumar, G.S., Jose, R., Deepthi, P., Mohan, S.S., Gandhi, T.K., Harsha, H.C., Deshpande, K.S., Sarker, M., Prasad, T.S., and Pandey, A. (2006). Human protein reference database--2006 update. *Nucleic Acids Res* 34, D411-414.
45. Daniels, M.J., Wang, Y., Lee, M., and Venkitaraman, A.R. (2004). Abnormal cytokinesis in cells deficient in the breast cancer susceptibility protein BRCA2. *Science* 306, 876-879.
46. Fabbro, M., Zhou, B.B., Takahashi, M., Sarcevic, B., Lal, P., Graham, M.E., Gabrielli, B.G., Robinson, P.J., Nigg, E.A., Ono, Y., and Khanna, K.K. (2005). Cdk1/Erk2- and Plk1-dependent phosphorylation of a centrosome protein, Cep55, is required for its recruitment to midbody and cytokinesis. *Dev Cell* 9, 477-488.

47. Litvak, V., Argov, R., Dahan, N., Ramachandran, S., Amarilio, R., Shainskaya, A., and Lev, S. (2004). Mitotic phosphorylation of the peripheral Golgi protein Nir2 by Cdk1 provides a docking mechanism for Plk1 and affects cytokinesis completion. *Mol Cell* *14*, 319-330.
48. Yamaguchi, T., Goto, H., Yokoyama, T., Sillje, H., Hanisch, A., Uldschmid, A., Takai, Y., Oguri, T., Nigg, E.A., and Inagaki, M. (2005). Phosphorylation by Cdk1 induces Plk1-mediated vimentin phosphorylation during mitosis. *J Cell Biol* *171*, 431-436.
49. Zhang, H., Shi, X., Paddon, H., Hampong, M., Dai, W., and Pelech, S. (2004). B23/nucleophosmin serine 4 phosphorylation mediates mitotic functions of polo-like kinase 1. *J Biol Chem* *279*, 35726-35734.
50. Goto, H., Kosako, H., Tanabe, K., Yanagida, M., Sakurai, M., Amano, M., Kaibuchi, K., and Inagaki, M. (1998). Phosphorylation of vimentin by Rho-associated kinase at a unique amino-terminal site that is specifically phosphorylated during cytokinesis. *J Biol Chem* *273*, 11728-11736.
51. Matsumura, F. (2005). Regulation of myosin II during cytokinesis in higher eukaryotes. *Trends Cell Biol* *15*, 371-377.
52. Kosako, H., Yoshida, T., Matsumura, F., Ishizaki, T., Narumiya, S., and Inagaki, M. (2000). Rho-kinase/ROCK is involved in cytokinesis through the phosphorylation of myosin light chain and not ezrin/radixin/moesin proteins at the cleavage furrow. *Oncogene* *19*, 6059-6064.
53. Brar, G.A., Kiburz, B.M., Zhang, Y., Kim, J.E., White, F., and Amon, A. (2006). Rec8 phosphorylation and recombination promote the step-wise loss of cohesins in meiosis. *Nature* *441*, 532-536.
54. Beausoleil, S.A., Villen, J., Gerber, S.A., Rush, J., and Gygi, S.P. (2006). A probability-based approach for high-throughput protein phosphorylation analysis and site localization. *Nat Biotechnol* *24*, 1285-1292.
55. Ishizaki, T., Maekawa, M., Fujisawa, K., Okawa, K., Iwamatsu, A., Fujita, A., Watanabe, N., Saito, Y., Kakizuka, A., Morii, N., and Narumiya, S. (1996). The small GTP-binding protein Rho binds to and activates a 160 kDa Ser/Thr protein kinase homologous to myotonic dystrophy kinase. *Embo J* *15*, 1885-1893.
56. Yokoyama, T., Goto, H., Izawa, I., Mizutani, H., and Inagaki, M. (2005). Aurora-B and Rho-kinase/ROCK, the two cleavage furrow kinases, independently regulate the progression of cytokinesis: possible existence of a novel cleavage furrow kinase phosphorylates ezrin/radixin/moesin (ERM). *Genes Cells* *10*, 127-137.

57. Emoto, K., Inadome, H., Kanaho, Y., Narumiya, S., and Umeda, M. (2005). Local change in phospholipid composition at the cleavage furrow is essential for completion of cytokinesis. *J Biol Chem* *280*, 37901-37907.
58. Wolf, A., Keil, R., Gotzl, O., Mun, A., Schwarze, K., Lederer, M., Huttelmaier, S., and Hatzfeld, M. (2006). The armadillo protein p0071 regulates Rho signalling during cytokinesis. *Nat Cell Biol* *8*, 1432-1440.
59. Amano, M., Chihara, K., Nakamura, N., Fukata, Y., Yano, T., Shibata, M., Ikebe, M., and Kaibuchi, K. (1998). Myosin II activation promotes neurite retraction during the action of Rho and Rho-kinase. *Genes Cells* *3*, 177-188.
60. Wilker, E.W., Grant, R.A., Artim, S.C., and Yaffe, M.B. (2005). A structural basis for 14-3-3sigma functional specificity. *J Biol Chem* *280*, 18891-18898.
61. Dickins, R.A., Hemann, M.T., Zilfou, J.T., Simpson, D.R., Ibarra, I., Hannon, G.J., and Lowe, S.W. (2005). Probing tumor phenotypes using stable and regulated synthetic microRNA precursors. *Nat Genet* *37*, 1289-1295.
62. Hjerrild, M., Stensballe, A., Rasmussen, T.E., Kofoed, C.B., Blom, N., Sicheritz-Ponten, T., Larsen, M.R., Brunak, S., Jensen, O.N., and Gammeltoft, S. (2004). Identification of phosphorylation sites in protein kinase A substrates using artificial neural networks and mass spectrometry. *J Proteome Res* *3*, 426-433.
63. Pinkse, M.W., Uitto, P.M., Hilhorst, M.J., Ooms, B., and Heck, A.J. (2004). Selective isolation at the femtomole level of phosphopeptides from proteolytic digests using 2D-NanoLC-ESI-MS/MS and titanium oxide precolumns. *Anal Chem* *76*, 3935-3943.
64. Rappsilber, J., Ishihama, Y., and Mann, M. (2003). Stop and go extraction tips for matrix-assisted laser desorption/ionization, nanoelectrospray, and LC/MS sample pretreatment in proteomics. *Anal Chem* *75*, 663-670.
65. Jang, Y.J., Ma, S., Terada, Y., and Erikson, R.L. (2002). Phosphorylation of threonine 210 and the role of serine 137 in the regulation of mammalian polo-like kinase. *J Biol Chem* *277*, 44115-44120.
66. Mundt, K.E., Golsteyn, R.M., Lane, H.A., and Nigg, E.A. (1997). On the regulation and function of human polo-like kinase 1 (PLK1): effects of overexpression on cell cycle progression. *Biochem Biophys Res Commun* *239*, 377-385.

# Chapter Three

## **Mitotic Specific Yeast Two Hybrid and Chemical Genetic Substrate Trap Reveal Roles for Budding Yeast Polo-like Kinase in Cytokinesis and Nuclear Positioning**

To be Published as:

Drew M. Lowery, Satoshi Yoshida, Duaa H. Mohammad, Jennifer L. Paulson,  
Kevan M. Shokat, David Pellman, and Michael B. Yaffe.

Mitotic Specific Yeast Two Hybrid Reveals Multiple Roles for Budding Yeast  
Polo-like Kinase Cdc5 in Late Mitosis (in preparation)  
and

Jennifer L. Paulson, M. Sullivan, Drew M. Lowery, M. S. Cohen, D. Randle, J. Taunton,  
Michael B. Yaffe, David O. Morgan, and Kevan M. Shokat.

A coupled chemical genetic and bioinformatic approach to  
Polo-like kinase pathway exploration (in preparation)

### Contributions:

Satoshi helped me perform the PBD pulldown assay, provided budding yeast method expertise, generated some of the yeast strains, and helped make the yeast genetic work happen through his encouragement. Duaa helped design the yeast two hybrid strategy after conception, performed the yeast two hybrid mating with me, consulted on the PBD peptide binding experiment, and was a significant intellectual influence. Jen generated the *cdc5-as1* allele and strains, performed the screen for Cdc5 substrates, wrote and made the figures dealing with this screen (Figures 3.8-3.9), and performed the work verifying Spc72 as a Cdc5 substrate (Figures 3.10 and 3.11A). Kevan provided intellectual support and experimental design for the Cdc5 substrate screen. David provided tremendous intellectual support, contributed greatly to the design of the yeast genetic experiments, and provided much encouragement. Michael helped conceive the context dependent yeast two hybrid strategy and provided intellectual support on all experiments. I performed all the experiments related to the yeast two hybrid screen, PBD pulldown assay, and *cy3* and *cnm67* work, conceived the specific second stage of the yeast two hybrid that was used here, performed the bioinformatic analysis, and wrote and made the figures dealing with all these aspects of the work presented here.

## **Abstract**

Protein phosphorylation is a ubiquitous regulatory mechanism for cellular signal propagation, and the complexity of signaling networks presents a challenge to protein kinase substrate identification. Substrates of Polo-like kinases are largely unknown, despite the significant role of these kinases in coordinating mitotic cell cycle progression. Here, we combine a novel application of the yeast two hybrid system to identify mitotic-specific interactors of the polo-box domain of the budding yeast polo-like kinase with chemical genetic, bioinformatic, and yeast proteomic tools for Polo-like kinase substrate identification. The results from the yeast two hybrid screen were validated through a polo-box domain pulldown screen from the TAP-tagged collection of yeast strains. In total, 27 proteins were validated to be phosphorylation-dependent polo-box domain interactors, out of 112 proteins attempted. Systematically-chosen candidate Cdc5 substrates were examined for loss of phosphorylation upon cellular Cdc5 inhibition using a mono-specific pharmacological inhibitor, revealing five novel Cdc5 substrates. We undertook further studies on *Cyk3* (identified by yeast two hybrid), *Cnm67* (identified by bioinformatics), and *Spc72* (identified as a Cdc5 substrate by chemical genetics). All three proteins are in vitro substrates of Polo-like kinases, and contain polo-box domain binding consensus motifs that, when mutated, eliminate Cdc-PBD binding. Interaction-defective genetic studies with these mutants to determine whether PBD binding affects their in vivo function are in process demonstrating a role for Cdc5 in regulating septum-dependent cytokinesis through *Cyk3*, and mitotic nuclear positioning through *Cnm67* and *Spc72*.



## **Introduction**

Ensuring accurate chromosome segregation is fundamental to survival of a species. Temporally and spatially regulated signaling events are required to monitor and direct multiple cellular events during cell division. The Polo-like family of serine/threonine protein kinases (Plks) have emerged as an important class of cell cycle regulators that coordinate mitotic progression, with multiple roles from mitotic entry to cytokinesis [1]. Humans have four Plks (Plk1-4), of which Plk1 is the most thoroughly characterized, motivated by its link to tumor development [1]. The budding yeast *S. cerevisiae* has a single Plk, Cdc5, with 49% identity to Plk1 in its kinase domain [2]. Cdc5 functions in adaptation to the DNA damage checkpoint, progression through G2/M, cohesin cleavage at anaphase entry, and cytokinesis, with an essential role in promoting mitotic exit as part of two signaling networks called FEAR and MEN [2].

The existence of a single Plk, the availability of several comprehensive strain libraries of epitope-tagged genes [3], and the availability of chemical genetic tools for dissection of kinases in budding yeast [4], makes it an attractive organism for the study of Plk signaling pathways. Despite the multiple mitotic functions of Cdc5, only a few of its substrates have been conclusively identified [5-8]. Cdc5 substrates are difficult to identify for several reasons. First, both Cdc5 and its known substrates are low abundance proteins present at less than 1500 copies per cell [3]. Additional Cdc5 substrates are also likely to be low abundance, as this is generally true for cell-cycle regulatory proteins [3]. Furthermore, characterized phosphorylation sites in Plk substrates have considerable sequence variation [9] and are of limited utility in identifying likely candidate substrates.

This variation in phosphorylation site preference suggests alternative specificity determinants, such as temporal and spatial regulation. Cdc5 levels are tightly cell cycle-regulated with maximal activity in mitosis [2]. Cdc5's distinct localization pattern includes the cytoplasmic face of the spindle pole body (SPB, the functional equivalent to the mammalian centrosome), chromosomes, and the bud neck (the future site of cytokinesis) [7, 10-12]. Accurate chromosome segregation requires coordination between these structures. Cytoplasmic microtubules project from the SPB projects to

move one set of duplicated chromosomes through the predetermined cleavage plane at the bud neck [13]. Cytokinesis initiation follows a MEN signal at the SPB, which monitors this anaphase spindle migration [13]. Mutations in a conserved C-terminal region of Plks called the polo box domain (PBD) disrupt this Cdc5 sub-cellular localization pattern [11]. The PBD is a phospho-serine/threonine binding module that can directly target Plks to their substrates after prior “priming” phosphorylation of the substrate by an upstream kinase [9, 14].

To identify further Cdc5 substrates, we used multiple independent methods. First, we developed a novel modification of the yeast two hybrid system to identify mitotic-specific interactors of the Cdc5-PBD, which are likely to also be Cdc5 substrates [9]. Secondly, we utilized a bioinformatic approach to rank-order all yeast proteins as potential Cdc5 substrates. Thirdly, we directly identified Cdc5 substrates using a mono-specific Cdc5 inhibitor, providing for interruption of the kinase substrate reaction at any point in the cell cycle with preservation of the endogenous expression levels of all the components. Hits from these screens were further verified as phosphospecific Cdc5 binders in a Cdc5-PBD pulldown assay. We are further analyzing the *in vivo* role of Cyk3, identified by yeast two hybrid, Cnm67, identified by bioinformatics, and Spc72, identified with the Cdc5 inhibitor assay. Spc72 and Cnm67 have known roles in anchoring cytoplasmic microtubules at the spindle pole body and function in nuclear positioning similar to the phenotype seen with Cdc5 inhibition. Cyk3 plays a role in the cytokinesis septum pathway. We show that all three proteins are *in vitro* substrates of Polo-like kinases, and experiments are in progress to analyze the regulation of these proteins by Cdc5 through interaction-defective genetics experiments, utilizing mutants of these proteins that no longer bind to the Cdc5-PBD.

## **Results and Discussion**

### **A Context Dependent Yeast Two Hybrid Screen for the Cdc5 Polo-box Domain**

To identify Cdc5-PBD interactors, we designed a novel yeast two hybrid screen. Standard yeast two hybrid screens have been successful in identifying some Plk interactors including six with full length Cdc5 [15-19], and a report that contained the full results of a PBD yeast two hybrid screen only identified eight interactors [20]. The total number of PBD interactors in yeast is likely to be much higher. Given our identification of over 600 specific Plk1-PBD interactors by a pulldown mass spectrometry approach (Chapter Two) [22], and a gene ratio of approximately five for human to yeast, we expect there to be 120 interactors of the Cdc5-PBD. Thus, there is a large discrepancy between the number of yeast two hybrid-identified PBD interactions and the actual number that exist. The reason that standard yeast two hybrids have not been more successful in identifying PBD interactors is because, for the most part, these interactors are context-dependent. Interactions between the PBD and its ligands take place only during mitosis and are dependent on phosphorylation of those ligands by CDKs or other mitotic kinases [14, 23]. Thus, the challenge was to design a novel yeast two hybrid approach that was sensitive to context-dependent interactions, and was able to separate these specific interactions that occur only at specific points during the cell cycle from the noise inherent in a yeast two hybrid assay.

One new application of the yeast two hybrid system had been designed for exactly this purpose. Guo and colleagues designed a yeast two hybrid strain that tethered a particular kinase or acetyltransferase to a bait protein of interest, and then performed a standard yeast two hybrid screen [24]. This strategy was able to identify either phosphorylation- or acetylation-dependent interactions of the particular bait proteins employed [24]. While this is certainly a viable strategy for many molecules, it requires the exogenous enzyme to function in yeast cells and in a cis configuration to its target. More critically, it only functions to identify the modification dependent interactions of one protein, and is not able to efficiently identify all the proteins that interact with a modification-dependent binding domain, such as the PBD. Also, overexpression or

altered activation of some enzymes, such as cell cycle kinases, will prevent normal yeast cell growth, which is a requirement for visualization of yeast two hybrid results, as the positive signal is a yeast colony. Thus, this strategy would not work to identify PBD interactors, though it may work to identify the PBD as an interactor of a particular bait protein if the upstream kinase is chosen correctly.

To overcome some of these difficulties, we chose to identify the interactors of the PBD of the budding yeast Plk, Cdc5, rather than the human homolog. Searching for interactions between yeast proteins within yeast cells eliminates many of the contextual challenges, as the appropriate kinases required for the phosphorylation-dependent interactions are expressed normally, eliminating the need to express an exogenous kinase or to rely on yeast kinases to phosphorylate human proteins. Also, since some of the endogenous Cdc5 is nuclear interactions between the Cdc5-PBD and its ligands can take place in the nucleus, which is required for interactions to drive gene expression in the yeast two hybrid system. Thus, for example, identification of growth factor signaling-dependent interactions in this system might be challenging since the kinases responsible for generating the binding sites are only present in the cytoplasm.

As the first step in identifying Cdc5-PBD interactions we undertook a standard yeast two hybrid screen as outlined in Figure 3.1A top. The Cdc5-PBD fused to the Gal4 DNA binding domain was used as the bait to screen for interaction with a library of yeast genomic DNA fused to the Gal4 activation domain. The Cdc5-PBD and library expressing strains were of separate mating type so interactions were detected by mating, selection of diploids that contained both genes, and growth on plates lacking adenine. The *ade2* gene is under the control of Gal4 in this strain, so only in yeast with an interaction between the Cdc5-PBD and the library fragment would this gene be expressed and the yeast be able to survive without adenine supplemented in the media. As expected, a vast number of colonies grew, indicating a large number of interactors. In order to weed out the non-specific interactors and the general noise in the system, a harsh selection criteria could have been employed, which likely would have resulted in similar results to previous studies with a few high affinity interactions being identified. Instead, as described earlier, a more comprehensive approach that strategically identified the mitotic-specific interactions was desired.

In order to achieve specificity for mitotic interactions, a measurement of interaction strength under normal conditions versus mitotic conditions was required. The budding yeast cell cycle is ninety minutes long with thirty minutes spent in mitosis, so the mitotic-specific interactions should be present among the more weakly interacting clones in the standard yeast two hybrid set-up. To enrich for cells in mitosis, we employed a strategy of growing the yeast on plates containing benomyl, which is a microtubule poison that disrupts the mitotic spindle and slows down or stops mitosis. Diploid yeast, of the yeast two hybrid strain used here, were tested for their ability to grow on different levels of benomyl (Figure 3.1B). The optimal concentration of benomyl for continued slow growth without massive death was determined to be 25 $\mu$ g/ml, and this was used in all further studies. As a way to measure the interaction strength, a qualitative colorimetric assay was employed (Figure 3.1A bottom). In addition to the commonly known  $\beta$ -galactosidase, budding yeast also produce  $\alpha$ -galactosidase under the control of a galactose inducible promoter, which is expressed upon interaction in the yeast two hybrid strain. This enzyme is secreted, and its activity can be monitored through the addition of X- $\alpha$ -galactose to the media, which the enzyme cleaves into a blue substrate. Thus, to measure the interaction strength of the hits from the first stage yeast two hybrid under the mitotically-enriched condition of growth in the presence of benomyl, the yeast clones were grown on plates containing X- $\alpha$ -gal with or without benomyl (Figure 3.1A bottom). A total of around 1500 colonies were picked as hits from the first stage yeast two hybrid and tested in the second stage mitotic enrichment screen. As this second stage is a qualitative assay the blue color was compared by eye and 264 colonies with significantly darker blue color on the plates containing benomyl were selected as hits (Figure 3.1C).

This second step has the added benefit of eliminating any self-activating sequences, because they would not have an enhanced signal with the benomyl treatment. Normally, with a genomic library, such as the one used here, a high percentage of hits in a yeast two hybrid are actually sequences that can act to directly activate gene transcription without an interaction with the bait protein. This requires another time-consuming step to independently test all hits for self-activation in the absence of the bait protein. None of the identified hits from the second stage of the yeast two hybrid were

found to self-activate when tested, whereas seven out of seventy-five of a random sample of hits that passed the first step of the yeast two hybrid were found to be self-activating.

Sequencing of the hits from the second stage identified 112 ORFs (Table 3.1) that are involved in many expected and unexpected processes. Classification of the ORFs by GO terms (Figure 3.2A) revealed that the second most populated category, after uncharacterized, was the expected category of cell cycle. A more specific breakdown of the cell cycle proteins (Figure 3.2B) revealed that these proteins participated in the known Cdc5-regulated processes of cytokinesis, spindle control, mitotic exit, general mitosis, meiosis, and the unexpected category of nuclear pore dynamics. The nuclear pore is known to dramatically alter its structure and function during mitosis and throughout the cell cycle [25-28] as suggested by the fact that these two nuclear pore proteins, Nup170 and Nup188, are categorized by GO terms as having a cell cycle regulatory role. Whether Cdc5 is involved in this process is presently unknown, although the yeast two hybrid interactions between Cdc5-PBD and these nuclear pore proteins suggest that this might be the case. The other major categories of interactors (Figure 3.2A) are similarly known to be regulated during the cell cycle, and in particular in mitosis, but are not currently known to be regulated by Cdc5 or other Plks [2, 9, 29-32].

Despite the fact that yeast two hybrid interactions are assumed to be direct the proteins identified as interacting with the Cdc5-PBD could be direct or could be part of complexes that interact with the Cdc5-PBD. To partially address this, we checked for the presence of optimal PBD binding motifs within all the identified ORFs (Table 3.1). The optimal binding motif for the Cdc5-PBD, as determined by oriented peptide library screening, is the same as for the Plk1-PBD, S(pS/pT)P with a minimal motif of S(pS/pT) [23]. All but two of the 112 sequenced ORFs contains this minimal motif (much higher than expected based on a random set of yeast proteins), suggesting that they may be direct interactors of the Cdc5-PBD, if the proteins are phosphorylated during mitosis. In addition 37 of the 112 (one third, significantly higher than the one quarter of a random set of yeast proteins that contain this motif) contain an optimal binding motif (Table 3.1) which could be generated by the budding yeast CDK Cdc28, and 11 of these 37 are known to be Cdc28 substrates [21]. Thus, for these 37 proteins, we can hypothesize that Cdc28 phosphorylates these proteins at their S(S/T)P motifs and generates a Cdc5-PBD

binding site. Intriguingly, 61 of the 112 identified proteins have human homologs, based on the identification of a human gene BLAST hit using the yeast gene with an E value greater than  $1 \times 10^6$ , so many of the interactions could be conserved in human cells.

### **Bioinformatic Screen for Additional Cdc5 Polo-box Domain Interactors**

The consensus phosphorylation motif of Cdc5 has not been determined, but there are a few pieces of information that allow us to infer Cdc5's optimal phosphorylation motif. Expression of both Plk1 and Plk3 can rescue a yeast strain harboring a *cdc5-1* allele at the restrictive temperature [33]. Thus, the phosphorylation motif of Cdc5 must overlap significantly with Plk1 and Plk3. The published phosphorylation motif of Plk1 is (E/D)X(S/T)(aliphatic) [34], and more recently, several sites have been mapped with an N in the -2 position consistent with our own in vitro results (Jes Alexander – personal communication). Unfortunately, the motif of Plk3 has not been published, but it is thought to be similar to Plk1 (Jes Alexander – personal communication). Of the mapped Cdc5 phosphorylation sites, they all fall within this general consensus [5-7, 35], and the N in the -2 position seems to be favored by Cdc5 [1]. A sequence alignment of the kinase domains of Plk1, Plk3, and Cdc5 reveals that all three kinases have similar degrees of homology with each other, with Cdc5 being slightly more similar to Plk1 (47% identical) than Plk3 (41% identical) (Figure 3.3A,B). The only known critical residue for regulation of Plks (T210 in Plk1) is conserved in all three kinases and the motif surrounding it is highly conserved (Figure 3.3B). A structure of the kinase domain of Plk1 is now available [36], and what limited information can be inferred about the preferred phosphorylation motif fits with the prior data. Similarly, models of the kinase domain structures of Plk1 and Plk3 [9] suggest that both kinases have the same phosphorylation motif. Thus, we conclude that the known phosphorylation motif for Plk1 is a good approximation of the phosphorylation motif for Cdc5.

Utilizing the approximate Cdc5 phosphorylation motif (E/D/N)X(S/T) and the known Cdc5-PBD binding motif S(S/T)P [23] allows identification of potential Cdc5 substrates through bioinformatics (Figure 3.4A). Briefly, the roughly six thousand predicted yeast proteins were searched with the Scansite profile scanning algorithm [37,

38] for Cdc5 binding and phosphorylation sequence motifs, generating a “Cdc5 substrate likelihood score” for each protein (more details are available in Methods). The distribution of scores is represented in Figure 3.4B, with high scores representing likely substrates. Notably, the group of best scoring-potential Cdc5 substrates was enriched in low abundance proteins relative to the entire proteome, requiring a sensitive test of candidate phosphorylation (Figure 3.4C). Cdc5 substrate likelihood scores, combined with functional criteria including previous demonstration of a cell cycle role and localization that matched that of Cdc5, led us to choose 192 total candidate substrates. Functional criteria are a useful filter for substrate sets [39], without which this approach would not have been possible. Among the proteins identified by this approach were the known Cdc5 substrates; Mcd1, Bfa1, and Swe1[5-7], with Swe1, notably, the only of the three previously shown to directly bind the PBD, ranked 12th highest overall.

#### **Validation of Cdc5 Polo-box Domain Interactors by Pull-down**

The Cdc5-PBD was known to be a phosphopeptide binding domain from previous studies [23] which identified a phosphobinding motif. However, since the Cdc5-PBD had not been crystalized, it was not entirely clear what mutant of the Cdc5-PBD should be made to eliminate the phosphopeptide binding. A sequence alignment of the Plk1-PBD and the Cdc5-PBD (Figure 3.5B) revealed that the critical residues for phosphopeptide binding, based on the Plk1-PBD structure [23, 40], were conserved in the Cdc5-PBD. Mutation of the analogous residues to the “pincer mutant” in Plk1-PBD [23] were generated (H641A/K643M) and tested in a phosphopeptide binding experiment. Cdc5-PBD wild-type or the mutant were *in vitro* transcribed and translated in the presence of [<sup>35</sup>S]-methionine, and then bound to a degenerate peptide library that matched the minimal consensus sequence of CDK phosphorylation or its non-phosphorylated counterpart. The wild-type Cdc5-PBD bound specifically to the phosphorylated peptide library as expected, and the mutant version bound weakly to both libraries (Figure 3.5C left). As a positive control, the Plk1-PBD and its mutant were also tested (Figure 3.5C right) and gave the same results as previously [23]. This confirms that the Cdc5-PBD is functioning as a phosphobinding domain, in an analogous way to



the Plk1-PBD, and identifies this mutant version of the Cdc5-PBD as an optimal negative control for Cdc5-PBD binding experiments. A domain map of Cdc5 with critical residues is shown in Figure 3.5A.

To further assess whether the proteins identified by the yeast two hybrid and the bioinformatic method were actual ligands of the Cdc5-PBD, we designed a PBD pulldown screen. The recently-generated TAP-tagged yeast strains were used as a source to generate lysates with tagged yeast proteins [3]. These lysates were then incubated with beads coated with either the wild-type Cdc5-PBD or the mutant Cdc5-PBD, identified earlier as not able to bind phosphopeptides. After extensive washing, interaction was detected by a western blot against the TAP tag using goat anti-rabbit IgG. Unfortunately, this detection procedure also recognized the Cdc5-PBD (Figures 3.6 and 3.7), preventing the interrogation of any proteins that run at the same size as the Cdc5-PBD. The criteria for choosing which proteins to interrogate was as follows: a TAP-tagged strain for the gene existed; the predicted size of the TAP-tagged protein did not overlap with the signal for the Cdc5-PBD; and a sufficient number of molecules per cell [3] had to exist to allow visualization of the protein. After applying these criteria all the remaining proteins identified by the yeast two hybrid method were attempted, as well as the top hits of the bioinformatic screen, up to a total of 110 TAP-tagged strains (Table 3.2). Of these 110 strains, 81 proteins could be seen in the lysate, 27 interacted specifically with the wild-type Cdc5-PBD (Figure 3.6), and 17 interacted non-specifically with both the wild-type and mutant versions of the Cdc5-PBD (Figure 3.7). This yields an approximately 75% success rate in visualizing a given TAP-tagged protein, and a 25% success rate in identifying specific Cdc5-PBD interactors. Of the proteins that bound the Cdc5-PBD specifically, 23 were originally identified in the yeast two hybrid, out of 79 total interrogated, giving a success rate of 30% for confirming the yeast two hybrid interaction. The success rate of the proteins originally identified by the bioinformatics screen was only 13%, as only four proteins were identified as being specific interactors; *cnm67*, *cbf5*, *lte1*, and *mcm2*. This suggests that the non-biased approach of the yeast two hybrid was more useful for the identification of real Cdc5-PBD interactors.

As with the yeast two hybrid results, the hits from the pulldown validation assay were categorized by GO terms and grouped by commonalities therein (Figures 3.6 and 3.7). Proteins involved in mitotic processes, in RNA regulation, and uncharacterized proteins were identified among both the specific and non-specific interactors, while all

three ribosome-associated proteins were non-specific interactors. Additionally, proteins that play roles in known Cdc5-dependent mitotic processes, such as spindle regulation, mitotic exit, and cytokinesis were also identified as specific Cdc5-PBD interactors. The categories of metabolic control and protein modification, also, were represented, though any connection between Cdc5 and these processes is currently unknown. Future work to connect Cdc5 function with these various cellular processes should prove an interesting and fruitful area of research. Only half of the specifically-interacting proteins contain an optimal Cdc5-PBD binding site that could be generated by CDK, suggesting that either other kinases also generate Cdc5-PBD binding sites, or these interactions are not direct, but instead are identified through another member of a complex that does contain a Cdc5-PBD binding site. Unfortunately, the minimal consensus phosphorylation site for Cdc5 is too common among yeast proteins to make any conclusions about its representation in the identified interactions, but all do contain a potential Cdc5 phosphorylation site.

The most obvious question from this list of Cdc5-PBD interactors is why some of the previously known Cdc5 interactors, such as Bfa1, Net1, Scc1, and Swe1 [5-7, 12, 35, 41, 42] are missing. These proteins may be absent for many reasons. For Scc1, it is likely that the Cdc5-PBD does not directly bind this protein, since it does not contain an optimal Cdc5-PBD binding site. Thus, it may have been missed in the yeast two hybrid and it would not have been selected in the bioinformatics search. This highlights a limitation of this approach, which is that proteins in complex with direct Cdc5-PBD interactors may be critical Cdc5 substrates, but they will not necessarily be identified by any of the approaches used here. Bfa1 is supposed to be inactivated by Cdc5 to allow mitotic exit to proceed [5]. This does not take place under conditions of spindle checkpoint so this may explain why the interaction was not seen in the benomyl enriched yeast two hybrid screen. Similarly, Swe1 is a ligand and substrate of Cdc5 that only interacts during the entry into mitosis, but would not be expected to remain bound to Cdc5 during an extended mitotic state. The non-identification of these two known Cdc5-PBD binders suggests that the screens presented here are also limited to identifying proteins that interact with the Cdc5-PBD during the core middle phase of mitosis, consisting of spindle and chromosome dynamics, rather than those that transiently interact with the Cdc5-PBD at early or late times during mitosis. By this line of reasoning, Net1 should have been identified, but it

was not. One possibility is that Net1 was not present in the library despite the library having a five-fold genomic coverage. Overall the Cdc5-PBD pulldown verifies several interesting Cdc5-PBD interactions, suggesting many future studies.

### **Generation of an Inhibitable Cdc5**

We sought to engineer budding yeast Cdc5 to be selectively inhibited by a small molecule, for identification of Plks substrates in intact cells. Our primary method for selective kinase inhibition is the introduction of a space-creating gatekeeper residue mutation coupled with a space-filling bulky derivative of the pyrazolopyrimidine (PP1) kinase inhibitor scaffold [43]. We replaced *CDC5* at its endogenous locus with the *cdc5-as1* allele (analog sensitive) encoding an L158G gatekeeper mutation. This change confers a modest 6-fold decrease in  $k_{cat}/K_m$  and slight increase in doubling time, indicating that Cdc5(L158G) is a functional kinase (data not shown). Surprisingly, we were unable to obtain significant inhibition of *cdc5-as1* using a variety of PP1 analogues, despite the fact that a diverse collection of other protein kinases have proven amenable to this approach (Jen Paulson – personal communication). Thus, the ATP binding site of Cdc5 differs enough from other kinases that a new inhibitor strategy is necessary.

Fortunately, the Cdc5 active site contains an uncommon cysteine, C96 (Figure 3.8A). A homologous cysteine in RSK and MSK was recently shown to be irreversibly inactivated by a pyrrolopyrimidine-based inhibitor containing an electrophile at the C-2 position [44]. We, therefore, reasoned that this, or a similar electrophilic inhibitor, might also bind and inactivate Cdc5(L158G) by virtue of the absence of a bulky gatekeeper residue and the presence of a naturally occurring Cys at position 96 (Figure 3.8B). As shown in Figure 3.8C, we observed that growth of the *cdc5-as1* strain, but not the wild-type strain, was prevented by treatment with the pyrrolopyrimidine-based inhibitor CMK. Together, the *cdc5-as1* strain and the CMK inhibitor provide a system for the potent and selective inhibition of Cdc5 in vivo. More extensive study revealed that the growth arrest upon Cdc5 inhibition is due to a spindle positioning defect such that the daughter nucleus fails to migrate into the daughter cell (Jen Paulson – personal communication).

## Cdc5 Substrates Identified in Candidate Based Screen

In addition to the use of the bioinformatic analysis to choose proteins for inclusion in the Cdc5-PBD pulldown validation assay, these proteins were also tested in a Cdc5 substrate assay. To test these candidate substrates for Cdc5-dependent phosphorylation *in vivo*, we also used the TAP tagged yeast strain collection. This approach is predicted not to alter the cellular concentration of the protein, while providing an ultra-sensitive handle for immunological detection [3]. To avoid false-positive phosphorylation effects caused by Cdc5 overexpression, *cdc5-as1* expressed from the endogenous Cdc5 locus as the sole source of Cdc5 was systematically introduced into TAP-tagged strains (Figure 3.9A). Since there is no general antibody that can detect all of the different Cdc5 phosphorylation sites, the Cdc5-dependent phosphorylation status of the TAP-tagged candidates was monitored by gel shift, a straightforward and well-established method for determining *in vivo* phosphorylation state [21]. We focused on the candidates that exhibited a gel shift in a nocodazole induced G2/M arrest, when Cdc5 is active, but not in a G1 arrest, when Cdc5 is not expressed [45]. These were then treated during the G2/M arrest for 20 minutes with 10  $\mu$ M CMK and compared with DMSO-treated controls.

Out of 74 proteins that shifted in G2/M, five proteins exhibited reproducible Cdc5-dependent changes in their gel shift (Figure 3.9B). These are likely to be direct Cdc5 substrates, since CMK was added for only 20 minutes. Significantly, of the three known Cdc5 substrates included in our screen, two, Bfa1 and Mcd1 [5, 6], showed a pronounced downshift upon Cdc5 inhibition. Similarly, two novel potential Cdc5 targets, Spc72 and Ulp2, also downshift upon Cdc5 inhibition. Spc72 is a previously described phosphoprotein, but the upstream kinase had not been identified [46]. Ulp2 is a desumoylase with roles in centromeric cohesion and recovery from checkpoint arrest [47, 48], processes in which Cdc5 functions [2]. Intriguingly, Cdc5 inhibition resulted in an upshift of Mih1; however, the chemical nature of the modified form of Mih1 is unclear, since it is unusual for loss of phosphorylation to result in a slower migrating form. However, Mih1 is the budding yeast homolog of the human protein, Cdc25, which is a known Plk1 target [14], though it is not clear that Mih1 has the same function in budding yeast cells that Cdc25 does in human cells. Notably, each identified protein reportedly

exists at less than 1400 molecules/cell. Unfortunately, we were limited by the proportion of phosphoproteins that demonstrate significant phosphorylation shifts. Further advances in mass spectrometric approaches that quantitatively detect differences in low stoichiometry phosphopeptides in a complex mixture are necessary to improve this approach [49].

### **Regulation of Cyk3, Cnm67, and Spc72 by Cdc5**

In order to further investigate the role of Cdc5 in controlling mitotic progression we chose to study some of the validated interactions in more detail. We chose one protein identified through the yeast two hybrid screen, Cyk3, one identified through bioinformatics and validated by Cdc5-PBD pulldown, Cnm67, and one identified as a Cdc5 substrate, Spc72. All three proteins are predicted to contain a single Cdc28-generated PBD binding site, contain multiple optimal Cdc5 phosphorylation sites, and have known functions in mitosis [50-57]. Cyk3 is the only known Cdc28 target among them [21]. The single predicted Cdc5-PBD binding site allows easy generation of non-binding mutants of Cyk3, Cnm67, and Spc72, which then can be used for interaction defective genetic studies to determine the role of Cdc5-PBD binding in the regulation of these proteins. Based on the full oriented peptide library screening data for the Cdc5-PBD [23], we decided to mutate the serine in the single STP motif in each protein to a valine, since this was the most disfavored residue for binding at this position. This should completely eliminate binding as a similar mutation blocks interaction between the Plk1-PBD and Cdc25C [14], and isothermal calorimetry data suggests that in vitro, a peptide with a valine at the -1 position relative to the phosphorylated residue binds with weaker than 150 $\mu$ M affinity to the Plk1-PBD [14].

First, we performed the Cdc5-PBD pulldown assay, as described previously, on Spc72, and found that it does indeed bind specifically to the Cdc5-PBD (Figure 3.10A), consistent with previous reports that suggested interaction between these proteins [17, 58]. The interaction is also regulated by cell cycle stage, since Spc72 binds the PBD less well in a G1 than in G2/M arrest (Figure 3.10B). Mutation of the predicted Cdc28-generated Cdc5-PBD binding site on Spc72 (S232) greatly reduces binding (Figure 3.10C). Some

residual binding was observed in this mutant and may reflect contributions from other sites in Spc72 or Cdc5-PBD interactions with Spc72 binding partners. However, the amount of mutant Spc72 that came down with the Cdc5-PBD is similar to the amount of wild-type Spc72 that came down with the Cdc5-PBD from G1 arrested cells. This suggests either a background level of Spc72 in this assay that cannot be eliminated, or that Spc72 binds the Cdc5-PBD weakly in a phospho-independent manner, in addition to its strong phospho-dependent interaction. The mutants of Cyk3 (S350V) and Cnm67 (S120V) have been generated, but tagged forms need to be made to allow detection in the pull-down assay.

In addition, to demonstrate that Cyk3, Cnm67, and Spc72 could serve as substrates for Plks in vitro, the wild-type TAP-tagged proteins were immunoprecipitated from yeast lysates and incubated with Plk1 kinase domain and radioactive ATP. Radioactivity was incorporated into all three proteins (Figure 3.11A, B) demonstrating that, in vitro, they can serve as substrates of Plks. This suggests that, in vivo, they are also substrates, since they directly interact with the Cdc5-PBD, placing them in an optimal position to be phosphorylated by Cdc5.

With the non-binding mutants in hand, interaction-defective genetics studies can be carried out. The deletion strain of *cyk3* is viable and exhibits a clumping phenotype when grown at 30°C or higher, that is minimized when grown at room temperature [50]. This phenotype results from the inability of mother and daughter yeast cells to completely separate after mitosis is complete. Mitotic exit is completed in these cells, because the cells proceed through the next round of the cell cycle thus eventually forming clumps of cells stuck together [50]. The defect in the  $\Delta cyk3$  strain appears to be improper septum deposition, as the bud neck septum is thicker than normal in these cells. Cyk3 probably plays a direct role in this process, as *cyk3* contains a transglutaminase domain, localizes to the bud neck [50, 59], and has synthetic lethality phenotypes consistent with it being a member of the septum pathway [50]. All of these phenotypes are rescued in the deletion strain by expression of the wild-type proteins [50]. To test whether the *cyk3* Cdc5-PBD non-binding mutant rescues these phenotypes it will be expressed in the deletion strain. In preliminary experiments, it appears that the non-Cdc5-PBD binding mutant is similar to the deletion strain in clumping, whereas

expression of wild-type *cyk3* fully rescues this phenotype (Figure 3.12A). This places Cdc5 as an upstream activator of both the septum and the actomyosin ring contraction pathways (Chapter Four) in budding yeast cytokinesis. In addition to demonstrate that the mutant *cyk3* is specifically defective in the septum pathway we will test its synthetic lethality with *myo1*.

Unfortunately, though the systematic deletion strains of *cnm67* and *spc72* are viable, they are functionally crippled due to a severe defect in chromosome segregation caused by the inability of the daughter nucleus to migrate into the daughter cell [51, 52, 54, 56]. Thus, to examine the properties of the *cnm67* and *spc72* non-Cdc5-PBD interacting mutants they were placed into a heterozygous diploid deletion strain. This strain will be sporulated and selected for the presence of the plasmid encoding the wild-type or mutant gene and the genomic deletion of the gene. These strains will always be grown at room temperature until assay, to alleviate the nuclear migration defect and avoid the introduction of mutations into the strain. For further ease of visualization, a GFP-tagged beta tubulin gene was inserted into the heterozygous diploid deletion strains at the genomic locus. Spindle orientation of the various strains will then be monitored by fluorescence microscopy. We expect that the strains harboring the mutant versions of the genes will have nuclear positioning defects, which will suggest that Cdc5 regulation of Cnm67 and Spc72 is required for proper mitotic spindle orientation and nuclear migration into the daughter cell. These Cdc5-PBD non-binding mutants might not be as severe as full deletions, but considering that Cnm67 and Spc72 have similar localizations at the spindle pole body and similar deletion phenotypes, a combination of the two non-binding mutants might produce a more severe effect.

## **Experimental Procedures**

### **Molecular Biology Techniques**

Residues 357-705 of Cdc5 (analogous to 345-603 of Plk1) were cloned between the BamHI and Sall sites in the pGBD vector. The same Cdc5 fragment was cloned between the BamHI and XhoI sites in the pGEX-4T1 vector and the pcDNA3.1+hisC vector. Site-directed mutagenesis was carried out using the QuikChange Site-Directed mutagenesis kit (Stratagene) to make a H641A/K643M version of the Cdc5-PBD. The pGEX-Cdc5-PBD constructs were transformed into the Rosetta2 bacterial expression strain, and GST-Cdc5PBD protein was produced by induction of  $OD_{600} = 0.7$  cells with 0.4mM IPTG for 16hrs at room temperature. Bacterial pellets were spun down from the overnight cultures, lysed by sonication in lysis buffer (50mM Tris pH7.5, 150mM NaCl, 5mM EDTA, 1mM PMSF), and GST fusion proteins purified by incubation with GSH beads overnight at 4°C. Beads were washed extensively with TBST and TBS, and resuspended in TBS with 1mM PMSF. The purity of protein was analyzed by coomassie blue staining of SDS-PAG and the amount of protein was determined by comparison to standard amounts of BSA. Protein was used within one week of generation, and checked for maintenance of full length protein at each time of use. Cyk3<sup>452-613</sup> was subcloned into pGEX-4T1 and a C522A mutation generated by the Quickchange method as above. GST-tagged Cyk3 proteins were induced and purified as above from BL21 cells. Cell cycle synchronization was obtained by G1 arrest with alpha factor for 3 hours, followed by washing to release (0 min time point). Alpha factor was re-added at 70-80 minutes when arresting in the following G1. Alpha factor was used at 1 µg/ml for bar- cells and 20 µg/ml for bar+ cells. G2/M arrests were obtained by nocodazole treatment at 15 µg/ml for 3 hours. For phosphorylation gel shifts, cell extracts were prepared in urea lysis buffer as described [21], and 5 µg of protein was loaded on 5%, 7.5%, or 10% Criterion gels (Biorad) for western blotting.

### **Yeast Genetic Techniques**

Media and genetic techniques were as previously described [60]. To generate *cnm67* constructs, the endogenous *cnm67* gene from 500bp upstream to 500bp



downstream of the genomic locus was cloned into pRS416 between the XhoI and BamHI sites by standard subcloning procedures. An analogous process was used to generate *cyk3* and *spc72* constructs in *leu* and *ura* marked plasmids, respectively. *Spc72* plasmids encoded an I302N difference from published sequence, which was confirmed in a W303 strain. Site-directed mutagenesis was carried out using the QuikChange Site-Directed mutagenesis kit (Stratagene) to generate *cnm67S120V*, *cyk3S350V*, *spc72S231A*, and *cyk3C522A*. Mutagenesis was confirmed using restriction digests and full gene DNA sequencing. The  $\Delta$ *cnm67* heterozygous diploid strain generated by the Yeast knockout consortium was purchased from Open Biosystems. GFP-beta-tubulin on a leucine marker was inserted into this strain, and correct integration was confirmed by colony PCR and by subsequent DNA sequencing of the genomic locus. The various *cnm67* constructs were transformed into this strain and spores were selected on media lacking uracil, leucine, and containing kanamycin to generate haploids with the GFP-beta-tubulin, the genomic *cnm67* deletion, and the covering *cnm67* plasmid. These strains were used for examination of *cnm67* function. The  $\Delta$ *cyk3* haploid strain generated by the Yeast knockout consortium was transformed with the various *cyk3* constructs and these strains were used for examination of *cyk3* function. The *cyk3* constructs were also transformed into a haploid  $\Delta$ *cyk3* $\Delta$ *myo1* strain with a *myo1* covering plasmid on a *ura* selectable plasmid. These strains were grown on 5-FOA plates to eliminate the *myo1* plasmid to determine whether the *cyk3* plasmids can rescue the double deletion of *cyk3* and *myo1*. TAP-tagged yeast strains were purchased from Open Biosystems as described [3]. Plasmids containing a *CDC5* (YMR001C) genomic fragment in pRS315 (p315-CDC5) and pRS306 (p306-CDC5) were gifts of J. Charles. The *cdc5-as1* allele (encoding Cdc5(L158G)) was introduced into p315-CDC5 and p306-CDC5 by QuikChange site-directed mutagenesis (Stratagene), generating p315-*cdc5-as1* and p306-*cdc5-as1*. The *cdc5-as1* allele was introduced at the *CDC5* locus by standard two-step gene replacement, except in the TAP-tagged library strains (Open Biosystems). The *cdc5-as1* allele was systematically introduced into TAP-tagged strains as follows. A *MAT $\alpha$*  strain derived from EY1274 carrying a *can1* $\Delta$ ::*MFA1p-LEU2* selectable marker (E.K. O'Shea, Harvard University) was transformed with a marker fusion PCR product generated by amplification of *cdc5-as1* and *k.lactis URA3* genes. The entire *cdc5-as1* gene was

sequenced in the resultant integrated strain. This strain was then crossed to selected *MATa HIS3* marked TAP-tagged library strains [3] using a manual 96-pinning tool (V&P Scientific). After sporulation, TAP-tagged *MATa* haploids were selected on synthetic media lacking histidine, arginine, leucine, and uracil and containing 50 µg/ml canavanine (Sigma).

### **Yeast Two Hybrid**

The Cdc5-PBD clone in pGBD was transformed into the PJ69-4a strain [61]. Self activation was tested by growth on SC –ade plates, and minimal self activation was observed. A yeast full genomic DNA library in pGAD in the PJ69-4α strain was obtained as a gift from A. Amon at MIT. Strains were grown, mated, and titered as described [61]. For the first yeast two hybrid selection, the  $4 \times 10^6$  diploid yeast were plated on each of ten plates of synthetic complete media without adenine and grew at 30°C for ten days. About 1500 single colonies were picked and streaked onto SC –leu/-trp plates to ensure diploid status and to re-generate single colonies. Single colonies were picked and grown as patches on SC –ade plates with 52 patches per plate. Actively growing patches were replica-plated onto plates containing 20µg/ml 5-bromo-4-chloro-3-indolyl alpha-D-galactopyranoside (X-a-gal) (Clontech) and then onto plates containing both 25µg/ml benomyl and 20µg/ml X-a-gal in YPD. X-a-gal is cleaved by the secreted enzyme α-galactosidase, which is under the control of a gal responsive promoter, into a blue precipitate. Plates were grown for two days at 30°C before pictures were taken of each plate on a light box with a digital camera. Nearly all of the patches turned blue on the X-a-gal containing plates. 264 of the patches on the benomyl containing plates were bright blue compared to the same strain on the plates without benomyl. These strains were picked and grew well on SC -leu/-trp/-ura, which once again confirmed the diploid status and interaction. The strains were grown in SC –leu media to enrich for the pGAD plasmid at the expense of the pGBD plasmid, and plasmid DNA was prepared by standard yeast miniprep procedure [60]. The insert in the pGAD plasmid was amplified by PCR using primers specific to the GAL4-AD fragment on the 5' end and a primer generic to both the pGAD and pGBD vectors on the 3' side. PCR products were run on agarose gels to determine size, and the concentration of DNA was determined by

spectrophotometer reading. 100ng of DNA per 1000bp of length of DNA was sent for sequencing using the upstream PCR primer as a sequencing primer. The resulting DNA sequences were blasted against the yeast genome to identify the region of interaction, and all intergenic and repetitive sequences were thrown out, leaving 112 distinct ORFs identified in the two stage mitotic-specific Y2H screen.

### **Yeast Lysate Generation**

50ml cultures of yeast strains were grown in appropriate media, YPD for TAP-tagged strains. Cultures were harvested by centrifugation 5min 2000g in 50ml conicals, and resuspended in 0.5ml PB (50mM Tris pH 8.0, 150mM NaCl) by vortexing. Cells were transferred to 2ml screw cap tube, spun down for 1min at full speed, the supernatant was vacuumed off, and the wash repeated. Cells were resuspended completely in 200ul 2X PBT (PB + 1% Triton X-100, 1mM DTT, 2mM EDTA, 1 mM AEBSF, 1 µg/mL aprotinin, 1 µg/mL leupeptin, 10 µM E64, 1 µg/mL pepstatin A, 1.6 µg/mL benzamidine, 2 mM Na<sub>3</sub>VO<sub>4</sub>, 10 mM NaF, 20 nM microcystin LR, 5 nM okadaic acid, 2 µM cantharidin, 0.00073% p-bromotetramisole, 0.4 nM cypermethrin, 100 µM dephostatin, 100 nM bestatin, 100 ng/mL TPCK). ~700ul acid washed glass beads were added (Sigma), and the tube completely filled with PBT buffer. Cells were lysed with a multi-bead beater Fastprep machine (Bio101) at speed 6.0m/s for 45s for eight cycles with at least 1min on ice between cycles. The lysate was spun out of the bottom of the tube through a hole poked in the bottom of the tube with a needle, and centrifuged at top speed in microfuge for 20min to pellet cell debris. The supernatant was used in experiments.

### **PBD Pulldown Assay**

The PBD pull-down assay was performed in Polo-box binding buffer (50 mM Tris, 150 mM NaCl, 2mM EDTA, 1 mM PMSF, 1 mM DTT, 1 % TritonX-100 and Complete protease inhibitor). Freshly prepared yeast cell lysates (containing 2 mg total protein in 300µl for each assay) were mixed with 20µl of GSH-beads saturated with 10ug pure GST-Cdc5PBD or mutant GST-Cdc5PBD H641A/K643M. Reactions were incubated for two hours at 4°C and then washed four times with binding buffer. Bound proteins were eluted from the beads by boiling in 20ul of 3X protein sample buffer, ran

on SDS-PAGE, transferred to nitrocellulose, and analyzed by western blotting with goat anti-rabbit IgG antibody to detect the TAP tag or other tag-appropriate antibody.

### **Phosphopeptide Binding Assay**

Cdc5-PBD wild-type and H641A/K643M, along with Plk1-PBD wild-type and H538A/K540M, were in vitro transcribed and translated in the presence of [<sup>35</sup>S]-methionine off of the pcDNA3.1+hisC vector with T7 polymerase using the TNT Quick T7 IVT kit (Promega). Streptavidin beads (Pierce, 75pmol/μL gel) were incubated with a ten-fold molar excess of each biotinylated library in 50 mM Tris/HCl (pH7.6), 150 mM NaCl, 0.5% NP-40, 1 mM EDTA, 2 mM DTT and washed five times with the same buffer to remove unbound peptide. The bead-immobilized libraries (10μL of gel) were added to 10 μL of the in vitro translated [<sup>35</sup>S]-labeled proteins in 150 μL binding buffer (50 mM Tris/HCl (pH7.6), 150 mM NaCl, 0.5% NP-40, 1 mM EDTA, 2 mM DTT, 8 μg/mL pepstatin, 8 μg/mL aprotinin, 8 μg/mL leupeptin, 800 μM Na<sub>3</sub>VO<sub>4</sub>, 25 mM NaF). After incubation at 4°C for 3 hours, the beads were washed three times 200 μL with binding buffer prior to SDS-PAGE (12.5%) and autoradiography. The peptide libraries used were biotin-Z-Met-Ala-X-X-X-X-pThr-Pro-X-X-X-Ala-Lys-Lys-Lys and biotin-Z-Met-Ala-X-X-X-X-Thr-Pro-X-X-X-Ala-Lys-Lys-Lys with Z indicating aminohexanoic acid and pThr indicating phospho-threonine.

### **Bioinformatic Analysis**

Candidate Cdc5 substrates were initially selected based on information available in September 2003 as follows. First, Cdc5-dependent processes were used as keywords in Gene Ontology (GO) term searches, and the resulting proteins were included in the screen if they contained a minimal phosphorylation or PBD motif. Second, yeast proteins in SWIS-PROT were evaluated with Scansite using position-specific scoring matrixes representing the phosphorylation and binding motifs of the Cdc5 kinase domain and Cdc5 Polo-box domain respectively. The Scansite algorithm assigns final scores (Sf) that range from 0 to 1 depending upon how closely the query sequence matches the optimal Cdc5 PBD or kinase motif, when normalized to all proteins in the database [37]. A Scansite final score of 0 corresponds to a perfect match, while a score of 1 corresponds to

the complete lack of even a minimal binding or phosphorylation motif. The Cdc5 substrate likelihood score was defined as  $1-[0.5 (Sf_{PBD}+Sf_{Kin})]$ , where  $Sf_{PBD}$  and  $Sf_{Kin}$  were the final Scansite scores for the individual PBD and kinase motifs, respectively. Candidates were selected based on top scores and by considering the remaining proteins in turn by score, including those with cell cycle function and localization in the same compartment as Cdc5 (nucleus or cytoplasm).

### **Plk1 Kinase Assay**

Plk1 kinase domain with a T210D activating mutation was expressed in bacteria and purified to homogeneity. TAP tagged proteins were isolated from cell extracts by pulldown with IgG sepharose (GE Healthcare). Several micrograms of each protein was incubated with or without Plk1 and 100 $\mu$ M ATP and 1 $\mu$ Ci of  $^{32}$ P- $\gamma$ -ATP in Plk1 kinase buffer (50mM Tris pH 7.5, 150mM NaCl, 10mM MgCl<sub>2</sub>, 1mM DTT) for two hours at 30°C. Samples were taken at several timepoints, run on an SDS-PAGE, and exposed to a phosphoimager plate for autoradiography. In this way, Cyk3, Cnm67, and Spc72 were confirmed to be in vitro substrates of Plk1, and by implication, Cdc5.

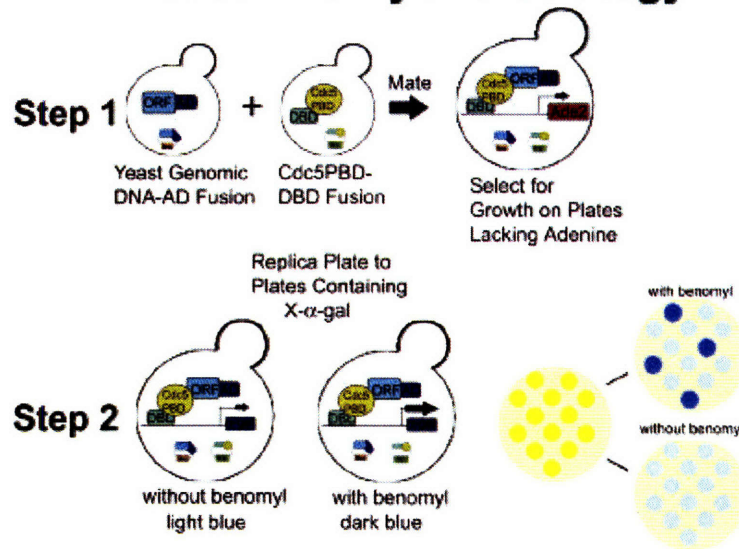
**Figure 3.1: Modified Yeast Two Hybrid Strategy Identifies Mitotic-Dependent Interactions.**

(A) Schematic of the two step yeast two hybrid strategy for identification of mitotic specific polo-box domain interactors.

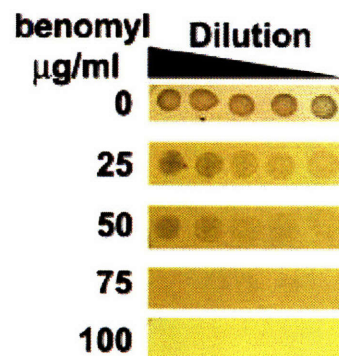
(B) Growth of the diploid yeast two hybrid strain was tested on plates containing various concentrations of benomyl. 50  $\mu$ l of a saturated overnight culture grown in YPD was plated as serial two-fold dilutions on plates containing the indicated amount of benomyl.

(C) Example of results of the second step of the yeast two hybrid, with dark blue colonies seen on the plates containing benomyl (top) and weak blue staining similar among all colonies on replica plates of the same yeast on plates without benomyl (bottom).

**A Yeast Two Hybrid Strategy**



**B**



**C**

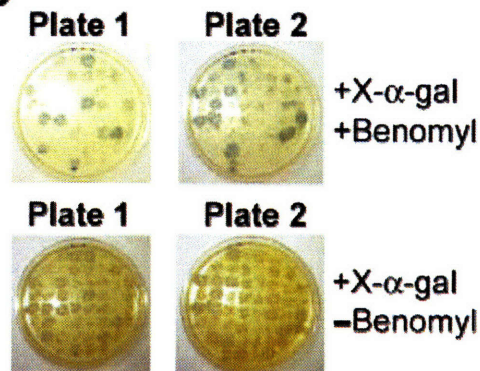
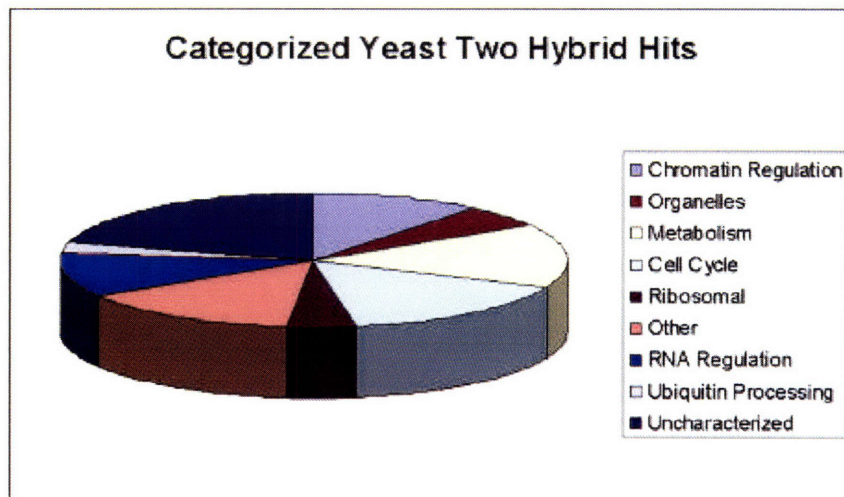


**Figure 3.2: Yeast Two Hybrid Results Summary.**

**(A)** Pie chart showing GO categories for all identified Cdc5-PBD interactors listed in Table 3.1.

**(B)** Pie chart showing more specific GO categories for those proteins originally identified as being part of the GO category “Cell Cycle” in Figure 3.2A.

**A**



**B**

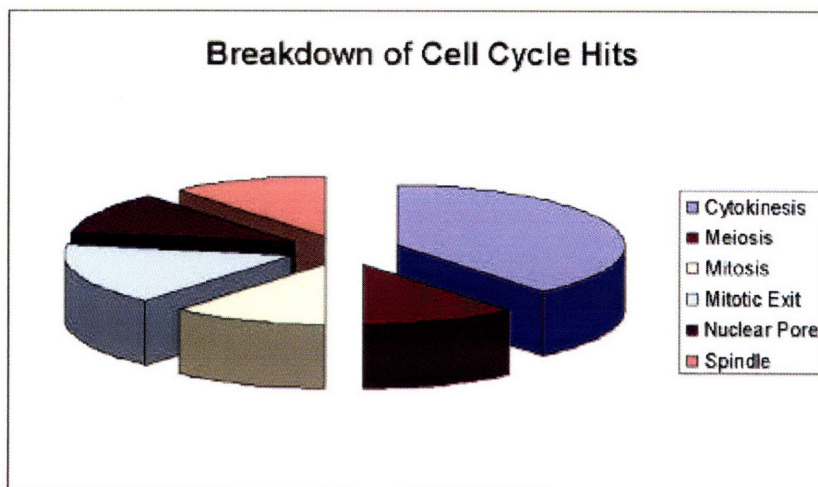
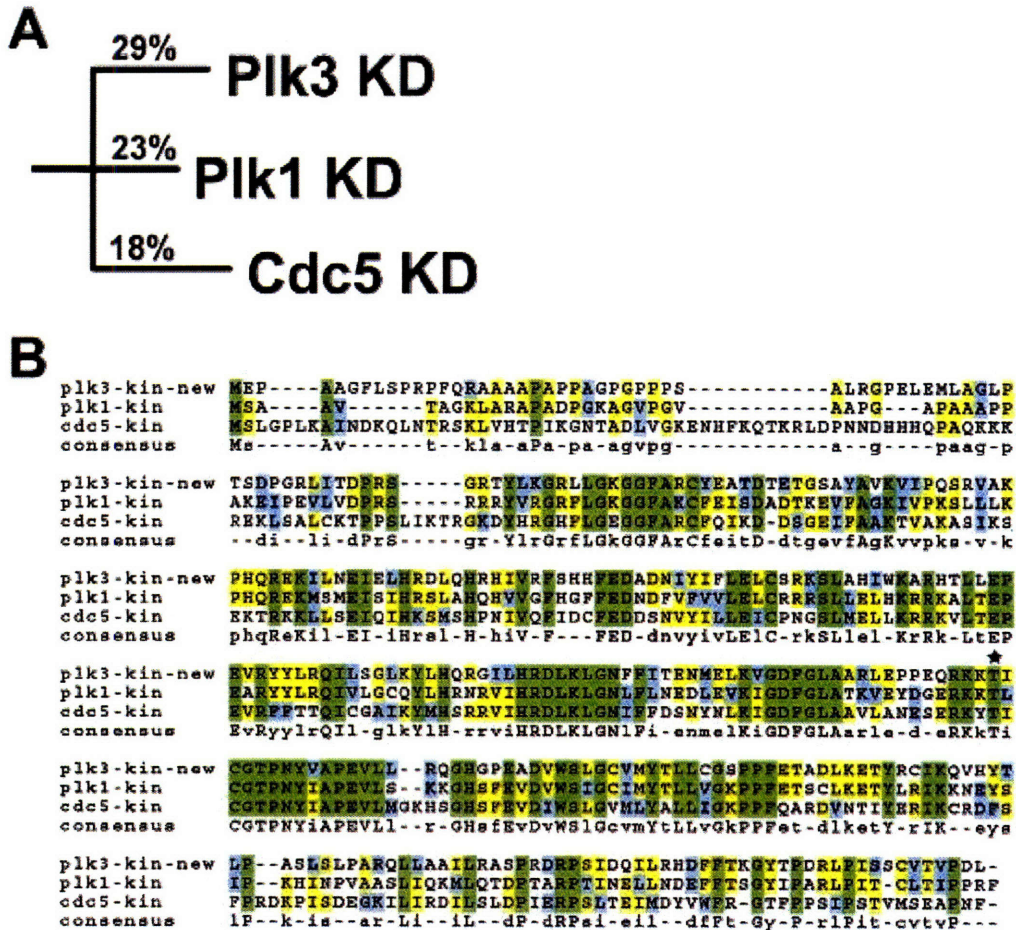




Figure 3.3: Cdc5 Kinase Domain is Similar to Plk1 Kinase Domain

(A) Rooted tree of conservation between Plk1, Plk3, and Cdc5 kinase domains.

(B) Sequence alignment of the kinase domains of human Plk1, human Plk3, and Cdc5 with the critical Thr in the phosphorylation loop indicated with a star above it.





### Figure 3.4: Bioinformatic Prediction of Cdc5 Substrates.

(A) Schematic representation of substrate recognition by Cdc5. The substrate is depicted to contain a Cdc5 phosphorylation motif, (D/E/N)X(S/T) and a binding motif, S(pS/pT)(P/X), which binds the Cdc5 polo boxes (PB1 and PB2). X represents any amino acid, p represents phosphorylation.

(B) Bioinformatic mining of the yeast proteome for candidate Cdc5 substrates. The distribution of assigned Cdc5 substrate likelihood scores is shown for Cdc5 candidate substrates compared with the proteome, with high scores reflecting likely candidates.

(C) Cdc5 candidate substrates are enriched in low abundance proteins. Normalized distribution of protein abundance [3] comparing candidate Cdc5 substrates to the entire proteome. The data set means were statistically different ( $P=0.0003$ ) by unpaired t-test. Proteins without abundance values [3] are excluded from the analysis.

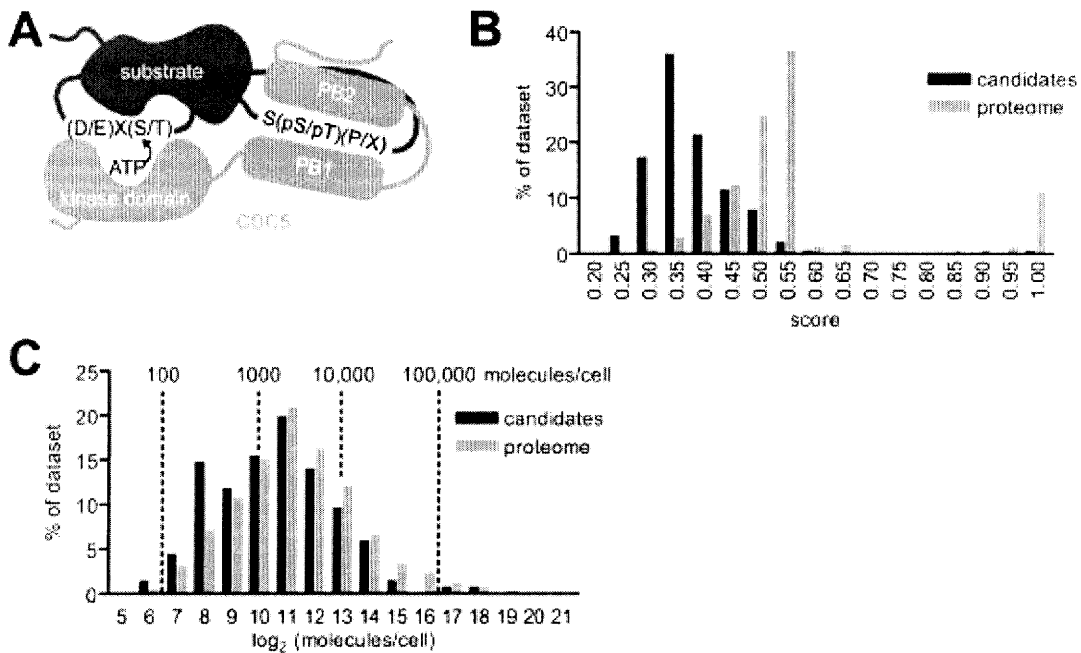


**Figure 3.5: Cdc5 Polo-box Domain Binds Phosphopeptides.**

(A) Cartoon drawing of Cdc5 domain structure with critical residues indicated.

(B) Sequence alignment of the PBD of Cdc5 and human Plk1 with conserved critical residues for phosphopeptide binding indicated with a star above them.

(C) Phosphopeptide binding assay of the Cdc5-PBD with a pTP and TP peptide library with Plk1-PBD as a positive control.

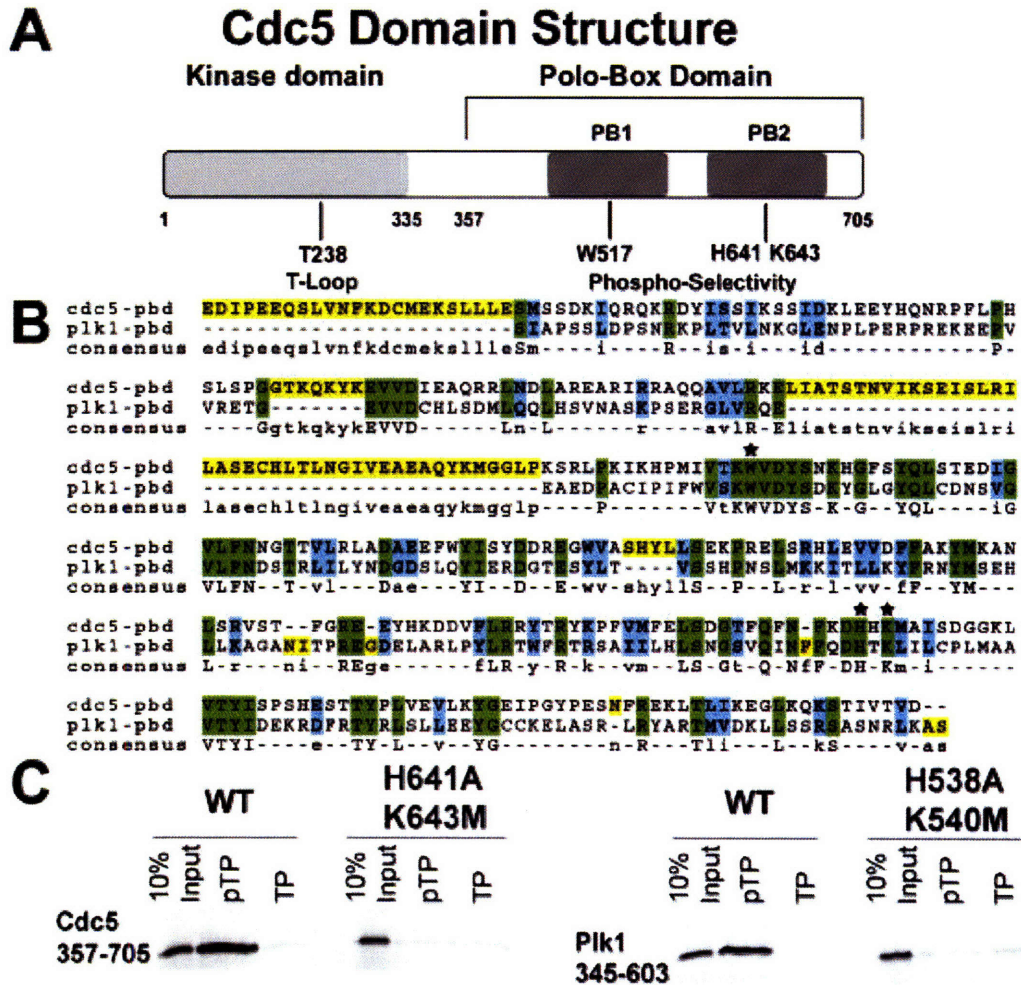


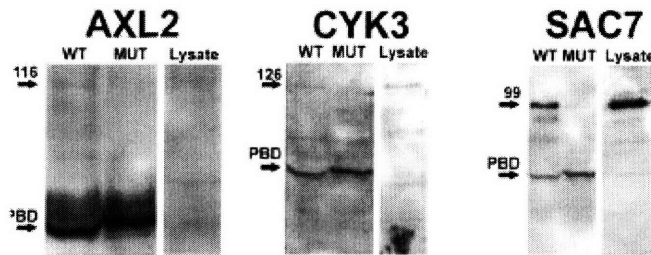
**Figure 3.6: Polo-box Domain Pulldown Confirms Specific Interactors.**

Western blot of Cdc5-PBD pulldowns with goat anti-rabbit IgG to visualize the proteinA region of the TAP tag. Each pulldown was from lysates from a particular TAP-tagged strain of yeast, as indicated by the gene name above each blot. Pulldowns were performed with wild-type Cdc5-PBD (left lane each blot) or mutant Cdc5-PBD (middle lane each blot), and the TAP-tagged protein was also confirmed to be expressed in the lysate (right lane each blot). Arrows indicate expected size of protein, and arrows with question mark indicated a suspected breakdown product of the expected protein. The Cdc5-PBD is also recognized by this antibody and is also marked with an arrow and the word PBD in each pulldown. All the proteins shown specifically interacted with the wild-type Cdc5-PBD and not the mutant version. Proteins were sorted by GO categories as indicated on the left side of each row.

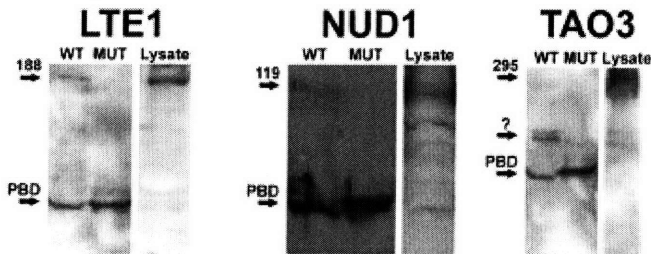
Figure 3.6 Continued:

## Specific Cdc5-PBD Interactors

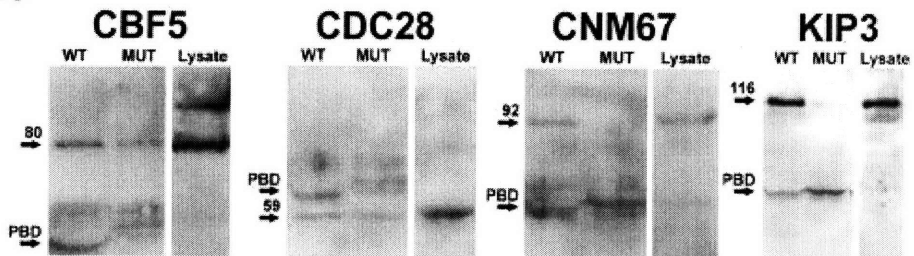
### Cytokinesis



### Mitotic Exit



### Spindle



### Nuclear Pore

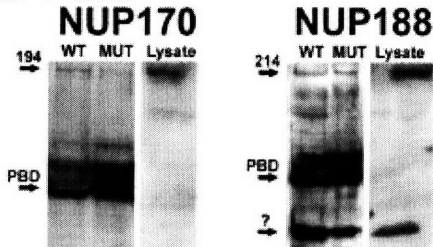
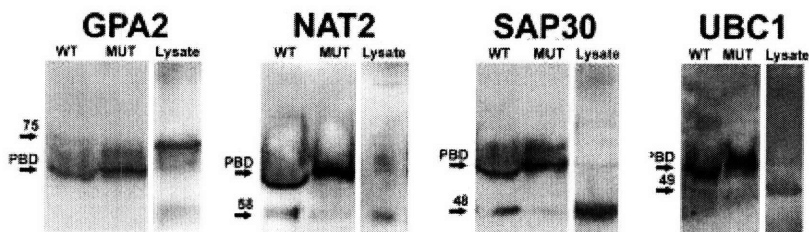


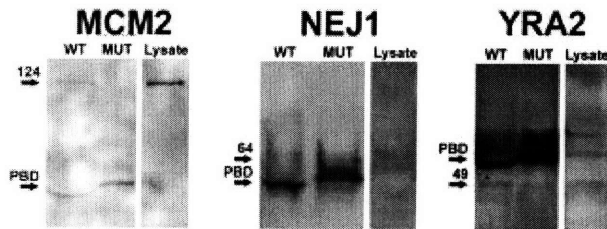
Figure 3.6 Continued:

## Specific Cdc5-PBD Interactors

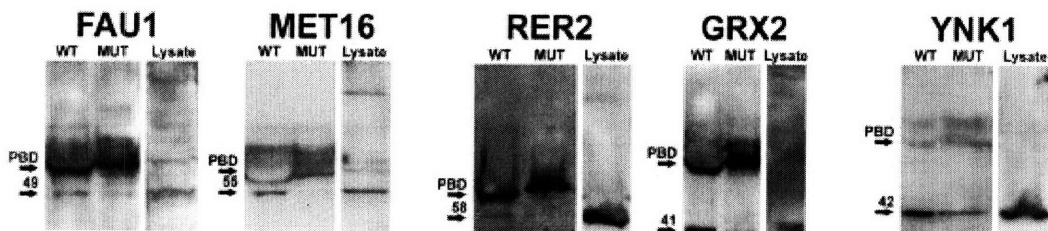
### Modifying Enzymes



### RNA/DNA Control



### Metabolism



### Uncharacterized

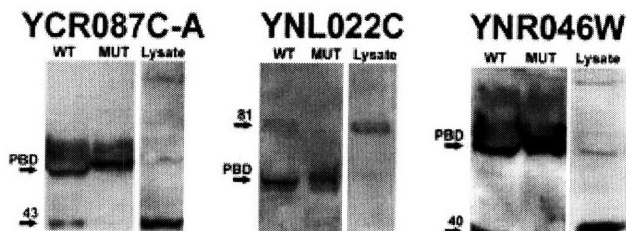
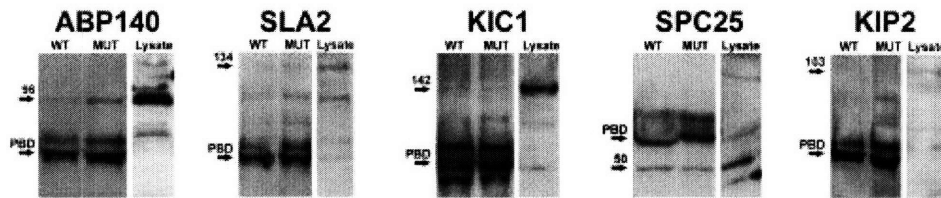


**Figure 3.7: Polo-box Domain Pulldown Identifies Non-specific Interactors.**

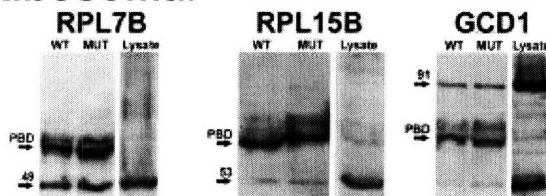
Same as Figure 3.6 except that the proteins identified in this group do not bind the wild-type Cdc5-PBD specifically. Instead they bind equally well or better to the mutant Cdc5-PBD.

## Non-Specific Cdc5-PBD Interactors

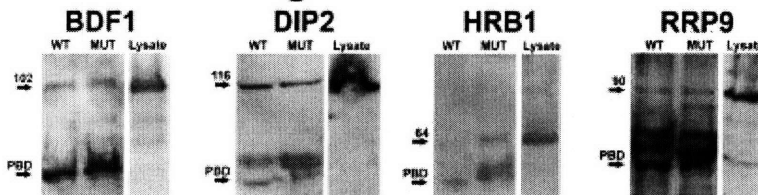
### Mitotic



### Ribosomal



### RNA Processing



### Various

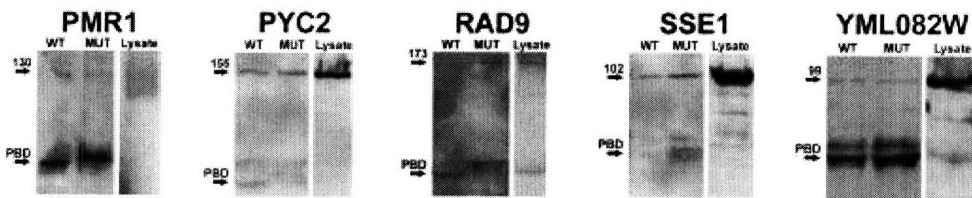


### Figure 3.8: Analog-sensitive Cdc5 is Inhibited by CMK.

(A) Sequence alignment of kinase domain regions spanning the gatekeeper residue and the reactive cysteine. The Cdc5 sequence is in bold, and the specificity filters critical for RSK2 inhibition by CMK [44] are highlighted in gray.

(B) Chemical structure of CMK. CMK (in gray), with features of the kinase active site depicted, including a cysteine to react with the electrophilic chloromethyl ketone and a gatekeeper residue that controls access to a hydrophobic binding pocket. A predicted steric clash between the Cdc5 leucine gatekeeper residue and CMK is illustrated.

(C) Cell viability halo assay of wild type and *cdc5-as1* yeast. Inhibition of cell growth in the region surrounding a disc spotted with 1 nmol CMK or scaffold molecule is observed only upon CMK application to *cdc5-as1* (center), indicating a requirement for both the gatekeeper mutation and the electrophilic reactivity of CMK.

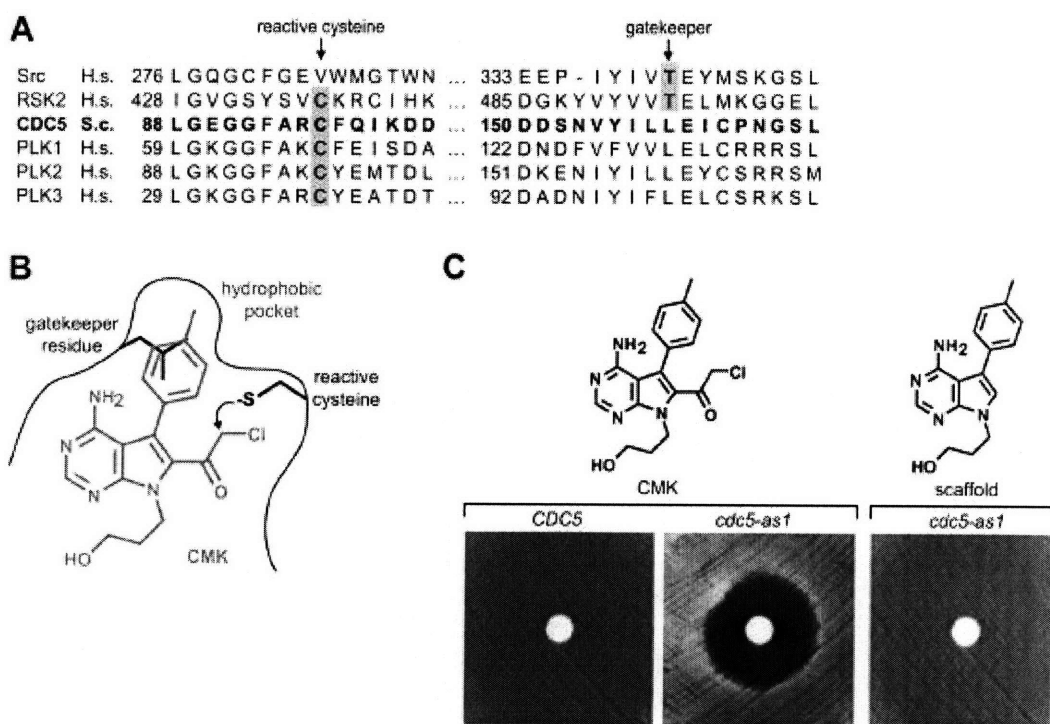


**Figure 3.9: A Candidate Based In Vivo Screen Identifies Cdc5 Substrates.**

(A) Approach to screening for substrates phosphorylated by Cdc5 *in vivo*.

(B) Result of the screen. The gel shifts of five TAP-tagged candidate substrates are altered upon Cdc5 inhibition with 10  $\mu$ M CMK (+) as compared with a DMSO control treatment (-).

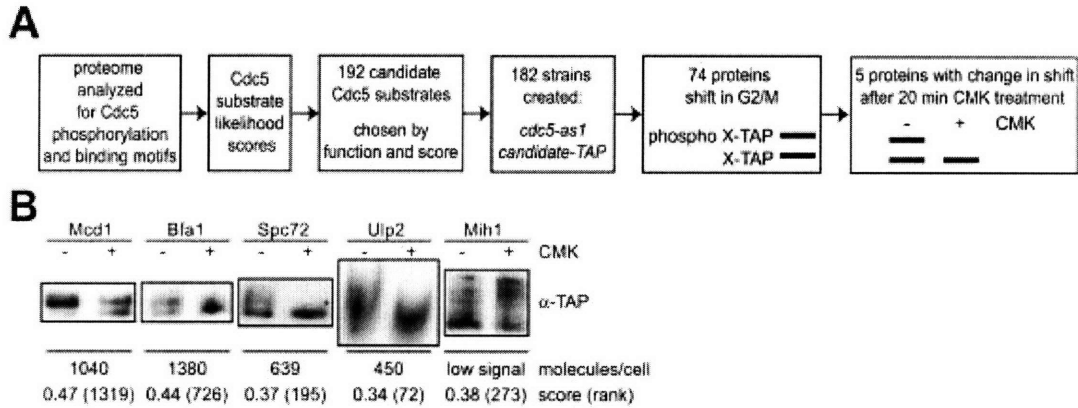




**Figure 3.10: Spc72 Binds to the Cdc5 Polo-box Domain**

(A) Spc72 is bound by the Cdc5 PBD, and PBD\* has reduced Spc72 binding. Anti-TAP (Spc72) western blot indicates Spc72 present in the input G2/M cell extract (I) or pulled down (P) with GST-PBD (PBD) or GST-PBD\* (PBD\*). Total protein staining indicates the amount of GST-fusion protein in pulldown lanes (P).

(B) Cdc5 preferentially binds mitotic Spc72. Wild type PBD pulldowns from G2/M phase cell extracts (as in A) or G1 phase cell extracts were probed for Spc72.

(C) Mutation of consensus Cdc5 binding residues in Spc72 reduces binding to the PBD. PBD binding to Spc72 or Spc72(S231A,S232A) as in A. I = 5% input, P = pulldown.

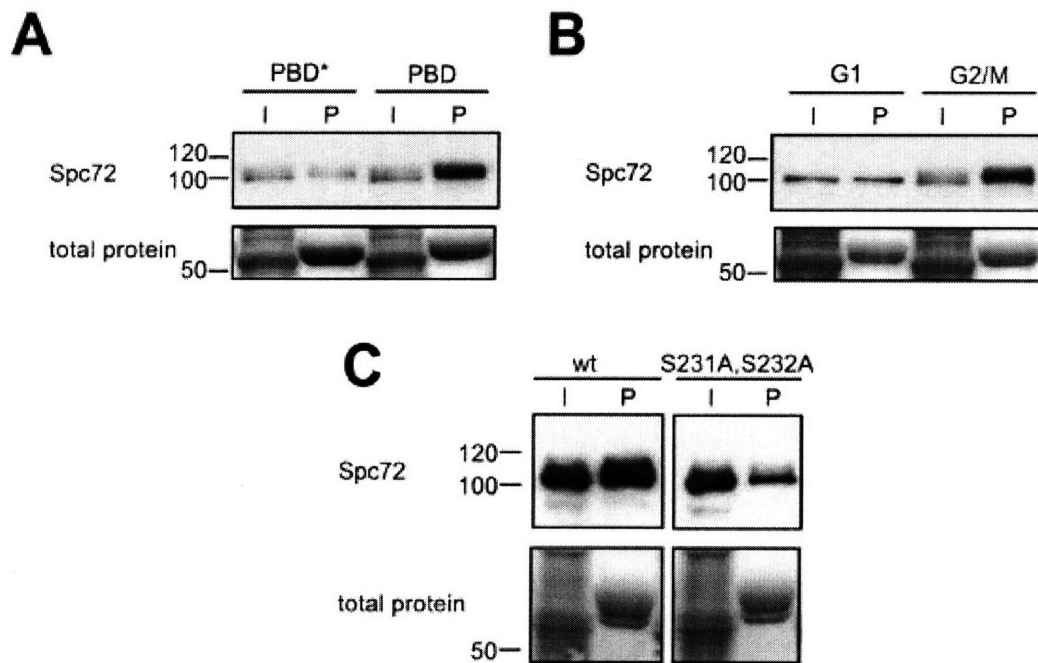


**Figure 3.11: Cyk3, Cnm67, and Spc72 are Plk Substrates In Vitro.**

(A) In vitro phosphorylation of Spc72 by Cdc5. Spc72 is phosphorylated ( $^{32}\text{P}$ ) upon addition of Cdc5 (left panels), and no Spc72 phosphorylation is seen when Cdc5 is added to a mock pulldown reaction (untagged Spc72, - Spc72-TAP, right panels).

(B) In vitro phosphorylation of immunoprecipitated full length TAP-cyk3 and TAP-cnm67 proteins. Proteins were incubated with Plk1 T210 kinase domain and  $\gamma^{32}\text{P}$ -ATP for indicated times.

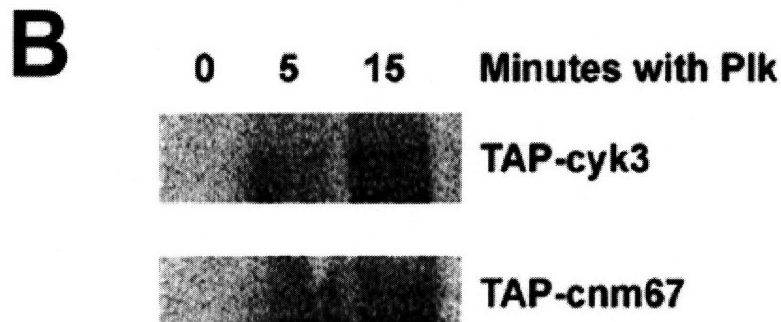
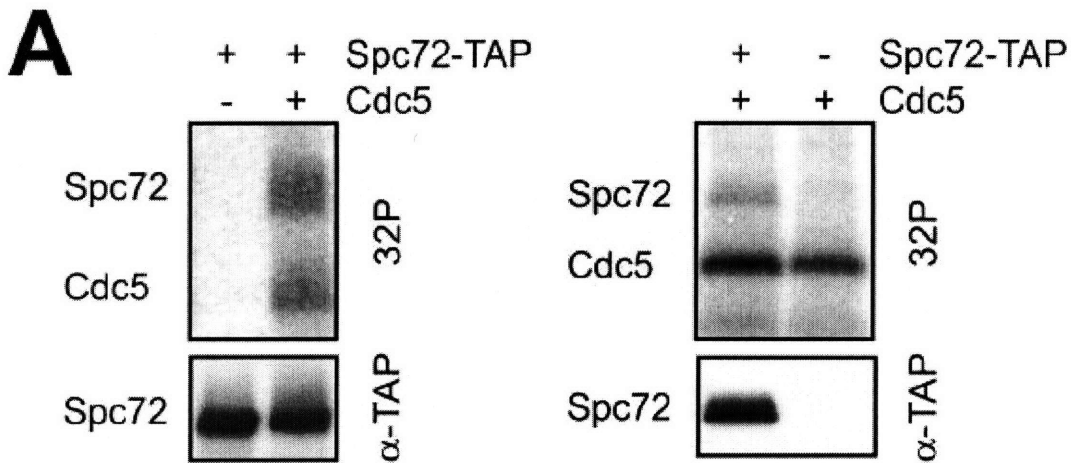


**Figure 3.12: Cyk3 is Regulated by Cdc5.**

(A) The  $\Delta$ cyk3 strain was complimented with wild-type cyk3, non-Cdc5-PBD binding cyk3, or vector alone. The wild-type cyk3 expressing strain overcame the cell clumping phenotype of the deletion strain whereas the non-Cdc5-PBD binding cyk3 expressing strain did not.

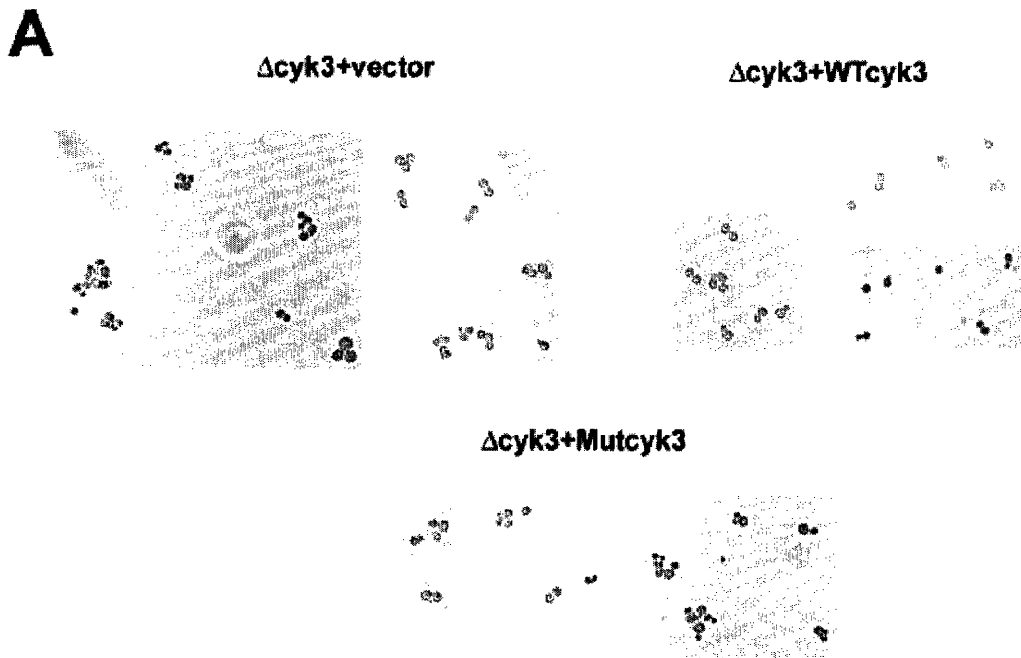






Table 3.2: TAP-tagged Strains used in Cdc5-PBD Pulldown

Systematic Name	Common Name	Identified By	Molecules Per Cell <sup>1</sup>	Molecular Weight <sup>2</sup>	PBDSite S(S/T)	PBDSite S(S/T)P	KinaseSite (E/D)X(S/T)	Saw in Lysate	Positive Hit	Negative Hit
YAL024C	LTE1	Bioinformatics	304	163	yes	yes	yes	x		x
YAR019C	CDC15	Bioinformatics	238	110	yes	yes	yes	x		
YBL023C	MCM2	Bioinformatics	1690 ±261	99	yes	yes	yes	x		x
YBL079W	NUP170	Y2H	1560	169	yes	no	yes	x		x
YBR002C	RER2	Y2H	8970	33	yes	no	yes	x		x
YBR060C	ORC2	Bioinformatics	1700 ±82.5	71	yes	yes	yes	x		
YBR143C	SUP45	Y2H	13100	49	yes	no	yes	x		
YBR200W	BEM1	Bioinformatics	6490	62	yes	yes	yes	x		
YBR218C	PYC2	Y2H	17000	130	yes	yes	yes	x		x
YCL014W	BUD3	Bioinformatics	technical problem	185	yes	yes	yes			
YCL024W	KCC4	Bioinformatics	538	116	yes	yes	yes	x		
YCR087C-A	LUG1	Y2H	3430	18	yes	no	yes	x		x
YCR088W	ABP1	Bioinformatics	606	66	yes	yes	yes	x		
YDL017W	CDC7	Bioinformatics	1600 ±816	58	yes	yes	yes	x		
YDL021W	GPM2	Y2H	2020	36	yes	yes	yes	x		
YDL117W	CYK3	Y2H	377	101	yes	yes	yes	x		x
YDR072C	IPT1	Y2H	606	61	yes	yes	yes			
YDR146C	SWI5	Bioinformatics	688	80	yes	yes	yes			
YDR177W	UBC1	Y2H	8940	24	yes	no	yes	x		x
YDR217C	RAD9	Bioinformatics	400	148	yes	yes	yes	x		x
YDR330W	UBX5	Y2H	6630	57	yes	no	yes	x		
YDR331W	GPI8	Y2H	1560	47	yes	no	yes	x		
YDR388W	RVS167	Y2H	14600	53	yes	no	yes	x		
YDR389W	SAC7	Y2H	1420	74	yes	yes	yes	x		x
YDR398W	UTP5	Y2H	33100	72	yes	no	yes			
YDR513W	GRX2	Y2H	31400	16	yes	yes	yes	x		x
YEL032W	MCM3	Bioinformatics	35100 ±5540	108	yes	yes	yes	x		
YEL043W	YEL043W	Y2H	149	106	yes	yes	yes			
YER018C	SPC25	Y2H	3280	25	yes	no	yes	x		x
YER020W	GPA2	Y2H	4570	50	yes	yes	yes	x		x
YER063W	THO1	Y2H	6580	24	yes	no	yes	x		
YER101C	AST2	Y2H	937	48	yes	no	yes			
YER164W	CHD1	Y2H	1620	168	yes	no	yes	x		
YER183C	FAU1	Y2H	468	24	yes	no	yes	x		x
YFL053W	DAK2	Y2H	low signal	62	yes	yes	yes			
YGL140C	YGL140C	Y2H	1080	138	yes	yes	yes			
YGL167C	PMR1	Y2H	6900	105	yes	yes	yes	x		x
YGL216W	KIP3	Y2H	736	91	yes	yes	yes	x		x
YGL219C	MDM34	Y2H	377	52	yes	yes	yes	x		
YGL248W	PDE1	Y2H	1400	42	yes	yes	yes			
YGR003W	CUL3	Bioinformatics	174	86	yes	yes	yes			
YGR005C	TFG2	Y2H	520 ±123	47	yes	no	yes	x		
YGR097W	ASK10	Bioinformatics	low signal	127	yes	yes	yes			
YGR147C	NAT2	Y2H	1240	33	yes	no	yes	x		x
YGR172C	CDC28	Y2H	6670	34	yes	no	yes	x		x
YHL007C	STE20	Bioinformatics	259	102	yes	yes	yes	x		
YHL025W	SNF6	Y2H	2900	38	yes	no	yes	x		
YHR102W	KIC1	Y2H	1040	117	yes	yes	yes	x		x
YHR104W	GRE3	Y2H	12900	37	yes	no	yes	x		
YHR118C	ORC6	Bioinformatics	2970 ±143	50	yes	yes	yes	x		
YIL031W	ULP2	Bioinformatics	450	117	yes	yes	yes	x		
YIL129C	TAO3	Y2H	206	270	yes	yes	yes	x		x
YIL140W	AXL2	Y2H	396	91	yes	no	yes	x		x
YJL095W	BCK1	Bioinformatics	112	164	yes	yes	yes			
YKL012W	PRP40	Y2H	low signal	69	yes	no	yes			
YKL067W	YNK1	Y2H	7130	17	yes	no	yes	x		x
YKL091C	YKL091C	Y2H	2870	36	yes	no	yes	x		

**Table 3.2 Continued: TAP-tagged Strains used in Cdc5-PBD Pulldown**

Systematic Name	Common Name	Identified By	Molecules Per Cell	Molecular Weight	PBDSite S(S/T)	PBDSite S(S/T)P	KinaseSite (E/D)X(S/T)	Saw in Lysate	Positive Hit	Negative Hit
YKL185W	ASH1	Bioinformatics	1800	66	yes	yes	yes			
YKL213C	DOA1	Y2H	6800	80	yes	no	yes	x		
YKL214C	YRA2	Y2H	1310	24	yes	no	yes	x	x	
YLR045C	STU2	Bioinformatics	1660	101	yes	yes	yes	x		
YLR057W	YLR057W	Y2H	71.6	97	yes	yes	yes			
YLR129W	DIP2	Y2H	9620	106	yes	no	yes	x		x
YLR175W	CBF5	Bioinformatics	33600 ±2870	55	yes	yes	yes	x	x	
YLR197W	SIK1	Y2H	13500 ±5780	57	yes	no	yes	x		
YLR219W	MSC3	Y2H	131	81	yes	no	yes			
YLR234W	TOP3	Y2H	468	74	yes	no	yes	x		
YLR257W	YLR257W	Y2H	18600	36	yes	yes	yes	x		
YLR265C	MSM1	Y2H	3120	67	yes	no	yes	x		
YLR265C	NEJ1	Y2H	377	39	yes	yes	yes	x	x	
YLR399C	BDF1	Y2H	8100	77	yes	yes	yes	x		x
YML034W	SRC1	Bioinformatics	2100	95	yes	yes	yes	x		
YML057W	CMP2	Y2H	7110	69	yes	no	yes	x		
YML082W	YML082W	Y2H	2810	74	yes	yes	yes	x		x
YML103C	NUP188	Y2H	11700	189	yes	yes	yes	x	x	
YMR115W	FMP24	Y2H	8970	58	yes	no	yes	x		
YMR121C	RPL15B	Y2H	721	24	yes	no	yes	x		x
YMR263W	SAP30	Y2H	704	23	yes	no	yes	x	x	
YNL004W	HRB1	Y2H	1990	49	yes	yes	yes	x		x
YNL022C	YNL022C	Y2H	922	56	yes	no	yes	x	x	
YNL023C	FAP1	Y2H	589	108	yes	no	yes	x		
YNL027W	CRZ1	Y2H	1160	76	yes	yes	yes			
YNL082W	PMS1	Bioinformatics	521	99	yes	yes	yes			
YNL126W	SPC98	Bioinformatics	56.9	98	yes	yes	yes	x		
YNL191W	YNL191W	Y2H	7300	40	yes	no	yes			
YNL197C	WHI3	Bioinformatics	5730	71	yes	yes	yes	x		
YNL225C	CNM67	Bioinformatics technical problem		67	yes	yes	yes	x	x	
YNL242W	ATG2	Y2H	876	178	yes	yes	yes			
YNL243W	SLA2	Y2H	40600	109	yes	yes	yes	x		x
YNR046W	TRM112	Y2H	4800	15	yes	no	yes	x	x	
YNR047W	YNR047W	Y2H	752	101	yes	yes	yes			
YOR058C	ASE1	Bioinformatics	556	102	yes	yes	yes			
YOR197W	MCA1	Y2H	1400	51	yes	no	no	x		
YOR231W	MKK1	Bioinformatics	1040	57	yes	yes	yes			
YOR239W	ABP140	Y2H	17000	71	yes	no	yes	x		x
YOR260W	GCD1	Y2H	9530 ±1760	66	yes	no	yes	x		x
YOR336W	KRE5	Y2H	815	156	yes	yes	yes	x		
YOR373W	NUD1	Y2H	892	94	yes	no	yes	x	x	
YPL105C	YPL105C	Y2H	830	94	yes	yes	yes	x		
YPL106C	SSE1	Y2H	71700	77	yes	yes	yes	x		x
YPL115C	BEM3	Bioinformatics	752	125	yes	yes	yes			
YPL119C	DBP1	Y2H	1480	68	yes	yes	yes			
YPL155C	KIP2	Bioinformatics	656	78	yes	yes	yes	x		x
YPL179W	PPQ1	Bioinformatics	319	61	yes	yes	yes			
YPL190C	NAB3	Y2H	5830 ±541	90	yes	yes	yes			
YPL198W	RPL7B	Y2H	7080	28	yes	no	no	x		x
YPL245W	YPL245W	Y2H	1130	52	yes	no	yes			
YPR083W	MDM36	Y2H	414	65	yes	no	yes			
YPR137W	RRP9	Y2H	5130	65	yes	no	yes	x		x
YPR167C	MET16	Y2H	217	30	yes	no	yes	x	x	
							<b>Totals</b>	<b>81</b>	<b>27</b>	<b>17</b>

**Notes:**

- As given in Ghammeiati et al. which is reference #3 in Chapter 3.
- Molecular Weight is given for endogenous protein without the addition of the TAP tag which adds 21kd.

## References

1. Brar, G.A., Kiburz, B.M., Zhang, Y., Kim, J.E., White, F., and Amon, A. (2006). Rec8 phosphorylation and recombination promote the step-wise loss of cohesins in meiosis. *Nature* *441*, 532-536.
2. Lee, K.S., Park, J.E., Asano, S., and Park, C.J. (2005). Yeast polo-like kinases: functionally conserved multitask mitotic regulators. *Oncogene* *24*, 217-229.
3. Ghaemmaghami, S., Huh, W.K., Bower, K., Howson, R.W., Belle, A., Dephoure, N., O'Shea, E.K., and Weissman, J.S. (2003). Global analysis of protein expression in yeast. *Nature* *425*, 737-741.
4. Bishop, A.C., Ubersax, J.A., Petsch, D.T., Matheos, D.P., Gray, N.S., Blethrow, J., Shimizu, E., Tsien, J.Z., Schultz, P.G., Rose, M.D., Wood, J.L., Morgan, D.O., and Shokat, K.M. (2000). A chemical switch for inhibitor-sensitive alleles of any protein kinase. *Nature* *407*, 395-401.
5. Hu, F., Wang, Y., Liu, D., Li, Y., Qin, J., and Elledge, S.J. (2001). Regulation of the Bub2/Bfa1 GAP complex by Cdc5 and cell cycle checkpoints. *Cell* *107*, 655-665.
6. Alexandru, G., Uhlmann, F., Mechtler, K., Poupart, M.A., and Nasmyth, K. (2001). Phosphorylation of the cohesin subunit Scc1 by Polo/Cdc5 kinase regulates sister chromatid separation in yeast. *Cell* *105*, 459-472.
7. Sakchaisri, K., Asano, S., Yu, L.R., Shulewitz, M.J., Park, C.J., Park, J.E., Cho, Y.W., Veenstra, T.D., Thorner, J., and Lee, K.S. (2004). Coupling morphogenesis to mitotic entry. *Proc Natl Acad Sci U S A* *101*, 4124-4129.
8. Yoshida, S., Kono, K., Lowery, D.M., Bartolini, S., Yaffe, M.B., Ohya, Y., and Pellman, D. (2006). Polo-like kinase Cdc5 controls the local activation of Rho1 to promote cytokinesis. *Science* *313*, 108-111.
9. Lowery, D.M., Lim, D., and Yaffe, M.B. (2005). Structure and function of Polo-like kinases. *Oncogene* *24*, 248-259.
10. Shirayama, M., Zachariae, W., Ciosk, R., and Nasmyth, K. (1998). The Polo-like kinase Cdc5p and the WD-repeat protein Cdc20p/fizzy are regulators and substrates of the anaphase promoting complex in *Saccharomyces cerevisiae*. *Embo J* *17*, 1336-1349.
11. Song, S., Grenfell, T.Z., Garfield, S., Erikson, R.L., and Lee, K.S. (2000). Essential function of the polo box of Cdc5 in subcellular localization and induction of cytokinetic structures. *Mol Cell Biol* *20*, 286-298.



12. Hornig, N.C., and Uhlmann, F. (2004). Preferential cleavage of chromatin-bound cohesin after targeted phosphorylation by Polo-like kinase. *Embo J* 23, 3144-3153.
13. Pearson, C.G., and Bloom, K. (2004). Dynamic microtubules lead the way for spindle positioning. *Nat Rev Mol Cell Biol* 5, 481-492.
14. Elia, A.E., Cantley, L.C., and Yaffe, M.B. (2003). Proteomic screen finds pSer/pThr-binding domain localizing Plk1 to mitotic substrates. *Science* 299, 1228-1231.
15. Song, S., and Lee, K.S. (2001). A novel function of *Saccharomyces cerevisiae* CDC5 in cytokinesis. *J Cell Biol* 152, 451-469.
16. Bartholomew, C.R., Woo, S.H., Chung, Y.S., Jones, C., and Hardy, C.F. (2001). Cdc5 interacts with the Wee1 kinase in budding yeast. *Mol Cell Biol* 21, 4949-4959.
17. Park, C.J., Song, S., Giddings, T.H., Jr., Ro, H.S., Sakchaisri, K., Park, J.E., Seong, Y.S., Winey, M., and Lee, K.S. (2004). Requirement for Bbp1p in the proper mitotic functions of Cdc5p in *Saccharomyces cerevisiae*. *Mol Biol Cell* 15, 1711-1723.
18. Mort-Bontemps-Soret, M., Facca, C., and Faye, G. (2002). Physical interaction of Cdc28 with Cdc37 in *Saccharomyces cerevisiae*. *Mol Genet Genomics* 267, 447-458.
19. Ito, T., Chiba, T., Ozawa, R., Yoshida, M., Hattori, M., and Sakaki, Y. (2001). A comprehensive two-hybrid analysis to explore the yeast protein interactome. *Proc Natl Acad Sci U S A* 98, 4569-4574.
20. Ji, J.H., and Jang, Y.J. (2006). Screening of domain-specific target proteins of polo-like kinase 1: construction and application of centrosome/kinetochore-specific targeting peptide. *J Biochem Mol Biol* 39, 709-716.
21. Ubersax, J.A., Woodbury, E.L., Quang, P.N., Paraz, M., Blethrow, J.D., Shah, K., Shokat, K.M., and Morgan, D.O. (2003). Targets of the cyclin-dependent kinase Cdk1. *Nature* 425, 859-864.
22. Lowery, D.M., Clauser, K.R., Hjerrild, M., Lim, D., Alexander, J., Kishi, K., Ong, S.E., Gammeltoft, S., Carr, S.A., and Yaffe, M.B. (2007). Proteomic screen defines the Polo-box domain interactome and identifies Rock2 as a Plk1 substrate. *Embo J* 26, 2262-2273.

23. Elia, A.E., Rellos, P., Haire, L.F., Chao, J.W., Ivins, F.J., Hoepker, K., Mohammad, D., Cantley, L.C., Smerdon, S.J., and Yaffe, M.B. (2003). The molecular basis for phosphodependent substrate targeting and regulation of Plks by the Polo-box domain. *Cell* *115*, 83-95.
24. Guo, D., Hazbun, T.R., Xu, X.J., Ng, S.L., Fields, S., and Kuo, M.H. (2004). A tethered catalysis, two-hybrid system to identify protein-protein interactions requiring post-translational modifications. *Nat Biotechnol* *22*, 888-892.
25. Mosammaparast, N., and Pemberton, L.F. (2004). Karyopherins: from nuclear-transport mediators to nuclear-function regulators. *Trends Cell Biol* *14*, 547-556.
26. Sazer, S. (2005). Nuclear envelope: nuclear pore complexity. *Curr Biol* *15*, R23-26.
27. Ball, J.R., and Ullman, K.S. (2005). Versatility at the nuclear pore complex: lessons learned from the nucleoporin Nup153. *Chromosoma* *114*, 319-330.
28. Roux, K.J., and Burke, B. (2006). From pore to kinetochore and back: regulating envelope assembly. *Dev Cell* *11*, 276-278.
29. Glover, D.M. (2005). Polo kinase and progression through M phase in *Drosophila*: a perspective from the spindle poles. *Oncogene* *24*, 230-237.
30. Liu, J., and Maller, J.L. (2005). *Xenopus* Polo-like kinase Plx1: a multifunctional mitotic kinase. *Oncogene* *24*, 238-247.
31. Barr, F.A., Sillje, H.H., and Nigg, E.A. (2004). Polo-like kinases and the orchestration of cell division. *Nat Rev Mol Cell Biol* *5*, 429-440.
32. van de Weerd, B.C., and Medema, R.H. (2006). Polo-like kinases: a team in control of the division. *Cell Cycle* *5*, 853-864.
33. Lee, K.S., and Erikson, R.L. (1997). Plk is a functional homolog of *Saccharomyces cerevisiae* Cdc5, and elevated Plk activity induces multiple septation structures. *Mol Cell Biol* *17*, 3408-3417.
34. Nakajima, H., Toyoshima-Morimoto, F., Taniguchi, E., and Nishida, E. (2003). Identification of a consensus motif for Plk (Polo-like kinase) phosphorylation reveals Myt1 as a Plk1 substrate. *J Biol Chem* *278*, 25277-25280.
35. Shou, W., Azzam, R., Chen, S.L., Huddleston, M.J., Baskerville, C., Charbonneau, H., Annan, R.S., Carr, S.A., and Deshaies, R.J. (2002). Cdc5 influences phosphorylation of Net1 and disassembly of the RENT complex. *BMC Mol Biol* *3*, 3.

36. Kothe, M., Kohls, D., Low, S., Coli, R., Cheng, A.C., Jacques, S.L., Johnson, T.L., Lewis, C., Loh, C., Nonomiya, J., Sheils, A.L., Verdries, K.A., Wynn, T.A., Kuhn, C., and Ding, Y.H. (2007). Structure of the catalytic domain of human Polo-like kinase 1. *Biochemistry* 46, 5960-5971.
37. Obenauer, J.C., Cantley, L.C., and Yaffe, M.B. (2003). Scansite 2.0: Proteome-wide prediction of cell signaling interactions using short sequence motifs. *Nucleic Acids Res* 31, 3635-3641.
38. Yaffe, M.B., Leparc, G.G., Lai, J., Obata, T., Volinia, S., and Cantley, L.C. (2001). A motif-based profile scanning approach for genome-wide prediction of signaling pathways. *Nat Biotechnol* 19, 348-353.
39. Dephoure, N., Howson, R.W., Blethrow, J.D., Shokat, K.M., and O'Shea, E.K. (2005). Combining chemical genetics and proteomics to identify protein kinase substrates. *Proc Natl Acad Sci U S A* 102, 17940-17945.
40. Cheng, K.Y., Lowe, E.D., Sinclair, J., Nigg, E.A., and Johnson, L.N. (2003). The crystal structure of the human polo-like kinase-1 polo box domain and its phospho-peptide complex. *Embo J* 22, 5757-5768.
41. Geymonat, M., Spanos, A., Walker, P.A., Johnston, L.H., and Sedgwick, S.G. (2003). In vitro regulation of budding yeast Bfa1/Bub2 GAP activity by Cdc5. *J Biol Chem* 278, 14591-14594.
42. Yoshida, S., and Toh-e, A. (2002). Budding yeast Cdc5 phosphorylates Net1 and assists Cdc14 release from the nucleolus. *Biochem Biophys Res Commun* 294, 687-691.
43. Bishop, A., Buzko, O., Heyeck-Dumas, S., Jung, I., Kraybill, B., Liu, Y., Shah, K., Ulrich, S., Witucki, L., Yang, F., Zhang, C., and Shokat, K.M. (2000). Unnatural ligands for engineered proteins: new tools for chemical genetics. *Annu Rev Biophys Biomol Struct* 29, 577-606.
44. Cohen, M.S., Zhang, C., Shokat, K.M., and Taunton, J. (2005). Structural bioinformatics-based design of selective, irreversible kinase inhibitors. *Science* 308, 1318-1321.
45. Cheng, L., Hunke, L., and Hardy, C.F. (1998). Cell cycle regulation of the *Saccharomyces cerevisiae* polo-like kinase cdc5p. *Mol Cell Biol* 18, 7360-7370.
46. Gruneberg, U., Campbell, K., Simpson, C., Grindlay, J., and Schiebel, E. (2000). Nud1p links astral microtubule organization and the control of exit from mitosis. *Embo J* 19, 6475-6488.

47. Li, S.J., and Hochstrasser, M. (2000). The yeast ULP2 (SMT4) gene encodes a novel protease specific for the ubiquitin-like Smt3 protein. *Mol Cell Biol* *20*, 2367-2377.
48. Bachant, J., Alcasabas, A., Blat, Y., Kleckner, N., and Elledge, S.J. (2002). The SUMO-1 isopeptidase Smt4 is linked to centromeric cohesion through SUMO-1 modification of DNA topoisomerase II. *Mol Cell* *9*, 1169-1182.
49. Morandell, S., Stasyk, T., Grosstessner-Hain, K., Roitinger, E., Mechtler, K., Bonn, G.K., and Huber, L.A. (2006). Phosphoproteomics strategies for the functional analysis of signal transduction. *Proteomics* *6*, 4047-4056.
50. Korinek, W.S., Bi, E., Epp, J.A., Wang, L., Ho, J., and Chant, J. (2000). Cyk3, a novel SH3-domain protein, affects cytokinesis in yeast. *Curr Biol* *10*, 947-950.
51. Schaerer, F., Morgan, G., Winey, M., and Philippsen, P. (2001). Cnm67p is a spacer protein of the *Saccharomyces cerevisiae* spindle pole body outer plaque. *Mol Biol Cell* *12*, 2519-2533.
52. Hoepfner, D., Brachat, A., and Philippsen, P. (2000). Time-lapse video microscopy analysis reveals astral microtubule detachment in the yeast spindle pole mutant *cnm67*. *Mol Biol Cell* *11*, 1197-1211.
53. Brachat, A., Kilmartin, J.V., Wach, A., and Philippsen, P. (1998). *Saccharomyces cerevisiae* cells with defective spindle pole body outer plaques accomplish nuclear migration via half-bridge-organized microtubules. *Mol Biol Cell* *9*, 977-991.
54. Hoepfner, D., Schaerer, F., Brachat, A., Wach, A., and Philippsen, P. (2002). Reorientation of mispositioned spindles in short astral microtubule mutant *spc72Delta* is dependent on spindle pole body outer plaque and Kar3 motor protein. *Mol Biol Cell* *13*, 1366-1380.
55. Knop, M., and Schiebel, E. (1998). Receptors determine the cellular localization of a gamma-tubulin complex and thereby the site of microtubule formation. *Embo J* *17*, 3952-3967.
56. Soues, S., and Adams, I.R. (1998). SPC72: a spindle pole component required for spindle orientation in the yeast *Saccharomyces cerevisiae*. *J Cell Sci* *111 (Pt 18)*, 2809-2818.
57. Chen, X.P., Yin, H., and Huffaker, T.C. (1998). The yeast spindle pole body component Spc72p interacts with Stu2p and is required for proper microtubule assembly. *J Cell Biol* *141*, 1169-1179.

58. Ho, Y., Gruhler, A., Heilbut, A., Bader, G.D., Moore, L., Adams, S.L., Millar, A., Taylor, P., Bennett, K., Boutilier, K., Yang, L., Wolting, C., Donaldson, I., Schandorff, S., Shewnarane, J., Vo, M., Taggart, J., Goudreault, M., Muskat, B., Alfarano, C., Dewar, D., Lin, Z., Michalickova, K., Willems, A.R., Sassi, H., Nielsen, P.A., Rasmussen, K.J., Andersen, J.R., Johansen, L.E., Hansen, L.H., Jespersen, H., Podtelejnikov, A., Nielsen, E., Crawford, J., Poulsen, V., Sorensen, B.D., Matthiesen, J., Hendrickson, R.C., Gleeson, F., Pawson, T., Moran, M.F., Durocher, D., Mann, M., Hogue, C.W., Figeys, D., and Tyers, M. (2002). Systematic identification of protein complexes in *Saccharomyces cerevisiae* by mass spectrometry. *Nature* 415, 180-183.
59. Huh, W.K., Falvo, J.V., Gerke, L.C., Carroll, A.S., Howson, R.W., Weissman, J.S., and O'Shea, E.K. (2003). Global analysis of protein localization in budding yeast. *Nature* 425, 686-691.
60. Rose, M.D., Winston, F., and Hieter, P. (1990). *Methods in Yeast Genetics* (Cold Spring Harbor, NY: Cold Spring Harbor Laboratory).
61. James, P., Halladay, J., and Craig, E.A. (1996). Genomic libraries and a host strain designed for highly efficient two-hybrid selection in yeast. *Genetics* 144, 1425-1436.

# Chapter Four

## **Cytokinesis-Specific Function of RhoGEFs Controlled by Polo-like Kinases in Yeast and Human**

Yeast Portion Shortened From  
Satoshi Yoshida, Keiko Kono, Drew M. Lowery, Sara Bartolini,  
Michael B. Yaffe, Yoshikazu Ohya, and David Pellman.  
Polo-like kinase Cdc5 controls the local activation of Rho1 to promote cytokinesis.  
Science 313, 2006.

Subsequently several papers on similar topics in mammalian cells were published, data for which I now reference concurrently with the text on the original yeast work along with inserting my own work on the mammalian RhoGEF, Ect2, in cytokinesis.

### Contributions:

Satoshi Yoshida performed all of the yeast work not explicitly mentioned below and wrote much of the manuscript. Keiko performed the Rho1 assays shown in Figure 4.7 and elsewhere. Sara generated a huge number of constructs and strains, and performed many of the genetic analyses with Satoshi. The mammalian Ect2 was done in collaboration with Mark Burkard in Prasad Jallapelli's laboratory. Mark and Prasad both made significant intellectual contributions to the project, and Mark performed the experiments shown in Figure 4.10A. Karl Clauser in Steve Carr's laboratory at the Broad Institute performed the mass spectrometry based identification of phosphorylation sites shown in Table 4.3 and 4.5. For the yeast work I designed and performed the PBD pulldown assay with Satoshi as shown in Figure 4.2, performed all the in vitro kinase reactions as detailed in Tables 4.1-2, performed sequence analysis of PBD interactors and suggested appropriate mutations, and provided advice on biochemical methods. For the mammalian work I performed the experiments, made the figures, and wrote all related text to Figures 4.3, 4.19, and 4.10B, and Tables 4.3 and 4.5.

## **Abstract**

The links between the cell cycle machinery and the cytoskeletal proteins controlling cytokinesis are poorly understood. The small guanine nucleotide triphosphate (GTP)-binding protein RhoA stimulates type II myosin contractility and formin-dependent assembly of the cytokinetic actin contractile ring. We found that budding yeast Polo-like kinase Cdc5 controls the targeting and activation of Rho1 (RhoA) at the division site via Rho1 guanine nucleotide exchange factors. This role of Cdc5 (Polo-like kinase) in regulating Rho1 is likely to be relevant to cytokinesis and asymmetric cell division in other organisms. Subsequently several groups demonstrated that in mammalian cells Plk1 controls the targeting and activation of RhoA at the division site through multiple mechanisms including via the RhoGEF Ect2 [1-3] though the role of Ect2 in RhoA targeting was already well established [4-6]. We go on to show that Ect2 is localized to the division site through a phosphorylation dependent interaction between the Ect2 tandem BRCT domains and the Plk1 substrate Cyk4.

## **Introduction**

Cytokinesis, the physical separation of daughter cells after mitosis, involves the dynamic reorganization of the cortical cytoskeleton and is precisely regulated both in time and space [7, 8]. Successful cytokinesis is critical to the maintenance of genome stability as cytokinesis failure can lead to chromosome aberrations and cancer [9]. The timing and mechanism of contractile actin ring (CAR) assembly is an important but poorly understood aspect of the eukaryotic cell cycle.

The Polo-like kinase Cdc5 controls many aspects of cell division, including cytokinesis [10, 11]. Plk1 is involved in cytokinesis in animal cells, but its precise role has been difficult to address because manipulations that inhibit Polo-like kinase produce spindle assembly defects, which affect CAR organization [7, 12, 13]. RhoA/1 is an attractive candidate to be under Polo-like kinase regulation because of its essential role in CAR assembly and contraction [7, 8, 14, 15]. In yeast, cytokinesis is largely independent of microtubules [14], making yeast an advantageous system to study the role of Polo-like kinase. Additionally, the contractile ring is not essential in most budding yeast strains; another mechanism involving cell wall deposition can substitute for CAR function [16, 17]. This facilitates genetic analysis because null alleles affecting CAR function can be studied in viable cells. Despite these differences, the core machinery for CAR assembly is conserved in budding yeast: CAR assembly requires Rho1, the functional homolog of RhoA in animal cells, which activates actin filament assembly via formins [14, 18].



## Results and Discussion

The timing of CAR assembly was characterized by actin staining and by labeling of the CAR with a fusion between tropomyosin and green fluorescent protein (Tpm2-GFP) (Figure 4.1A). To identify cell cycle regulators required for CAR assembly, we reexamined CAR assembly in mutants that block mitotic exit [17, 19]. The CAR assembled in *cdc15-2* or *cdc14-1* strains, mutations that compromise the canonical mitotic exit network (MEN) (Figure 4.1A). By contrast, CAR assembly was impaired in mutants lacking Cdc5 (Figure 4.1A). The defect in CAR assembly in cells lacking Cdc5 was not a secondary consequence of the anaphase defect in these cells as mutations in other Cdc5 regulated processes, such as *cdc14* which is a member of the FEAR network (Figure 4.1A), did not overcome this defect [20]. To test whether Cdc5 was also required to maintain CAR formation we performed the experiment in Figure 4.1B. In this experiment, cells were first arrested in telophase by overexpression of Bfa1, an inhibitor of mitotic exit [21, 22] at 23°C. This cell cycle block is after CAR assembly (Figure 4.1B). After the temperature shift to the restrictive temperature (34.5 °C), the *cdc5-2* strain failed to maintain a visible CAR (Figure 4.1B). In the absence of Cdc5, a residual fraction of cells were observed that had thin CARs (Figure 4.1A). Thus, Cdc5, although not absolutely essential for CAR assembly, is an important regulator. Similarly Plk1 activity is required for the assembly of many components of the contractile ring in mammalian cells including anillin and myosinII [1-3] though it is not required for chromosome separation in anaphase [2, 3]. Plk1 activity is required after CDK1 inactivation and independently of Aurora B to promote initiation of cytokinesis [2].

Next we characterized the nature of the CAR assembly defect in *cdc5-2* cells at the restrictive temperature, with the use of the MEN mutant *cdc15-2* as a control. By contrast, although the formin Bni1 and Rho1 localized normally to the neck in *cdc15-2*-arrested cells, neither Bni1 nor Rho1 was detectable at the bud neck in *cdc5-2*-arrested cells (Figure 4.1C). Furthermore, Bni1 was often mistargeted to the bud tip in *cdc5-2*-arrested cells (Figure 4.1C). Thus, Cdc5 is required for the neck recruitment of Rho1 and Bni1, a key downstream factor required for CAR assembly. Plk1 activity is similarly required for the localization of RhoA to the future cleavage furrow site [1-3].

To identify potential Cdc5 substrates relevant to Rho1 regulation, we screened all known budding yeast Rho guanine triphosphate (GTPase) regulators for interaction with the Polo-box domain (PBD) of Cdc5 [13, 23, 24]. PBD binding partners include the Rho1 guanine nucleotide exchange factors (GEFs) Rom2 and Tus1, the Rho1 GTPase activating protein (GAP) Sac7, and a putative Rho-GAP, Ecm25 (Figure 4.2A and 4.2B). The PBD also binds Bem3, a GAP for Cdc42, the major small GTPase that controls polarized morphogenesis in budding yeast. These interactions are highly specific to the priming phosphorylation of the candidates, because the interaction was lost with a Polobox pincer mutation, PBD\* (Figure 4.2A and 4.2B), that abolishes phosphospecific recognition of the substrates by PBD [24]. All the candidates had multiple potential Polo-box binding sequences, binding motifs that are often primed by cyclin-dependent kinase (CDK)-dependent phosphorylation [23]. Tus1, Bem3, Sac7, and Ecm25 are also good CDK substrates [25]. The only RhoA regulator known to bind the Plk1-PBD is the Rom2 and Tus1 homologue, Ect2 (Figure 4.3A) [26].

Because of the requirement of Rho1 [27] and RhoA [8] for CAR assembly, we focused our subsequent analysis on the Rho GEFs, Tus1, Rom2, and in human cells Ect2. Genetic analyses demonstrate that null mutants of TUS1 and ROM2 impair the CAR/Myosin II pathway. The null mutant of ROM2 also partially impaired the CAR-independent cytokinesis pathway suggesting ROM2 has multiple cytokinesis roles [20]. Consistent with this, the combination of *tus1Δ* with *rom2Δ* resulted in a synergistic defect in CAR assembly while deletion of the third Rho1 GEF, Rom1, did not have any effect on CAR assembly [20]. These findings are consistent with the requirement for the fission yeast Tus1 homolog in cytokinesis [28-30]. The pattern of synthetic lethality observed with *cdc5-2* also provided genetic evidence for a role for Cdc5 in the CAR-dependent mechanism [20], though CAR-independent roles for Cdc5 were also observed [20]. This is not surprising given that Cdc5 is required for global activation of Rho1 as described later (Figure 4.7B) and that overexpression of a dominant-negative form of Cdc5 interferes with both the CAR-dependent and CAR-independent pathways for cytokinesis [11].

We next evaluated the possibility that Tus1 is a direct Polo-like kinase substrate. The N terminus of Tus1 (Tus1<sup>1-300</sup>), containing two Polo-box binding motifs (Ser-

Ser/Thr-Pro), is sufficient for Polo-box binding (Figure 4.4A and 4.4B). The serine residues immediately preceding the CDK consensus site in the Polo-box binding motifs of Tus1 (Ser7 and Ser92) were mutated to threonine (hereafter referred to as ST mutations), a well-characterized change that disrupts binding to the PBD [23, 24] but that should not affect CDK-dependent phosphorylation. Glutathione S-transferase (GST)–PBD precipitation experiments revealed that neither Tus1-ST1–300 nor full-length Tus1-ST protein bound to the PBD (Figure 4.2C and 4.4B). Similar ST substitutions were introduced into the coding sequence for Rom2; the Rom2-ST protein also had a reduced affinity for the Cdc5 PBD (Figure 4.5). Thus, Tus1 and Rom2 interact with Cdc5 by a mechanism similar to that of other known Polo substrates. Ect2 also binds to the Plk1-PBD in a phosphorylation dependent manner through phosphorylation of Thr413 in Ect2 by CDK1 (Figure 4.3B) [26].

Biochemical experiments suggested that Tus1 is a bona fide in vivo Cdc5 substrate. Although we were not able to detect a clear mobility shift of the full-length Tus1 (1307 amino acids), the Tus1 Polo-box interacting domain (PID), Tus1<sup>1-300</sup>, was phosphorylated in vivo as evidenced by a motility shift that was abolished by phosphatase treatment in *cdc15-2*-arrested cells (Figure 4.4C). Most notably, the slowest migrating form of Tus1<sup>1-300</sup> (hereafter referred to as hyperphosphorylated) was absent in *cdc5-2*-arrested cells (Figure 4.2D). This hyperphosphorylated form could also be induced in cycling cells by overexpression of Cdc5 (Figure 4.4D). Furthermore, Tus1-ST<sup>1-300</sup> also lost this hyperphosphorylated band (Figure 4.2D). Thus, Tus1<sup>1-300</sup> is phosphorylated in late mitosis in a manner that depends on Cdc5. The fact that this Cdc5-dependent phosphorylation also required physical interaction between Tus1<sup>1-300</sup> and the Polo box strongly suggests that the Cdc5-dependent phosphorylation of Tus1<sup>1-300</sup> is direct. Indeed, mass spectrometry confirmed that the Tus1<sup>1-300</sup> was readily phosphorylated by a human Polo-like kinase, Plk1, in vitro (Table 4.1), identifying at least 12 phosphorylated residues. Although we were not able to map phosphorylation sites directly on full-length Tus1 because of its low expression [31], together with our genetic data these findings strongly suggest that Tus1 is a Cdc5 substrate.

We attempted similar experiments to characterize the potential Polo-like kinase dependent phosphorylation of Rom2. We identified several in vitro Plk1 phosphorylation

sites by mass spectrometry (Table 4.2). However, we were not able to identify a mobility shift for full-length Rom2, nor were we able to detect a mobility shift for several N-terminal Rom2 fragments. These fragments were not well expressed in *Escherichia coli* and thus may not fold properly. Nevertheless, the similar phenotypes of *rom2-ST* and *tus1-ST* strains (Table 4.4, and Figure 4.6, text below) suggest that in vivo Cdc5 regulates Rom2 similarly to Tus1. Ect2 is a known in vitro target of Plk1 [26] which we confirmed (Figure 4.3C), and we were able to map two phosphorylation sites in Ect2 through mass spectrometry (Table 4.3) at sites T319 and S636. In vivo evidence that Ect2 is a Plk1 substrate is lacking though the expression of a PBD binding site mutant of Plk1 does cause RhoA activation problems [26]. Since these two sites do not conform to any known Plk consensus phosphorylation motif they could be an in vitro artifact that do not have an in vivo functional role.

The synthetic lethal interactions observed with *tus1-ST* and *rom2-ST* suggested that these mutations were specifically defective in the CAR-dependent pathway for cytokinesis but not other Rho1-dependent cellular functions (Table 4.4, and Figure 4.6). *tus1-ST hof1Δ* strains displayed a striking reduction in fitness whereas *tus1-ST myo1Δ* strains grew like the *myo1Δ* single deletion strain (Figure 4.6). This suggests that *tus1-ST* has a specific defect in the CAR pathway. Furthermore, unlike *tus1Δ*, *tus1-ST* was viable when combined with a deletion of *MPK1* (Table 4.4). *Mpk1/Slt2* is a component of the Rho1-Pkc1-MAP kinase cascade that responds to cell wall defects [32]. Thus, *Tus1-ST*, though defective for CAR assembly, is proficient for its role in maintaining cell wall integrity. Consistent with the hypothesis that the "ST" mutation in *ROM2* partially compromised the CAR pathway, *rom2-ST hof1Δ* double mutants also exhibited a moderate growth defect and *rom2-ST* did not enhance the growth defect of *myo1Δ* strains (Figure 4.6). Furthermore, although Rom2, together with Rom1, is essential for cell wall biosynthesis during bud emergence [33], *rom1Δ rom2-ST* strains were viable with normal bud morphology unlike *rom1Δ rom2Δ* strains (Table 4.4). Finally, *tus1Δ rom2Δ* strains are inviable because of a cell wall integrity defect [32] whereas *tus1-ST rom2-ST* strains, despite a severe cytokinesis defect, grow even at 37°C (Table 4.4). Thus, the ST mutants are separation-of-function alleles that are specifically defective in contractile ring function. Supporting this hypothesis, *tus1-ST* strains arrested in telophase were defective

in CAR assembly, and this defect was enhanced in *tus1-ST rom2-ST* double mutant strains (Figure 4.7A).

A Tus1 protein containing several phosphomimetic mutations at putative Cdc5 phosphorylation sites provided further evidence for the importance of Cdc5-dependent phosphorylation of Tus1 for CAR assembly. Phosphomimetic mutations (Ser to Asp or Thr to Glu) were introduced at Ser or Thr residues within Plk1 phosphorylation consensus sites (Asp/Glu-X-Ser/Thr, where X is any amino acid). This consensus is optimal for Plk1-dependent phosphorylation of vertebrate Cdc25 [34] and perfectly matches the *in vivo* Cdc5 target phosphorylation sites on Mcd1 (Scc1) [35]. Three out of four Plk1 phosphorylation consensus sites within Tus1<sup>1-300</sup> were phosphorylated by Plk1 *in vitro* (Table 4.1). A Tus1 mutant containing six putative phosphomimetic changes (Tus1-6DE) partially bypassed the requirement for Cdc5, both for CAR formation and for Rho1 localization to the division site (Figure 4.2E). A control Tus1 mutant where the putative phosphorylation sites were mutated to Ala failed to restore CAR assembly and Rho1 localization in *cdc5-2* cells, demonstrating that only the negatively charged residues caused a gain-of-function effect at these sites. The magnitude of the gain-of-function phenotype induced by *TUS1-6DE* is likely to be an underestimate, because the introduction of negatively charged residues appears to reduce the already low steady state expression of Tus1 (Figure 4.4E) [31].

Our experiments suggest that Cdc5 controls Rho1 through Tus1 and Rom2. This was directly tested by monitoring the amount of active Rho1 both globally and locally at the bud neck. The total amount of active GTP-bound Rho1 was detected by a precipitation assay with the Rho1-binding domain (RBD) of Pkc1 (Figure 4.7B). The amount of active Rho1 was diminished in *cdc5-2*-arrested cells in comparison with *cdc15-2*-arrested cells (Figure 4.7B). We also visualized active Rho1 by immunofluorescence using an antibody that specifically detects GTP-bound Rho1 [36]. Consistent with the precipitation experiment of active Rho1, activated Rho1 was barely detectable in *cdc5-2*-arrested cells but was abundant and recruited to the bud neck region in *cdc15-2*-arrested cells (Figure 4.7A). By contrast, *tus1-ST rom2-ST* cells arrested at the *cdc15-2* block had active Rho1 at the bud cortex but lacked active Rho1 at the bud neck (Figure 4.7A). Consistent with this observation, the precipitation assay indicated

that Rho1 activity was not diminished in *tus1-ST rom2-ST* strains and in fact was slightly elevated (Figure 4.7B). The fact that total Rho1 activity was high in *tus1-ST rom2-ST* strains but low in *cdc5-2* strains suggests that Cdc5 also controls global Rho1 activity through another mechanism, perhaps through Rho1 GAPs such as Sac7 (Figure 4.2B). Thus, Cdc5-dependent regulation of Tus1 and Rom2 controls the local activation of Rho1 at the division site but not the global levels of active Rho1 in the cell. This is still unclear in mammalian cells as though clearly Plk1 is required for RhoA localization [1-3] the connection with RhoA activation has not been fully worked out though work is in progress (see below).

Next, we determined whether Cdc5-dependent phosphorylation is required to recruit Tus1 and Rom2 to the bud neck. Consistent with its important role in CAR assembly, Tus1-GFP was recruited to the bud neck just before CAR constriction. The bud neck localization of Tus1 was dependent on Cdc5 activity but not on other MEN components (Figure 4.8A). Furthermore, Tus1-ST-GFP failed to localize to the division site in *cdc15-2*-arrested cells that had high Cdc5 activity (Figure 4.8A). Similarly Ect2 was dependent on Plk1 activity for localization to the cell division site [1-3]. Previously Ect2 localization to the division site had been shown to be required for localization of active RhoA to the division site [4]. Thus taken together it seems Plk1, like Cdc5, is responsible for localization of active RhoA, though the direct connection between Cdc5 phosphorylation of Tus1 is not yet present in the Plk1 and Ect2 system.

We next tested whether the requirement for Cdc5 regulation of Tus1 could be bypassed by tethering the ST variant to the bud neck. The coding sequence for Tus1-ST-GFP was fused to the coding sequence for Mlc2, a nonessential type II myosin light chain [37], and expressed from the endogenous *TUS1* promoter. Indeed, in *cdc15-2*-arrested cells, Tus1-ST-Mlc2-GFP protein localized to the bud neck and activated CAR assembly, unlike Tus1-ST-GFP (Figure 4.8B). Furthermore, Tus1-Mlc2-GFP could partially restore CAR assembly in *cdc5-2*-arrested cells (Figure 4.8B). Thus, a critical function of the Cdc5-dependent regulation of cytokinesis is to recruit Tus1, and thus Rho1, to the site of CAR assembly. These results do not exclude the additional possibility that Cdc5 also affects Tus1 GEF activity. However, in mammalian cells it does not seem likely that Plk1 does not regulate the GEF activity of Ect2 as I have not seen a difference in Ect2

GEF assays in the presence of Plk1 (data not shown). Nor does the GEF activity of Ect2 seem to be critical for RhoA activity during cytokinesis as siRNA depletion of Ect2 results in loss of active RhoA localization but no change in bulk active RhoA levels [38]. Thus, the relative importance of GEF activity versus localization for both RhoA and Rho1 remains unclear.

Our study reveals a molecular pathway by which Cdc5 and Plk1 control contractile ring assembly in budding yeast and mammalian cells. Cdc5/Plk1 is required for the recruitment of Rho GEFs to the division site that in turn is necessary for recruitment and activation of Rho1/A. The failure of this mechanism results in the mistargeting of the formin Bni1 from the bud neck to the bud tip in budding yeast. This causes a defect in CAR assembly, because the actin filaments in the contractile ring are assembled by formins [7, 8, 14]. It is possible that Cdc5 and Plk1 have more broad roles in Rho-type GTPase regulation than the local activation of Rho1 at the division site. Cdc5 is required for the global activation of Rho1 in late mitosis (unknown for Plk1), whereas the Cdc5/Plk1 regulation of Tus1, Rom2, and Ect2 is required for local Rho1/A recruitment and activation. Cdc5/Plk1 could exert additional control of Rho1/A via Rho GAPs. It is also possible that Cdc5/Plk1 could exert Polo-box independent regulation of Rho1/A GEFs. Lastly, given that fission yeast Polo kinase was recently shown to be required for stress-induced polarized growth [39], it is intriguing that our biochemical screen identified Bem3, a Cdc42 GAP, as a Polo-box binding partner. Our findings thus elucidate a mechanism by which Polo-like kinase governs Rho1/A during cytokinesis and raise the possibility that Polo-like kinase controls other aspects of the cortical cytoskeleton through other Rho GTPases.

Cdc5 control of the localization of the RhoGEFs Tus1 and Rom2 (and therefore localization of active Rho1) is directly dependent on Cdc5-PBD binding and Cdc5 phosphorylation of Tus1 and Rom2. In the Plk1 and Ect2 case this has not been shown. Instead Ect2 localization is dependent on the centralspindlin complex and specifically binds Cyk-4 (also known as MgcRacGAP) [4] in a manner that requires Plk1 activity [1, 2]. This interaction has been narrowed down to require the tandem BRCT domains of Ect2 and the N-terminus of Cyk-4, and occurs in a phosphodependent manner in anaphase cells but not metaphase cells [4]. Intriguingly I helped identify tandem BRCT

domains as phospho-dependent binding domains (Appendix One) [40], so Ect2 might bind to Cyk-4 in a manner analogous to that of Brca1 and Bach1 (Appendix One) [41]. A sequence alignment of Brca1, PTIP, and Ect2 (Figure 4.9A) reveals that they all have conserved residues at the sites where Brca1 directly binds phosphate as revealed by Brca1 crystal structures (Appendix One) [41]. Mutation of these residues in PTIP also eliminates phosphopeptide binding (Duaa Mohammad - personal communication). Thus it seems likely that Ect2 binds phosphopeptides in a similar manner. However, when I performed peptide library binding experiments (for methods see Appendix One) I did not observe any specific phospho-binding by the Ect2 BRCTs (Figure 4.9B). It is possible that none of the libraries tested have enough specificity for the Ect2 BRCTs despite the fact that they all can be bound by both PTIP and Brca1 BRCTs (Appendix One and Figure 4.9B). Another possibility is that the Ect2 BRCT phosphorylation-dependent binding is weaker than those of PTIP and Brca1, and requires either a full protein for binding or multiple binding sites to create an avidity effect.

Since the weight of the evidence suggested that the Ect2 BRCTs and Cyk-4 (also known as MgcRacGAP) interacted in a phosphorylation and Plk1 dependent manner [1, 2, 4] we directly investigated whether Plk1 could generate binding sites that contributed to the Ect2/Cyk-4 interaction in vitro. Active full length Plk1 kinase was incubated with either CDB-Cyk4 or the Ect2 E5 fragment (residues 1-421) which encompass the BRCT domains. The kinase reactions were stopped by adding excess EDTA, various combinations of proteins were mixed, and complexes were pulled-down using chitin beads which bind to the CBD tag on Cyk-4. Only when Cyk-4 was pre-incubated with Plk1 did a complex form between Cyk-4 and Ect2 (Figure 4.10A). Pre-incubation of Ect2 with Plk1 produced no change in the amount of Ect2 pulled down with Cyk-4. Interestingly Cyk-4 that had been pre-incubated with Plk1 also pulled-down Plk1 suggesting a direct interaction between the two proteins (Figure 4.10A). To further examine this complex active Plk1 kinase domain was used instead of full length Plk1. Similar results were seen as pre-incubation of Cyk-4 with Plk1 kinase domain generated binding sites for Ect2 on Cyk-4 and for the PBD of Plk1 on Cyk-4, though the background seen without the kinase was higher than in the previous experiment, perhaps due to using ten-fold less detergent in the wash buffer (Figure 4.10B). In order to map



the phosphorylation sites on Cyk-4 a larger sample of Cyk-4 was incubated with Plk1 kinase domain and sent for mass spectrometry identification of phospho-peptides. Four phospho-peptides were identified (S157, S170, S214, T260) (Table 4.5) which all perfectly matched the consensus motif for Plk1 phosphorylation [34] (Jes Alexander - personal communication). Also two of them (S170 and T260) when phosphorylated by Plk1 make perfect (S(pS/pT)P) PBD binding sites [23, 24]. Mutation of all the Plk1-dependent phosphorylation sites in Cyk-4 is ongoing, so that the sites necessary for PBD and Ect2 binding can be determined by the same pulldown assay. With the mutant versions of Cyk-4 that can no longer bind Ect2 or the PBD in hand, in vivo experiments can be done to determine if these mutants can fulfill the various roles of Cyk-4. In particular the localization of Ect2, RhoA, and Plk1 to the spindle midzone and cleavage furrow will be assessed in cells expressing the non-binding mutant versions of Cyk-4 where the endogenous protein has also been knocked down by siRNA.

Thus, In mammalian cells one can construct a model where Plk1 targets Cyk-4 after the metaphase to anaphase transition to create a docking site for the Ect2 BRCT domains, recruiting Ect2 and ultimately RhoA to the cleavage initiation site. The mechanism whereby this is inhibited until anaphase is unclear, but at a minimum, consists of inhibitory CDK1 phosphorylation of Ect2 [4]. The finding that Ect2 can bind the PBD and is a potential substrate of Plk1 (Figure 4.3) [26] remains without known functional consequences though perhaps Plk1 targeting of Ect2 also helps to relieve the inhibition that Ect2 is under in early mitosis [4] or otherwise modify Ect2 to activate its binding capacity [26, 42]. Overall there is a clear direct role for Cdc5 in targeting Tus1 and Rom2 to the bud neck to create a zone of active Rho1, but Plk1 is just as effective in an indirect manner in targeting Ect2 to generate a zone of active RhoA at the cleavage furrow.

## **Experimental Procedures**

### **Yeast genetics and molecular biology techniques**

Media and genetic techniques were as previously described [43]. All the yeast strains were isogenic to BY4741 (*MATa his3 leu2 met15 ura3* from Open Biosystems). *cdc5-2*, *cdc15-2* and *cdc14-1* strains were backcrossed at least four times to BY4741 background from W303-1A and 3 out of 3 independent clones of each mutant showed indistinguishable terminal phenotypes in telophase arrest and in CAR formation at 34.5°C. Gene deletion or modifications were performed with PCR mediated gene replacement [44] and correct integrations were confirmed by colony PCR. For a description of the strains and plasmids, see Tables 4.6 and 4.6. *tus1-ST* mutant constructs were created as follows. Briefly, a wild type truncated *TUS1* [containing 600 base pairs (bp) upstream of the ATG translation start site to 900 bp downstream of ATG] fragment was cloned into a pRS306 vector using EcoRI and PstI. Site-directed mutagenesis was carried out using QuikChange Site-Directed mutagenesis kit (Stratagene, La Jolla, CA). Ser7 and Ser92 were mutated to Thr generating Tus1-ST mutant. Mutagenesis was confirmed using restriction digests followed by DNA sequencing. All constructs were targeted by linearization with BglII to the *TUS1* locus in a wild type diploid. The strains were sporulated and tetrads were dissected to obtain a haploid isolate of the integrant. Correct integration and introduction of all the mutations were confirmed by colony PCR and by subsequent DNA sequencing of the genomic locus. *tus1-6A* and *tus1-6DE* were constructed essentially the same as *tus1-ST*. Mutations were introduced on the pRS304 plasmid containing a wild type truncated *TUS1* fragment (containing 600 bp upstream of the ATG translation start site to 1892 bp downstream of ATG). The indicated Ser/Thr were mutated to Ala in Tus1-6A or Asp/Glu in Tus1-6DE (Ser181, Ser191, Ser221, Thr257, Thr392 and Thr408). All constructs were targeted by linearization with SacII to the *TUS1* locus. *rom2-st* mutant constructs and strains were made analogously.

### **Functionality of the epitope-tagged constructs**

The coding sequence for a linker (Gly-Gly-Ser-Gly-Gly-Ser) was introduced between the coding sequence for the epitopes and the carboxyl terminus of Tus1, Rom2

and Tpm2. For the tagged constructs, the functionality was examined as follows. *TUS1-myc* and *TUS1-GFP* were crossed to *rom2Δ* and tested for the growth at 24°C, 30°C, 34°C, and 37°C. We did not observe either a synthetic growth defect or cytokinesis failure. Rom2-myc and Rom2-GFP also fully supported cell viability at 24°C, 30°C, 34°C, and 37°C in the absence of Tus1 or Rom1. *BNI1-3xGFP* was introduced to *bnr1Δ* cells by a genetic cross and the *BNI1-3xGFP bnr1Δ* cells grew normally at 24°C, 30°C, 34°C, and 37°C. They also did not exhibit round bud morphology or a cytokinesis defect, characteristics of *bni1Δ* strains. *MYO1-GFP*, *IQG1-GFP*, *HOF1-GFP*, and *SHS1-GFP* didn't cause cytokinesis defects at 24°C, 30°C, 34°C, or 37°C. *Tpm2-GFP* is only partially functional because *tpm1ΔTPM2-GFP* cells were viable but grew poorly. However, *TPM2-GFP* had no dominant inhibitory effect on cell cycle progression or cytokinesis and CAR assembly and CAR constriction occurred with identical kinetics in *TPM2* and *TPM2-GFP* cells. Tus1-Mlc2-GFP is a functional Tus1 protein because *rom2ΔTUS1-MLC2-GFP* strains grew even at 37°C whereas *rom2Δtus1Δ* was lethal. Localization of Tus1-Mlc2-GFP mimicked Mlc2 and was recruited to the bud neck at the bud emergence (unlike Tus1-GFP, which localized to the neck just prior to the mitotic exit) and disappeared after its constriction during cytokinesis. We could not determine whether Tus1-Mlc2-GFP is fully functional as Mlc2 protein because a *mlc2* deletion strain has no obvious growth defects. The coding sequence for a linker (Gly-Gly-Ser-Gly-Gly-Ser) was introduced between the carboxyl terminus of Tus1 and amino terminus of Mlc2.

### **Fluorescence imaging and image analysis**

Cells were observed in an automated Zeiss 200M inverted microscope (Carl Zeiss, Thornwood, NY) as previously described [45]. All image processing was performed using SlideBook software. To characterize the localization of proteins to the bud neck, we acquired images at 0.3 μm intervals in the Z focal plane, enabling visualization of the relatively small budding yeast bud neck region (usually less than 1 μm in diameter). Shown are selected Z focal plane slices through the bud neck. Cells were fixed in 3.7 % formaldehyde for 10 minutes and washed twice in phosphate-buffered saline solution before microscopic observation of GFP tagged proteins (or GFP variants). For timelapse

live cell microscopy 2  $\mu$ l of the culture [in the synthetic complete (SC) medium supplemented with adenine] were spotted onto a glass slide and immediately imaged at room temperature (approximately 24°C). Staining of actin cytoskeleton by Alexa-568 phalloidin was described previously [46]. Immunofluorescence method for Rho1 and HA-Rho1 was as described [36] with thanks to M. Abe for providing the antibody specific to Rho1-GTP. For visualizing Bni1-3xGFP in *cdc15-2* and in *cdc5-2* block, the cells were treated with 100  $\mu$ M latrunculin A for 5 minutes before fixation to enhance the polarized (e.g. bud tip or bud neck) localization of Bni1 since cytoplasmic high background of Bni1-3xGFP masks the cortical and neck localized signals.

### **Biochemical methods**

Western blotting and phosphatase treatment was performed as described [47]. The cell lysates for the Western blotting were prepared by treating the yeast cells with 120 mM Sodium hydroxide for 15 minutes at 4°C. The cell pellets were boiled for 5 minutes with SDS-sample buffer. Mouse monoclonal anti-myc antibody (9E10), mouse monoclonal anti-HA antibody (12CA5), rabbit polyclonal anti-Mpk1/Slk2 antibody and mouse monoclonal anti-GFP antibody were obtained from commercial sources. Rabbit anti- Rho1 antibody and anti-active Rho1 antibody were described previously [36, 48].

The pull-down assay for active Rho1p was performed as follows. Yeast cells were lysed in a lysis buffer [50 mM Tris-HCl (pH 7.5), 150 mM NaCl, 1 mM EDTA, 12 mM MgCl<sub>2</sub>B<sub>2</sub>, 1 mM DTT, 1 mM PMSF, 25  $\mu$ g/ml TPCK, 25  $\mu$ g/ml TLCK, 25  $\mu$ g/ml leupeptin, 25  $\mu$ g/ml pepstatin, 25  $\mu$ g/ml antipain, 25  $\mu$ g/ml aprotinin, 25  $\mu$ g/ml chymostatin, 0.6% CHAPS, 0.12% cholesteryl hemisuccinate], incubated with a bead-bound GST fusion of an RBD of Pkc1 or that of Bni1, washed, and subjected to SDS-PAGE. Bound Rho1p was detected by western blot analysis.

The PBD pull-down assay was performed in Polo-box binding buffer (50 mM Tris, 150 mM NaCl, 2mM EDTA, 1 mM PMSF, 1 mM DTT, 1 % TritonX-100 and Complete protease inhibitor). Freshly prepared yeast cell lysates (containing 2 mg total protein in 300  $\mu$ l for each assay) were mixed with 20  $\mu$ l of the beads saturated with pure PBD or PBD\*. Bound proteins were analyzed by Western blotting with goat anti-Rabbit IgG antibody to detect the TAP tag [31] or other tag appropriate antibody.

Plk1 kinase domain with a T210D activating mutation was expressed in bacteria and purified to homogeneity. Tus1<sup>1-300</sup>, Rom2<sup>1-400</sup>, mouse Ect2<sup>1-421</sup>, mouse Ect2<sup>414-639</sup>, and Cyk-4<sup>1-288</sup> were all expressed and purified from bacteria. Several micrograms of each protein was incubated with Plk1 and 100μM ATP in Plk1 kinase buffer (50mM Tris pH 7.5, 150mM NaCl, 10mM MgCl<sub>2</sub>, 1mM DTT) for two hours at 30°C. The entire reaction was run on a single lane of a SDS-PAGE, stained with coomassie blue, and the band corresponding to the desired protein was cut out. Tus1<sup>1-300</sup> and Rom2<sup>1-400</sup> were sent to the Taplin Biological Mass Spectrometry Facility at Harvard Medical School for phospho-peptide determination by mass spectrometry (thanks to R. Tomaino and S. Gygi). The mouse Ect2 fragments and Cyk-4 fragment were sent to our collaborator K. Clauser in S. Carr's laboratory for phospho-peptide determination by LC/MS/MS after in-gel trypsin cleavage. Separate kinase reactions were also performed with one tenth the amount of protein and Plk1 kinase domain with 10μCi of <sup>32</sup>P-γ-ATP added to the mixture. Samples were taken at several timepoints, ran on an SDS-PAGE, and exposed to a phosphoimager plate for autoradiography. In this way all of the proteins were confirmed to be in vitro phosphorylated by Plk1.

Ect2 tandem BRCT domain phosphopeptide binding studies were performed as described in Appendix One. Alignments of tandem BRCT domains were generated using standard algorithms. Ect2/Cyk4 binding studies were performed as follows. GST-Ect2<sup>1-421</sup>, CBD-Ect2<sup>1-421</sup>, and CBD-Cyk4<sup>1-288</sup> proteins were expressed and purified from bacteria. To generate untagged forms the tags were cleaved with TEV (for CBD tags) or thrombin (for GST tags) on beads freeing the untagged version. Proteins were phosphorylated with Plk1 full length, Plk1 kinase domain, Plk1 kinase domain kinase dead, or mock as described above without the radioactive ATP. After phosphorylation proteins were mixed and pulled-down with chitin beads which bind the CBD tag on Cyk4 for two hours or overnight at 4°C in binding buffer (20mM Hepes pH 7.2, 50mM NaCl, 5mM MgCl<sub>2</sub>, 1% Triton, 1mM DTT, 1mM PMSF). Beads were washed four times in binding buffer, boiled in protein sample buffer, and analyzed by SDS-PAGE and western blotting.

**Figure 4.1: Cdc5 is required for CAR assembly.**

(A) CAR assembly is defective in *cdc5*- but not *cdc15*- or *cdc14*-arrested cells. Cells were released from a G1 block ( $\alpha$  factor) and examined at intervals after release at the nonpermissive temperature 34.5°C for budding index (diamonds), percentage of anaphase cells by labeling nuclear DNA (squares), and bud neck localization of Tpm2-GFP (triangles). The  $\alpha$  factor was re-added at 60 min to prevent progression into a second cell cycle. (Bottom) Representative images of cells from the 120-min time point. Scale bar indicates 5  $\mu$ m.

(B) Cdc5 is required to maintain the CAR. Log-phase cultures of *cdc5-2* and control cells were arrested in telophase by overexpression of *BFA1* from the *GALI* promoter for 3 hours. The telophase-arrested cells were shifted to a restrictive temperature (34.5°C) to inactivate *cdc5-2* and *cdc15-2*, fixed, and the CAR formation was visualized with the use of Tpm2-GFP.

(C) Cdc5 is required for the subcellular targeting of Bni1 and Rho1. Bni1-3xGFP expressed at an endogenous level was visualized after 2-hour incubation of the cells at 34.5°C. Rho1 was visualized by immunofluorescence labeling with a rabbit antibody against Rho1 130 min after release to 34.5°C from a G1 block. Arrows point to the bud neck signals in *cdc15* cells and the bud tip signals in *cdc5* cells.

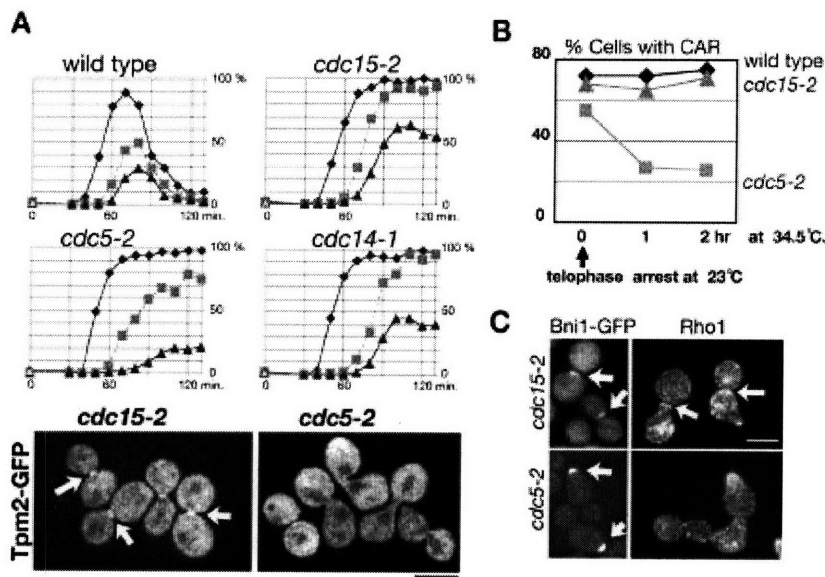


**Figure 4.2: A screen for Polo-box binding partners suggests that Cdc5 controls multiple Rho-type GTPase regulators.**

All potential Rho GTPase regulators in the yeast genome were screened for physical interaction with the Cdc5 PBD and a control pincer mutation (PBD\*).

(A) In cases where epitope-tagged constructs were not available from the yeast tandem affinity purification (TAP)-tagged library [31], epitope-tagged constructs were generated. Tus1 and Rom1 were overexpressed from the *GALI* promoter for this initial screen. After precipitation assay, Western blotting was performed to detect the indicated epitope tags of the bound proteins. + indicates the wild-type GST-PBD; +\* indicates the pincer mutant.

(B) PBD or PBD\* precipitation assays with lysates from strains from the yeast TAP-tag fusion library.

(C) Endogenous-level Tus1 binds to the PBD. This binding is abolished by the ST mutation and thus requires the Polo-box binding motif. WT, wild type.

(D) Hyperphosphorylation of Tus1<sup>1-300</sup>-myc requires Cdc5 and the Polo-box binding motifs. Shown are Western blots to detect endogenous-level Tus1<sup>1-300</sup>-myc or its ST derivative in the indicated strains after 2.5 hours at the restrictive temperature of 34.5°C.

(E) Phosphomimetic mutations at Polo-consensus phosphorylation sites partially bypass the requirement for Cdc5 for CAR assembly and Rho1 recruitment. The indicated strains were arrested with  $\alpha$  factor and released at the nonpermissive temperature (33.5°C) for 140 min. The CAR was visualized with the use of Tpm2-GFP, and Rho1 was visualized by immunofluorescence. More than 400 cells were counted for each sample. The experiment was repeated three times with near-identical results. By a Student's t test, the difference in Tpm2-GFP labeling in cells expressing Tus1-6DE versus Tus1 was significant ( $P = 0.011$ ). Error bars indicate SEM. Scale bar, 5  $\mu\text{m}$ ; arrows point to the bud neck signal.

Figure 4.2 Continued

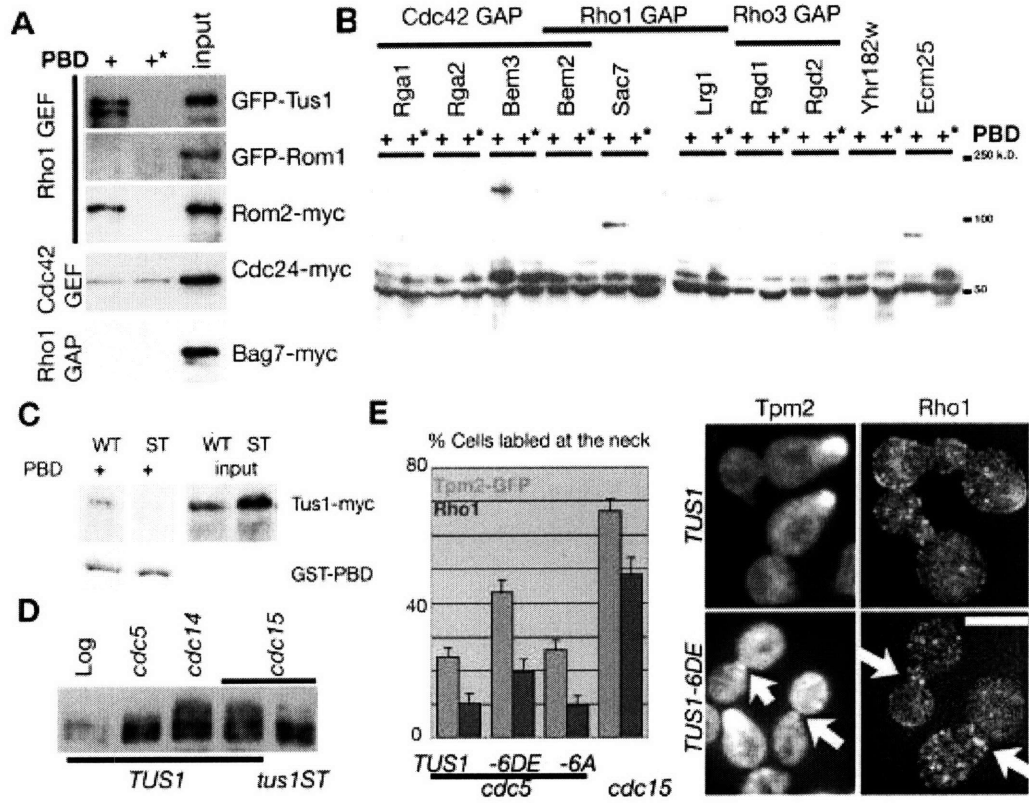




**Figure 4.3: Ect2 binds the PBD and is a Plk1 substrate in vitro**

(A) Flag-Ect2 was expressed in U2OS cells, and either treated with nocodazole or mock treated. Lysates were used in Plk1-PBD pulldowns with wild-type or the non-binding mutant of the Plk1-PBD, and blotted for the presence of Flag-Ect2. Ect2 specifically came down with the wild-type Plk1-PBD during mitosis.

(B) The indicated Flag-Ect2 constructs were expressed in U2OS cells, and immunoprecipitated with anti-Flag resin. Blotting for endogenous Plk1 indicates that Plk1 interacts with full length Ect2 and the N-terminus, but not the PBD site mutants.

(C) Ect2 serves as a substrate of Plk1 in vitro. The indicated Ect2 fragments were incubated with Plk1 kinase domain and  $\gamma^{32}\text{P}$ -ATP for the indicated times and phosphate incorporation was monitored by autoradiograph.

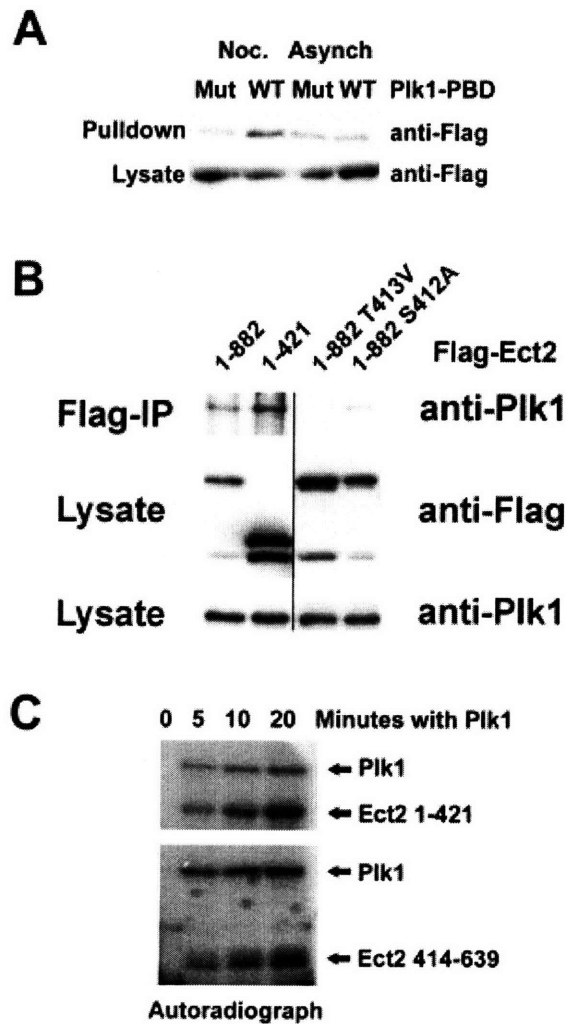


**Figure 4.4: Characterization of Tus1 protein.**

(A) Domain structure of Tus1. The Dbl-PH domain is the catalytic domain for nucleotide exchange. The function of the CNH domain is not known. Tus1 contains two potential Polo box binding motifs in the N-terminal Polo box interaction domain (PID).

(B) Endogenous level Tus1<sup>1-300</sup> binds to the PBD. This binding is abolished by the “ST” mutation and thus requires the Polo box binding motif. Shown is a pull down assays as in Fig. 5.3C.

(C) Tus1<sup>1-300</sup> is a phosphoprotein. Tus1<sup>1-300</sup> was immunoprecipitated from *cdc15*-arrested cells. The immunoprecipitate was divided and subjected to the indicated treatments.

(D) Overexpression of Cdc5 induces hyper phosphorylation of Tus1<sup>1-300</sup>-myc. *GAL1-CDC5* or *GAL1-cdc5N209A* [encoding a kinase dead mutant [49]] were induced by galactose for 3 hrs.

(E) Expression level of full length Tus1-myc. Shown is a Western blot to detect endogenous level, Tus1-myc or its derivatives from log phase cultures. Mpk1 was detected as a loading control.

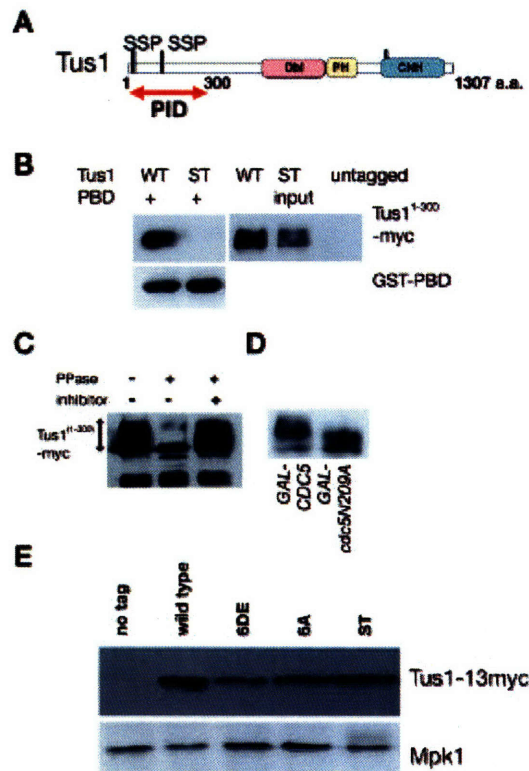


**Figure 4.5: Characterization of Rom2-ST.**

**(A) Domain structure of Rom2.** The Dbl-PH domain is the catalytic domain for nucleotide exchange. The function of the DEP and CNH domains are not known. Rom2 contains two potential Polo-box binding motifs in the N-terminal region.

**(B) Endogenous level full-length Rom2 binds to the PBD but not the pincer mutation PBD\*.** Lane 1, 3, 5; pull-down with PBD. Lane 2, 4, 6; pull-down with PBD\*. Lane 7-9; total lysates. Rom2-myc extract was applied for lanes 1, 2 and 7. Rom2-ST-13 myc extract was applied in lanes 3, 4 and 8. Untagged controls are in lanes 5, 6 and 9. This binding is strongly diminished by the “ST” mutation and thus requires the Polo-box binding motif.

**(C) Localization of Rom2-GFP and Rom2-ST-GFP.** The “ST” mutation does not affect Rom2 localization in small budded cells (percentages indicated in white lower left, n= 200 from a log-phase culture). By contrast, Rom2-ST-GFP was severely compromised for neck localization in large budded cells.

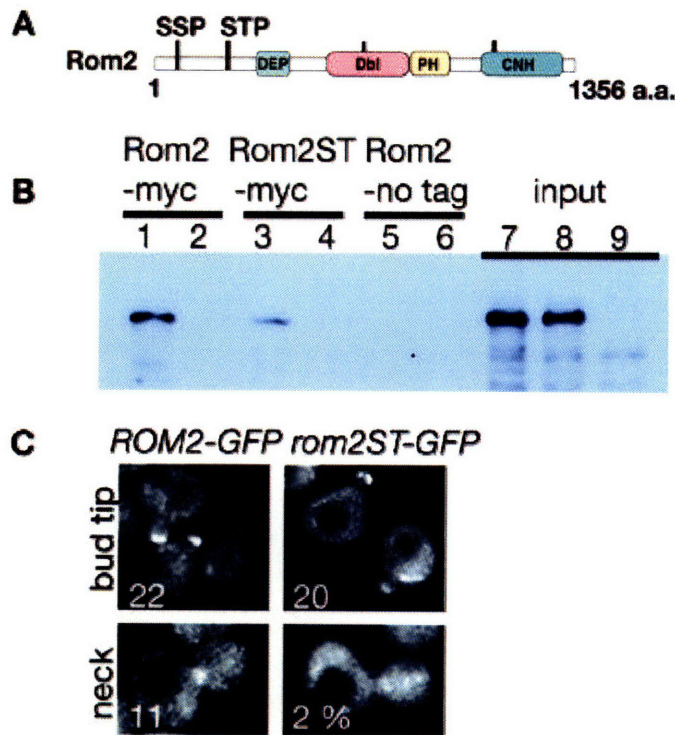


**Figure 4.6: *tus1-ST* and *rom2-ST* are separation-of-function alleles that have reduced fitness when combined with *hof1Δ* but not *myo1Δ*.**

Shown are 5-fold serial dilutions of the indicated strains grown for 3 days at 37°C.

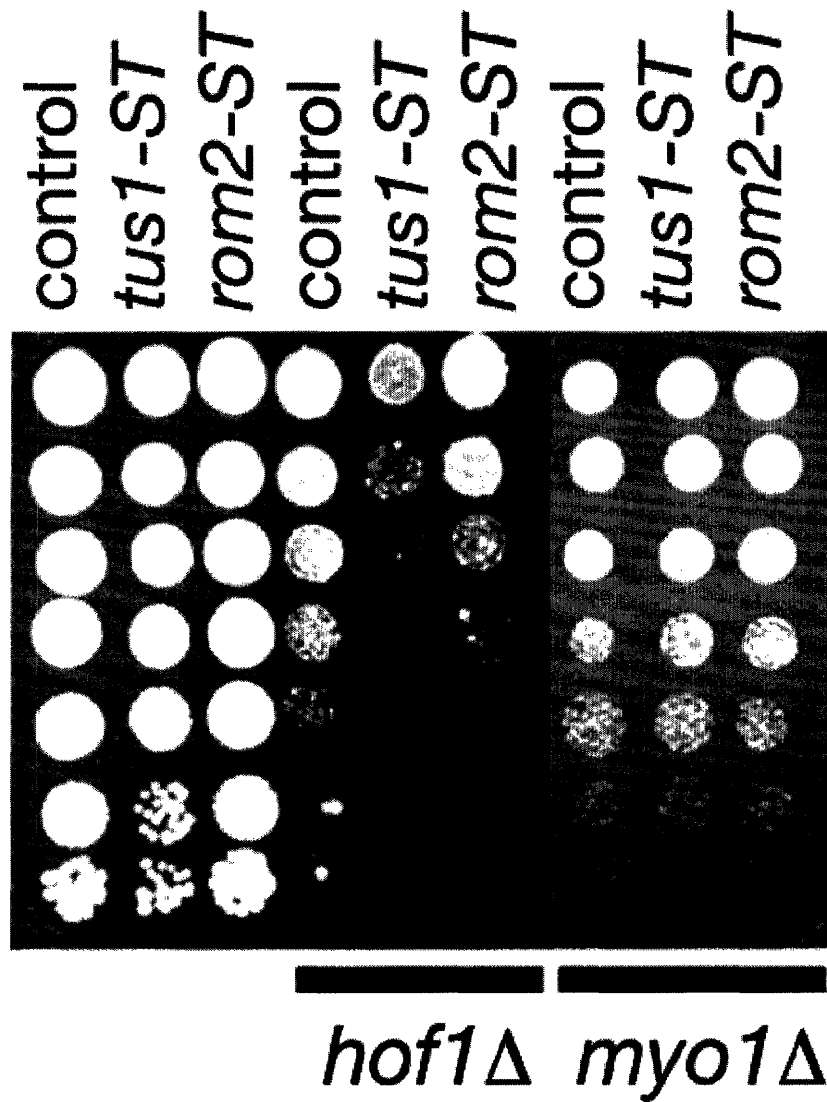


**Figure 4.7: Polo regulation of Tus1 and Rom2 is critical for CAR assembly and local Rho1 activation.**

(A) Polo regulation of Tus1 and Rom2 is required for CAR assembly and for recruitment of active Rho1 to the bud neck. CAR assembly was assayed with use of Tpm2-GFP.

Active Rho1 was detected by immunofluorescence by using an antibody that specifically recognizes Rho1-GTP but not Rho1-GDP [36]. Error bars indicate SEM; scale bar, 5  $\mu$ m; arrows point to the bud neck signals.

(B) The total cellular level of active Rho1 requires Cdc5- but not Polo-dependent phosphorylation of Tus1 and/or Rom2. The precipitation assay was performed with the use of Pkc1-RBD.

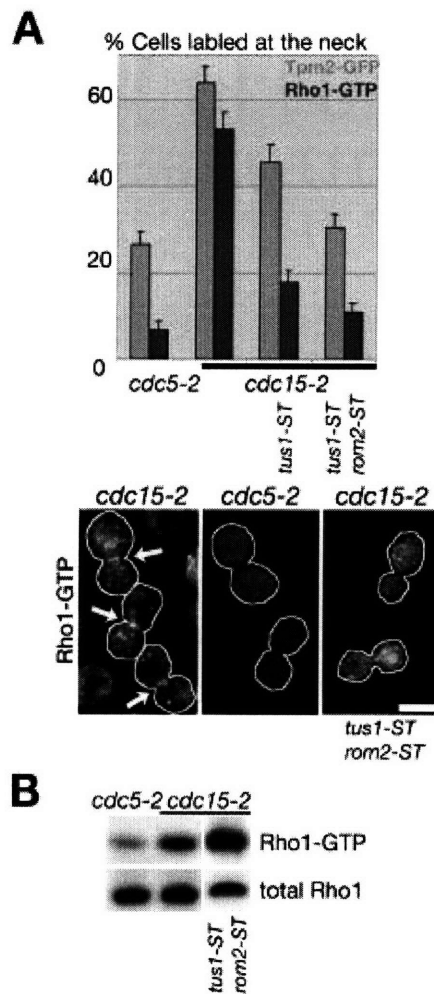


**Figure 4.8: Cdc5 targets Tus1 to the division site.**

(A) Tus1-GFP requires Cdc5 and its Polo-box binding motifs to localize to the bud neck. Tus1-GFP or the ST derivatives were imaged in *cdc5-2* or in *cdc15-2* 2 hours after incubation at 34.5°C (n > 100), along with the percentages of the large budded cells with GFP signal at the bud neck. Scale bar, 5 μm.

(B) Tethering Tus1-ST to the bud neck by fusion to Mlc2 corrects the CAR assembly defect of *tus1-ST rom2-ST* strains and partially bypasses the requirement for Cdc5 in CAR assembly. (Left) Numerical summary of the data. The bars indicate the percentage of cells with detectable contractile rings. Error bars indicate SEM. The dark bars indicate the percentage of cells with robust contractile rings. (Right) Examples of cells. (Top) GFP imaging of the indicated fusions. (Bottom) Actin was visualized with alexa568-phalloidin. Arrows indicate cells with robust CAR labeling.

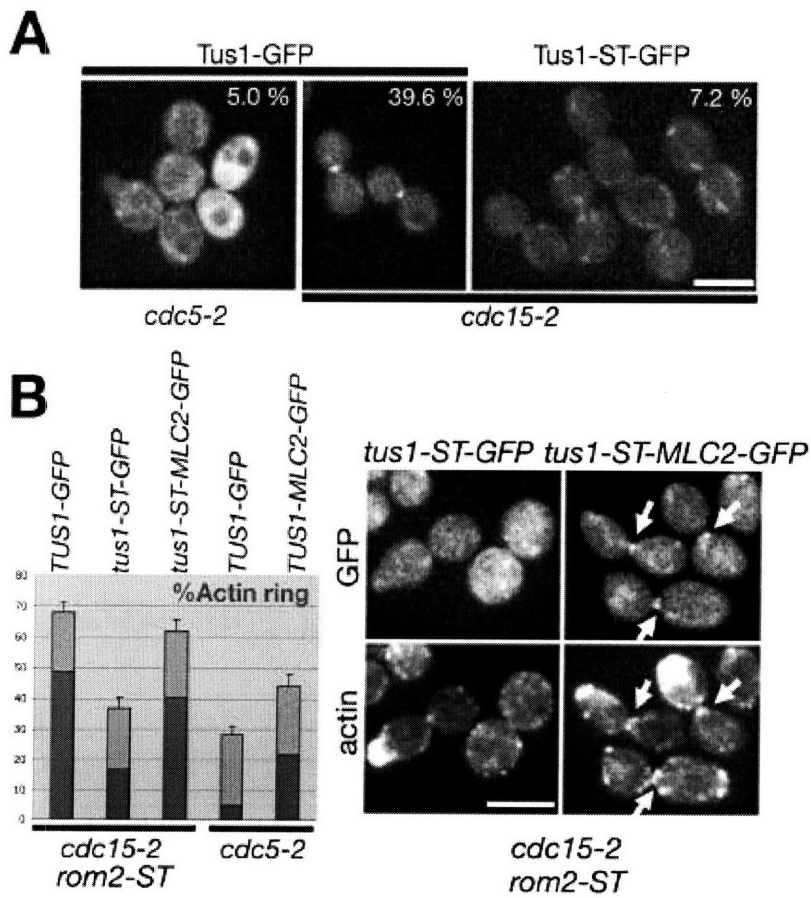






**Figure 4.10: Ect2 binds Cyk4 after Plk1 phosphorylation of Cyk4**

(A) Ect2 and CBD-Cyk4 N-terminal fragments were generated in bacteria and pre-treated with active full length Plk1 or mock treated. The treated proteins were then used in a CBD pulldown to identify what proteins interacted with Cyk4.

(B) The same experiment as A was performed except using active Plk1 kinase domain instead of full length Plk1. The GST-Ect2 N-terminal fragment was added to the two left lanes and the GST-Plk1-PBD was added to the right two lanes. Increased binding to the Cyk-4 N-terminal fragment was seen with both proteins after pre-incubation of the Cyk-4 N-terminal fragment with active Plk1 kinase domain.

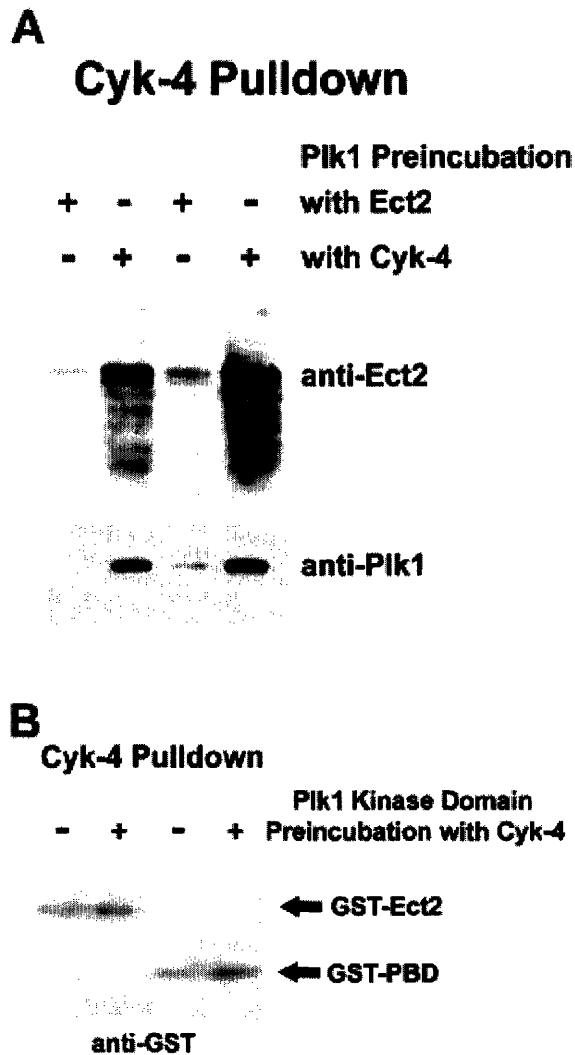




**Table 4.1 Plk1-dependent phosphorylation sites on Tus1<sup>1-300</sup> in vitro**

Peptide Sequences identified

1. <sup>243</sup>VSEALESVYSDSDYTFNNS\*NAR<sup>264</sup>
2. <sup>243</sup>VSEALESVYSDSDYT\*FNNSNARP<sup>264</sup>
3. <sup>243</sup>VSEALESVYSDSDYT\*FNNS\*NAR<sup>264</sup>
4. <sup>243</sup>VSEALES\*VYSDSDYT\*FNNSNAR<sup>264</sup>
5. <sup>135</sup>SPNKLS\*FIGNSEER<sup>148</sup>
6. <sup>104</sup>RPPPPPPLLYS\*TESIR<sup>119</sup> or <sup>104</sup>RPPPPPPLLYST\*ESIR<sup>119</sup>
7. <sup>236</sup>NVSGNS\*R<sup>242</sup>
8. <sup>149</sup>HHMEYISNHS\*R<sup>159</sup>
9. <sup>179</sup>DSS\*KQQAHFSDSDLR<sup>194</sup> or <sup>179</sup>PDS\*SKQQAHFSDSDLR<sup>194</sup>
10. <sup>183</sup>QQAHFSDS\*DLR<sup>194</sup>
11. <sup>139</sup>LS\*FIGNSEERP<sup>148</sup>
12. <sup>201</sup>PALPIPFT\*T\*T\*LLLS\*PFDDDEDSEFFTKPPPPLSTSRP<sup>235</sup>  
one site on four possible locations
13. <sup>201</sup>ALPIPFT\*T\*T\*LLLS\*PFDDDEDSEFFTKPPPPLS\*T\*S\*R<sup>235</sup>  
two sites – one on four possible locations (T,T,T or S)  
the other on three possible locations (S,T or S)

Legend to Table 4.1

Phosphorylated residues were determined by microcapillary LC/MS/MS techniques after trypsin digestion. Shown are peptides that were identified at least twice. Residues indicated with a star (\*) are phosphorylation sites that were definitively identified. Underlined phosphorylation sites were mutated in the Tus1-6DE or Tus1-6A mutants.

**Table 4.2 Plk1-dependent phosphorylation sites on Rom2<sup>1-400</sup> in vitro**

Peptide Sequences identified

1. <sup>289</sup>SMS\*LNSSTLK<sup>298</sup>
2. <sup>76</sup>S\*GVEAAIDDS\*DIPNNEMK<sup>93</sup>
3. <sup>205</sup>QSS\*FSTGSASTTPTQAR<sup>221</sup> or <sup>205</sup>QS\*SFSTGSASTTPTQAR<sup>221</sup>
4. <sup>109</sup>EVPDTQS\*LSSADNTPVSSPK<sup>128</sup>

Legend to Table 4.2

Phosphorylation sites were determined by microcapillary LC/MS/MS techniques after sequential digestion by trypsin and by chymotrypsin. Shown are peptides that were identified at least twice. Residues indicated with a star (\*) are phosphorylated residues that were definitively identified.

**Table 4.3 Plk1-dependent phosphorylation sites on Ect2 in vitro**

Peptide Sequences identified

1. <sup>316</sup>AGET\*MYLYEK<sup>325</sup>
2. <sup>327</sup>VDGCPANLLS\*SHR<sup>639</sup>

Legend to Table 4.3

Phosphorylated residues were determined by microcapillary LC/MS/MS techniques after trypsin digestion. Shown are peptides that were identified at least twice.

Residues indicated with a star (\*) are phosphorylation sites that were definitively identified.

**Table 4.4 Summary of the rom2-ST and tus1-ST genetic analysis**

Genotype	YPD (24°C)	YPD (37°C)	YPD+Sorbitol (37°C)	SC (37°C)
Wild type	+++	+++	+++	+++
<i>rom2</i> Δ	+++	++	+++	+++
<i>rom2-ST</i>	+++	+++	+++	+++
<i>tus1</i> Δ <i>rom2-ST</i>	+++	++	+++	+++
<i>tus1</i> Δ	+++	++	+++	+++
<i>tus1-ST</i>	+++	+++	+++	+++
<i>rom2</i> Δ <i>tus1-ST</i>	+++	++	+++	+++
<i>rom2</i> Δ <i>tus1</i> Δ	+/-	-	++	+
<i>tus1-ST rom2-ST</i>	+++	+++	+++	+++
<i>rom1</i> Δ	+++	+++	+++	+++
<i>rom1</i> Δ <i>rom2</i> Δ	-			
<i>rom1</i> Δ <i>rom2-ST</i>	+++	+++	+++	+++
<i>rom1</i> Δ <i>tus1</i> Δ	+++	++	+++	+++
<i>rom1</i> Δ <i>tus1-ST</i>	+++	+++	+++	+++
<i>mpk1</i> Δ	+++	+	++	++
<i>mpk1</i> Δ <i>tus1</i> Δ	+	-	++	+
<i>mpk1</i> Δ <i>tus1-ST</i>	+++	+	++	++

**Legend to Table 4.4**

All the mutants were generated by genetic crosses and 3 independent clones were tested for growth. *rom2*Δ *tus1*Δ, *rom1*Δ *rom2*Δ, *mpk1*Δ *tus1*Δ, and *mpk1*Δ *tus1*ST were germinated on YPD plates containing 1 M sorbitol as an osmotic stabilizer. The growth was judged after 3 days at the indicated temperature. The number of “+” reflects the robustness of the growth. “-“ indicates no growth.

**Table 4.5 Plk1-dependent phosphorylation sites on Cyk-4 in vitro**

Peptide Sequences identified

1. <sup>149</sup>SGSILSDIS\*FDKTDE<sup>163</sup>
2. <sup>164</sup>SLDWSS\*LVK<sup>173</sup>
3. <sup>203</sup>SIGSAVDQGNES\*IVA<sup>217</sup>
4. <sup>255</sup>LTQPWNSDST\*LNSR<sup>264</sup>

Legend to Table 4.5

Phosphorylated residues were determined by microcapillary LC/MS/MS techniques after trypsin digestion. Shown are peptides that were identified at least twice.

Residues indicated with a star (\*) are phosphorylation sites that were definitively identified.

**Table 4.6 List of the yeast strains**

<b>Strain</b>	<b>Mat</b>	<b>Relevant genotype</b>
PY3295	<i>a</i>	wild type <i>his3 leu2met15ura3</i>
PY5237	<i>a</i>	<i>cdc14-1</i>
PY5255	<i>a</i>	<i>cdc14-1 tpm2::TPM2-GFP-HIS3</i>
PY5220	<i>a</i>	<i>cdc15-2</i>
PY5217	<i>a</i>	<i>cdc15-2 tpm2::TPM2-GFP-HIS3</i>
PY5206	<i>a</i>	<i>cdc15-2 shs1::SHS1-GFP-HIS3</i>
PY5207	<i>a</i>	<i>cdc15-2 myo1::MYO1-GFP-HIS3</i>
PY5327	<i>a</i>	<i>cdc15-2 iqg::IQG1-GFP-HIS3</i>
PY5328	<i>a</i>	<i>cdc15-2 bni1::BNI1-3xGFP-LEU2</i>
PY5329	<i>a</i>	<i>cdc15-2 tus1::TUS1-GFP-HIS3</i>
PY5199	<i>a</i>	<i>cdc15-2 tus1::TUS1-13myc-HIS3</i>
PY5261	<i>a</i>	<i>cdc15-2 tus1::TUS1<sup>1-300</sup>-13myc-HIS3</i>
PY5254	<i>a</i>	<i>cdc15-2 tus1::tus1-ST-URA3</i>
PY5300	<i>a</i>	<i>cdc15-2 tus1::tus1-ST-GFP-HIS3</i>
PY5330	<i>a</i>	<i>cdc15-2 tus1::tus1-ST-13myc-HIS3</i>
PY5331	<i>a</i>	<i>cdc15-2 tus1::tus1-ST<sup>1-300</sup>-13myc-HIS3</i>
PY5332	<i>a</i>	<i>cdc15-2 tus1::tus1-ST-URA3 tpm2::TPM2-GFP-HIS3</i>
PY5253	<i>a</i>	<i>cdc15-2 rom2::rom2ST-LEU2</i>
PY5333	<i>a</i>	<i>cdc15-2 rom2::rom2ST-LEU2 tpm2::TPM2-GFP-HIS3</i>
PY5252	<i>a</i>	<i>cdc15-2 tus1::tus1-ST-URA3 rom2::rom2ST-LEU2</i>
PY5334	<i>a</i>	<i>cdc15-2 tus1::tus1-ST-URA3 rom2::rom2ST-LEU2 tpm2::TPM2-GFP-HIS3</i>
PY5323	<i>a</i>	<i>cdc5::cdc5-2-URA3</i>
PY5335	<i>a</i>	<i>cdc5-2::URA3 tpm2::TPM2-GFP-HIS3</i>
PY5292	<i>a</i>	<i>cdc5::cdc5-2-URA3 Δswel::KAN</i>
PY5336	<i>a</i>	<i>cdc5::cdc5-2-URA3 shs1::SHS1-GFP-HIS3</i>
PY5337	<i>a</i>	<i>cdc5::cdc5-2-URA3 myo1::MYO1-GFP-HIS3</i>
PY5339	<i>a</i>	<i>cdc5::cdc5-2-URA3 iqg1::IQG1-GFP-HIS3</i>
PY5340	<i>a</i>	<i>cdc5::cdc5-2-URA3 bni1::BNI1-3xGFP-LEU2</i>
PY5341	<i>a</i>	<i>cdc5::cdc5-2-URA3 tus1::TUS1-GFP-HIS3</i>
PY5198	<i>a</i>	<i>cdc5::cdc5-2-URA3 tus1::TUS1-13myc-HIS3</i>
PY5260	<i>a</i>	<i>cdc5::cdc5-2-URA3 tus1::TUS1<sup>1-300</sup>-13myc-HIS3</i>
PY5343	<i>a</i>	<i>cdc5::cdc5-2-URA3 tus1::TUS1-6A-LEU2 tpm2::TPM2-GFP-HIS3</i>
PY5318	<i>a</i>	<i>cdc5::cdc5-2-URA3 tus1::TUS1-6DE-LEU2 tpm2::TPM2-GFP-HIS3</i>
PY5344	<i>a</i>	<i>cdc5::cdc5-2-ura3::HIS3</i>
PY5345	<i>a</i>	<i>cdc5::GAL-3HA-CDC5-KanR</i>
PY5346	<i>a</i>	<i>cdc5::GAL-3HA-CDC5-KanR tpm2::TPM2-GFP-HIS3</i>
PY5347	<i>a</i>	<i>cdc5::GAL-3HA-CDC5-KanR tpm2::TPM2-GFP-HIS3 ura3::CFP-TUB1-GFP-URA3</i>
PY5256	<i>a</i>	<i>tpm2::TPM2-GFP-HIS3 ura3::CFP-TUB1-GFP-URA3</i>
PY5349	<i>a</i>	<i>tus1Δ::KANR</i>
PY5350	<i>a</i>	<i>tus1::TUS1-GFP-HIS3</i>

**Table 4.6 Continued List of the yeast strains**

<b>Strain</b>	<b>Mat</b>	<b>Relevant genotype</b>
PY5197	<i>a</i>	<i>tus1::TUS1-13myc-HIS3</i>
PY5259	<i>a</i>	<i>tus1::TUS1<sup>1-300</sup>-13myc-HIS3</i>
PY5351	<i>a</i>	<i>tus1::TUS1<sup>1-300</sup>-13myc-HIS3 CDC5::GAL1-CDC5-URA3</i>
PY5352	<i>a</i>	<i>tus1::TUS1<sup>1-300</sup>-13myc-HIS3 CDC5::GAL1-cdc5<sup>N209A</sup>-URA3</i>
PY5202	<i>a</i>	<i>tus1::tus1-ST-URA3</i>
PY5353	<i>a</i>	<i>tus1::tus1-ST-GFP-HIS3</i>
PY5354	<i>a</i>	<i>tus1::tus1-ST-13myc-HIS3</i>
PY5355	<i>a</i>	<i>tus1::tus1-ST1-300-13myc-HIS3</i>
PY5279	<i>a</i>	<i>tus1::tus1-6DE-LEU2</i>
PY5356	<i>a</i>	<i>tus1::tus1-6DE-GFP-HIS3</i>
PY5357	<i>a</i>	<i>tus1::tus1-6DE-13myc-HIS3</i>
PY5358	<i>a</i>	<i>tus1::tus1-6A-LEU2</i>
PY5359	<i>a</i>	<i>tus1::tus1-6A-GFP-HIS3</i>
PY5360	<i>a</i>	<i>tus1::tus1-6A-13myc-HIS3</i>
PY5156	<i>a</i>	<i>myo1Δ::HIS3</i>
PY5158	<i>a</i>	<i>hof1Δ::HIS3</i>
PY5361	<i>a</i>	<i>rom1Δ::KanR</i>
PY5031	<i>a</i>	<i>rom2Δ::KanR</i>
PY5362	<i>a</i>	<i>mpk1Δ::KanR</i>
PY5363	<i>a</i>	<i>rom1Δ::KanR tus1Δ::KanR</i>
PY5364	<i>a</i>	<i>rom2Δ::KanR tus1Δ::KanR</i>
PY5365	<i>a</i>	<i>rom2Δ::KanR hof1Δ::HIS3</i>
PY5366	<i>a</i>	<i>rom2Δ::KanR myo1Δ::HIS3 (complemented with PB2521)</i>
PY5367	<i>a</i>	<i>tus1Δ::KanR hof1Δ::HIS3 (complemented with PB2520)</i>
PY5368	<i>a</i>	<i>tus1Δ::KanR myo1Δ::HIS3</i>
PY5369	<i>a</i>	<i>rom2::rom2-ST-LEU2</i>
PY5370	<i>a</i>	<i>tus1Δ::KanR rom2::rom2-ST-LEU2</i>
PY5371	<i>a</i>	<i>rom1Δ::KanR rom2::rom2-ST-LEU2</i>
PY5372	<i>a</i>	<i>myo1Δ::KanR rom2::rom2-ST-LEU2</i>
PY5373	<i>a</i>	<i>hof1Δ::KanR rom2::rom2-ST-LEU2</i>
PY5374	<i>a</i>	<i>rom2Δ::KanR tus1::tus1-ST-URA3</i>
PY5375	<i>a</i>	<i>rom1Δ::KanR tus1::tus1-ST-URA3</i>
PY5376	<i>a</i>	<i>myo1Δ::KanR tus1::tus1-ST-URA3</i>
PY5377	<i>a</i>	<i>hof1Δ::KanR tus1::tus1-ST-URA3</i>
PY5378	<i>a</i>	<i>mpk1Δ::KanR tus1::tus1-ST-URA3</i>
PY5379	<i>a</i>	<i>mpk1Δ::KanR tus1Δ::KanR</i>
PY5380	<i>a</i>	<i>tus1::tus1-ST-URA3 rom2::rom2-ST-LEU2</i>
PY5201	<i>a</i>	<i>myo1::MYO1-CFP tus1::TUS1-GFP-HIS3</i>
PY5257	<i>a</i>	<i>myo1::MYO1-CFP tpm2::TPM2-GFP-HIS3</i>
PY5235	<i>a</i>	<i>myo1::MYO1-CFP rom2::ROM2-3xGFP-HIS3</i>
PY5381	<i>a</i>	<i>ura3::CFP-TUB1 tus1::TUS1-GFP-HIS3</i>
PY5256	<i>a</i>	<i>ura3::CFP-TUB1 tpm2::TPM2-GFP-HIS3</i>
PY5382	<i>a</i>	<i>ura3::CFP-TUB1 rom2::ROM2-3xGFP-LEU2</i>

**Table 4.6 Continued List of the yeast strains**

<b>Strain</b>	<b>Mat</b>	<b>Relevant genotype</b>
PY4315	<i>α</i>	<i>trp1Δ::NatR</i>
PY5384	<i>α</i>	<i>rom1::GAL1-GFP-ROM1-TRP1 trp1Δ::NatR</i>
PY5385	<i>a</i>	<i>cdc24::CDC24-13myc-HIS3</i>
PY5386	<i>a</i>	<i>bag7::BAG7-13myc-HIS3</i>
PY5387	<i>a</i>	<i>bfa1::GAL1-HA-BFA1-HIS3 tpm2::TPM2-GFP-HIS3</i>
PY5388	<i>a</i>	<i>cdc15-2 bfa1::GAL1-HA-BFA1-HIS3 tpm2::TPM2-GFP-HIS3</i>
PY5389	<i>a</i>	<i>cdc5::cdc5-2-URA3 bfa1::GAL1-HA-BFA1-HIS3 tpm2::TPM2-GFP-HIS3</i>

TAP tagged strains used for Fig. 4.2B are from the commercially available TAP fusion library [31] and are not described in this list.



**Table 4.7 List of the plasmids**

Name	GENE (ORF)	Marker	Other*	Source
PB2520	TUS1-GFP	URA3	YCp	
PB2521	ROM2-GFP	URA3	YCp	
PB2202	CDC5	URA3	YCp	A. Amon
PB2522	MYO1	URA3	YCp	E. Bi
PB2523	HOF1	URA3	YEp	E. Bi
PB1993	BNI1-3xGFP	LEU2	YIp	
PB2525	TUS1 (1-600)	LEU2	YIp	
PB2526	TUS1 (1-600)-6A	LEU2	YIp	
PB2527	TUS1 (1-600)-6DE	LEU2	YIp	
PB2476	TUS1 (1-300)	URA3	YIp	
PB2477	TUS1 (1-300)-ST	URA3	YIp	
PB2478	ROM2 (1-500)	LEU2	YIp	
PB2528	ROM2 (1-500)-ST	LEU2	YIp	
PB2529	ROM2-3xGFP	LEU2	YIp	

\* YCp= Yeast Centromeric Plasmid  
 YEp= Yeast Episomal Plasmid  
 YIp= Yeast Integrative Plasmid

#### Bacterial expression

PB2530	GST-Cdc5PBD	Amp+
PB2531	GST-Cdc5PBD*	Amp+
PB2532	GST-Rom2 (1-400)	Kan+
PB2533	GST-Tus1 (1-300)	Kan+
PB2534	GST-Tus1 (216-450)	Kan+
PB2535	GST-RBD (Pkc1)	Amp+

#### Mammalian Work

GST-mEct2 (1-421)	Amp+
GST-mEct2 (414-639)	Amp+
Plk1 kinase domain T210D	Kan+
CBD-CYK4 (1-288)	Kan+
GST-Plk1PBD	Amp+

## References

1. Burkard, M.E., Randall, C.L., Larochele, S., Zhang, C., Shokat, K.M., Fisher, R.P., and Jallepalli, P.V. (2007). Chemical genetics reveals the requirement for Polo-like kinase 1 activity in positioning RhoA and triggering cytokinesis in human cells. *Proc Natl Acad Sci U S A* *104*, 4383-4388.
2. Petronczki, M., Glotzer, M., Kraut, N., and Peters, J.M. (2007). Polo-like kinase 1 triggers the initiation of cytokinesis in human cells by promoting recruitment of the RhoGEF Ect2 to the central spindle. *Dev Cell* *12*, 713-725.
3. Brennan, I.M., Peters, U., Kapoor, T.M., and Straight, A.F. (2007). Polo-like kinase controls vertebrate spindle elongation and cytokinesis. *PLoS ONE* *2*, e409.
4. Yuce, O., Piekny, A., and Glotzer, M. (2005). An ECT2-centralspindlin complex regulates the localization and function of RhoA. *J Cell Biol* *170*, 571-582.
5. Chalamalasetty, R.B., Hummer, S., Nigg, E.A., and Sillje, H.H. (2006). Influence of human Ect2 depletion and overexpression on cleavage furrow formation and abscission. *J Cell Sci* *119*, 3008-3019.
6. Nishimura, Y., and Yonemura, S. (2006). Centralspindlin regulates ECT2 and RhoA accumulation at the equatorial cortex during cytokinesis. *J Cell Sci* *119*, 104-114.
7. D'Avino, P.P., Savoian, M.S., and Glover, D.M. (2005). Cleavage furrow formation and ingression during animal cytokinesis: a microtubule legacy. *J Cell Sci* *118*, 1549-1558.
8. Piekny, A., Werner, M., and Glotzer, M. (2005). Cytokinesis: welcome to the Rho zone. *Trends Cell Biol* *15*, 651-658.
9. Fujiwara, T., Bandi, M., Nitta, M., Ivanova, E.V., Bronson, R.T., and Pellman, D. (2005). Cytokinesis failure generating tetraploids promotes tumorigenesis in p53-null cells. *Nature* *437*, 1043-1047.
10. Lee, K.S., Park, J.E., Asano, S., and Park, C.J. (2005). Yeast polo-like kinases: functionally conserved multitask mitotic regulators. *Oncogene* *24*, 217-229.
11. Song, S., and Lee, K.S. (2001). A novel function of *Saccharomyces cerevisiae* CDC5 in cytokinesis. *J Cell Biol* *152*, 451-469.
12. van Vugt, M.A., and Medema, R.H. (2005). Getting in and out of mitosis with Polo-like kinase-1. *Oncogene* *24*, 2844-2859.

13. Barr, F.A., Sillje, H.H., and Nigg, E.A. (2004). Polo-like kinases and the orchestration of cell division. *Nat Rev Mol Cell Biol* 5, 429-440.
14. Balasubramanian, M.K., Bi, E., and Glotzer, M. (2004). Comparative analysis of cytokinesis in budding yeast, fission yeast and animal cells. *Curr Biol* 14, R806-818.
15. Bement, W.M., Benink, H.A., and von Dassow, G. (2005). A microtubule-dependent zone of active RhoA during cleavage plane specification. *J Cell Biol* 170, 91-101.
16. Schmidt, M., Bowers, B., Varma, A., Roh, D.H., and Cabib, E. (2002). In budding yeast, contraction of the actomyosin ring and formation of the primary septum at cytokinesis depend on each other. *J Cell Sci* 115, 293-302.
17. Vallen, E.A., Caviston, J., and Bi, E. (2000). Roles of Hof1p, Bni1p, Bnr1p, and myo1p in cytokinesis in *Saccharomyces cerevisiae*. *Mol Biol Cell* 11, 593-611.
18. Tolliday, N., VerPlank, L., and Li, R. (2002). Rho1 directs formin-mediated actin ring assembly during budding yeast cytokinesis. *Curr Biol* 12, 1864-1870.
19. Lippincott, J., Shannon, K.B., Shou, W., Deshaies, R.J., and Li, R. (2001). The Tem1 small GTPase controls actomyosin and septin dynamics during cytokinesis. *J Cell Sci* 114, 1379-1386.
20. Yoshida, S., Kono, K., Lowery, D.M., Bartolini, S., Yaffe, M.B., Ohya, Y., and Pellman, D. (2006). Polo-like kinase Cdc5 controls the local activation of Rho1 to promote cytokinesis. *Science* 313, 108-111.
21. Lee, J., Hwang, H.S., Kim, J., and Song, K. (1999). Ibd1p, a possible spindle pole body associated protein, regulates nuclear division and bud separation in *Saccharomyces cerevisiae*. *Biochim Biophys Acta* 1449, 239-253.
22. Ro, H.S., Song, S., and Lee, K.S. (2002). Bfa1 can regulate Tem1 function independently of Bub2 in the mitotic exit network of *Saccharomyces cerevisiae*. *Proc Natl Acad Sci U S A* 99, 5436-5441.
23. Elia, A.E., Cantley, L.C., and Yaffe, M.B. (2003). Proteomic screen finds pSer/pThr-binding domain localizing Plk1 to mitotic substrates. *Science* 299, 1228-1231.
24. Elia, A.E., Rellos, P., Haire, L.F., Chao, J.W., Ivins, F.J., Hoepker, K., Mohammad, D., Cantley, L.C., Smerdon, S.J., and Yaffe, M.B. (2003). The molecular basis for phosphodependent substrate targeting and regulation of Plks by the Polo-box domain. *Cell* 115, 83-95.

25. Ubersax, J.A., Woodbury, E.L., Quang, P.N., Paraz, M., Blethrow, J.D., Shah, K., Shokat, K.M., and Morgan, D.O. (2003). Targets of the cyclin-dependent kinase Cdk1. *Nature* *425*, 859-864.
26. Niiya, F., Tatsumoto, T., Lee, K.S., and Miki, T. (2006). Phosphorylation of the cytokinesis regulator ECT2 at G2/M phase stimulates association of the mitotic kinase Plk1 and accumulation of GTP-bound RhoA. *Oncogene* *25*, 827-837.
27. Levin, D.E. (2005). Cell wall integrity signaling in *Saccharomyces cerevisiae*. *Microbiol Mol Biol Rev* *69*, 262-291.
28. Tajadura, V., Garcia, B., Garcia, I., Garcia, P., and Sanchez, Y. (2004). *Schizosaccharomyces pombe* Rgf3p is a specific Rho1 GEF that regulates cell wall beta-glucan biosynthesis through the GTPase Rho1p. *J Cell Sci* *117*, 6163-6174.
29. Mutoh, T., Nakano, K., and Mabuchi, I. (2005). Rho1-GEFs Rgf1 and Rgf2 are involved in formation of cell wall and septum, while Rgf3 is involved in cytokinesis in fission yeast. *Genes Cells* *10*, 1189-1202.
30. Morrell-Falvey, J.L., Ren, L., Feoktistova, A., Haese, G.D., and Gould, K.L. (2005). Cell wall remodeling at the fission yeast cell division site requires the Rho-GEF Rgf3p. *J Cell Sci* *118*, 5563-5573.
31. Ghaemmaghami, S., Huh, W.K., Bower, K., Howson, R.W., Belle, A., Dephoure, N., O'Shea, E.K., and Weissman, J.S. (2003). Global analysis of protein expression in yeast. *Nature* *425*, 737-741.
32. Schmelzle, T., Helliwell, S.B., and Hall, M.N. (2002). Yeast protein kinases and the RHO1 exchange factor TUS1 are novel components of the cell integrity pathway in yeast. *Mol Cell Biol* *22*, 1329-1339.
33. Ozaki, K., Tanaka, K., Imamura, H., Hihara, T., Kameyama, T., Nonaka, H., Hirano, H., Matsuura, Y., and Takai, Y. (1996). Rom1p and Rom2p are GDP/GTP exchange proteins (GEPs) for the Rho1p small GTP binding protein in *Saccharomyces cerevisiae*. *Embo J* *15*, 2196-2207.
34. Nakajima, H., Toyoshima-Morimoto, F., Taniguchi, E., and Nishida, E. (2003). Identification of a consensus motif for Plk (Polo-like kinase) phosphorylation reveals Myt1 as a Plk1 substrate. *J Biol Chem* *278*, 25277-25280.
35. Alexandru, G., Uhlmann, F., Mechtler, K., Poupart, M.A., and Nasmyth, K. (2001). Phosphorylation of the cohesin subunit Scc1 by Polo/Cdc5 kinase regulates sister chromatid separation in yeast. *Cell* *105*, 459-472.

36. Abe, M., Qadota, H., Hirata, A., and Ohya, Y. (2003). Lack of GTP-bound Rho1p in secretory vesicles of *Saccharomyces cerevisiae*. *J Cell Biol* *162*, 85-97.
37. Luo, J., Vallen, E.A., Dravis, C., Tcheperegine, S.E., Drees, B., and Bi, E. (2004). Identification and functional analysis of the essential and regulatory light chains of the only type II myosin Myo1p in *Saccharomyces cerevisiae*. *J Cell Biol* *165*, 843-855.
38. Birkenfeld, J., Nalbant, P., Bohl, B.P., Pertz, O., Hahn, K.M., and Bokoch, G.M. (2007). GEF-H1 modulates localized RhoA activation during cytokinesis under the control of mitotic kinases. *Dev Cell* *12*, 699-712.
39. Petersen, J., and Hagan, I.M. (2005). Polo kinase links the stress pathway to cell cycle control and tip growth in fission yeast. *Nature* *435*, 507-512.
40. Manke, I.A., Lowery, D.M., Nguyen, A., and Yaffe, M.B. (2003). BRCT repeats as phosphopeptide-binding modules involved in protein targeting. *Science* *302*, 636-639.
41. Clapperton, J.A., Manke, I.A., Lowery, D.M., Ho, T., Haire, L.F., Yaffe, M.B., and Smerdon, S.J. (2004). Structure and mechanism of BRCA1 BRCT domain recognition of phosphorylated BACH1 with implications for cancer. *Nat Struct Mol Biol* *11*, 512-518.
42. Kim, J.E., Billadeau, D.D., and Chen, J. (2005). The tandem BRCT domains of Ect2 are required for both negative and positive regulation of Ect2 in cytokinesis. *J Biol Chem* *280*, 5733-5739.
43. Rose, M.D., Winston, F., and Hieter, P. (1990). *Methods in Yeast Genetics* (Cold Spring Harbor, NY: Cold Spring Harbor Laboratory).
44. Longtine, M.S., McKenzie, A., 3rd, Demarini, D.J., Shah, N.G., Wach, A., Brachat, A., Philippsen, P., and Pringle, J.R. (1998). Additional modules for versatile and economical PCR-based gene deletion and modification in *Saccharomyces cerevisiae*. *Yeast* *14*, 953-961.
45. Carvalho, P., Gupta, M.L., Jr., Hoyt, M.A., and Pellman, D. (2004). Cell cycle control of kinesin-mediated transport of Bik1 (CLIP-170) regulates microtubule stability and dynein activation. *Dev Cell* *6*, 815-829.
46. Sagot, I., Klee, S.K., and Pellman, D. (2002). Yeast formins regulate cell polarity by controlling the assembly of actin cables. *Nat Cell Biol* *4*, 42-50.
47. Yoshida, S., and Toh-e, A. (2002). Budding yeast Cdc5 phosphorylates Net1 and assists Cdc14 release from the nucleolus. *Biochem Biophys Res Commun* *294*, 687-691.

48. Qadota, H., Python, C.P., Inoue, S.B., Arisawa, M., Anraku, Y., Zheng, Y., Watanabe, T., Levin, D.E., and Ohya, Y. (1996). Identification of yeast Rho1p GTPase as a regulatory subunit of 1,3-beta-glucan synthase. *Science* 272, 279-281.
49. Charles, J.F., Jaspersen, S.L., Tinker-Kulberg, R.L., Hwang, L., Szidon, A., and Morgan, D.O. (1998). The Polo-related kinase Cdc5 activates and is destroyed by the mitotic cyclin destruction machinery in *S. cerevisiae*. *Curr Biol* 8, 497-507.

# Chapter Five

## **Conclusions, Other Observations, and Future Directions**

### **PBD binding site timing and accessibility: Temporal distribution of Plk substrates**

One of the more confusing aspects of Plk1's (and orthologs) function is how various Plk substrates are targeted at different time-points during mitosis. There is a clear linear order to some mitotic events, yet how different substrates of the same kinase are targeted at different points is not clear. For Plk1 (and orthologs), this could be a simple consequence of PBD binding site generation by different kinases at different points during mitosis. Particularly puzzling is why PBD binding sites generated by Plk1 itself are not created until late mitosis. This suggests a shift in Plk1 targets from early mitosis, where Cdk1 is active and the PBD binding sites are mostly Cdk1-generated with other kinases contributing at particular subcellular locales such as the centrosome, to late mitosis, where Cdk1 is inactive and the PBD binding sites are mostly generated by Plk1 itself or other cytokinesis kinases. One explanation of this shift is that Cdk1 might block the ability of Plk1 to phosphorylate its self-generated PBD binding sites through phosphorylation at other sites in the same protein. This has been observed for PRC1 [1] and is also likely for MKPL2 [2]. Similarly, in budding yeast, Scc1 is targeted by Cdc5 in metaphase, and Bfa1 is not targeted until anaphase [3], though the PBD binding site-generating kinases for these proteins are unknown. PBD binding site-generating kinases, other than Cdk1 and Plk1, probably only function on a few select substrates and do not contribute to this overarching shift in PBD targeting from early to late mitosis.

However, even within early mitosis, certain targets are phosphorylated at different rates and at different times than other substrates. This is very evident for Cdk1 and has been studied in some detail. To assess whether the current state of the mitotic cell or some intrinsic factor to the substrates themselves controlled the kinetics, Georgi et al. [4] looked at the phosphorylation of a number of different Cdk1 substrates in cell extracts that had entered mitosis at various times. They found that no matter how long the extract had been in mitosis, the substrates were phosphorylated with the same kinetics (which varied widely between the different substrates tested), indicating that the kinetics of Cdk1 phosphorylation are somehow controlled by the substrates themselves. The same thing likely occurs for Plk1, suggesting that PBD targeting is not nearly the entire story. Instead, there must be some differentiation of substrates through another mechanism.



One interesting theory is that Plk1 targets with strong single PBD binding sites might be early substrates, whereas Plk1 targets with multiple weak PBD binding sites might be later substrates, though this has not been tested. Another theory is that there is a previously undiscovered regulatory subunit of Plk1 that additionally modulates its targeting to substrates. A regulatory subunit of Plk1 could control Plk1's function during early mitosis but be degraded by the APC at the metaphase to anaphase transition allowing different Plk1 behavior during late mitosis. Or a series of regulatory subunits controlled by other mitotic kinases could modify Plk1 behavior at different stages of mitosis.

Other external factors might also be at work, such as kinases that can phosphorylate the Ser immediately preceding the Ser that needs to be phosphorylated to generate a PBD binding site. PBD binding site accessibility, and thus Plk1 substrate status, could be controlled through a kinase/phosphatase pair, as was suggested for vimentin above. Even the PBD binding site itself might be controlled by a phosphatase to prevent PBD binding and Plk1 phosphorylation too early. Shugoshin binds to PP2A and brings it to the centromere where PP2A probably acts on Shugoshin and cohesin to keep them dephosphorylated until the spindle association checkpoint has been satisfied [5-7]. Plk1 and orthologs are responsible for phosphorylation of both Shugoshin and cohesin to release them from chromosomes [8-11], but as long as PP2A activity is present, this does not occur. Whether PP2A dephosphorylates the Plk1-generated phosphorylation site or the PBD binding site is not clear. Interestingly, Separase function is required for Shugoshin delocalization in *Drosophila* [12] and high Separase activity can prompt Cdc5 to phosphorylate its anaphase targets while the cells are still in metaphase [3]. Separase cleavage of its targets is not required for this phenomenon so how Separase controls Plk function is unclear though Separase could control a theoretical Plk regulatory subunit described earlier. Overall, multiple mechanisms collaborate to produce a temporal pattern of Plk1 substrates through mitosis, with PBD binding site-accessibility at the core of the regulation.

## **Phospho-dependent binding reactions downstream of Plk phosphorylation events**

Just as the PBD binds to phosphorylated sites downstream of CDK and other kinases, there might be domains that bind to sites that have been phosphorylated by Plks. Plks can generate the epitope for the phospho-specific antibody known as 3F3/2 [13, 14], suggesting that Plk-generated motifs are accessible to binding interactions. There are several possible candidates for domains that could bind Plk-generated sites based on current literature. The first is the Ect2 BRCT domains as described extensively in Chapter Four. Another promising candidate is 14-3-3 sigma which is the only 14-3-3 protein with a specific mitotic role [15]. Many of the translational machinery proteins that were found to bind to 14-3-3 sigma [15] also were identified as binding targets of the Plk1 PBD (Chapter Two). Perhaps the PBD and 14-3-3 sigma could compete for the same binding sites, but the optimal binding motifs for these domains are quite different and no sites within EIF4B appear to be able to bind both 14-3-3 and the PBD [16-18]. Instead, it seems more likely that the PBD binds these proteins to direct Plk1 to phosphorylate them at another site, which generates 14-3-3 sigma binding sites. The protein EIF4B was shown to be a critical target of 14-3-3 in mitosis, as overexpression of EIF4B overcame the 14-3-3 sigma-dependent suppression of translation in mitosis [15]. EIF4B was also identified as a PBD interactor (Table 2.1). Looking at all the possible 14-3-3 sigma binding sites in EIF4B reveals that several of them also match consensus Plk1 phosphorylation sites, and there is a potential CDK-generated PBD binding site (Figure 5.1). This leads to the straightforward hypothesis that Cdk1 activity in early mitosis phosphorylates EIF4B, allowing binding by the PBD, which in turn targets Plk1 activity to phosphorylate EIF4B so it can be bound by 14-3-3 sigma. Binding of EIF4B by 14-3-3 sigma disrupts cap-dependent, and leads to cap-independent, translation, which is a hallmark of mitotic cells [15]. To demonstrate that Plk1 generates the 14-3-3 sigma binding sites, a 14-3-3 sigma pull-down can be done with bacterial-produced EIF4B that is pre-incubated with Plk1 kinase. Mapping of the relevant sites through mutational analysis and/or mass spectrometry should easily follow. Then, the relevant mutations can be tested in vivo for functionality using the add back system described in Wilker et al. [15]. There should be less mutant EIF4B required (that cannot bind 14-3-3 sigma) to

overwhelm the 14-3-3 sigma-dependent suppression of mitotic translation than wild-type EIF4B. Similarly, knockdown of Plk1 by siRNA using the method of van Vugt et al. [19] should give the same mitotic translation defect as seen in the 14-3-3 sigma knockdown cells. The Ect2 tandem BRCTs and 14-3-3 sigma have dramatically different folds and appear to recognize dramatically different motifs, however, they may both bind to specific Plk1-dependent phosphorylation sites. As Plk1 participates in such a vast range of mitotic functions ([20, 21], Figure 2.4), other domains that recognize Plk1-phosphorylated motifs likely exist.

### **Suspected Polo-like kinase targets**

#### **Cdc14/Net1**

Cdc14 and Net1 were identified in the bioinformatic screen for Cdc5 substrates, but were not verified to bind the Cdc5-PBD. Cdc14 is a phosphatase conserved from yeast to humans that dephosphorylates CDK sites during late mitosis [22], and Cdc14 is held inactive in the nucleolus by Net1 until the FEAR (cdc14 early anaphase release network) and MEN (mitotic exit network) pathways cause Cdc14 release [23, 24]. Both of these pathways require Cdc5 kinase activity though the mechanism of Cdc5 action is unknown [25, 26].

Net1 has been shown to be an *in vitro* Cdc5 substrate and multiple Cdc5-dependent phosphorylation sites have been mapped, but mutation of these sites caused minimal phenotypic consequences [27, 28]. On the other hand, Net1 has been shown to be an *in vivo* CDK substrate, and mutation of three of these sites in the N-terminal 341 amino acids, which are required for Net1 to hold Cdc14 in the nucleolus, eliminates the ability of Net1 to release Cdc14 [29]. One of these three sites makes a perfect PBD binding site. Of course, mutation of this residue eliminates both the CDK phosphorylation and the potential PBD binding. Single mutations have not been tested in the reported literature, but it will be interesting to see whether mutation of this single residue, T212, has the same phenotypic consequences. Also critical is to test whether mutation of the -1 Ser (S211) also results in the same phenotypic consequences. This mutant will presumably be a separation-of-function allele for CDK phosphorylation and PBD binding.

PBD binding studies of wild-type and mutant Net1, as well as phosphorylation site mapping experiments by mass spectrometry, will be necessary to confirm this.

If the expected results are obtained, this would lead to a model that the Cdc5-PBD targets Cdc5 to Net1. But since Cdc5 activity against Net1 is not biologically relevant [27], it is likely that, as has been suggested [28], Cdc5 phosphorylates Cdc14, which contains five optimal, and more than ten minimal, Plk consensus phosphorylation motifs but no consensus motifs for PBD binding. This phosphorylation of Cdc14 by Cdc5 could be the driving force behind the separation of Net1 and Cdc14. Thus, Net1 and Cdc14 are a likely example of the distributive phosphorylation model, where PBD binding to Net1 allows Plk phosphorylation of Cdc14. Very recently human Cdc14A was found to bind Plk1 *in vivo* and to be a Plk1 substrate *in vitro* [30], confirming the possible connection between Cdc14 and Plks.

### **Lte1**

In my Cdc5-PBD pulldown screen from the TAP-tagged yeast collection, I identified Lte1, a member of the mitotic exit network [26], as a specific PBD interactor (Chapter Three). This is in agreement with a previous report that full-length Cdc5 interacts with Lte1 by both pulldown and co-immunoprecipitation [31]. Lte1 is a member of the MEN pathway described just above. Activity of Lte1 is only required at low temperatures [32], and Lte1 is synthetically lethal with Spo12 [33], which is part of the FEAR network [25], even at normal temperatures. This allows easy assessment of Lte1 function through the use of an Lte1/Spo12 double deletion strain with a covering *ura*-marked Spo12 plasmid. Growth of this strain on 5-FOA plates will eliminate the *ura*-marked plasmid and cause cell death which can be rescued by expression of a wild-type Lte1 covering plasmid. Alternatively, an Lte1 deletion strain can be grown at low temperature (15°C), causing death which again can be rescued by the presence of a wild-type Lte1 covering plasmid. Overexpression of the central CHD domain region of Lte1 rescues the cold sensitivity [34]. This region contains five optimal CDK phosphorylation sites of the sequence (S/T)PX(K/R), and mutation of all five of these sites in full-length Lte1 still rescues both the cold sensitivity and *spo12* synthetic lethality of a Lte1 deletion strain [35]. This allele of Lte1 with five mutations can still function as a CDK target in

vitro and in vivo [35], indicating other minimal CDK target sites, (S/T)P, are also phosphorylated.

Intriguingly, within this region there are three optimal PBD binding sites (S630, S643, S667) of the form S(S/T)P, of which two are within optimal CDK phosphorylation sites. My hypothesis is that CDK phosphorylation of these sites targets the Cdc5-PBD to Lte1 causing subsequent phosphorylation of Lte1 by Cdc5 to regulate Lte1 function. Thus, mutation of these three sites will eliminate Lte1 function in the assays described earlier. Ideally, wild-type Lte1 will be compared to the double mutant in the two optimal CDK phosphorylation sites and the triple mutant in all three potential PBD binding sites. Presumably, the double mutant would rescue the low temperature and *spo12* synthetic lethality just as well as the wild-type protein, considering that a mutant of five sites, including these two, rescued these phenotypes [35]. If the triple mutant fails to rescue, it will be imperative to show that this mutant does not bind the PBD like the wild-type protein, and that the triple mutant Lte1 is still a substrate for CDK in vitro, to show that CDK regulation has not been completely lost. Also, the single mutant at S643 should also be tested, though this will likely rescue similarly to wild-type. Lte1 has more than a dozen potential Cdc5-phosphorylation sites based on the known phosphorylation motif for Plk's [36, 37], further suggesting Plk regulation of this molecule. A shift to a non-permissive temperature of a temperature-sensitive Cdc5 allele does not eliminate the gel shift associated with Lte1 phosphorylation in mitosis [31], but this gel shift has been fairly convincingly demonstrated to be CDK-dependent [35].

### **Npm1**

Npm1, nucleophosmin, was identified as a specific Plk1 PBD interactor in my PBD-pulldown mass spectrometry screen (Table 2.1). Npm1 is a mammalian RNA binding protein involved in preribosomal assembly and transport of ribonucleoproteins between cellular compartments (ref). In addition, we identified a phosphopeptide corresponding to phosphorylation of T219 in Npm1 (Table 2.2). This threonine sits within the sequence STP which, when phosphorylated, matches the optimal PBD binding site. As this is the only optimal PBD binding site found within Npm1, it is likely to

directly bind the PBD. To test this, S218A and T219A mutants can be made in Npm1 and tested for binding in a PBD pulldown assay.

Npm1 is already known to be regulated by Plk1 during mitosis through phosphorylation of serine four in Npm1 by Plk1 [38]. Mutation of this site to alanine results in lack of centrosome duplication and failure of chromosome segregation, whereas mutation of this site to the phosphomimic residue D results in centrosome over-duplication and cytokinesis defects [38]. If the S218A and T219A mutations do eliminate PBD binding, then it will be interesting to test whether expression of these mutants in tissue culture cells mimics the phenotypes seen with expression of the S4A mutant. (It may be necessary to siRNA-deplete the endogenous Npm1 to see the phenotype.) If the S4A and PBD site mutants have the same phenotype, this will confirm that Npm1 is regulated through Plk1 phosphorylation subsequent to PBD binding. A double mutant in the PBD binding site with the S4D would be expected to result in the same phenotype as the S4D mutant alone, because Plk1 phosphorylation is downstream of PBD binding. However, the phenotypes may be different, indicating a separate need for PBD binding and Plk1-dependent phosphorylation, or the presence of additional PBD-dependent Plk1 phosphorylation sites. This is unlikely, however, because no other consensus Plk1 phosphorylation motifs are present on Npm1. Npm1 likely represents a model protein for demonstrating the processive phosphorylation model.

More intriguingly, there is growing evidence that Npm1 is a dynamically-regulated molecule during the cell cycle that contributes to genomic stability and ribosome processing along with being a proto-oncogene [39]. The localization of Npm1 to nucleoli during interphase is disrupted during mitosis, through phosphorylation by CDKs, and this phosphorylation blocks the RNA binding function of Npm1, that it uses to bind pre-ribosomal particles [40]. Whether Plk1 activity is required for these changes in Npm1 activity is unclear, and it could be easily tested using the mutants described above. The function of Npm1 at centrosomes is also a bit unclear, but it appears Npm1 is involved in physical separation of paired centrioles after CDK phosphorylation. Interestingly, this function is mediated through Npm1 activation of Rock2, and in fact Npm1 binding to Rock2 enhances the kinase activity of Rock2 [41]. Considering that Npm1 [38] and Rock2 (Chapter Two) are both regulated by Plk1, and that both Npm1

[41] and Plk1 (Chapter Two) activate Rock2, there is likely to be three-way regulation between all three proteins. The binding of Npm1 and Rock2 could be Plk1-stimulated, in addition to being CDK-stimulated [41], which could easily be tested using the mutants of Npm1 described above. If this turns out to be true, then Plk1 will have three mechanisms for activating Rock2: direct phosphorylation of Rock2 (Chapter Two), activation of Ect2 (Chapter Four) (which activates furrow-localized Rock2), and activation of Npm1 (which activates centrosome-localized Rock2). Loss of Npm1 in mouse models leads to aneuploid tumors [39], suggesting spindle and/or cytokinesis failure, consistent with the phenotypes seen with Plk1 and Rock2 gain or loss (Chapter Two). Lastly, Npm1 has been found to be a target of the Brca1/Bard1 Ubiquitin Ligase at the centrosome [42], suggesting an additional layer of control that could be tested in the HCC1937 cell line (Appendix One).

## **NIPA**

A mechanism, whereby Cdk1/cyclinB1 is kept inactive during interphase, is through ubiquitination and degradation of cyclinB1 by an SCF complex with NIPA (nuclear interacting partner of ALK) as the substrate specificity factor [43]. Recently, NIPA has been identified as a mitotic phosphoprotein [43, 44]. At least two sites in NIPA, S354 and S359, are phosphorylated during G2, disrupting the association of NIPA with its SCF complex, and thus preventing NIPA from directing cyclinB1 degradation [44]. Interestingly, the S359 site is within an SSP motif that could be bound by the PBD. Subsequent to the partial activation of Cdk1/cyclinB1 allowed by the disruption of NIPA, Cdk1/cyclinB1 phosphorylates NIPA on S395, in the context of another SSP motif [44]. All three of these sites have been shown to be *in vivo*-relevant, through the use of point mutations, whereas several other mapped Cdk1/cyclinB1 *in vitro* phosphorylation sites on NIPA were shown to be irrelevant *in vivo* [44]. Plk1 did not phosphorylate NIPA *in vitro* without prior phosphorylation by Cdk1/cyclinB1 [44], so there is a strong possibility that Plk1 is involved in the regulation of this molecule, considering the two PBD binding motifs that are generated. These sites are all fully conserved in mouse NIPA, though only the sequence context of the S395 site is conserved in *Xenopus*. This

would bring yet another layer of Plk1 regulation into the story of how Cdk1/cyclinB1 gets activated to promote mitotic entry [21, 45].

### **MCMs and ORCs**

One interesting set of proteins that has not been implicated in any process overlapping with Plk1 are the mini-chromosome maintenance proteins (MCMs) and the origin recognition complex proteins (ORCs). Six separate MCMs (MCM2-7) are known to form a complex which is thought to be the replicative helicase in eukaryotic organisms [46]. They form part of the pre-replicative initiation complex along with several members of the ORC protein family [47]. After replication initiation, several ORC proteins are phosphorylated by CDK family members to exclude formation of new pre-replication initiation complexes until after chromosome segregation is completed during anaphase [48, 49]. The MCM complex stays with the replication complex until replication is complete, and then several members of it are regulated through CDK phosphorylation [48]. The details on the regulation of ORC and MCM proteins differ between organisms, but in all cases, multiple members are either degraded through ubiquitin-dependent pathways, excluded from the nucleus, or otherwise prevented from performing their replication function [49]. Outside S phase several of these proteins have different functions, including Orc6, which, when disrupted, interferes with chromosome segregation and cytokinesis [50] and binds septins at the cleavage furrow [51]. Mcm2 [52] and Orc2 [52, 53] are located at the centrosome throughout mitosis, and depletion of Mcm2 and Orc2 by siRNA causes similar defects to those seen with depletion of Orc6 [52]. Orc2 also recruits Cdk1 to chromatin to promote RPA (replication protein A) foci disassembly to allow mitotic chromosome condensation [54].

Plk1 PBD can bind various MCMs and probably the entire MCM2-7 complex [55], though no function was ascribed to this interaction. We identified Mcm2, Mcm4, and Mcm6, in the PBD pulldown mass spectrometry screen, as specific PBD interactors (Chapter Two). All three of these have optimal PBD binding sites, whereas the other three members of the complex, Mcm3/5/7, do not have any optimal PBD binding sites. Several PBD binding motifs in MCM2 and MCM4 have been mapped as *in vivo* phosphorylation sites ([56], Table 2.2), leading to a strong possibility that the PBD can



directly bind these proteins. In a yeast two-hybrid experiment, interaction was seen between full-length Plk1, Mcm2, and Orc2, but not any of the other MCM or ORC proteins [52]. The role of PBD binding of these MCMs is unclear, and there are multiple possibilities. If this interaction normally takes place during mitosis, it might be a secondary inhibition mechanism to prevent pre-replicative initiation complexes from forming too early, beyond just phosphorylation by CDKs. Since the nucleus breaks down during mitosis, perhaps PBD binding and/or phosphorylation by Plk1 maintains the separation of the MCMs from chromatin. Alternatively, Plk1 regulation of MCMs in mitosis might extend the period of inhibition of MCMs past when CDK activity is lost at the beginning of anaphase, considering that MCMs are thought to re-associate with chromatin starting in telophase [48, 49]. Furthermore, Plk1 regulation of MCMs could have relieved the CDK-generated inhibition of MCMs, if the PBD interaction takes place in late mitosis, like the PBD interactions of cytokinesis regulators. The re-association of pre-replicative complexes with DNA might be monitored in a checkpoint fashion in late mitosis, since elimination of Mcm2, Orc2, and Orc6 causes cytokinesis failure [50, 52]. The activity of Plk1 may be required to satisfy this checkpoint, by being partially responsible for the re-establishment of pre-replicative complexes. More simply, Plk1 may regulate mitotic-specific functions of Mcm2 and Orc2, rather than having any impact on the DNA replication activities of these proteins.

### **Rho-activated Kinases and Myosin Phosphatase Targeting Subunit**

In Chapter Two, we demonstrated extensively that Rock2 is under the control of Plk1. In addition Rock1, citron kinase, and myosin phosphatase targeting subunit (MYPT) were all identified as specific PBD binders (Table 2.1 and Figure 2.6 F,H). All four of these proteins are known to be involved in cytokinesis and regulate the phosphorylation of myosin regulatory light chain, which in turn controls the activation state of myosin in the acto-myosin ring [57]. The three kinases are all regulated by binding RhoA. It will be interesting to see if Rock1 and citron kinase are also activated by Plk1, like Rock2 (Figure 2.8F). Rock2 has a single potential CDK-generated PBD binding site, but I have not been able to demonstrate that this site mediates the interaction with the PBD, as mutation of this site does not eliminate the Rock2/PBD interaction by

pull-down. Potentially, the PBD binding site on Rock2 could be generated by Plk1, as is known for several other proteins involved in cytokinesis ([1, 2], and Chapter Four). Rock1 does not contain any potential CDK-generated PBD binding sites, so again it may be regulated through Plk1-generation of its own PBD binding site. Citron kinase, on the other hand, has six potential CDK-generated PBD binding sites, of which we mapped one as being an *in vivo* phosphorylation site (Table 2.2). Finally, the phosphatase, MYPT, also has two potential CDK-generated PBD binding sites. All have lots of potential Plk1 phosphorylation sites, as judged by optimal consensus motifs. These four proteins all contribute to the same pathway, so it may make sense for Plk1 to regulate all of them in similar fashion, at the same time, in order to promote the forward progression of cytokinesis. Considering the large role of Plk1 in regulating RhoA networks, as discussed in Chapter Four, it seems likely that Plk1 also helps control these downstream RhoA targets.

### **RAM Network Components**

Another late mitotic pathway in budding yeast is the RAM (regulation of Ace2 activity and cellular morphogenesis) network. It is similar in structure to the MEN, with a small G-protein regulating the activity of a kinase cascade, with the ultimate target being the daughter cell-specific transcription factor, Ace2 [58]. I identified the RAM network scaffold, Tao3, in my Cdc5-PBD yeast two-hybrid and pulldown assay (Chapter Three). The upstream RAM network kinase, Kic1, also came down with the Cdc5-PBD, though it came down equally well with the mutant version (Chapter Three). Intriguingly, the laboratory of Eric Weiss at Northwestern has identified Kic1 to be a Cdc5 substrate (Eric Weiss - personal communication). Also, the downstream kinase Cbk1, which is a member of the NDR family of kinases, is an *in vitro* substrate of Plk1 (unpublished observations). Though Cbk1 does not have any consensus binding sites for the PBD, its obligate binding partner, Mob2, does have a consensus PBD binding site. Further genetic experiments need to be performed to show that Cdc5 regulates the RAM network and to identify which components are the targets.

### **Other Proteins Identified as PBD Interactors in This Thesis**

For the proteins identified as specific Cdc5-PBD interactors (Chapter Three – Table 3.1 and 3.2), it will be interesting to continue to perform interaction-defective genetics. For those proteins where identification of the PBD binding site is straightforward, mutants can be made that lose Cdc5-PBD binding. The genomic copy of the gene can be easily replaced with this non-binding mutant, or single copy plasmids containing the wild-type or non-binding mutant version of the gene can be placed in strains with the genomic copy deleted. Either way, this represents a powerful genetic system for examining the effects of Cdc5 regulation of many key mitotic processes. Furthermore, the availability of the *cdc5-as1* allele and the corresponding inhibitor (Chapter Three) allows for direct assessment of whether these yeast proteins are also Cdc5 substrates in addition to Cdc5-PBD binders.

For other human proteins with mapped phosphorylation sites that match optimal PBD binding sites (Table 2.2), it will be interesting to examine whether PBD binding is indeed mediated through the phosphorylation, and whether mutation of that site to eliminate PBD binding has any phenotypic consequences. Ideally, mutants of both the phosphorylation site and the -1 serine will be tested in a PBD pulldown assay and in vivo assay. This will allow for separation of function between the consequences of phosphorylation of the residue by CDK, which should be normal in the -1 serine mutant, and the consequence of loss of PBD binding. Ideally, to test the biological significance of PBD-binding, the endogenous copy of the gene will be knocked down by siRNA or other methods, and the wild-type copy of non-binding mutants will be added back in a form that cannot be targeted by the siRNA. Over- and mis-expression effects will be difficult to overcome, which is why the yeast system is so much more powerful.

### **The Function of Plk1 at the Central Spindle**

There are a large number of PBD binding partners and Plk1 substrates at the central spindle, as described previously in Chapter Two, and as more fully illuminated by recent papers. In order to put all these proteins in context, I generated a new protein-protein interaction map (as previously done in Chapter Two) of the central spindle

machinery that connects the central spindle (shown as tubulin in figure) to the actomyosin ring focused on Plk1 and Aurora B (Figure 5.2). Many of the core components known to be involved in central spindle formation (Mklp1, Mklp2, Cyk4, and vimentin) are regulated by these two kinases [59-65], though the only direct link known between these two kinases is the phosphorylation of the Aurora B modulator, INCENP, by Plk1 [66]. The microtubule bundling protein PRC1 recruits the kinesins, Mklp1, Mklp2, KIF4, and KIF14, to the central spindle where they, in turn, recruit many of the other central spindle components [59]. As described in Chapters Two and Four, this core spindle machinery connects to the RhoA-mediated cytokinesis pathways through the RhoGEF, Ect2, with Plk1 as a regulator of both processes. Rho-dependent kinases control the activation of myosin, through phosphorylation of regulatory myosin light chain and, in turn, contraction of the actomyosin ring [57]. Plk1 also regulates these kinases (Chapter Two) as well as anillin [67], which plays a role in the construction and contractility of the actomyosin ring [68]. In addition, not shown are the Plk1-regulated proteins, NudC, Cep170, Cep55, Nir2, and TTDN1, which all localize to the central spindle, and depletion of which causes cytokinesis defects, though none of these proteins have any known direct connection to the central spindle or RhoA mediated processes [69-73].

Why are there so many binding partners of the PBD at the central spindle and so many Plk1 substrates? Depletion of almost any of these PBD binding partners prevents Plk1 localization to the central spindle, which suggests that either all the binding events are somehow co-dependent or, more likely, that depletion of any of these components causes mitotic defects that prevent proper central spindle assembly. The ability of Plk1 to localize in cells expressing non-PBD binding mutants of these proteins has not been tested, but could serve to identify an order of importance of these proteins in Plk1 localization. Similarly, after the Plk1-dependent phosphorylation sites on all these proteins have been mapped, cell lines expressing non-phosphorylatable mutants can be used to determine the relevance of these sites to cytokinesis function. Perhaps some of the Plk1-dependent phosphorylation sites are extraneous to the actual functioning of cytokinesis and only occur due to the proximity of Plk1 and the proteins. Still, the coordinated phosphorylation of so many proteins by one kinase at one time in one

process suggests that Plk1 phosphorylation of all the proteins may be required to get timely and accurate cytokinesis. Similarly, Aurora B-mediated phosphorylation of many of the same components creates a system where a large number of potentially-independent events have to match up, in time and space, in order for the irreversible process of cytokinesis to occur. In this view, the vast number of Plk1 and Aurora B substrates can simply be seen as an exquisite unidirectional control mechanism.

### **On the Implications of the Number of Plk Substrates and PBD Binders**

The sheer number of known and suspected Plk1 targets requires that Plk1 does not bind to its substrates for a long time. PBD binding to a ligand seems like a fairly strong interaction with a measured  $K_d$  of 280nm with an isolated phosphopeptide [18]. This is similar to  $K_d$ s of 40nm for the Lck SH2 domain with an optimal peptide [74], 510nm for 14-3-3 with its binding peptide from Raf [16], and 330nm for the FHA domain of Rad53 with an optimal peptide [75]. Whether this number has anything to do with the  $K_d$  of an interaction between the PBD and a full-length protein is unclear. Certainly, the autoinhibition of the kinase domain and the PBD in the full-length molecule may contribute to a lower  $K_d$ , as seen for peptides *in vitro* [17]. However, it is thought that during mitosis, when Plk1 is activated by phosphorylation on T210 [76-79], this autoinhibition is mostly eliminated [80]. This could be more fully tested *in vitro* by phosphopeptide binding studies using full length Plk1, with or without pre-treatment with PKA to phosphorylate the T210 site [81]. Arguing that the PBD does bind tightly *in vivo*, in full-length Plk1, is the data that expression of a kinase-dead Plk1, or the isolated PBD, causes mitotic defects [79, 80, 82]. If the PBD interacted weakly with full length substrates *in vivo* due to a fast off rate, the endogenous wild-type Plk1 should be able to drive mitosis even in the presence of kinase-dead Plk1 or isolated PBD, though a mitotic delay might occur. Taking all the evidence together, it seems that the PBD's interaction strength *in vivo* must be modified by the activity of the Plk kinase. The obvious hypothesis is that Plk1 phosphorylation of PBD ligands somehow modifies the PBD interaction, either through disruption or preventing re-binding after dissociation. This

could happen due to structural rearrangements of Plk1 substrates, direct interference with the PBD binding site by the Plk1-generated phosphorylation, or other mechanisms.

The degree of interference with PBD binding by Plk1 phosphorylation could, and probably will, vary widely between Plk1 substrates. Proteins with a single PBD site and a Plk phosphorylation site in close proximity might be nearly completely inhibited from PBD binding after Plk phosphorylation. On the other hand, for those PBD binders that have a large number of low affinity PBD binding sites, it seems unlikely that Plk phosphorylation will greatly diminish PBD binding, unless there are a similarly large number of Plk-dependent phosphorylation sites. Proteins that have Plk1-generated PBD binding sites might be on those proteins that Plk1 needs to stay attached to for significant periods of time. These proteins would be the scaffolds in the distributive phosphorylation model (Figure 1.3). Spacing requirements, at least in two dimensions, for the distance between a PBD binding site and a Plk phosphorylation site, could also be tested in vitro using peptides containing a PBD binding site and an optimal Plk phosphorylation site at various distances away. Kinase assays, to measure the incorporation of phosphate into the Plk phosphorylation site, and equilibrium binding studies, to measure the binding affinity of the PBD to its binding site, of these peptides would show the interplay between Plk phosphorylation and PBD binding. At short distances, Plk will probably not be able to phosphorylate its target efficiently, and thus the observed PBD binding affinity will not change much. At long distances, the Plk phosphorylation site will not interfere with PBD binding despite full phosphorylation. But, presumably, at some intermediate distance, Plk phosphorylation of its target site will interfere with PBD binding.

### **Summary and Future Directions**

Before this project started a fair bit was known about the role of Plks in mitosis [21], and about the function of the polo-box domain with the identification of it as a phosphopeptide binding domain [18]. These studies have added a large number of additional PBD interactors and potential Plk1 and Cdc5 substrates to a list that has been growing rapidly over the past few years (Table 1.1). More specifically we have demonstrated a mechanistic role for Plk1 and Cdc5 in the control of Rho-mediated

cytokinesis signaling through Plk control of RhoGEFS and Rho-activated kinases. Additionally we will demonstrate a role for Cdc5 in control of septum deposition and nuclear migration which have not been previously described. The methods and assays designed for these projects can be harnessed for a number of other potential uses.

The pulldown mass spectrometry screen described in Chapter Two can be readily extended to other phosphopeptide binding domains under other cellular conditions. Utilizing a mutant that no longer binds phosphopeptides provides an optimal negative control to identify specific interactors. This has already been done for the phosphobinding protein, 14-3-3 sigma, for cell cycle stage specific interactions by another member of our laboratory [15]. In addition any protein-protein interaction domain that has a known mutation that interferes with the protein-protein interaction surface could be used in this system. For example, the mammalian inhibitor of apoptosis protein, survivin, is known to interact with the pro-apoptotic protein, Smac, and mutation of Arg-71 in survivin to alanine blocks this interaction. Performance of the pulldown mass spectrometry screen with wild-type and mutant surviving should detect Smac as a specific survivin interactor, and might detect other survivin interactors that bind the same surface. Perhaps more interestingly, this approach could be used to map differential interactions among cell types or mutant proteins associated with disease states. For example, there are a number of known cancer-associated mutations in the tandem BRCT domain of BRCA1 (Appendix One). A panel of these mutants could be used in a pulldown mass spectrometry screen from human tumor cell lysates to determine how these mutations affect the binding pattern of BRCA1. The mutant BRCA1 proteins could fail to interact with critical BRCA1 ligands, or they could interact with ligands that wild-type BRCA1 does not bind, to promote a transformed cellular state.

The context-dependent yeast two hybrid scheme described in Chapter Three has a multitude of potential uses for both identification of phosphorylation-dependent interactions along with identification of any activity-dependent interaction. Initially other phosphopeptide binding domains can be tested under appropriate conditions where they bind their ligands. For example the budding yeast protein, Rad9, is required for cell cycle arrest after DNA damage, and contains a tandem BRCT domain that is a phosphopeptide binding module. The tandem BRCT domain of Rad9 could be used in a context-

dependent yeast two hybrid screen looking for interactions that occur after exposure of yeast cells to various agents that activate the DNA damage response network, such as methyl-methonyl-sulfate (MMS), UV irradiation, hydroxyurea, or gamma irradiation. Different interactions may be identified with different treatments giving a broad picture of the range of Rad9 responses to DNA damage. The screening strategy is clearly extendable to domains that bind post-translational modifications other than phosphorylations, but even more broadly it could be used to look for any interactions that occur only under a particular cellular state. For example, in mammalian cells, p53 and mdm2 interact upon unstressed conditions, but upon a variety of cellular stresses this interaction is lost. This interaction could be identified by performing the same screen as above for Rad9, but looking at those hits that bind stronger in the untreated condition compared to the treated condition.



**Figure 5.1: Potential 14-3-3 Sigma and Plk1 Related Sites in EIF4B**

**(A) Potential 14-3-3 Sigma Related Sites in EIF4B**

MAASAKKKNKKGTISLTDFLAEDGGTGGGSTYVSKPVSWADETDDLEGDVSTTWHSNDDDVYRAPPIDR  
SILPTAPRAAREPNIDRSRLPKSPPYTAFLGNLPYDVTEESIKEFFRGLNISAVRLPREPSNPERLKGFG  
YAEFEDLDSLLSALSLSLNEESLGNRRIRVDVADQAQDKDRDRSFRDRNRSDKTDTDWRARPATDSFDD  
YPPRRGSDSFGDKYRDYSDRYRDGYRDGYRDGPRRMDRYGGRDRYDDRGSRDYDRGYDSRIGSGRRA  
FGSGYRRDDDYRGGDRYEDRYDRDRSRSRSDYRDRDRGPPQRPKLNKPRSTPKEDDSSAS  
TSQSTRAASIFGGAKPVDTAAREREVEERLQKEQEKLQRLDEPKLERRPRERHPSWRSEETQERERSRT  
GSESSQTGTSTTSSRNAARRRESEKSLNETLNKEEDCHSPTSKPPKPDQPLKVMPPPPKENAWVKRSSN  
PPARSQSSDTEQQSPTSGGGKVAPAQPSSEEGPGRKDENKVDGMNAPKGQGTGNSSRGPGDGGNRDHWKESD  
RKDGKKDQDSRSAPPEPKPEENPASKFSSASKYAALSVDGEDENEGEDYAD

Red = 14-3-3 binding mode #1 RSX(pS/pT)XP

Pink = 14-3-3 binding mode #2 RXPhiX(pS/pT)XP

**(B) Potential Plk1 Related Sites in EIF4B**

MAASAKKKNKKGTISLTDFLAEDGGTGGGSTYVSKPVSWADETDDLEGDVSTTWHSNDDDVYRAPPIDR  
SILPTAPRAAREPNIDRSRLPKSPPYTAFLGNLPYDVTEESIKEFFRGLNISAVRLPREPSNPERLKGFG  
YAEFEDLDSLLSALSLSLNEESLGNRRIRVDVADQAQDKDRDRSFRDRNRSDKTDTDWRARPATDSFDD  
YPPRRGSDSFGDKYRDYSDRYRDGYRDGYRDGPRRMDRYGGRDRYDDRGSRDYDRGYDSRIGSGRRA  
FGSGYRRDDDYRGGDRYEDRYDRDRSRSRSDYRDRDRGPPQRPKLNKPRSTPKEDDSSAS  
TSQSTRAASIFGGAKPVDTAAREREVEERLQKEQEKLQRLDEPKLERRPRERHPSWRSEETQERERSRT  
GSESSQTGTSTTSSRNARRRESSEKSLNETLNKEEDCHSPTSKPPKPDQPLKVMPPPPKENAWVKRSSN  
PPARSQSSDTEQQSPTSGGGKVAPAQPSSEEGPGRKDENKVDGMNAPKGQGTGNSSRGPGDGGNRDHWKESD  
RKDGKKDQDSRSAPPEPKPEENPASKFSSASKYAALSVDGEDENEGEDYAD

Green = strong potential Plk1 phosphorylation site (E/D/N)X(S/T)(F/Y/W/V/I/L/M)

Yellow = weak potential Plk1 phosphorylation site (E/D/N/Q)X(S/T)

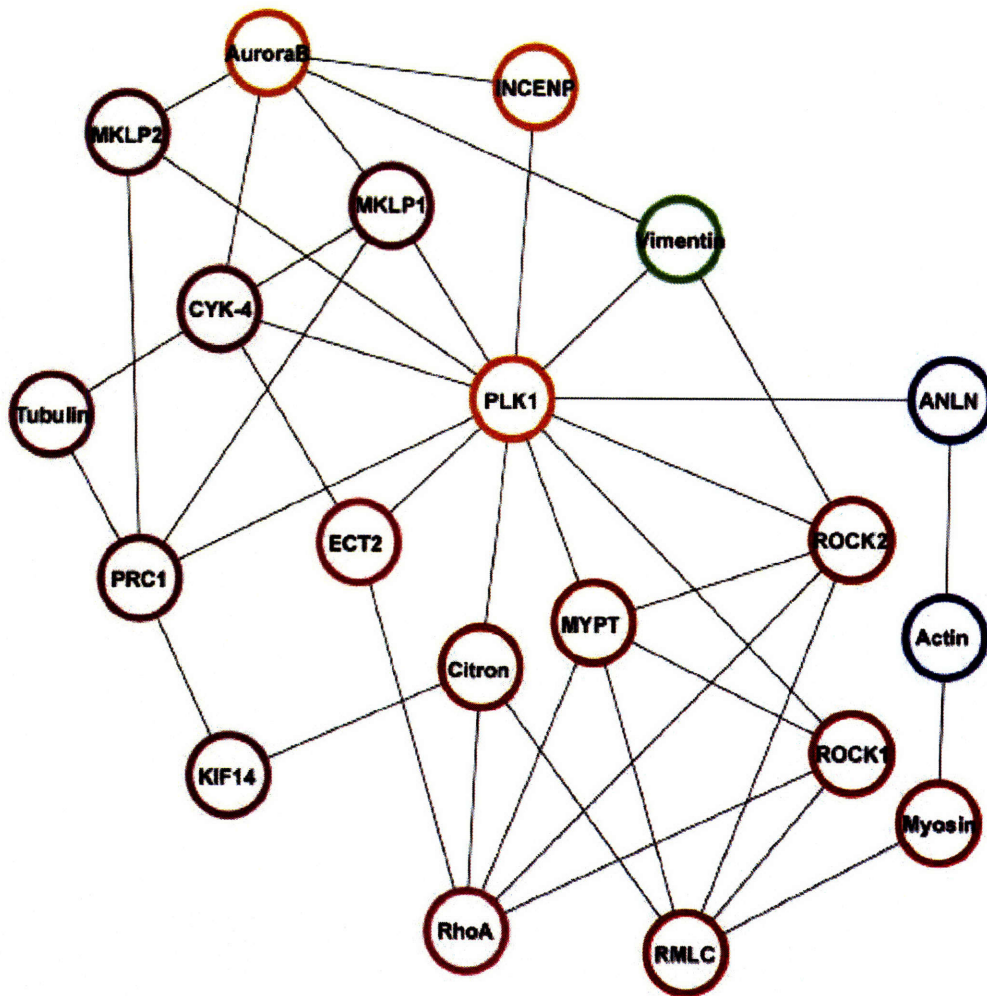
Blue = potential PBD binding site S(S/T)P

**(C) Potential 14-3-3 Sigma Binding Sites Generated by Plk1**

MAASAKKKNKKGTISLTDFLAEDGGTGGGSTYVSKPVSWADETDDLEGDVSTTWHSNDDDVYRAPPIDR  
SILPTAPRAAREPNIDRSRLPKSPPYTAFLGNLPYDVTEESIKEFFRGLNISAVRLPREPSNPERLKGFG  
YAEFEDLDSLLSALSLSLNEESLGNRRIRVDVADQAQDKDRDRSFRDRNRSDKTDTDWRARPATDSFDD  
YPPRRGSDSFGDKYRDYSDRYRDGYRDGYRDGPRRMDRYGGRDRYDDRGSRDYDRGYDSRIGSGRRA  
FGSGYRRDDDYRGGDRYEDRYDRDRSRSRSDYRDRDRGPPQRPKLNKPRSTPKEDDSSAS  
TSQSTRAASIFGGAKPVDTAAREREVEERLQKEQEKLQRLDEPKLERRPRERHPSWRSEETQERERSRT  
GSESSQTGTSTTSSRNARRRESEKSLNETLNKEEDCHSPTSKPPKPDQPLKVMPPPPKENAWVKRSSN  
PPARSQSSDTEQQSPTSGGGKVAPAQPSSEEGPGRKDENKVDGMNAPKGQGTGNSSRGPGDGGNRDHWKESD  
RKDGKKDQDSRSAPPEPKPEENPASKFSSASKYAALSVDGEDENEGEDYAD

### Figure 5.2: Central Spindle Protein-Protein Interaction Network

Protein-protein interactions that occur during cytokinesis connecting the central spindle (tubulin) to the actomyosin ring are shown as lines between protein nodes. Proteins are indicated with their common names rather than official gene names. All interactions shown are verified *in vivo* interactions except for those between Plk1 and Rock1, Citron, and MYPT which are suggested in Chapter Two. Colors are consistent with Figure 2.6 with Aurora B and INCENP also in orange like Plk1 as central kinase regulators.



## References

1. Neef, R., Gruneberg, U., Kopajtich, R., Li, X., Nigg, E.A., Sillje, H., and Barr, F.A. (2007). Choice of Plk1 docking partners during mitosis and cytokinesis is controlled by the activation state of Cdk1. *Nat Cell Biol* 9, 436-444.
2. Neef, R., Preisinger, C., Sutcliffe, J., Kopajtich, R., Nigg, E.A., Mayer, T.U., and Barr, F.A. (2003). Phosphorylation of mitotic kinesin-like protein 2 by polo-like kinase 1 is required for cytokinesis. *J Cell Biol* 162, 863-875.
3. Stegmeier, F. (2004). Regulation of Mitotic Exit in *Saccharomyces cerevisiae*, Massachusetts Institute of Technology.
4. Georgi, A.B., Stukenberg, P.T., and Kirschner, M.W. (2002). Timing of events in mitosis. *Curr Biol* 12, 105-114.
5. Tang, Z., Shu, H., Qi, W., Mahmood, N.A., Mumby, M.C., and Yu, H. (2006). PP2A is required for centromeric localization of Sgo1 and proper chromosome segregation. *Dev Cell* 10, 575-585.
6. Riedel, C.G., Katis, V.L., Katou, Y., Mori, S., Itoh, T., Helmhart, W., Galova, M., Petronczki, M., Gregan, J., Cetin, B., Mudrak, I., Ogris, E., Mechtler, K., Pelletier, L., Buchholz, F., Shirahige, K., and Nasmyth, K. (2006). Protein phosphatase 2A protects centromeric sister chromatid cohesion during meiosis I. *Nature* 441, 53-61.
7. Kitajima, T.S., Sakuno, T., Ishiguro, K., Iemura, S., Natsume, T., Kawashima, S.A., and Watanabe, Y. (2006). Shugoshin collaborates with protein phosphatase 2A to protect cohesin. *Nature* 441, 46-52.
8. Alexandru, G., Uhlmann, F., Mechtler, K., Poupart, M.A., and Nasmyth, K. (2001). Phosphorylation of the cohesin subunit Scc1 by Polo/Cdc5 kinase regulates sister chromatid separation in yeast. *Cell* 105, 459-472.
9. Clarke, A.S., Tang, T.T., Ooi, D.L., and Orr-Weaver, T.L. (2005). POLO kinase regulates the *Drosophila* centromere cohesion protein MEI-S332. *Dev Cell* 8, 53-64.
10. Hornig, N.C., and Uhlmann, F. (2004). Preferential cleavage of chromatin-bound cohesin after targeted phosphorylation by Polo-like kinase. *Embo J* 23, 3144-3153.
11. Sumara, I., Vorlaufer, E., Stukenberg, P.T., Kelm, O., Redemann, N., Nigg, E.A., and Peters, J.M. (2002). The dissociation of cohesin from chromosomes in prophase is regulated by Polo-like kinase. *Mol Cell* 9, 515-525.

12. Lee, J.Y., Dej, K.J., Lopez, J.M., and Orr-Weaver, T.L. (2004). Control of centromere localization of the MEI-S332 cohesion protection protein. *Curr Biol* *14*, 1277-1283.
13. Wong, O.K., and Fang, G. (2005). Plx1 is the 3F3/2 kinase responsible for targeting spindle checkpoint proteins to kinetochores. *J Cell Biol* *170*, 709-719.
14. Ahonen, L.J., Kallio, M.J., Daum, J.R., Bolton, M., Manke, I.A., Yaffe, M.B., Stukenberg, P.T., and Gorbsky, G.J. (2005). Polo-like kinase 1 creates the tension-sensing 3F3/2 phosphoepitope and modulates the association of spindle-checkpoint proteins at kinetochores. *Curr Biol* *15*, 1078-1089.
15. Wilker, E.W., van Vugt, M.A., Artim, S.A., Huang, P.H., Petersen, C.P., Reinhardt, H.C., Feng, Y., Sharp, P.A., Sonenberg, N., White, F.M., and Yaffe, M.B. (2007). 14-3-3sigma controls mitotic translation to facilitate cytokinesis. *Nature* *446*, 329-332.
16. Yaffe, M.B., Rittinger, K., Volinia, S., Caron, P.R., Aitken, A., Leffers, H., Gamblin, S.J., Smerdon, S.J., and Cantley, L.C. (1997). The structural basis for 14-3-3:phosphopeptide binding specificity. *Cell* *91*, 961-971.
17. Elia, A.E., Rellos, P., Haire, L.F., Chao, J.W., Ivins, F.J., Hoepker, K., Mohammad, D., Cantley, L.C., Smerdon, S.J., and Yaffe, M.B. (2003). The molecular basis for phosphodependent substrate targeting and regulation of Plks by the Polo-box domain. *Cell* *115*, 83-95.
18. Elia, A.E., Cantley, L.C., and Yaffe, M.B. (2003). Proteomic screen finds pSer/pThr-binding domain localizing Plk1 to mitotic substrates. *Science* *299*, 1228-1231.
19. van Vugt, M.A., and Medema, R.H. (2005). Polo-like kinase-1: activity measurement and RNAi-mediated knockdown. *Methods Mol Biol* *296*, 355-369.
20. van de Weerd, B.C., and Medema, R.H. (2006). Polo-like kinases: a team in control of the division. *Cell Cycle* *5*, 853-864.
21. Barr, F.A., Sillje, H.H., and Nigg, E.A. (2004). Polo-like kinases and the orchestration of cell division. *Nat Rev Mol Cell Biol* *5*, 429-440.
22. Stegmeier, F., and Amon, A. (2004). Closing mitosis: the functions of the Cdc14 phosphatase and its regulation. *Annu Rev Genet* *38*, 203-232.
23. Visintin, R., Hwang, E.S., and Amon, A. (1999). Cfi1 prevents premature exit from mitosis by anchoring Cdc14 phosphatase in the nucleolus. *Nature* *398*, 818-823.

24. Yoshida, S., and Toh-e, A. (2002). Budding yeast Cdc5 phosphorylates Net1 and assists Cdc14 release from the nucleolus. *Biochem Biophys Res Commun* 294, 687-691.
25. Stegmeier, F., Visintin, R., and Amon, A. (2002). Separase, polo kinase, the kinetochore protein Slk19, and Spo12 function in a network that controls Cdc14 localization during early anaphase. *Cell* 108, 207-220.
26. Bardin, A.J., and Amon, A. (2001). Men and sin: what's the difference? *Nat Rev Mol Cell Biol* 2, 815-826.
27. Shou, W., Azzam, R., Chen, S.L., Huddleston, M.J., Baskerville, C., Charbonneau, H., Annan, R.S., Carr, S.A., and Deshaies, R.J. (2002). Cdc5 influences phosphorylation of Net1 and disassembly of the RENT complex. *BMC Mol Biol* 3, 3.
28. Visintin, R., Stegmeier, F., and Amon, A. (2003). The role of the polo kinase Cdc5 in controlling Cdc14 localization. *Mol Biol Cell* 14, 4486-4498.
29. Azzam, R., Chen, S.L., Shou, W., Mah, A.S., Alexandru, G., Nasmyth, K., Annan, R.S., Carr, S.A., and Deshaies, R.J. (2004). Phosphorylation by cyclin B-Cdk underlies release of mitotic exit activator Cdc14 from the nucleolus. *Science* 305, 516-519.
30. Yuan, K., Hu, H., Guo, Z., Fu, G., Shaw, A.P., Hu, R., and Yao, X. (2007). Phospho-regulation of HSCDC14A by polo-like kinase 1 is essential for mitotic progression. *J Biol Chem*.
31. Neutzner, M. (2003). Regulatoren des Zellteilungszyklus der Hefe *Saccharomyces cerevisiae*: die Polo-Kinase Cdc5 und der Ubiquitinierungsfaktor Hct1, Universität Stuttgart.
32. Wickner, R.B., Koh, T.J., Crowley, J.C., O'Neil, J., and Kaback, D.B. (1987). Molecular cloning of chromosome I DNA from *Saccharomyces cerevisiae*: isolation of the MAK16 gene and analysis of an adjacent gene essential for growth at low temperatures. *Yeast* 3, 51-57.
33. D'Aquino, K.E., Monje-Casas, F., Paulson, J., Reiser, V., Charles, G.M., Lai, L., Shokat, K.M., and Amon, A. (2005). The protein kinase Kin4 inhibits exit from mitosis in response to spindle position defects. *Mol Cell* 19, 223-234.
34. Yoshida, S., Ichihashi, R., and Toh-e, A. (2003). Ras recruits mitotic exit regulator Lte1 to the bud cortex in budding yeast. *J Cell Biol* 161, 889-897.

35. Jensen, S., Geymonat, M., Johnson, A.L., Segal, M., and Johnston, L.H. (2002). Spatial regulation of the guanine nucleotide exchange factor Lte1 in *Saccharomyces cerevisiae*. *J Cell Sci* 115, 4977-4991.
36. Nakajima, H., Toyoshima-Morimoto, F., Taniguchi, E., and Nishida, E. (2003). Identification of a consensus motif for Plk (Polo-like kinase) phosphorylation reveals Myt1 as a Plk1 substrate. *J Biol Chem* 278, 25277-25280.
37. Brar, G.A., Kiburz, B.M., Zhang, Y., Kim, J.E., White, F., and Amon, A. (2006). Rec8 phosphorylation and recombination promote the step-wise loss of cohesins in meiosis. *Nature* 441, 532-536.
38. Zhang, H., Shi, X., Paddon, H., Hampong, M., Dai, W., and Pelech, S. (2004). B23/nucleophosmin serine 4 phosphorylation mediates mitotic functions of polo-like kinase 1. *J Biol Chem* 279, 35726-35734.
39. Grisendi, S., Mecucci, C., Falini, B., and Pandolfi, P.P. (2006). Nucleophosmin and cancer. *Nat Rev Cancer* 6, 493-505.
40. Okuwaki, M., Tsujimoto, M., and Nagata, K. (2002). The RNA binding activity of a ribosome biogenesis factor, nucleophosmin/B23, is modulated by phosphorylation with a cell cycle-dependent kinase and by association with its subtype. *Mol Biol Cell* 13, 2016-2030.
41. Ma, Z., Kanai, M., Kawamura, K., Kaibuchi, K., Ye, K., and Fukasawa, K. (2006). Interaction between ROCK II and nucleophosmin/B23 in the regulation of centrosome duplication. *Mol Cell Biol* 26, 9016-9034.
42. Sato, K., Hayami, R., Wu, W., Nishikawa, T., Nishikawa, H., Okuda, Y., Ogata, H., Fukuda, M., and Ohta, T. (2004). Nucleophosmin/B23 is a candidate substrate for the BRCA1-BARD1 ubiquitin ligase. *J Biol Chem* 279, 30919-30922.
43. Bassermann, F., von Klitzing, C., Munch, S., Bai, R.Y., Kawaguchi, H., Morris, S.W., Peschel, C., and Duyster, J. (2005). NIPA defines an SCF-type mammalian E3 ligase that regulates mitotic entry. *Cell* 122, 45-57.
44. Bassermann, F., von Klitzing, C., Illert, A.L., Munch, S., Morris, S.W., Pagano, M., Peschel, C., and Duyster, J. (2007). Multisite Phosphorylation of Nuclear Interaction Partner of ALK (NIPA) at G2/M Involves Cyclin B1/Cdk1. *J Biol Chem* 282, 15965-15972.
45. van Vugt, M.A., and Medema, R.H. (2005). Getting in and out of mitosis with Polo-like kinase-1. *Oncogene* 24, 2844-2859.
46. Masai, H., You, Z., and Arai, K. (2005). Control of DNA replication: regulation and activation of eukaryotic replicative helicase, MCM. *IUBMB Life* 57, 323-335.



47. Takisawa, H., Mimura, S., and Kubota, Y. (2000). Eukaryotic DNA replication: from pre-replication complex to initiation complex. *Curr Opin Cell Biol* *12*, 690-696.
48. Tye, B.K. (1999). MCM proteins in DNA replication. *Annu Rev Biochem* *68*, 649-686.
49. DePamphilis, M.L. (2003). The 'ORC cycle': a novel pathway for regulating eukaryotic DNA replication. *Gene* *310*, 1-15.
50. Prasanth, S.G., Prasanth, K.V., and Stillman, B. (2002). Orc6 involved in DNA replication, chromosome segregation, and cytokinesis. *Science* *297*, 1026-1031.
51. Chesnokov, I.N., Chesnokova, O.N., and Botchan, M. (2003). A cytokinetic function of Drosophila ORC6 protein resides in a domain distinct from its replication activity. *Proc Natl Acad Sci U S A* *100*, 9150-9155.
52. Stuermer, A., Hoehn, K., Faul, T., Auth, T., Brand, N., Kneissl, M., Putter, V., and Grummt, F. (2007). Mouse pre-replicative complex proteins colocalise and interact with the centrosome. *Eur J Cell Biol* *86*, 37-50.
53. Prasanth, S.G., Prasanth, K.V., Siddiqui, K., Spector, D.L., and Stillman, B. (2004). Human Orc2 localizes to centrosomes, centromeres and heterochromatin during chromosome inheritance. *Embo J* *23*, 2651-2663.
54. Cuvier, O., Lutzmann, M., and Mechali, M. (2006). ORC is necessary at the interphase-to-mitosis transition to recruit cdc2 kinase and disassemble RPA foci. *Curr Biol* *16*, 516-523.
55. Tsvetkov, L., and Stern, D.F. (2005). Interaction of chromatin-associated Plk1 and Mcm7. *J Biol Chem* *280*, 11943-11947.
56. Ishimi, Y., Komamura-Kohno, Y., Kwon, H.J., Yamada, K., and Nakanishi, M. (2003). Identification of MCM4 as a target of the DNA replication block checkpoint system. *J Biol Chem* *278*, 24644-24650.
57. Matsumura, F. (2005). Regulation of myosin II during cytokinesis in higher eukaryotes. *Trends Cell Biol* *15*, 371-377.
58. Nelson, B., Kurischko, C., Horecka, J., Mody, M., Nair, P., Pratt, L., Zougman, A., McBroom, L.D., Hughes, T.R., Boone, C., and Luca, F.C. (2003). RAM: a conserved signaling network that regulates Ace2p transcriptional activity and polarized morphogenesis. *Mol Biol Cell* *14*, 3782-3803.

59. Gruneberg, U., Neef, R., Li, X., Chan, E.H., Chalamalasetty, R.B., Nigg, E.A., and Barr, F.A. (2006). KIF14 and citron kinase act together to promote efficient cytokinesis. *J Cell Biol* *172*, 363-372.
60. Goto, H., Yasui, Y., Kawajiri, A., Nigg, E.A., Terada, Y., Tatsuka, M., Nagata, K., and Inagaki, M. (2003). Aurora-B regulates the cleavage furrow-specific vimentin phosphorylation in the cytokinetic process. *J Biol Chem* *278*, 8526-8530.
61. Yamaguchi, T., Goto, H., Yokoyama, T., Sillje, H., Hanisch, A., Uldschmid, A., Takai, Y., Oguri, T., Nigg, E.A., and Inagaki, M. (2005). Phosphorylation by Cdk1 induces Plk1-mediated vimentin phosphorylation during mitosis. *J Cell Biol* *171*, 431-436.
62. Liu, X., Zhou, T., Kuriyama, R., and Erikson, R.L. (2004). Molecular interactions of Polo-like-kinase 1 with the mitotic kinesin-like protein CHO1/MKLP-1. *J Cell Sci* *117*, 3233-3246.
63. Lee, K.S., Yuan, Y.L., Kuriyama, R., and Erikson, R.L. (1995). Plk is an M-phase-specific protein kinase and interacts with a kinesin-like protein, CHO1/MKLP-1. *Mol Cell Biol* *15*, 7143-7151.
64. Guse, A., Mishima, M., and Glotzer, M. (2005). Phosphorylation of ZEN-4/MKLP1 by aurora B regulates completion of cytokinesis. *Curr Biol* *15*, 778-786.
65. Minoshima, Y., Kawashima, T., Hirose, K., Tonozuka, Y., Kawajiri, A., Bao, Y.C., Deng, X., Tatsuka, M., Narumiya, S., May, W.S., Jr., Nosaka, T., Semba, K., Inoue, T., Satoh, T., Inagaki, M., and Kitamura, T. (2003). Phosphorylation by aurora B converts MgcRacGAP to a RhoGAP during cytokinesis. *Dev Cell* *4*, 549-560.
66. Goto, H., Kiyono, T., Tomono, Y., Kawajiri, A., Urano, T., Furukawa, K., Nigg, E.A., and Inagaki, M. (2006). Complex formation of Plk1 and INCENP required for metaphase-anaphase transition. *Nat Cell Biol* *8*, 180-187.
67. Straight, A.F., Field, C.M., and Mitchison, T.J. (2005). Anillin binds nonmuscle myosin II and regulates the contractile ring. *Mol Biol Cell* *16*, 193-201.
68. Zhao, W.M., and Fang, G. (2005). Anillin is a substrate of anaphase-promoting complex/cyclosome (APC/C) that controls spatial contractility of myosin during late cytokinesis. *J Biol Chem* *280*, 33516-33524.
69. Guarguaglini, G., Duncan, P.I., Stierhof, Y.D., Holmstrom, T., Duensing, S., and Nigg, E.A. (2005). The forkhead-associated domain protein Cep170 interacts with Polo-like kinase 1 and serves as a marker for mature centrioles. *Mol Biol Cell* *16*, 1095-1107.



70. Fabbro, M., Zhou, B.B., Takahashi, M., Sarcevic, B., Lal, P., Graham, M.E., Gabrielli, B.G., Robinson, P.J., Nigg, E.A., Ono, Y., and Khanna, K.K. (2005). Cdk1/Erk2- and Plk1-dependent phosphorylation of a centrosome protein, Cep55, is required for its recruitment to midbody and cytokinesis. *Dev Cell* 9, 477-488.
71. Litvak, V., Argov, R., Dahan, N., Ramachandran, S., Amarilio, R., Shainskaya, A., and Lev, S. (2004). Mitotic phosphorylation of the peripheral Golgi protein Nir2 by Cdk1 provides a docking mechanism for Plk1 and affects cytokinesis completion. *Mol Cell* 14, 319-330.
72. Zhou, T., Aumais, J.P., Liu, X., Yu-Lee, L.Y., and Erikson, R.L. (2003). A role for Plk1 phosphorylation of NudC in cytokinesis. *Dev Cell* 5, 127-138.
73. Zhang, Y., Tian, Y., Chen, Q., Chen, D., Zhai, Z., and Shu, H.B. (2007). TTDN1 is a Plk1-interacting protein involved in maintenance of cell cycle integrity. *Cell Mol Life Sci* 64, 632-640.
74. Cousins-Wasti, R.C., Ingraham, R.H., Morelock, M.M., and Grygon, C.A. (1996). Determination of affinities for Ick SH2 binding peptides using a sensitive fluorescence assay: comparison between the pYEEIP and pYQQP consensus sequences reveals context-dependent binding specificity. *Biochemistry* 35, 16746-16752.
75. Durocher, D., Taylor, I.A., Sarbassova, D., Haire, L.F., Westcott, S.L., Jackson, S.P., Smerdon, S.J., and Yaffe, M.B. (2000). The molecular basis of FHA domain:phosphopeptide binding specificity and implications for phospho-dependent signaling mechanisms. *Mol Cell* 6, 1169-1182.
76. Jang, Y.J., Ma, S., Terada, Y., and Erikson, R.L. (2002). Phosphorylation of threonine 210 and the role of serine 137 in the regulation of mammalian polo-like kinase. *J Biol Chem* 277, 44115-44120.
77. Lee, K.S., and Erikson, R.L. (1997). Plk is a functional homolog of *Saccharomyces cerevisiae* Cdc5, and elevated Plk activity induces multiple septation structures. *Mol Cell Biol* 17, 3408-3417.
78. Qian, Y.W., Erikson, E., and Maller, J.L. (1998). Purification and cloning of a protein kinase that phosphorylates and activates the polo-like kinase Plx1. *Science* 282, 1701-1704.
79. Mundt, K.E., Golsteyn, R.M., Lane, H.A., and Nigg, E.A. (1997). On the regulation and function of human polo-like kinase 1 (PLK1): effects of overexpression on cell cycle progression. *Biochem Biophys Res Commun* 239, 377-385.

80. Jang, Y.J., Lin, C.Y., Ma, S., and Erikson, R.L. (2002). Functional studies on the role of the C-terminal domain of mammalian polo-like kinase. *Proc Natl Acad Sci U S A* 99, 1984-1989.
81. Kelm, O., Wind, M., Lehmann, W.D., and Nigg, E.A. (2002). Cell cycle-regulated phosphorylation of the *Xenopus* polo-like kinase Plx1. *J Biol Chem* 277, 25247-25256.
82. Tang, J., Erikson, R.L., and Liu, X. (2006). Ectopic Expression of Plk1 Leads to Activation of the Spindle Checkpoint. *Cell Cycle* 5.

# Appendix One

## **Tandem BRCT Domains Function as Phosphopeptide Binding Modules and Control the DNA Damage Responsive Functions of BRCA1**

Portions Published In:

Isaac A. Manke, Drew M. Lowery, Ancho Nguyen, and Michael B. Yaffe.  
BRCT repeats as phosphopeptide-binding modules involved in protein targeting.  
*Science* 302, 2003.

and

Julie A. Clapperton, Isaac A. Manke, Drew M. Lowery, Timmy Ho, Leslie F. Haire,  
Michael B. Yaffe, and Stephen J. Smerdon.  
Structure and mechanism of BRCA1 BRCT domain recognition of phosphorylated  
BACH1 with implications for cancer. *Nat Struct Mol Biol* 11, 2004.

### Contributions:

Isaac was the lead organizer of the project and performed all experiments not otherwise explicitly mentioned. Katja Hoepker assisted Isaac in performing the original screen shown in figure A1.1A. Ancho helped to generate the localization data shown in figures A1.10-11. Julie along with Steve and Michael generated the crystals, solved the crystal structure, performed some of the ITC, and made the figures involving the structure. Timmy Ho helped with BRCT domain protein and DNA production. Irma Rangel-Alarcon performed the peptide binding experiment shown in figure A1.8A. Christian Reinhardt helped me with the experiment in Figure A1.12. I cloned nearly all of the tandem BRCT and mutant BRCA1 constructs, performed all western blotting in collaboration with Isaac, helped with protein production, helped generate the data in figures A1.3, A1.12, and A1.13, assisted with IVT pulldown experiments, analyzed data and decided on direction in collaboration with Isaac, participated in writing the manuscripts, and made the figures involving western blotting.

## Abstract

We used a proteomic approach to identify phosphopeptide-binding modules mediating signal transduction events in the DNA damage response pathway. Using a library of partially degenerate phosphopeptides biased to resemble the phosphorylation motif of the phosphatidylinositol 3-kinase-related kinase (PIKK) family members, ataxia-telangiectasia-mutated (ATM), ataxia-telangiectasia- and RAD3-related (ATR), we identified tandem BRCA1 carboxy-terminal (BRCT) domains in Pax transactivation domain-interacting protein (PTIP) and BRCA1 as phosphoserine (pSer)- or phosphothreonine (pThr)-specific binding modules that recognize a subset of substrates phosphorylated by the PIKKs in response to  $\gamma$ -irradiation (IR). These interactions direct the localization of the tandem BRCT domains to foci in response to IR. Furthermore, we report the 1.85Å X-ray crystal structure of the Brca1 tandem BRCT domains in complex with a phosphorylated peptide representing the minimal interacting region of the DEAH-box helicase Bach1. Germline mutations in the tandem BRCT domains of the Brca1 tumor suppressor often result in a significant increase in susceptibility to breast and ovarian cancers, and we show that a subset of disease-linked mutations appear to act through specific disruption of phospho-dependent Brca1 interactions.

## Introduction

Signal transduction by protein kinases in eukaryotes results in the directed assembly of multi-protein complexes at specific locations within the cell [1]. This process is particularly evident following DNA damage, where activation of DNA damage response kinases results in the formation of protein-protein complexes at discrete foci within the nucleus [2]. In many cases, kinases directly control the formation of these multi protein complexes by generating specific phosphorylated-motif sequences; modular binding domains then recognize these short phospho-motifs to mediate protein-protein interactions [3, 4]. We used a proteomic screening approach [5] to identify novel modular pSer- or pThr-binding domains involved in the DNA damage response, and found that BRCT (Brca1 C-terminal) domains function downstream of DNA damage dependent protein kinases.

The original gene found to contain tandem BRCT domains is the breast-cancer susceptibility gene product, Brca1, which plays important roles in cell cycle control, transcriptional regulation, chromatin remodeling, and the response to DNA-damage [6-9]. Brca1 is a large, modular protein of 1863 amino-acid residues containing an N-terminal RING domain, a central region rich in SQ/TQ dipeptide pairs, and the tandem BRCT domains at its C-terminus (Figure A1.1C). Brca1 interacts with a large number of protein partners at different stages of the cell cycle, or following genotoxic stress. For example, Brca1 interacts with the DNA helicase BACH1 during S and G2 in normally cycling cells [10, 11], whereas Brca1 interacts with a subset of ATM/ATR substrates in response to DNA damage (Figure A1.4B,D). In both S-phase and irradiated/mutagen-treated cells, Brca1 localizes to distinct nuclear foci thought to represent sites of DNA-damage [12, 13] where Brca1 is thought to function, at least in part, as a scaffold for the assembly of DNA-repair complexes.

Mutations in Brca1 occur in 50% of women with inherited breast cancer and up to 90% of women with combined breast and ovarian cancer [14-17]. Most frameshift and deletion mutants truncate all or part of the BRCT repeats, while more than 70 missense mutations lie within the BRCT domains themselves (<http://research.nhgri.nih.gov/projects/bic/>). BRCT domains occur singly or as multiple

repeats in a number of proteins in addition to Brca1 that are involved in cell-cycle regulation and DNA-damage responses [18, 19]. Comprised of 80–100 amino acids, BRCT domains are generally thought to function as protein-protein recognition modules [19]. The molecular basis underlying Brca1 BRCT function, and how cancer-causing mutations in the BRCT domains act at the structural level, however, remains unresolved, despite significant structural, biochemical, and mutagenic analysis [19-23]. It has been suggested that mutational effects are manifested through structural destabilization, however a number of mutations are located on the protein surface, indicating that they may specifically affect BRCT interactions with other Brca1-associated targets.

We present here the identification of BRCT domain containing proteins as phosphorylation dependent binding partners of DNA damage responsive proteins downstream of DNA damage dependent kinases. To determine the structural basis for phosphopeptide binding and phosphopeptide-motif selection, and investigate alternative structural mechanisms underlying Brca1 BRCT mutations and cancer predisposition, we solved the high resolution X-ray crystal structure of the Brca1 tandem BRCT repeats bound to a Bach1 phosphopeptide. We show that a set of cancer-associated Brca1 BRCT mutations eliminate phosphopeptide binding *in vitro* and Bach1 phosphoprotein binding *in vivo*, or alter the phosphopeptide recognition motif for the Brca1 tandem BRCT domains, revealing a molecular and structural basis for mutation-associated loss of Brca1 function.

## Results

### Identification of tandem BRCT domains as phosphopeptide binding modules

We used a proteomic screening approach [5] to identify novel modular pSer- or pThr-binding domains involved in the DNA damage response. In cells exposed to IR, the PIKK family members phosphorylate transcription factors, DNA repair proteins, protein kinases, and scaffolds on Ser-Gln and Thr-Gln motifs [24]. We therefore constructed an oriented peptide library biased to resemble the motif generated by ATM and ATR [25, 26] (Figure A1.1 legend and methods). The phosphorylated and non-phosphorylated peptide libraries were immobilized and screened against approximately 96,000 in vitro translated (IVT) polypeptides (960 pools each encoding ~ 100 transcripts) over a 10-week period in a high-throughput approach. The majority of IVT products either failed to bind to either of the immobilized peptide libraries or bound slightly better to the non-phosphorylated control (Figure A1.1A). Several pools, however, contained cDNAs encoding proteins that bound preferentially to the (pSer or pThr)-Gln library.

Pool EE11 contained the strongest phosphopeptide-binding clone, EE11-9, which encoded the C-terminal 70% of human PTIP (Figure A1.1B). PTIP was originally identified as a transcriptional control protein although later data suggests that PTIP also appears to also play a critical role in the DNA damage response pathway [27-29]. Human PTIP contains at least 4 BRCT domains, known protein-protein interaction modules present in many DNA damage response and cell cycle checkpoint proteins [19]. Unfortunately the PTIP clone used throughout this study and referred to as full length PTIP is not actually the entire protein. Subsequent to the completion of this work it was recognized that PTIP is a much longer protein with an extended N-terminus that possibly contains another two BRCT domains. A series of deletion constructs was generated and analyzed for the minimal phosphopeptide-specific binding region (Figure A1.1B). A construct containing only the tandem 3<sup>rd</sup> and 4<sup>th</sup> BRCT domains displayed strong and specific binding to the (pSer or pThr)-Gln library. Constructs of PTIP lacking both of these domains failed to bind or lacked phospho-discrimination. Furthermore, neither the 3<sup>rd</sup> or 4<sup>th</sup> BRCT domains alone bound to phosphopeptides, suggesting that the PTIP

tandem C-terminal BRCT pair functions as a single module that is necessary and sufficient for phospho-specific binding.

BRCT domains are often found in tandem pairs, or multiple copies of tandem pairs, and the tandem BRCA1 BRCT domains behave as a single stable domain ((BRCT)<sub>2</sub>) [20]. To investigate whether (pSer or pThr)-binding is a general feature of (BRCT)<sub>2</sub> domains, we screened (BRCT)<sub>2</sub> domains from a number of other DNA damage response proteins (Figure A1.2A). Like those in PTIP, the BRCA1-(BRCT)<sub>2</sub> domain showed phospho-specific binding and individual BRCA1 BRCT domains were insufficient for phospho-specific interactions. Phospho-specific binding by the (BRCT)<sub>2</sub> domains of MDC1, 53BP1, or the PTIP N-terminal pair was not observed, and only a low amount of phospho-specific binding for *S. cerevisiae* RAD9 was detected, suggesting that the phosphopeptide-binding function is present in only a subset of (BRCT)<sub>2</sub> domains.

We used oriented peptide library screening to determine the optimal phospho-binding motifs for the C-terminal (BRCT)<sub>2</sub> domains of PTIP and BRCA1 (Figure A1.2B and Table A1.1) [30]. PTIP- and BRCA1-(BRCT)<sub>2</sub> displayed strongest binding to similar, but not identical, motifs with extremely strong selection for either aromatic or aliphatic residues, and aromatic residues only, respectively, in the (pSer or pThr)+3 position when screened with a (pSer or pThr)-Gln library. Prominent amino acid selection was also observed in the (pSer or pThr)+2 and +5 positions, with more moderate selection at other positions. We investigated the relative importance of Gln in the (pSer or pThr)+1 position, since this residue is critical for ATM and ATR phosphorylation, using individual pSer-, pThr- and (pSer-X-X-Phe)-oriented peptide libraries. This revealed selection for Gln, Ile, Phe, and Tyr in the degenerate +1 position. Furthermore, the absence of a Gln in the +1 position reduced the selection for aromatic and aliphatic residues in the +3 and +5 positions, suggesting that although Gln in the (pSer or pThr)+1 position was not essential, it is a favored residue.

We defined an optimal (BRCT)<sub>2</sub> domain-binding peptide (BRCTide) as Y-D-I-(pSer or pThr)-Q-V-F-P-F. Isothermal titration calorimetry showed that the optimal phosphoserine-containing peptide bound to the C-terminal (BRCT)<sub>2</sub> domain of PTIP with a dissociation constant of 280 nM, and to the (BRCT)<sub>2</sub> domain of BRCA1 with a dissociation constant of 540 nM (Table A1.2). Replacement of pThr for pSer reduced the



affinity of the peptide for the PTIP- and BRCA1-(BRCT)<sub>2</sub> domains by a factor of ~7 and substitution of Ser or Thr for pSer abrogated binding altogether. To further verify motif selection, binding of the PTIP- and BRCA1-(BRCT)<sub>2</sub> domains to a solid-phase array of immobilized phosphopeptides was performed in which each amino acid flanking the pThr-Gln or the pSer core in the optimal BRCTtide was varied (Figure A1.3). The resulting selectivities were generally consistent with the results obtained using oriented peptide libraries in solution and confirmed the importance of the (pSer or pThr) +3 position in (BRCT)<sub>2</sub> domain binding.

To examine the role of (BRCT)<sub>2</sub> domains in binding to proteins phosphorylated by ATM and ATR, lysates from U2OS cells that had been treated with 10 Gy IR or mock treated were incubated with GST-(BRCT)<sub>2</sub> fusion proteins. Bound proteins were detected by immunoblotting with an antibody to the (pSer or pThr)-Gln motif generated by ATM and ATR (Cell Signaling Technologies) (Figure A1.4). After IR, both PTIP- and BRCA1-(BRCT)<sub>2</sub> domains interact with different phospho-proteins, despite similar phospho-peptide recognition motifs. The PTIP-(BRCT)<sub>2</sub> phospho-protein interactions are inhibited by incubating the (BRCT)<sub>2</sub> domains with a (pSer or pThr)-Gln peptide library, but not with a pThr-Pro library or the non-phosphorylated (Ser or Thr)-Gln library (Figure A1.4A). Binding of both PTIP- and BRCA1-(BRCT)<sub>2</sub> domains to phospho-proteins was largely eliminated by treatment of the cells with caffeine to inhibit the activity of ATM and ATR[31] and by the BRCTtide but not by the non-phosphorylated analogue (Figure A1.4B and A1.4D).

In response to IR, the DNA damage protein 53BP1 undergoes phosphorylation by ATM and facilitates the ability of ATM to phosphorylate additional cellular substrates [32-34]. Endogenous 53BP1 from U2OS cell lysates bound to the C-terminal PTIP-(BRCT)<sub>2</sub> domain only in lysates from cells treated with IR (Figure A1.4C). Binding was inhibited by the optimal BRCTtide but not by its non-phosphorylated counterpart. Binding was also eliminated by incubation of the (BRCT)<sub>2</sub> domain with the (pSer or pThr)-Gln peptide library, but not by pre-incubation with a pThr-Pro library or the non-phosphorylated (Ser or Thr)-Gln library, and binding was also eliminated in cells treated with caffeine before IR, or in lysates treated with λ-phosphatase after irradiation.

## Structure of the Brca1 BRCT:Bach1 Phosphopeptide Complex

BRCA1-(BRCT)<sub>2</sub> domains bound to the interacting phosphopeptide from BACH1 (residues 986–995) were crystallized and the structure solved at 1.85Å resolution by X-ray diffraction (Figure A1.5A,B). Phases were determined by molecular replacement using the previously determined structure of the un-liganded BRCA1-(BRCT)<sub>2</sub> domains (PDB ID 1JNX) as a search model [20], (Table A1.1 and Methods). Difference Fourier maps revealed well-defined electron density for the phosphopeptide allowing modeling of eight residues corresponding to Bach1 Ser 988 – Lys 995. Each BRCT repeat forms a compact domain (Figure A1.5A) in which a central, four-stranded beta-sheet is packed against two helices,  $\alpha$ 1 and  $\alpha$ 3, on one side and a single helix,  $\alpha$ 2 on the other. The two domains pack together through interaction between  $\alpha$ 2 of BRCT1 and the  $\alpha$ 1'/ $\alpha$ 3' pair of BRCT2. A linker region connecting the two BRCT domains contains a  $\beta$ -hairpin-like structure  $\beta$ L and a short helical region,  $\alpha$ L, that forms part of the interface through interactions with  $\alpha$ 2 of BRCT1 and the N-terminal end of  $\alpha$ 3' from BRCT2. Overall, the structure of the BRCA1-(BRCT)<sub>2</sub> domains:phosphopeptide complex is similar to that of the un-liganded domains (rmsd  $\sim$  0.4Å for all C $\alpha$  atoms). However, superposition of the individual BRCT repeats reveals that phosphopeptide-binding is associated with a slight relative rotation of each BRCT domain and a translation of BRCT1 helix  $\alpha$ 1 towards the cleft between the domains.

The Bach1 phosphopeptide binds in an extended conformation to a groove located at the highly conserved interface between the N- and C-terminal BRCT domains (Figures A1.5A and A1.6A), consistent with the requirement of both domains for efficient phosphopeptide binding [35, 36]. This mode of binding is distinct from that observed in the phospho-independent interaction between p53 and the 53BP-1-(BRCT)<sub>2</sub> domains, which occurs primarily through the linker region [37, 38]. Our structure clearly shows that the phospho-dependent interactions that are necessary and sufficient for formation of the Bach1/Brca1 complex occur on the opposite side of the BRCT-BRCT interface from those involved in the p53:53BP-1 interaction.

BRCA1-(BRCT)<sub>2</sub> domains binding to library-selected peptides *in vitro* [35, 36], and to phosphorylated Bach1 *in vivo* [11] is dominated by the presence of a

phosphoserine/threonine and a phenylalanine three residues C-terminal to it (Phe +3). This is now confirmed by our structure which shows that the Bach1 pSer 990 phosphate moiety binds to a basic pocket through three direct hydrogen-bonding interactions involving the side chains of Ser 1655 and Lys 1702, and the main-chain NH of Gly 1656 (Figure A1.7A). All three of these residues are located in BRCT1 and all are absolutely conserved in Brca1 homologues. Ser 1655 and Gly 1656 are situated within the loop preceding  $\alpha$ 1 and are brought into proximity with the phosphate moiety as a result of a conformational change in the loop that occurs upon phosphopeptide binding. Intriguingly, a S1655F mutation has been identified in a single breast cancer patient, although its link to disease has not been confirmed. In addition to these direct interactions, the phosphate, and some peptide main-chain atoms are also tethered through a highly organized network of water molecules, many of which are tetrahedrally hydrogen bonded (Figure A1.7A). Indirect protein-solvent-phosphate contacts are unusual in phospho-dependent protein-protein interactions but have been observed previously in structures of phosphopeptide complexes of the human Plk1 Polo-box domain [39, 40].

The Phe +3 peptide side-chain fits into a hydrophobic pocket at the BRCT interface consisting of the side chains of Phe 1704, Met 1775 and Leu 1839 contributed from both BRCT domains (Figures A1.7A and A1.8A). This finding rationalizes the strong selection for aromatic amino acids in the +3 position of the binding motif seen in peptide library experiments [35, 36], as well as the observation of Yu et al that mutation of Phe 993 to Ala eliminates Brca1:Bach1 binding [11]. Additional hydrogen-bonds with the main-chain N and C=O atoms of Phe +3 are supplied by main- and side-chain atoms from Arg 1699, a site of mutation also associated with cancer predisposition. The phosphorylated Ser 990 of Bach1 is preceded by an Arg residue in the -3 position and followed by a proline residue in the +1 position, suggesting potential Ser 990 phosphorylation by either basophilic and/or proline-directed kinases. BRCA1-(BRCT)<sub>2</sub> domains are also known to interact with pSQ-containing motifs characteristic of PI 3-kinase-like kinases such as ATM and ATR (Figure A1.4B,D). In the tandem BRCT:Bach1 phosphopeptide co-crystal structure, there are no direct interactions between the +1 Pro side chain and the BRCT domains. Instead, this residue participates in only a single water-mediated hydrogen bond involving its carbonyl oxygen (Figure

A1.7A), consistent with the idea that various types of protein kinases can generate tandem BRCT phospho-binding motifs. The Lys +5 side chain makes two salt-bridging interactions with residues in BRCT2 (Figure A1.7A), consistent with the Lys selection observed in this position by spot blot and peptide library experiments [35, 36].

### **Cancer-Associated Brca1 BRCT Mutations**

Residues that form or stabilize the phosphopeptide binding surface, and the domain-domain interface, are among the most highly conserved portions of the molecule in Brca1 orthologs from humans, primates, rats and mice (Figure A1.6A). Interestingly, these regions correlate strongly with the location of cancer-associated mutations (Figure A1.6B). Some cancer-associated mutations may disrupt the global BRCT fold while others are more likely to specifically interfere with ligand binding [19, 21-23, 37]. Approximately 80 tumor-derived mutations have been identified within the BRCA1-(BRCT)<sub>2</sub> domains, though only a few of these have been subsequently confirmed to result in cancer predisposition, including D1692Y, C1697R, R1699W, A1708E, S1715R, G1738E, P1749R, M1775R, 5382InsC (a frameshift mutation that results in a stop codon at position 1829), and Y1853X (which truncates the last 11 residues). Most of these cluster at or near the phosphopeptide-interacting surface (Figure A1.6B). Two of these mutated residues, Arg 1699 and Met 1775, directly interact with residues in the phosphopeptide (Figure A1.7A). Two others, Pro 1749 and Gly 1738, are located at the BRCT1/BRCT2 interface beneath the molecular surface and their effects are likely to be mediated through alterations in the relative orientation of the tandem BRCT motifs that our structure suggests is necessary for phospho-dependent interactions with partner proteins.

To verify the phosphoserine phosphate interactions observed in the X-ray structure and to investigate the effects of the most common tumor-derived point mutations, we investigated the binding of a panel of site-directed mutant BRCA1-(BRCT)<sub>2</sub> domains to the interacting region of Bach1. Binding was determined by measuring the ability of in vitro transcribed and translated proteins to bind to either phosphorylated and non-phosphorylated biotinylated peptides (Figure A1.7B). Wild-type

BRCA1-(BRCT)<sub>2</sub> domains clearly bind to phosphorylated but not non-phosphorylated peptides, while mutation of the conserved Ser 1655 and Lys 1702, alone or in combination, completely abolished the interaction. Five bona fide cancer-linked mutations, P1749R, G1738E, M1775R, Y1853X and 5382InsC all result in complete loss of phosphopeptide binding. A mutation R1699W is cancer-linked and a second, R1699Q, has been detected in breast cancer patients but has not yet been directly related to disease-predisposition. We surmised that the glutamine side-chain might still participate in main-chain hydrogen bonding to the peptide and this is, indeed, the only BRCA1-(BRCT)<sub>2</sub> domains mutant that retained a small degree of binding in our assays. Somewhat surprisingly, however, the R1699Q mutant largely loses phospho-specificity, and instead bound to both phosphorylated and non-phosphorylated peptides.

To investigate the *in vivo* binding of cancer-predisposing mutant BRCA1-(BRCT)<sub>2</sub> domains to endogenous Bach1, we transfected U2OS cells with a vector encoding the C-terminal 550 amino acids of Brca1 containing a myc tag and an SV40 nuclear localization sequence as described by Chen et al [41]. As shown in Figure A1.7C, interaction between the wild type BRCA1-(BRCT)<sub>2</sub> domains with full-length Bach1 was easily detected. In contrast, no *in vivo* interaction was observed between Bach1 and mutant BRCA1-(BRCT)<sub>2</sub> domains that disrupt phosphate-binding or predispose to breast and ovarian cancer. All of these cancer-associated mutant proteins were expressed at comparable levels when transfected into mammalian cells [42] (Figure A1.7C).

Subsequently we generated two other BRCA1 cancer associated mutations (D1692Y and R1751Q) that did not act the same as the previous mutations in the IVT-pulldown or Bach1 co-immunoprecipitation experiment. Both proteins showed phospho-specific binding to the pSXXF and pS peptide libraries that were described in Figure A1.2A (Figure A1.8A), and interacted with Bach1 (Figure A1.8B). In all cases the interactions were weaker than that seen with the wild-type BRCA1-(BRCT)<sub>2</sub> domains, but significant based on a complete lack of interaction seen with the M1775R and S1655A/K1702M negative controls. In addition we tested the R1699Q mutant with these peptide libraries, and saw weak phospho-specific binding to the pS library though as before this mutant failed to interact with Bach1 (Figure A1.8A,B). This data shows that not every cancer-associated BRCA1-(BRCT)<sub>2</sub> domains has lost its phosphobinding

activity, and there must be some other reason that these mutations predispose women to breast and ovarian cancer. One explanation is that these mutations, as well as many of the previously tested ones, may be intrinsically unstable [20, 21, 43]. However, we observed equal expression of our wild-type and mutant BRCA1-(BRCT)<sub>2</sub> domains constructs in both in vitro translation and overexpression in tissue culture cells systems (Figure A1.8 A,B), in agreement with a previous study [42]. Alternatively these mutants that retain phosphopeptide binding may disrupt other interaction surfaces on Brca1 not required for phosphopeptide binding [19].

Interpretation of the structural effects of the M1775R mutation is simplified since the X-ray crystal structure of the M1775R BRCA1-(BRCT)<sub>2</sub> domains mutant has been determined (PDB ID 1N5O) [21], revealing a nearly identical structure as the wild-type protein with an average rmsd of 0.35 Å for all C $\alpha$  atoms. Superposition of the mutant structure with that of our Bach1 complex shows that the guanidine portion of the substituent arginine side-chain extrudes into the tandem BRCT cleft, where it occupies the binding site for the essential Phe +3 of the phosphopeptide (Figure A1.9A, B). In this case, loss of phosphopeptide-binding in vitro and Bach1 binding in vivo appear to be attributable to the severe steric clash of the Arg 1775 side-chain with an important determinant of phosphopeptide specificity and affinity. The M1775R mutant protein does, however, bind weakly to a BACH1 phosphopeptide in which the +3 Phe is mutated to Asp or Glu (Figure A1.9C). This is consistent with the introduction of a basic residue at the pSer +3 binding site (Figure A1.6B) and with the observation that this mutation creates new anion binding sites in the M1775R crystal structure [21]. Thus, in addition to disrupting the native Brca1:BACH1 interaction, this mutation may also result in the formation of inappropriate BRCA1-(BRCT)<sub>2</sub> domains interactions.

### **Phosphopeptide-Binding and Nuclear Foci Formation**

The binding of the PTIP-(BRCT)<sub>2</sub> domain to ATM and ATR phosphorylated proteins could localize PTIP at sites of DNA damage in vivo. To investigate this, we transfected U2OS cells with GFP fusions of full-length PTIP, PTIP lacking the C-terminal (BRCT)<sub>2</sub> domain, or the C-terminal (BRCT)<sub>2</sub> domain (Figure A1.10). In the

absence of DNA damage, PTIP was diffusely nuclear with a small amount of cytosolic staining. Two hours after IR, PTIP re-localized into discrete nuclear foci that co-localized with (pSer or pThr)-Gln phosphoepitopes, 53BP1 and  $\gamma$ -H2AX (Figure A1.10A). PTIP from which the C-terminal (BRCT)<sub>2</sub> domain was deleted, was not predominantly detected in the (pSer or pThr)-Gln and 53BP1 foci after IR (Figure A1.10B). However, the fragment containing the C-terminal (BRCT)<sub>2</sub> domain, was nuclear and formed minor amounts of foci in the absence of DNA damage, but re-localized into prominent nuclear foci that co-localized with 53BP1 after IR (Figure A1.10C). Further supporting the role of ATM and ATR in PTIP localization, caffeine treatment prior to IR reduced the full-length PTIP foci formation (Figure A1.11).

Subcellular localization and nuclear foci formation by the wild type, S1655A/K1702M phosphopeptide-binding mutant and the M1775R cancer-associated mutant BRCA1-(BRCT)<sub>2</sub> domains were studied before and after DNA damage in unsynchronized U2OS cells (Figure A1.12). To maximize visualization of nuclear foci, the cells were permeabilized with buffers containing 0.5% Triton X-100 prior to fixation and immunostaining [44]. In un-extracted cells the wild-type BRCT domains and both of the mutant BRCT proteins showed equivalent diffuse nuclear localization. Extraction of the un-irradiated cells prior to fixation resulted in near complete loss of BRCT domain staining in all cases (Figure A1.12A). Under these conditions, less than 5% of the wild-type and M1775R tandem BRCT-containing cells displayed 5 or more nuclear foci, and no foci were observed with the S1655A/K1702M double mutant. When the cells were irradiated with 10 Gy of  $\gamma$ -irradiation, and 2 hrs later permeabilized, fixed, and stained, nearly all of the cells containing the wild-type Brca1 tandem BRCT domains demonstrated sharp punctate nuclear foci that largely co-localized with the staining pattern of an anti-pSer/pThr-Gln epitope antibody that recognizes ATM- and ATR-phosphorylated substrates (Figure A1.12B). In contrast, the S1655A/K1702M mutant protein displayed only faint staining with a very fine granular pattern that completely failed to co-localize with pSer/pThr-Gln staining. This failure of foci formation and pSer/pThr-Gln co-localization is strong evidence that the phospho-binding function of the Brca1 tandem BRCT domains is critical for normal subcellular localization following DNA damage. The M1775R mutant protein that binds weakly to phosphopeptides with a

different specificity than the wild-type Brca1 BRCT domains also formed punctate nuclear foci, although these were slightly reduced in number and showed less colocalization with pSer/pThr-Gln staining foci than the wild-type protein. This localization might result from synergistic weak binding to alternative non-optimal phosphorylated ligands present in high abundance in nuclear foci following DNA damage, as has been observed for other phosphopeptide-binding domain interactions [45].



## Discussion

(BRCT)<sub>2</sub> domains are unusual in binding to pSer-containing peptides more strongly than to pThr-containing peptides since 14-3-3 proteins, WW domains, WD40 domains, FHA domains and Polobox domains either bind pThr-peptides better than pSer-peptides, or do not bind to pSer-peptides at all [5, 46, 47]. Intriguingly, ATM and ATR preferentially phosphorylate Ser-Gln over Thr-Gln motifs [25], suggesting functional convergence between the motifs generated by the PIKKs and the motifs recognized by BRCT domains. The observed (BRCT)<sub>2</sub> domains selection for aromatic and aliphatic residues in the (pSer or pThr)+3 positions exceeds their selection for Gln in the +1 position. Thus, only a subset of ATM and ATR phosphorylated substrates are likely to bind with high affinity, and kinases other than Gln-directed kinases might also generate potential (BRCT)<sub>2</sub> domain-binding motifs.

The specific role of PTIP in the DNA damage response though remains exceedingly unclear. Few studies have been performed looking at PTIP function, and its biological role is still mysterious. Initially, PTIP was identified as an interactor of the Pax2 transcription factor, and found to play a role in transcriptional silencing of Pax2 targets [27, 48]. In fact, PTIP is now thought to be a member of a histone methyltransferase complex [49] further supporting its role as a transcriptional regulator. The knockout mouse phenotype of PTIP first indicated that it could be involved in the DNA damage response, as the mouse was inviable with similar phenotypes to the ATR, Chk1, and Brca1 knockout mice [28]. Trophoblast cells grown from these mice were more sensitive to IR, and overall, the embryos had few cells in mitosis [28], consistent with a role for PTIP in the DNA damage response. The fact that an interaction of PTIP with a known DNA damage response protein, 53BP1, is enhanced by IR, and the formation of PTIP foci following IR (Figure A1.4) confirms this potential for PTIP regulation of the DNA damage response. A more recent study has confirmed that PTIP forms nuclear foci after IR (but not other DNA damaging agents), and that knockdown of PTIP by siRNA reduced ATM-mediated phosphorylation of p53 at Ser15 [50].

This still leaves many open questions regarding the role for PTIP in cycling and non-cycling cells. PTIP clearly has multiple functions, perhaps functioning as a transcriptional regulator during development and in specialized cell populations, and

functioning in the DNA damage response pathway in cycling cells. The fact that PTIP only forms foci after IR suggests that PTIP plays a role in the ATM signaling network, though the mouse knockout data suggests PTIP is part of the ATR/Chk1 pathway [2]. One interesting question is whether formation of foci by PTIP is dependent on 53BP1 foci formation. This can easily be answered through the use of a 53BP1 siRNA depletion strategy, which has been successfully used before to order foci formation pathways [34]. Once at foci, what is the role of PTIP? Considering the loss of p53 phosphorylation following PTIP knockdown, it appears that PTIP functions as a scaffold for DNA damage-responsive kinase activity, similarly to the other BRCT domain-containing proteins in the DNA damage response network such as 53BP1, MDC1, and Brca1 [2]. Are there other PTIP BRCT domain interactors, as indicated by the multiple bands pulled down by the PTIP BRCTs after IR (Figure A1.4), or is 53BP1 the only *in vivo* interactor? Mass spectrometry identification of the bands would at least allow further candidates to be tested. The availability of mouse Cre-Lox PTIP cells [51] will allow further studies to look at the role of PTIP in multiple DNA damage-signaling responses in otherwise wild-type MEFs, without the limitations of incomplete knockdown by siRNA or redundant pathway upregulation during development. It remains an open question whether PTIP has a distinct and necessary role in the DNA damage response, though evidence is slowly accumulating.

The 1.85Å BRCA1-(BRCT)<sub>2</sub> domains:phosphopeptide structure described here is the highest resolution X-ray structure of any BRCT domain structure solved to date, and provides an enhanced structural framework within which the molecular basis of breast and ovarian cancer can be further investigated. The structure reveals why tandem BRCT repeats, rather than single BRCT domains, are required for binding to pSer- or pThr-containing phosphopeptides with high affinity and specificity, since motif recognition is mediated by residues contributed from both domains across the domain-domain interface. In addition, the structure rationalizes the observation that the BRCA1-(BRCT)<sub>2</sub> domains do not bind to pTyr-containing sequences (Figure A1.3), since the phosphate recognition pocket appears too shallow to accept a bulky phenyl ring. Despite the fact that mutations in Brca1 ultimately predispose women to cancer, wild-type Brca1 paradoxically constitutes a target for anti-cancer therapy. Given the importance of Brca1 in homologous

recombination and DNA repair [9, 52-54], disruption of the pSer-binding function would be expected to result in enhanced sensitivity to chemotherapy and radiation, as has been observed in Brca1 null murine embryonic stem cells [53]. Thus, the structural delineation of the pSer binding surface provides a new target for rational drug design.

The BRCA1-(BRCT)<sub>2</sub> domains:phosphopeptide structure, in combination with biochemical and cell biological analysis, shows that some pro-oncogenic mutations in the Brca1 C-terminal domains directly disrupt phosphopeptide binding or perturb the BRCT interface that forms the phospho-dependent binding surface. Four bona fide cancer-linked mutations, P1749R, G1738E, 5382InsC, and Y1853X all result in loss of phosphopeptide binding. A fifth mutation, M1775R, binds weakly to phosphopeptides with altered motif specificity, and can still form nuclear foci after DNA damage, however it completely loses the ability to interact with wild-type Bach1. These effects of the P1749 and M1775 lesions confirm the previous observations that these mutations are sufficient to abrogate Brca1-Bach1 interactions in vivo [10]. Since Bach1 mutations have also been shown to be associated with the development of cancer [55], these findings suggest that the loss of this critical Brca1 M1775R:Bach1 interaction may be the critical event responsible for cancer predisposition [11, 55]. However, the observation that some (D1692Y, R1751Q) mutants can still bind to Bach1 suggests this theory may not be fully correct. These mutants do bind Bach1 more weakly than wild-type Brca1 suggesting that there could be a critical threshold of the Brca1:Bach1 interaction required for the tumor suppressor activity of Brca1 in vivo.

It remains unclear how phosphopeptide binding by the BRCA1 (BRCT)<sub>2</sub> domain contributes to propagating signals in the DNA damage response network. In order to study the role of Brca1 BRCT phospho-binding activity, we attempted to generate a Brca1 knockout system, where different mutants of Brca1 could be added back for assay. Unfortunately, depletion of Brca1 by siRNA or by a microRNA vector caused massive cell death, preventing simple interpretations of follow-up experiments. Fortunately, there is a cell line available from a breast cancer patient, HCC1937, which has one deleted Brca1 allele and one 5832InsC allele, which has a missense mutation that causes premature termination before the BRCTs. Thus, this cell line can be used for in vivo assays of (BRCT)<sub>2</sub> domain function. The cell line grows very slowly and cannot be

transfected to an appreciable rate using standard techniques, but it can be infected with retro- or lenti- viruses. Addition of wild-type Brca1 rescues the function of the cell line in response to DNA damage [42], while certain cancer associated mutations still lose function [42]. We were able to replicate the rescue using a wild-type Brca1 virus, and found that MAPKAPK2 activation after certain DNA damage signals is dependent on Brca1 (Figure A1.13). Future experiments are planned to characterize whether other cancer-associated mutations are deficient in various DNA damage-responsive events, particularly the D1692Y and R1751Q mutants, which retain BACH1 binding function. Also, the S1655A/K1702M mutant will be tested to see whether phospho-binding activity is generically required for Brca1 function in these processes.

Our experimental evidence and crystal structure-based sequence alignments suggest that not all tandem BRCT domains can bind to phosphorylated ligands, despite the fact that several residues involved in the binding are relatively conserved. The only other definitive phosphorylation-dependent tandem BRCT domain besides PTIP and Brca1 was found in MDC1 by another member of our lab, and it appears that MDC1 binding is specialized because it requires a free carboxy terminus at the +3 position for binding [56]. A set of tandem BRCT domains of TopBP1 might also bind in a phospho-dependent manner, as the sixth BRCT domain of TopBP1 was found to bind to E2F1 in a manner that was enhanced upon phosphorylation of E2F1 by ATM [57], and the tandem BRCT domains of the yeast homolog of TopBP1 (Rad4) bind to Rad9 in a phosphorylation-dependent manner [58]. There is a clear suggestion that the tandem BRCT domains of Ect2 also are phospho-specific binders, but they do not bind in the IVT-pulldown assay (Chapter Four), perhaps due to lack of an appropriate phosphopeptide library. Other tandem BRCT domains may function like Ect2, with too low, or like Mdc1, with too specialized, of a binding affinity to be seen in the standard IVT-pulldown assays used in the screen to identify new phosphobinding domains (Figure A1.1A). It appears likely, however, that a minority of BRCT domains have a phospho-binding function, as there are many examples of single BRCT domains [59], BRCT domains have been previously thought to be non-phosphorylation-mediated interaction surfaces [59], and BRCT domains are conserved in bacteria which presumably do not have any need for phosphoSer/Thr-dependent binding. Even PTIP itself has four other BRCT domains that

do not have phosphobinding ability (Duaa Mohammad - personal communication) and no known function. Non-phosphorylation-dependent binding events are not unprecedented in a class of phosphorylation-dependent binding domains, as seen in FHA domains [60], in tandem BRCT domains themselves in 53BP1 [37, 38], and even in Brca1 [61]. Perhaps BRCT domains are simply protein interaction surfaces which in some cases have evolved to be phosphorylation-dependent.

## Experimental Procedures

### ATM/ATR phospho-motif screen for phosphoserine/threonine binding domains.

An oriented (pSer/pThr) phosphopeptide library biased toward the phosphorylation motifs for ATM/ATR kinases, and its non-phosphorylated counterpart were constructed as follows: biotin-Z-Gly-Z-Gly-Gly-Ala-X-X-X-B-(pS/pT)-Gln-J-X-X-X-Ala-Lys-Lys-Lys and biotin-Z-Gly-Z-Gly-Gly-Ala-X-X-X-B-(Ser/Thr)-Gln-J-X-X-X-Ala-Lys-Lys-Lys where pS denotes phosphoserine, pT phosphothreonine, Z indicates aminohexanoic acid, B represents a biased mixture of the amino acids Ala, Ile, Leu, Met, Asn, Pro, Ser, Thr, Val and J represents a biased mixture of 25% Glu, 75% X, where X denotes all amino acids except Arg, Cys, His, Lys. The amino acids Arg, Lys, and His were intentionally omitted from the degenerate positions in the peptide library to decrease the likelihood of identifying phosphopeptide-binding domains such as 14-3-3 which target basophilic motifs generated by kinases such as AKT, PKA, and PKCs. Streptavidin beads (Pierce, 75pmol/ $\mu$ L gel) were incubated with a ten-fold molar excess of each biotinylated library in 50 mM Tris/HCl (pH7.6), 150 mM NaCl, 0.5% NP-40, 1 mM EDTA, 2 mM DTT and washed five times with the same buffer to remove unbound peptide. The bead-immobilized libraries (10 $\mu$ L of gel) were added to 10  $\mu$ L of an in vitro translated [<sup>35</sup>S]-labeled protein pool in 150  $\mu$ L binding buffer (50 mM Tris/HCl (pH7.6), 150 mM NaCl, 0.5% NP-40, 1 mM EDTA, 2 mM DTT, 8  $\mu$ g/mL pepstatin, 8  $\mu$ g/mL aprotinin, 8  $\mu$ g/mL leupeptin, 800  $\mu$ M Na<sub>3</sub>VO<sub>4</sub>, 25 mM NaF) in a 96 well plate format. Each pool consisted of ~100 radiolabeled proteins produced by the ProteoLink in vitro expression cloning system (Promega). After incubation at 4°C for 3 hours, the beads were rapidly washed three times 200  $\mu$ L with binding buffer using a 96 well vacuum manifold prior to SDS-PAGE (12.5%) and autoradiography. Positively scoring hits were identified as protein bands that interacted more strongly with the phosphorylated immobilized library than with the unphosphorylated counterpart. Pools containing positively scoring clones were progressively subdivided and re-screened for phosphobinding until single clones were isolated and identified by DNA sequencing. The same procedure was used on individual plasmids to test the phosphobinding ability of various tandem BRCT containing proteins and all the BRCA1 mutant.

## **Protein Cloning, Expression, and Purification**

For deletion mapping of the PTIP and BRCA1 BRCT phospho-binding region and for expression of MDC1, Rad9, and 53BP1 (Figures A1.1 and A1.2), fragments were generated by PCR, cloned into pcDNA3.1 (Invitrogen), and subjected to *in vitro* transcription and translation. The original MDC1 and 53BP1 plasmids were gifts from S. Elledge and K. Iwabuchi respectively. For production of recombinant GST-PTIP BRCT domains and GST-BRCA1 BRCT domains, residues 550-757 of PTIP and residues 1634-1863 of BRCA1 were ligated into the EcoRI and NotI sites of pGEX-4T1 (Pharmacia) and subsequently transformed into DH5 $\alpha$  E. Coli. Protein induction occurred at 37°C for 4 hrs or at 25°C for 16 hrs in the presence of 0.2-0.4 mM IPTG. GST-PTIP BRCT domains and GST-BRCA1 BRCT domains were isolated from bacterial lysates using glutathione agarose, eluted with 40mM glutathione/50mM Tris/HCl (pH 8.1), and dialyzed into 50mM Tris/HCl (pH 8.1)/300mM NaCl. For ITC experiments, purified GST-PTIP BRCT domains were dialyzed into cleavage buffer (25mM Tris-HCl, 100mM NaCl, 2mM CaCl<sub>2</sub>), and cleaved in solution with thrombin (Sigma). Free GST was removed by incubation with glutathione agarose and the PTIP BRCT domains were further purified on a mono-Q column and eluted with a NaCl gradient. The appropriate fractions were dialyzed into 25mM Tris/HCl (pH 8.1), 100mM NaCl. The GFP-PTIP constructs FL (residues 1-757), ? BRCT (residues 1-549), or (BRCT)<sub>2</sub> (residues 550-757) were cloned into the EcoRI and SalI sites of pEGFP-C2 (Clontech). For crystallization experiments, human Brca1 BRCTs (residues 1646–1859) were expressed as glutathione S-transferase (GST) fusions in pGEX-4T1 (Amersham Pharmacia Biotech) in *Escherichia coli* BL21 at 18°C. The GST was removed by 48-hour treatment with thrombin before gel filtration. Synthetic peptides for crystallization were prepared by W. Mawby, University of Bristol, U.K. A Brca1 BRCT clone (residues 1313–1863) in pcDNA3 containing a N-terminal Myc-tag and a SV40 nuclear localization sequence was a gift from R. Scully and D. Livingston [41], and was used for the co-immunoprecipitation and immunofluorescence assays. All mutations were generated using the Stratagene Quick Change Mutagenesis Kit, and verified by sequencing.

### **Peptide library screening**

Phosphoserine and phosphothreonine oriented degenerate peptide libraries consisting of the sequences Gly-Ala-X-X-X-B-(pS/pT)-Gln-J-X-X-X-Ala-Lys-Lys-Lys, Met-Ala-X-X-X-X-pThr-X-X-X-X-Ala-Lys-Lys-Lys, Met-Ala-X-X-X-X-pSer-X-X-X-X-X-Ala-Lys-Lys-Lys, and Gly-Ala-X-X-X-X-pSer-X-X-Phe-X-X-Ala-Tyr-Lys-Lys-Lys, where X denotes all amino acids except Cys. In the (pS/pT)-Gln library pS denotes phosphoserine, pT phosphothreonine, B represents a biased mixture of the amino acids Ala, Ile, Leu, Met, Asn, Pro, Ser, Thr, Val and J represents a biased mixture of 25% Glu, 75% X, where X denotes all amino acids except Arg, Cys, His, Lys. Peptides were synthesized using N-a-FMOC-protected amino acids and standard BOP/HOBt coupling chemistry. Peptide library screening was performed using 125-250  $\mu$ l of glutathione beads containing saturating amounts of GST-PTIP BRCT or GST-BRCA1 BRCT domains (1-1.5 mg) [30]. Beads were packed in a 1mL column and incubated with 0.45 mg of the peptide library mixture for 10 min at room temperature in PBS (150 mM NaCl, 3 mM KCl, 10 mM Na<sub>2</sub>HPO<sub>4</sub>, 2 mM KH<sub>2</sub>PO<sub>4</sub>, pH 7.6). Unbound peptides were removed from the column by three washes with PBS containing 1.0% NP-40 followed by three washes with PBS. Bound peptides were eluted with 30% acetic acid for 10 min at room temperature, lyophilized, resuspended in H<sub>2</sub>O, and sequenced by automated Edman degradation on a Procise protein microsequencer. Selectivity values for each amino acid were determined by comparing the relative abundance (mole percentage) of each amino acid at a particular sequencing cycle in the recovered peptides to that of each amino acid in the original peptide library mixture at the same position.

### **Isothermal Titration Calorimetry**

Peptides were synthesized by solid phase technique with three C-terminal lysines to enhance solubility. Peptides were then purified by reverse phase HPLC following deprotection and confirmed by MALDI-TOF mass spectrometry. Calorimetry measurements were performed using a VP-ITC microcalorimeter (MicroCal Inc.). Experiments involved serial 10 $\mu$ L injections of peptide solutions (20 $\mu$ M-150 $\mu$ M) into a sample cell containing 15 $\mu$ M PTIP BRCT domains (residues 550-757) or 15 $\mu$ M GST-BRCA1 BRCT domains (residues 1634-1863) in 25-50mM Tris/HCl (pH 8.1), 100-



300mM NaCl. Twenty injections were performed with 240s intervals between injections and a reference power of 25  $\mu$ Cal/s. Binding isotherms were plotted and analyzed using Origin Software (MicroCal Inc.)

### **Peptide Filter Array**

An ABIMED peptide arrayer with a computer controlled Gilson diluter and liquid handling robot was used to synthesize peptides onto an amino-PEG cellulose membrane using N-a-FMOC-protected amino acids and DIC/HOBT coupling chemistry. The membranes were blocked in 5% milk/TBS-T (0.1%) for 1hr at room temperature, incubated with 0.025-0.1  $\mu$ M GST-PTIP BRCT domains (residues 550-757) or GST-BRCA1 BRCT domains (residues 1634-1863) or 0.25  $\mu$ M GST-Brc1 BRCTs M1775R in 5% milk, 50 mM Tris/HCl (pH 7.6), 150 mM NaCl, 2 mM EDTA, 2mM DTT for 1 hr at room temperature and washed four times with TBS-T (0.1%). The membranes were then incubated with anti-GST conjugated HRP (Amersham) in 5% milk/TBS-T (0.1%) for 1 hr at room temperature, washed five times with TBS-T (0.1%), and subjected to chemiluminescence using ECL (Perkin-Elmer).

### **PTIP BRCT domains and BRCA1 BRCT domains binding to cellular substrates**

U2OS cells were either treated with 10 Gy of ionizing radiation or mock irradiated and allowed to recover for 30-120 min. Cells were subsequently lysed in 50 mM Tris/HCl (pH7.6), 150 mM NaCl, 1.0% NP-40, 5 mM EDTA, 2 mM DTT, 8  $\mu$ g/mL pepstatin, 8  $\mu$ g/mL aprotinin, 8  $\mu$ g/mL leupeptin, 2 mM  $\text{Na}_3\text{VO}_4$ , 10 mM NaF, 1  $\mu$ M microcystin. The lysates (0.5-2mg) were incubated with 20  $\mu$ L glutathione beads containing 10-20  $\mu$ g of GST-PTIP BRCT domains (residues 550-757), GST-BRCA1 BRCT domains (residues 1634-1863) or GST for 120 min at 4°C. Beads were washed three times with lysis buffer. Precipitated proteins were eluted in sample buffer and detected by blotting with anti-ATM/ATR substrate (pSer/pThr)Gln antibody (Cell Signaling), polyclonal anti-53BP1 (Oncogene), or monoclonal anti-HA (Covance). For peptide competition experiments, GST-PTIP BRCT domains or GST-BRCA1 BRCT domains were immobilized on glutathione beads and preincubated with 350  $\mu$ M of BRCTtide-(7pSer, 7pThr, 7Thr, 7Ser) (Table A1.2), (pSer/pThr)Gln-library,

(Ser/Thr)Gln-library, or pThrPro-library for 1 hr at 4°C and washed three times with lysis buffer. For the phosphatase experiment the lysate was treated for one hour with lambda protein phosphatase (Sigma) prior to incubation with glutathione beads containing GST-PTIP BRCT domains.

### **Co-immunoprecipitation of Brca1 BRCTs and Bach1**

U2OS cells were grown to 50% confluency in 100cm<sup>2</sup> dishes and transfected with the myc-tagged wild-type or mutant Brca1 BRCT constructs (residues 1313–1863) using FuGene6 transfection reagent (Roche) according to manufacturer's protocol. Cells were collected 30 hrs following transfection, lysed in lysis buffer (50 mM Tris/HCl (pH7.6), 150 mM NaCl, 1.0% NP-40, 5 mM EDTA, 2 mM DTT, 8 µg/mL AEBSF, 8 µg mL<sup>-1</sup> aprotinin, 8 µg mL<sup>-1</sup> leupeptin, 2 mM Na<sub>3</sub>VO<sub>4</sub>, 10 mM NaF and the phosphatase inhibitors microcystin and okadaic acid). Lysates containing equal amounts of protein (3 mg) was incubated with 3 µL of a mouse anti-myc antibody (Cell Signaling) for 2 hr at 4°C and then 10 µL of protein G-sepharose beads (Sigma-Aldrich) were added and samples incubated for an additional 2 hr at 4°C. Beads were washed four times with lysis buffer, bound proteins eluted in SDS-PAGE sample buffer, analyzed on 6% polyacrylamide gels, transferred to PVDF membrane, and detected by blotting with rabbit anti-Bach1 antibody (a gift from D. Livingston and R. Drapkin). A portion of the lysates were also run and blotted with the anti-Bach1 antibody and the anti-myc antibody to further ensure equal protein loading.

### **Immunofluorescence and Microscopy**

U2OS cells were seeded onto 18mm<sup>2</sup> coverslips and transfected with GFP-PTIP constructs [FL (residues 1-757), ? BRCT (residues 1-549), or (BRCT)<sub>2</sub> (residues 550-757)] or myc-Brca1 BRCT constructs (residues 1313-1863) using FuGene6 transfection reagent (Roche) according to manufacturer's protocol. Twenty to thirty hours following transfection, the cells were either treated with 10 Gy of ionizing radiation or mock irradiated and allowed to recover for 30-480 minutes. Cells were fixed in 3% paraformaldehyde/2% sucrose for 15 min at RT and permeabilized with a 0.5% Triton X-100 solution containing 20 mM Tris-HCl (pH 7.8), 75 mM NaCl, 300 mM sucrose, and 3

mM MgCl<sub>2</sub> for 15 min at RT. When necessary, cytosolic proteins were extracted after IR treatment as described previously[44]. In brief, cells were incubated with extraction buffer (10mM PIPES pH6.8, 100mM NaCl, 300mM sucrose, 3mM MgCl<sub>2</sub>, 1mM EGTA, 0.5% (v/v) Triton X-100) for 5 minutes on ice followed by incubation with extraction stripping buffer (10mM Tris-Hcl pH 7.4, 10mM NaCl, 3mM MgCl<sub>2</sub>, 0.5% (v/v) Triton X-100) for 5 minutes on ice followed by successive washes in ice cold PBS. Slides were stained with primary antibodies at 4°C overnight, then stained with a Texas Red conjugated anti-mouse or anti-rabbit secondary antibody for 60 min (Molecular Probes) at RT. Primary antibodies used were rabbit polyclonal anti-53BP1 (Oncogene), mouse anti-γ-H2AX (Upstate), mouse anti-myc (Cell Signaling), and rabbit anti-(pSer/pThr)Gln (Cell Signaling). Images were either collected on a Deltavision microscope (Carl Zeiss) and digitally deconvolved using Softworx graphics processing software (SGI) or captured using a spinning disk confocal detector mounted on a Nikon TE2000 microscope using OpenLab software (Improvision).

### **Crystallization and Structure Determination**

Crystals were grown at 18°C by microbatch methods. The Bach1 phosphopeptide (SRSTpS<sup>990</sup>PTFNK) was mixed with the Brca1 BRCTs in a 1.5:1 stoichiometric excess and concentrated to 0.35mM in a buffer containing 50mM Tris-HCl (pH 7.5), 0.4M NaCl, and 3mM DTT. Crystals grew from 50 mM MES (pH 6.5), 0.1 M (NH<sub>4</sub>)<sub>2</sub>SO<sub>4</sub>, and 13% PEG 8K (w/v) Crystals belonged to the trigonal space group P3<sub>2</sub>21 ( $a = b = 65.8 \text{ \AA}$ ,  $c = 93.1 \text{ \AA}$ ,  $\alpha = \beta = 90.0^\circ$ ,  $\gamma = 120.0^\circ$ ) with one complex in the asymmetric unit. Data were collected from flash-cooled crystals at 100K on a Raxis-II detector mounted on a Rigaku RU200 generator. Diffraction data were integrated and scaled using DENZO and SCALEPACK [62]. The structure was solved by molecular replacement using the coordinates 1JNX.brk [20] as a model with AMORE [63]. Subsequent refinement was carried out using REFMAC5 [63] and manual model building in O [64]. Figures were constructed using Pymol. The atomic coordinates and structure factors have been deposited in the Protein Data Bank (Accession code 1T15).

**Figure A1.1: Identification of phosphoSer/Thr-binding domains using an ATM/ATR-motif library vs. expression library screen.**

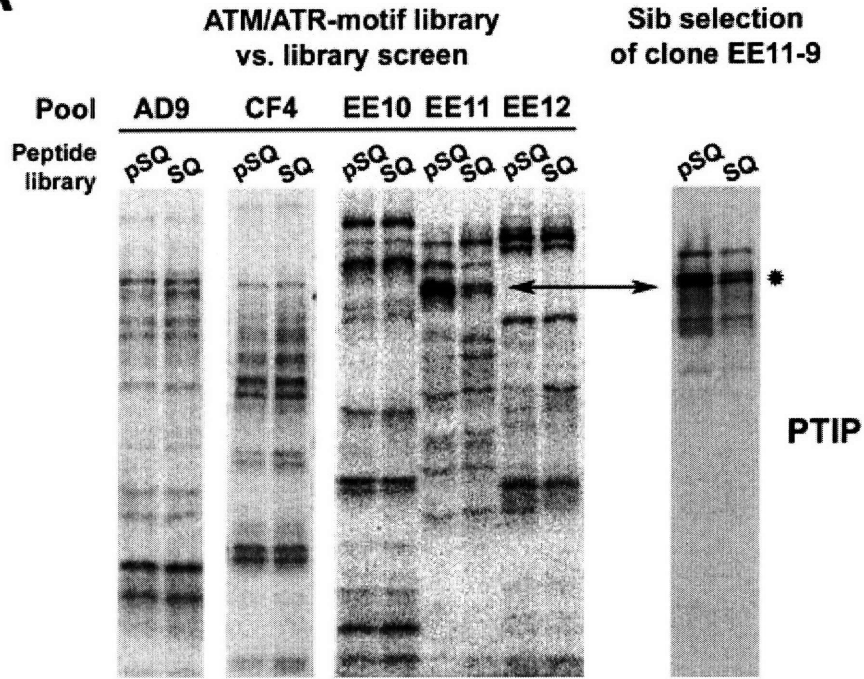
**(A)** An oriented (pSer/pThr) phosphopeptide library, biased toward the phosphorylation motifs of ATM and ATR, was immobilized on Streptavidin beads. The library [pSQ=biotin-ZGZGGAXXXB(pS/pT)QJXXXAKKK] and its non-phosphorylated counterpart (SQ) were screened against *in vitro* translated <sup>35</sup>S-Met labeled proteins. (pS/pT) denotes 50% phosphoserine and 50% phosphothreonine, Z indicates aminohexanoic acid, B represents a biased mixture of the amino acids (A, I, L, M, N, P, S, T, V) and J represents a biased mixture of (25% E, 75% X), where X denotes all amino acids except (R, C, H, K) (see methods). In each panel, the first and second lanes show binding of proteins within the pool to the phosphorylated (pSQ) and non-phosphorylated (SQ) libraries, respectively. Identification of PTIP, denoted by arrow and asterisk, occurred through progressive subdivision of the EE11 pool to a single clone.

**(B)** Deletion mapping of the phospho-binding domain of PTIP. Truncations of PTIP assayed for selective binding to the pSQ library (Figure A1.1A). BRCT domain boundaries were determined from sequence alignments [65].

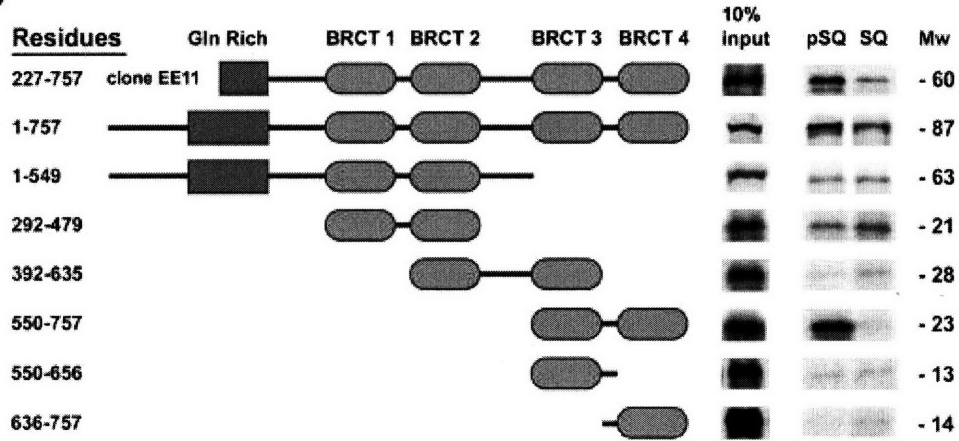
**(C)** Domain structure of BRCA1 is indicated in cartoon format.

Figure A1.1 Continued

**A**



**B**



**C**

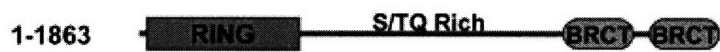
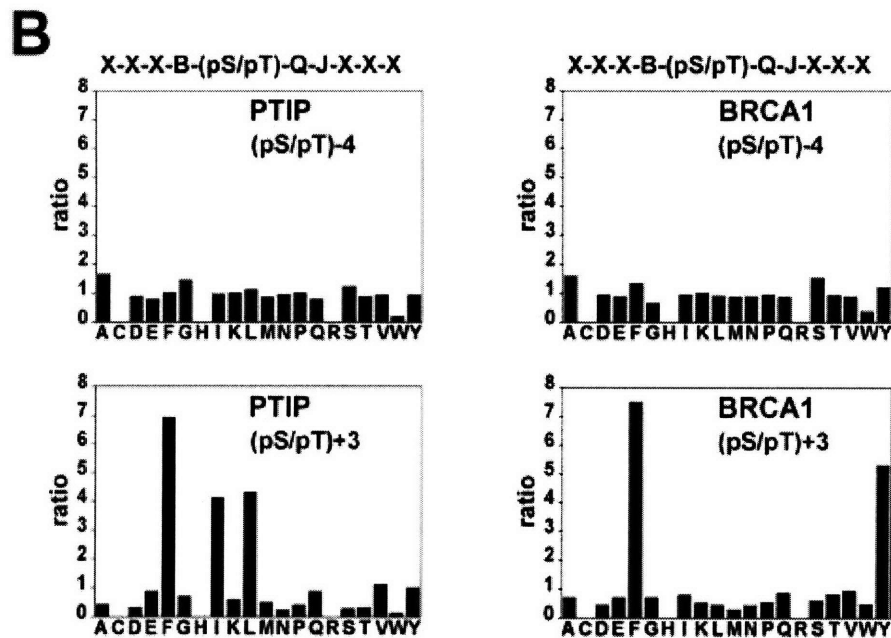
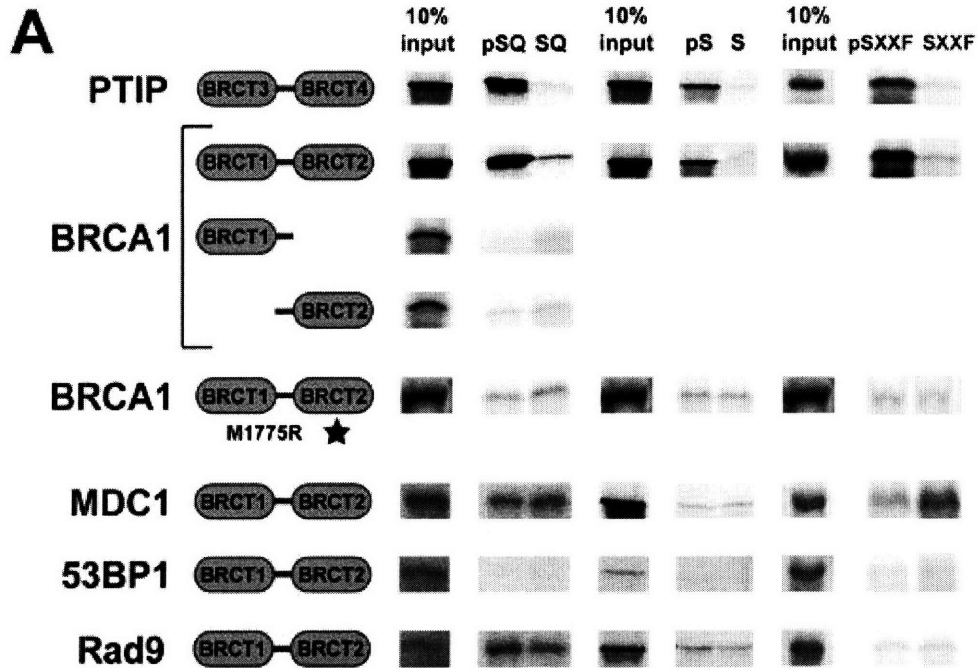


**Figure A1.2: Comparison of the tandem BRCT domains and determination of the PTIP and BRCA1 BRCT optimal phosphopeptide-binding motifs.**

(A) PTIP, BRCA1, BRCA1 M1775R, MDC1, 53BP1 and Rad9 (BRCT)<sub>2</sub> domains were assayed for binding as in Figure 1A. The peptide libraries used were pSQ (Figure A1.1A), pS= biotin-ZGZGGAXXXXpSXXXXXAKKK, pT=biotin-ZGZGGAXXXXpTXXXXXAKKK, pSXXF=biotin-ZGZGGAXXXXpSXXFXXAYKKK, where pS is phosphoserine, pT is phosphothreonine, Z indicates aminohexanoic acid, X denotes all amino acids except Cys. Domain boundaries: PTIP as indicated in Fig 1; BRCT1 and 2, aa 1633-1863; BRCT1 alone, aa 1633-1740; BRCT2 alone, 1741-1863; MDC1, aa 1874-2089; 53BP1, aa 1622-1972; Rad9, 985-1309.

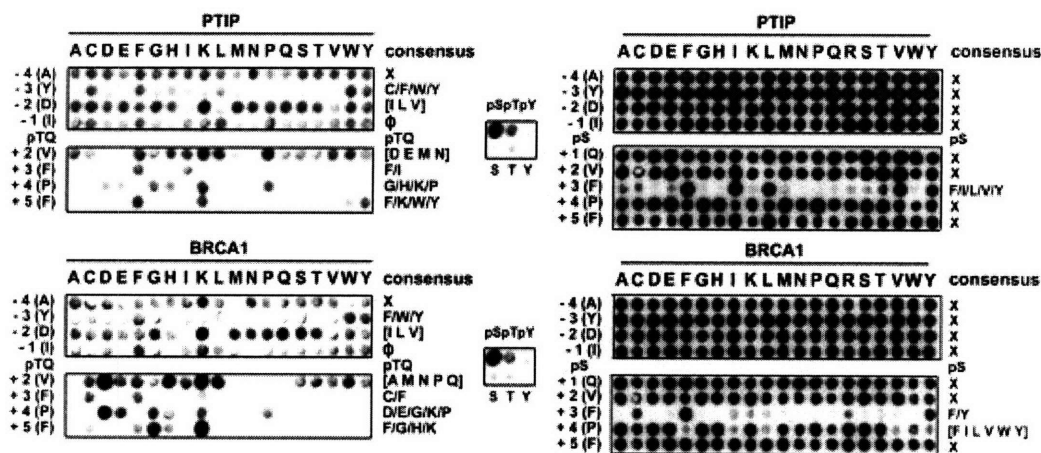
(B) Strong selection by the PTIP- and BRCA1-(BRCT)<sub>2</sub> domains for Phe at the (pSer/pThr)-Gln +3 position (7.0 or 7.5), respectively (Table A1.1). Bar graphs show the relative abundance of each amino acid at a given cycle of sequencing compared to its abundance in the starting peptide library mixture[30]. In these types of assays ratios greater than 1.8 are considered to indicate significant selection and ratios greater than 2.5 are very significant.

Figure A1.2 Continued



### Figure A1.3: PTIP and BRCA1 BRCT domains binding to a filter array of phosphopeptides

Binding of GST-PTIP and BRCA1 (BRCT)<sub>2</sub> domains to a filter array of peptide spots, comprising single point mutants of the optimal BRCT domain phosphopeptide (left column). Bound GST-(BRCT)<sub>2</sub> domains were detected by blotting with HRP-conjugated anti-GST antibody. The resulting consensus binding motif is indicated in the right column; X denotes no dominant selection, φ denotes residues with aliphatic or aromatic side chains, and letters enclosed in square brackets are specifically de-selected. The top row indicates the amino acid that was substituted for the optimal amino acid. Substitution of pSer for pThr enhanced binding for both PTIP and BRCA1 (BRCT)<sub>2</sub> domains, consistent with the ITC results. Substitution of pTyr for pThr eliminated binding altogether, verifying that (BRCT)<sub>2</sub> domains are pSer/pThr-specific binding modules. Replacement of pThr with Thr, Ser or Tyr abrogated (BRCT)<sub>2</sub> domain binding. The pTQ oriented blots on the left show strong selection at several positions for both PTIP and BRCA1 BRCT domains; especially for Phe in the +3 position in agreement with the oriented peptide library screening data. The pS oriented blots on the right show that the +3 position is the most important position for peptide selection.





**Figure A1.4: Association of tandem PTIP and BRCA1 BRCT domains with DNA damage-induced phosphoproteins through their phosphopeptide-binding pockets.**

(A) Lysates from U2OS cells before or 2 hours after 10 Gy of IR were incubated with GST-PTIP-(BRCT)<sub>2</sub>. Bound proteins were detected by immunoblotting with an antibody to the (pSer/pThr)-Gln motif generated by ATM and ATR.

(B) Interaction of the PTIP-(BRCT)<sub>2</sub> domain with phosphoproteins. U2OS cells were treated with caffeine (5 mM) before IR exposure or the beads were incubated with an optimal BRCT-binding peptide (7pT) or the non-phosphorylated counterpart (7T).

(C) Tandem BRCT domains of PTIP interact with 53BP1 following DNA damage. Endogenous 53BP1 from IR treated U2OS cells was precipitated with GST-PTIP-(BRCT)<sub>2</sub> and detected by immunoblotting with an antibody to 53BP1. Interaction of GST-PTIP-(BRCT)<sub>2</sub> with HA-tagged 53BP1, detected by anti-HA blotting, was analyzed as in panels A and B.

(D) Lysates from U2OS cells 2 hrs following IR were incubated with GST-BRCA1 tandem BRCT domains. DNA damage-induced phosphoproteins were detected by blotting with the anti-ATM/ATR phosphoepitope motif antibody. The interaction of the GST-BRCA1 tandem BRCT domains with the phosphoproteins were analyzed as in panel B.

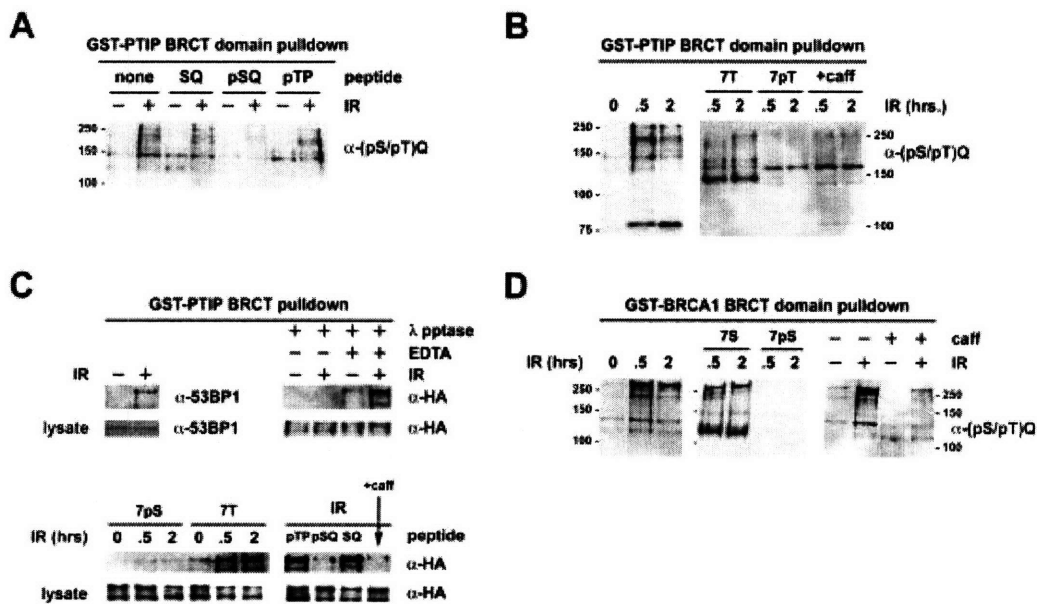


**Figure A1.5: Structure of the Brca1 tandem BRCT domains: Bach1 phosphopeptide complex.**

(A) Ribbons representation of the BRCA1-(BRCT)<sub>2</sub> domains domains in complex with the pSer-containing Bach1 peptide shown as stick representation in yellow. The Bach1 phosphopeptide binds at the interface between the two BRCT repeats. The secondary-structure elements in BRCT2 are labeled 'prime' to differentiate them from the secondary-structure elements in BRCT1. The BRCT inter-domain linker is shown in green. Areas of 3<sub>10</sub>-helix are not labeled.

(B) Electron density map (2F<sub>o</sub>-F<sub>c</sub>) covering the Bach1 phosphopeptide.

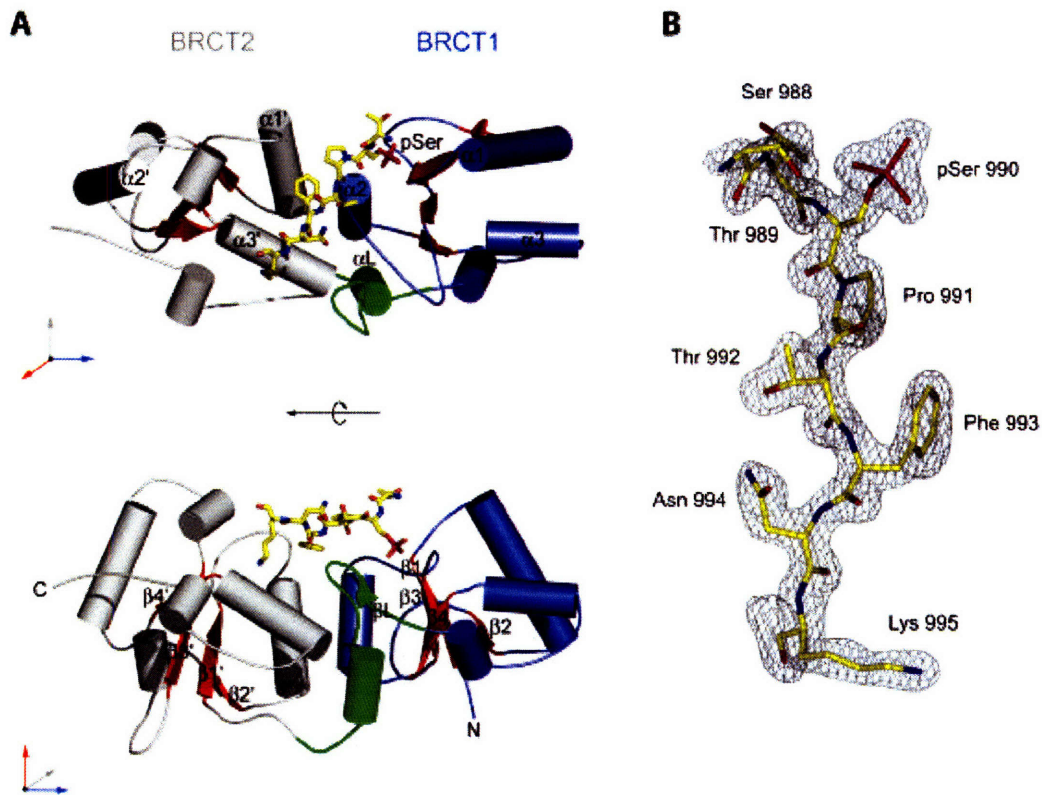


**Figure A1.6: Sites of Brca1 tandem BRCT domain cancer-linked mutations and sequence conservation in relation to the Bach1 phosphopeptide binding-site.**

**(A)** Comparison of the front and back views of the molecular surface showing the clustering of residues (magenta) conserved in human, chimp, mouse, rat, chicken and *Xenopus* BRCA1-(BRCT)<sub>2</sub> domains. The Bach1 peptide binds in a conserved phosphopeptide binding-groove.

**(B)** A molecular surface representation of BRCA1-(BRCT)<sub>2</sub> domains showing how the cancer-associated mutations S1655F, D1692Y, C1697R, R1699Q, S1715R, M1775R and Y1853X cluster with respect to the phosphopeptide binding-site. BRCT1 is colored blue, BRCT2 is colored grey, and the mutations are colored red, except for the S1655 which is colored green as its cancer predisposition has not been confirmed by pedigree analysis.

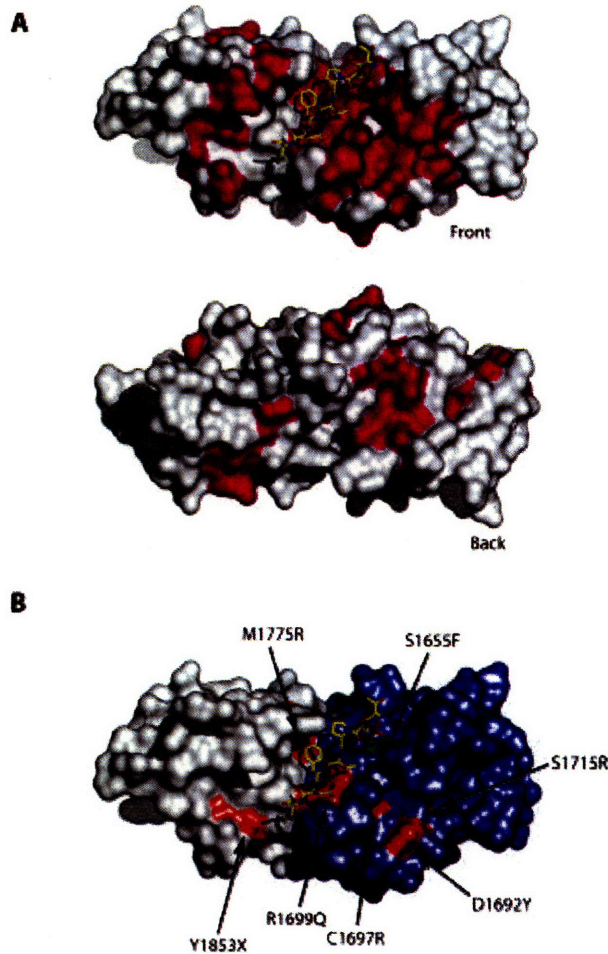


**Figure A1.7: Functional effects of tandem BRCT domain mutations.**

(A) Schematic representation of protein-peptide contacts between BRCA1-(BRCT)<sub>2</sub> domains and the Bach1 phosphopeptide. Hydrogen bonds, Van der Waals interactions and water molecules are denoted by dashed lines, pink crescents, and green circles respectively.

(B) The wild-type and mutant myc-tagged BRCA1-(BRCT)<sub>2</sub> domains constructs containing the indicated mutations were transcribed and translated *in vitro* in the presence of [<sup>35</sup>S]-methionine and analyzed for binding to a bead-immobilized optimal tandem BRCT domain-interacting phosphopeptide, YDIpSQVFPE, or its non-phosphorylated counterpart. The weak phospho-independent binding of the R1699Q mutant was observed using 10-fold more sample input than that in the other lanes.

(C) U2OS cells were transfected with the wild-type and mutant myc-tagged BRCA1-(BRCT)<sub>2</sub> domains constructs containing the indicated mutations. Protein lysates were immunoprecipitated with a mouse anti-myc antibody and analyzed for association with endogenous Bach1.

Figure A1.7 Continued

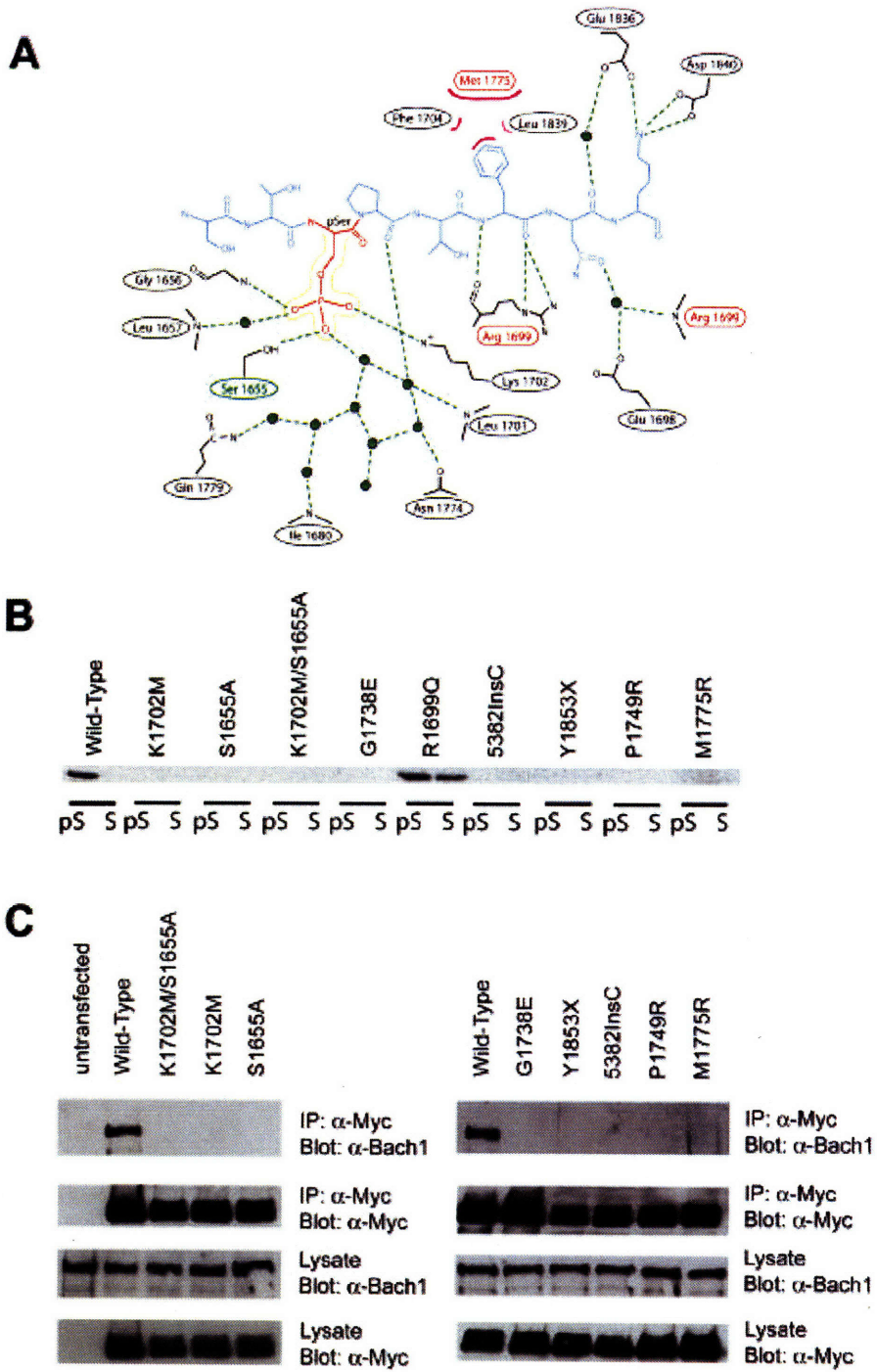


**Figure A1.8: Some Cancer-Associated Mutations in the Brca1 (BRCT)<sub>2</sub> Domain Retain Phospho-binding**

(A) The wild-type and mutant myc-tagged BRCA1-(BRCT)<sub>2</sub> domains constructs containing the indicated mutations were transcribed and translated in vitro in the presence of [<sup>35</sup>S]-methionine and analyzed for binding to a bead-immobilized optimal tandem BRCT domain-interacting phosphopeptide, YDIpSQVFPF, or its non-phosphorylated counterpart.

(B) U2OS cells were transfected with the wild-type and mutant myc-tagged BRCA1-(BRCT)<sub>2</sub> domains constructs containing the indicated mutations. Protein lysates were immunoprecipitated with a mouse anti-myc antibody and analyzed for association with endogenous Bach1.

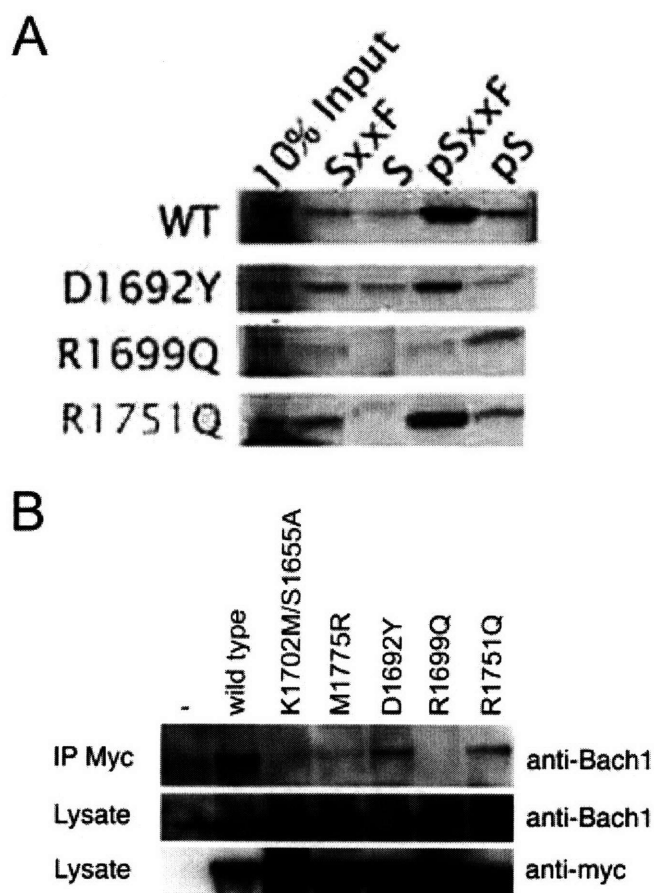




**Figure A1.9: The Phe +3 position of the Bach1 phosphopeptide is essential for Brca1 tandem BRCT domain binding-specificity.**

**(A)** Residues Phe 1704, Met 1775, and Leu 1839 from Brca1 tandem BRCT domains form a hydrophobic pocket to accommodate the Phe +3 position of the Bach1 phosphopeptide.

**(B)** Superposition of the crystal structure of Brca1 M1775R (BRCT)<sub>2</sub> domains mutant [21] with the wild-type: Bach1 phosphopeptide complex reveals that this mutation occludes the Bach1 Phe +3 position.

**(C)** Brca1 wild type (BRCT)<sub>2</sub> domains and the M1775R mutant binding to a Bach1 phosphopeptide spot array. The M1775R mutant spot blot was performed using 10 times the amount of protein and was exposed to film for a significantly longer amount of time than the wild-type protein.

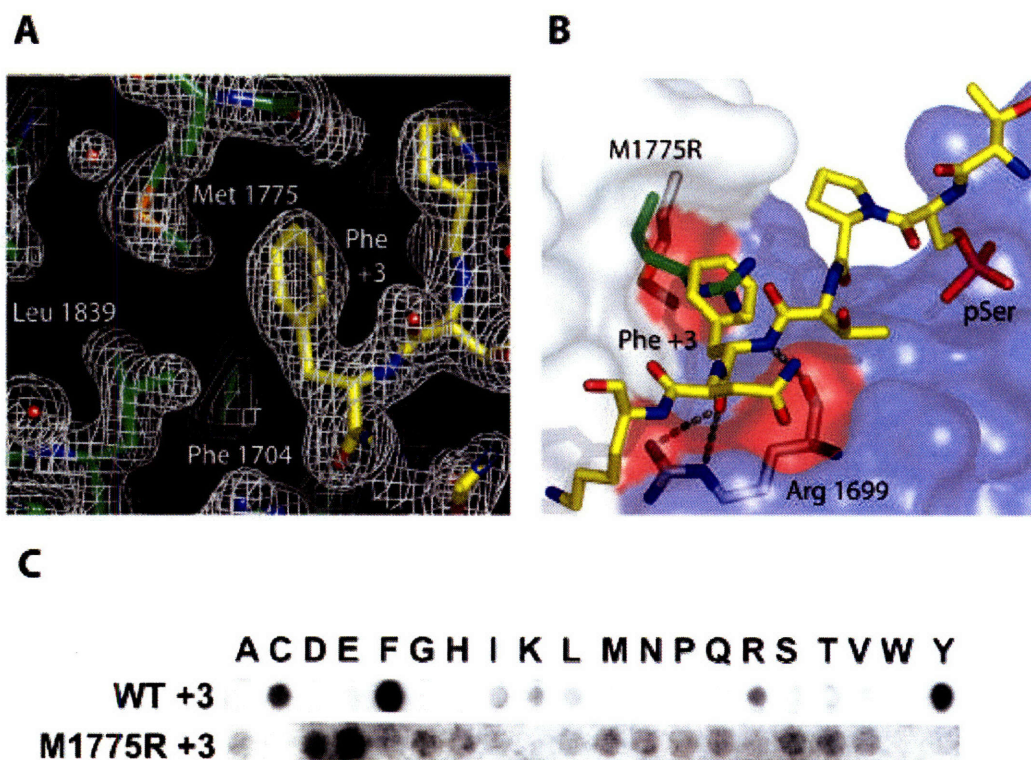


**Figure A1.10: Full length PTIP forms DNA damage induced foci and co-localizes with (pSer/pThr)-Gln proteins, 53BP1, and  $\gamma$ -H2AX.**

**(A)** U2OS cells were transfected with a full length PTIP-GFP construct (PTIP-FL residues 1-757).

**(B)** U2OS cells were transfected with a PTIP deletion construct in which the last two BRCT domains had been removed (PTIP- $\Delta$ BRCT, residues 1-550)

**(C)** U2OS cells were transfected with a PTIP construct containing only the last two BRCT domains ((BRCT)<sub>2</sub>, residues 550-757). In A-C, 24 hrs following transfection cells were either treated with 10 Gy of ionizing radiation or mock irradiated, allowed to recover for 2 hrs, stained, and analyzed by immunofluorescence microscopy.

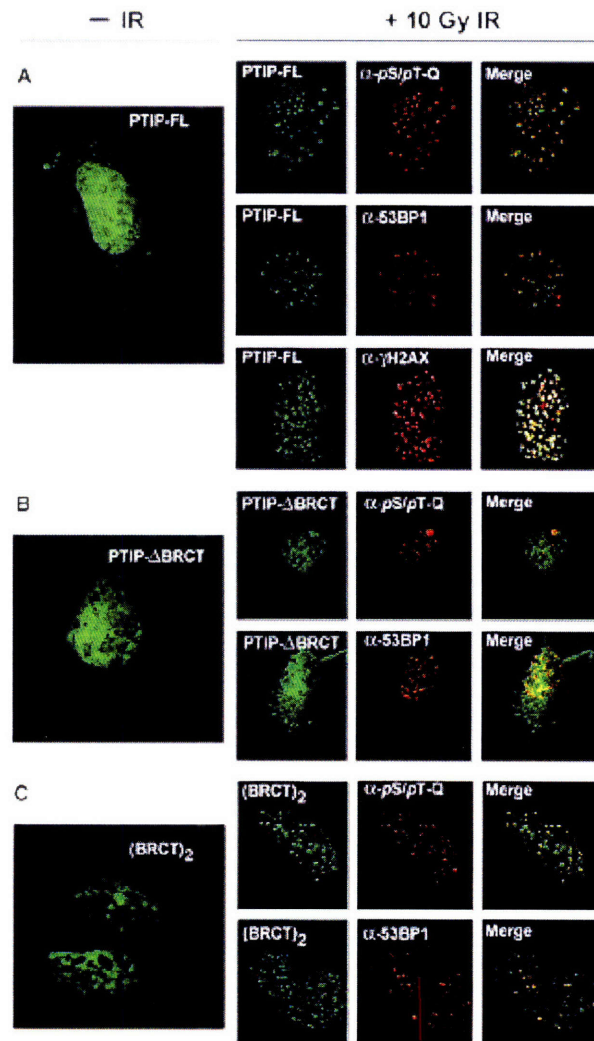




**Figure A1.11: Caffeine attenuates recruitment of PTIP to DNA damage foci in response to ionizing radiation.**

U2OS cells transfected with full-length PTIP-GFP cDNA were mock treated or pretreated with 10mM caffeine for 70 minutes before exposure to 10Gy ionizing radiation.

(A) In response to IR, mock-treated U2OS cells formed nuclear foci containing PTIP (in green) and H2AXp (in red); these two proteins co-localize at sites of DNA damage (merge).

(B) In response to IR, caffeine treated U2OS cells formed reduced numbers of nuclear foci; PTIP was mislocalized and did not form discrete nuclear foci (in green) and there were reduced numbers of H2AXp (in red) containing foci; pretreatment with caffeine effectively abolished co-localization of PTIP and H2AXp (merge).

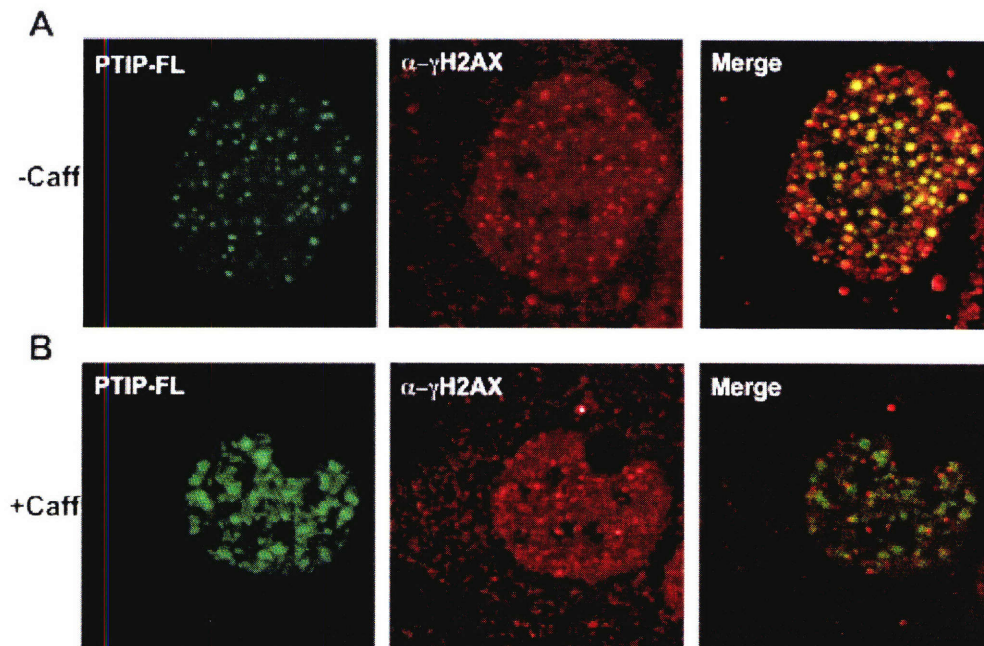


**Figure A1.12: Localization of the Brca1-BRCT Domains to Phosphoproteins.**

U2OS cells were transfected with the wild-type, M1775R, or K1702M/S1655A versions of the myc-tagged BRCA1-(BRCT)<sub>2</sub> domains construct.

(A) Un-irradiated cells were stained using an anti-myc antibody prior to (left panels) or following (right panels) extraction using Triton X-100-containing buffers.

(B) Two hours after exposure of cells to 10 Gy of ionizing irradiation, extracted cells were stained using an anti-myc antibody and an anti-pSer/pThr-Gln epitope antibody that recognizes the phosphorylation motif generated by the DNA damage-response kinases ATM and ATR.

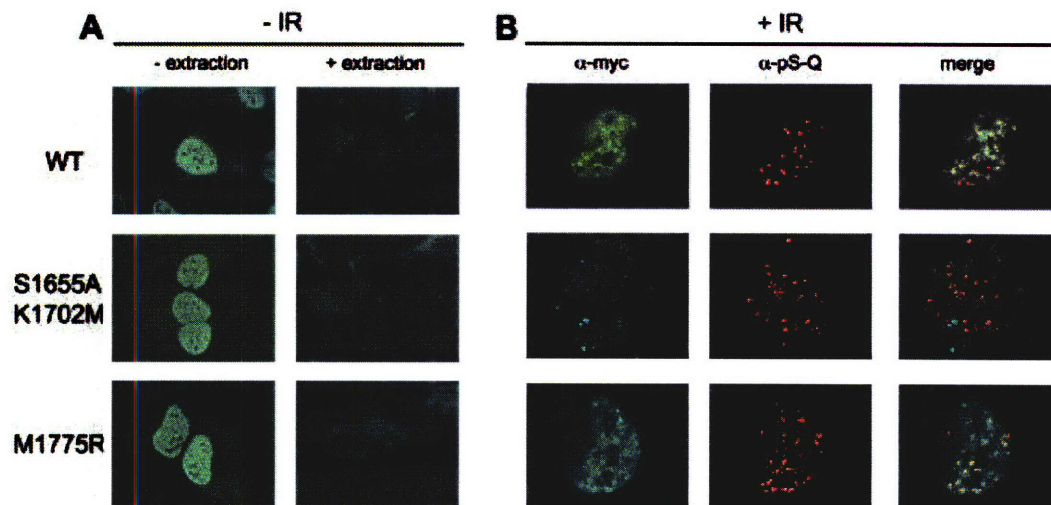


**Figure A1.13: Brca1 controls activation of MAPKAPK2**

HCC1937 cells, which do not have any functional Brca1, were complemented with full-length wild-type Brca1 (right three lanes) or vector alone (left three lanes). Cells were treated with doxorubicin or UV, in order to create a DNA damage response using DMSO as a control. Lysates were generated and probed for total MAPKAPK2, active MAPKAPK2, Brca1, and actin as a loading control. Brca1 was required to activate MAPKAPK2 after doxorubicin treatment, but not UV treatment.

<b>DMSO</b>	<b>+</b>	<b>-</b>	<b>-</b>	<b>+</b>	<b>-</b>	<b>-</b>
<b>doxorubicin</b>	<b>-</b>	<b>+</b>	<b>-</b>	<b>-</b>	<b>+</b>	<b>-</b>
<b>UV</b>	<b>-</b>	<b>-</b>	<b>+</b>	<b>-</b>	<b>-</b>	<b>+</b>

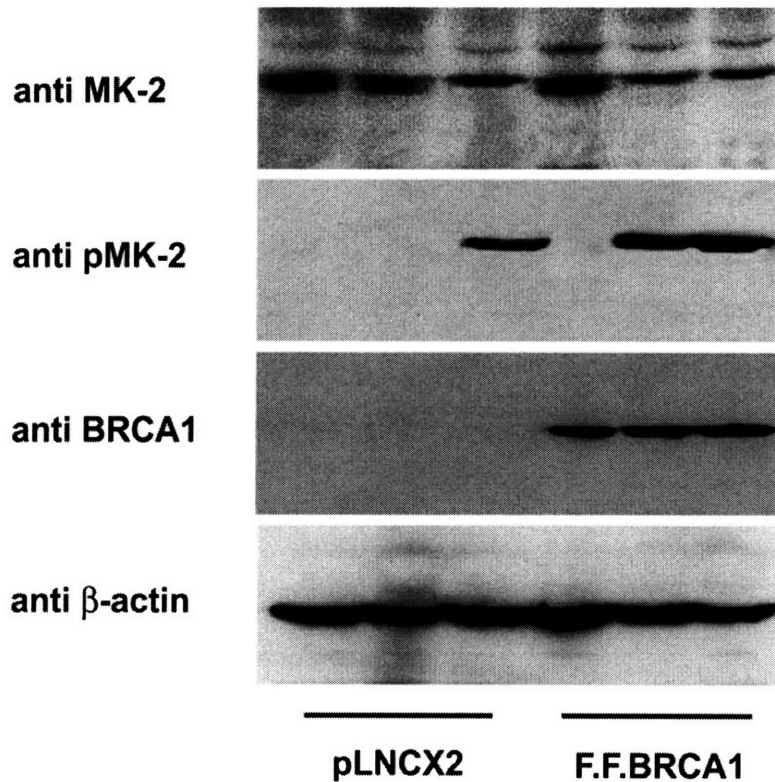


Table A1.1

Phosphoserine and Phosphothreonine Peptide									
Motif Selection by PTIP and BRCA1 Tandem BRCT Domains									
PTIP									
-4	-3	-2	-1		+1	+2	+3	+4	+5
X	Y (1.5)	G (2.3) D (1.5) E (1.4)	L (2.6) I (2.5) M (2.5) V (1.9)	<b>pS/pT</b>	Q	<u>V</u> (3.8) I (2.8)	<u>F</u> (7.0) <u>L</u> (4.3) <u>I</u> (4.1)	P (1.6)	I (2.9) F (2.7) L (2.4) V (2.0) Y (2.0)
X	X	E (1.3)	I (1.4) M (1.4) V (1.4) L (1.3)	<b>pS</b>	F (1.7) I (1.5) Q (1.5) Y (1.3)	V (1.8) T (1.5)	F	X	I (1.9) F (1.7) M (1.6) L (1.4)
G (1.6)	Y (1.1)	D (1.2) E (1.1)	L (1.2) I (1.2) M (1.2)	<b>pS</b>	Q (1.3) I (1.3) P (1.2)	V (2.1) I (1.7)	F (2.3) I (2.3) V (1.8) L (1.7) Y (1.5)	P (1.2)	Y (1.3)
X	X	X	I (2.1) L (1.8) W (1.3)	<b>pT</b>	Q (1.5) F (1.4) I (1.3)	Y (1.4)	I (1.4) L (1.3) V (1.2)	F (1.5) Y (1.4) P (1.3)	<b>A</b>
BRCA1									
-4	-3	-2	-1		+1	+2	+3	+4	+5
X	F (1.7) Y (1.6)	D (1.2) E (1.1)	I (1.4) V (1.3) L (1.2) M (1.2)	<b>pS/pT</b>	Q	<u>V</u> (3.1) T (2.6) I (2.2) S (1.7)	<u>F</u> (7.5) <u>Y</u> (5.2)	V (1.5) P (1.4)	<u>F</u> (4.5) G (1.8)
X	R (1.5) Y (1.4)	E (1.3) D (1.2)	V (1.4) I (1.3) M (1.3)	<b>pS</b>	F (2.1) Y (1.6) I (1.4) Q (1.4)	T (1.9) V (1.7)	F	X	F (1.6) M (1.4) Y (1.3)
X	X	Y (1.2)	X	<b>pS</b>	Q (1.4) F (1.3)	V (1.2) I (1.2)	F (2.4) Y (1.5)	I (1.2)	X
X	E (1.5)	D (1.9) E (1.5)	I (1.6) L (1.4)	<b>pT</b>	Q (1.5) E (1.4) F (1.3)	D (1.5) Y (1.3) I (1.2)	F (1.9) Y (1.2)	D (1.4) P (1.2)	<b>A</b>

A GST fusion of the PTIP or BRCA1 tandem BRCT domains was screened for binding to four phosphopeptide libraries, which contained the sequences GAXXXB(pS/pT)QJXXXAKKK, GAXXXpSXXFXXAYKKK, MAXXXpTXXXAKKK, and MAXXXSpXXXXAKKK, where X indicates all amino acids except Cys. In the library MAXXXB(pS/pT)QJXXXAKKK B indicates A, I, L, M, N, P, S, T, V, and J represents a biased mixture of 25% E, 75% X, while X indicates all amino acids except Arg, Cys, His, Lys for all positions in this library. Residues showing strong enrichment are underlined.

Table A1.2

<b>Peptide Binding Affinities for the Tandem BRCT Domains</b>			
<b>Peptide</b>	<b>Sequence</b>	<b>(BRCT)<sub>2</sub> Domain</b>	<b>K<sub>d</sub></b>
BRCTtide-7pS	GAAYDI- <b>pS</b> - QVFPPFAKKK	PTIP	280 nM
BRCTtide-7pT	GAAYDI- <b>pT</b> - QVFPPFAKKK	PTIP	2.1 μM
BRCTtide-7S	GAAYDI- <b>S</b> - QVFPPFAKKK	PTIP	N.D.B.
BRCTtide-7T	GAAYDI- <b>T</b> - QVFPPFAKKK	PTIP	N.D.B.
BRCTtide-7pS	GAAYDI- <b>pS</b> - QVFPPFAKKK	BRCA1	540 nm
BRCTtide-7pT	GAAYDI- <b>pT</b> - QVFPPFAKKK	BRCA1	4.5 μM
BRCTtide-7S	GAAYDI- <b>S</b> - QVFPPFAKKK	BRCA1	N.D.B.
BRCTtide-7T	GAAYDI- <b>T</b> - QVFPPFAKKK	BRCA1	N.D.B.

## References

1. Pawson, T., and Nash, P. (2003). Assembly of cell regulatory systems through protein interaction domains. *Science* 300, 445-452.
2. Zhou, B.B., and Elledge, S.J. (2000). The DNA damage response: putting checkpoints in perspective. *Nature* 408, 433-439.
3. Yaffe, M.B. (2002). Phosphotyrosine-binding domains in signal transduction. *Nat Rev Mol Cell Biol* 3, 177-186.
4. Yaffe, M.B., and Elia, A.E. (2001). Phosphoserine/threonine-binding domains. *Curr Opin Cell Biol* 13, 131-138.
5. Elia, A.E., Cantley, L.C., and Yaffe, M.B. (2003). Proteomic screen finds pSer/pThr-binding domain localizing Plk1 to mitotic substrates. *Science* 299, 1228-1231.
6. Scully, R., and Livingston, D.M. (2000). In search of the tumour-suppressor functions of BRCA1 and BRCA2. *Nature* 408, 429-432.
7. Venkitaraman, A.R. (2002). Cancer susceptibility and the functions of BRCA1 and BRCA2. *Cell* 108, 171-182.
8. Starita, L.M., and Parvin, J.D. (2003). The multiple nuclear functions of BRCA1: transcription, ubiquitination and DNA repair. *Curr Opin Cell Biol* 15, 345-350.
9. Powell, S.N., and Kachnic, L.A. (2003). Roles of BRCA1 and BRCA2 in homologous recombination, DNA replication fidelity and the cellular response to ionizing radiation. *Oncogene* 22, 5784-5791.
10. Cantor, S.B., Bell, D.W., Ganesan, S., Kass, E.M., Drapkin, R., Grossman, S., Wahrer, D.C., Sgroi, D.C., Lane, W.S., Haber, D.A., and Livingston, D.M. (2001). BACH1, a novel helicase-like protein, interacts directly with BRCA1 and contributes to its DNA repair function. *Cell* 105, 149-160.
11. Yu, X., Chini, C.C., He, M., Mer, G., and Chen, J. (2003). The BRCT domain is a phospho-protein binding domain. *Science* 302, 639-642.
12. Scully, R., Chen, J., Ochs, R.L., Keegan, K., Hoekstra, M., Feunteun, J., and Livingston, D.M. (1997). Dynamic changes of BRCA1 subnuclear location and phosphorylation state are initiated by DNA damage. *Cell* 90, 425-435.
13. Wang, Y., Cortez, D., Yazdi, P., Neff, N., Elledge, S.J., and Qin, J. (2000). BASC, a super complex of BRCA1-associated proteins involved in the recognition and repair of aberrant DNA structures. *Genes Dev* 14, 927-939.

14. Miki, Y., Swensen, J., Shattuck-Eidens, D., Futreal, P.A., Harshman, K., Tavtigian, S., Liu, Q., Cochran, C., Bennett, L.M., Ding, W., and et al. (1994). A strong candidate for the breast and ovarian cancer susceptibility gene BRCA1. *Science* 266, 66-71.
15. Couch, F.J., and Weber, B.L. (1996). Mutations and polymorphisms in the familial early-onset breast cancer (BRCA1) gene. *Breast Cancer Information Core. Hum Mutat* 8, 8-18.
16. Nathanson, K.L., Wooster, R., Weber, B.L., and Nathanson, K.N. (2001). Breast cancer genetics: what we know and what we need. *Nat Med* 7, 552-556.
17. Ford, D., Easton, D.F., Stratton, M., Narod, S., Goldgar, D., Devilee, P., Bishop, D.T., Weber, B., Lenoir, G., Chang-Claude, J., Sobol, H., Teare, M.D., Struewing, J., Arason, A., Scherneck, S., Peto, J., Rebbeck, T.R., Tonin, P., Neuhausen, S., Barkardottir, R., Eyfjord, J., Lynch, H., Ponder, B.A., Gayther, S.A., Zelada-Hedman, M., and et al. (1998). Genetic heterogeneity and penetrance analysis of the BRCA1 and BRCA2 genes in breast cancer families. The Breast Cancer Linkage Consortium. *Am J Hum Genet* 62, 676-689.
18. Callebaut, I., and Morion, J.P. (1997). From BRCA1 to RAP1: a widespread BRCT module closely associated with DNA repair. *FEBS Lett* 400, 25-30.
19. Huyton, T., Bates, P.A., Zhang, X., Sternberg, M.J., and Freemont, P.S. (2000). The BRCA1 C-terminal domain: structure and function. *Mutat Res* 460, 319-332.
20. Williams, R.S., Green, R., and Glover, J.N. (2001). Crystal structure of the BRCT repeat region from the breast cancer-associated protein BRCA1. *Nat Struct Biol* 8, 838-842.
21. Williams, R.S., and Glover, J.N. (2003). Structural consequences of a cancer-causing BRCA1-BRCT missense mutation. *J Biol Chem* 278, 2630-2635.
22. Ekblad, C.M., Wilkinson, H.R., Schymkowitz, J.W., Rousseau, F., Freund, S.M., and Itzhaki, L.S. (2002). Characterisation of the BRCT domains of the breast cancer susceptibility gene product BRCA1. *J Mol Biol* 320, 431-442.
23. Vallon-Christersson, J., Cayanan, C., Haraldsson, K., Loman, N., Bergthorsson, J.T., Brondum-Nielsen, K., Gerdes, A.M., Moller, P., Kristoffersson, U., Olsson, H., Borg, A., and Monteiro, A.N. (2001). Functional analysis of BRCA1 C-terminal missense mutations identified in breast and ovarian cancer families. *Hum Mol Genet* 10, 353-360.
24. Abraham, R.T. (2001). Cell cycle checkpoint signaling through the ATM and ATR kinases. *Genes Dev* 15, 2177-2196.

25. Kim, S.T., Lim, D.S., Canman, C.E., and Kastan, M.B. (1999). Substrate specificities and identification of putative substrates of ATM kinase family members. *J Biol Chem* 274, 37538-37543.
26. O'Neill, T., Dwyer, A.J., Ziv, Y., Chan, D.W., Lees-Miller, S.P., Abraham, R.H., Lai, J.H., Hill, D., Shiloh, Y., Cantley, L.C., and Rathbun, G.A. (2000). Utilization of oriented peptide libraries to identify substrate motifs selected by ATM. *J Biol Chem* 275, 22719-22727.
27. Lechner, M.S., Levitan, I., and Dressler, G.R. (2000). PTIP, a novel BRCT domain-containing protein interacts with Pax2 and is associated with active chromatin. *Nucleic Acids Res* 28, 2741-2751.
28. Cho, E.A., Prindle, M.J., and Dressler, G.R. (2003). BRCT domain-containing protein PTIP is essential for progression through mitosis. *Mol Cell Biol* 23, 1666-1673.
29. Shimizu, K., Bourillot, P.Y., Nielsen, S.J., Zorn, A.M., and Gurdon, J.B. (2001). Swift is a novel BRCT domain coactivator of Smad2 in transforming growth factor beta signaling. *Mol Cell Biol* 21, 3901-3912.
30. Yaffe, M.B., and Cantley, L.C. (2000). Mapping specificity determinants for protein-protein association using protein fusions and random peptide libraries. *Methods Enzymol* 328, 157-170.
31. Sarkaria, J.N., Busby, E.C., Tibbetts, R.S., Roos, P., Taya, Y., Karnitz, L.M., and Abraham, R.T. (1999). Inhibition of ATM and ATR kinase activities by the radiosensitizing agent, caffeine. *Cancer Res* 59, 4375-4382.
32. Rappold, I., Iwabuchi, K., Date, T., and Chen, J. (2001). Tumor suppressor p53 binding protein 1 (53BP1) is involved in DNA damage-signaling pathways. *J Cell Biol* 153, 613-620.
33. Schultz, L.B., Chehab, N.H., Malikzay, A., and Halazonetis, T.D. (2000). p53 binding protein 1 (53BP1) is an early participant in the cellular response to DNA double-strand breaks. *J Cell Biol* 151, 1381-1390.
34. Wang, B., Matsuoka, S., Carpenter, P.B., and Elledge, S.J. (2002). 53BP1, a mediator of the DNA damage checkpoint. *Science* 298, 1435-1438.
35. Manke, I.A., Lowery, D.M., Nguyen, A., and Yaffe, M.B. (2003). BRCT repeats as phosphopeptide-binding modules involved in protein targeting. *Science* 302, 636-639.



36. Rodriguez, M., Yu, X., Chen, J., and Songyang, Z. (2003). Phosphopeptide binding specificities of BRCA1 COOH-terminal (BRCT) domains. *J Biol Chem* 278, 52914-52918.
37. Joo, W.S., Jeffrey, P.D., Cantor, S.B., Finnin, M.S., Livingston, D.M., and Pavletich, N.P. (2002). Structure of the 53BP1 BRCT region bound to p53 and its comparison to the Brca1 BRCT structure. *Genes Dev* 16, 583-593.
38. Derbyshire, D.J., Basu, B.P., Serpell, L.C., Joo, W.S., Date, T., Iwabuchi, K., and Doherty, A.J. (2002). Crystal structure of human 53BP1 BRCT domains bound to p53 tumour suppressor. *Embo J* 21, 3863-3872.
39. Elia, E.A.H., Rellos, P., Haire, L.F., Chao, J.W., Ivins, F.J., Hoepker, K., Mohammad, D., Cantley, L.C., Smerdon, S.J., and Yaffe, M.B. (2003). The Molecular Basis for Phosphodependent Substrate Targeting and Regulation of Plks by the Polo-box Domain. *Cell*.
40. Cheng, K.Y., Lowe, E.D., Sinclair, J., Nigg, E.A., and Johnson, L.N. (2003). The crystal structure of the human polo-like kinase-1 polo box domain and its phospho-peptide complex. *Embo J* 22, 5757-5768.
41. Chen, J., Silver, D.P., Walpita, D., Cantor, S.B., Gazdar, A.F., Tomlinson, G., Couch, F.J., Weber, B.L., Ashley, T., Livingston, D.M., and Scully, R. (1998). Stable interaction between the products of the BRCA1 and BRCA2 tumor suppressor genes in mitotic and meiotic cells. *Mol Cell* 2, 317-328.
42. Scully, R., Ganesan, S., Vlasakova, K., Chen, J., Socolovsky, M., and Livingston, D.M. (1999). Genetic analysis of BRCA1 function in a defined tumor cell line. *Mol Cell* 4, 1093-1099.
43. Williams, R.S., Chasman, D.I., Hau, D.D., Hui, B., Lau, A.Y., and Glover, J.N. (2003). Detection of protein folding defects caused by BRCA1-BRCT truncation and missense mutations. *J Biol Chem* 278, 53007-53016.
44. Mirzoeva, O.K., and Petrini, J.H. (2001). DNA damage-dependent nuclear dynamics of the Mre11 complex. *Mol Cell Biol* 21, 281-288.
45. Nash, P., Tang, X., Orlicky, S., Chen, Q., Gertler, F.B., Mendenhall, M.D., Sicheri, F., Pawson, T., and Tyers, M. (2001). Multisite phosphorylation of a CDK inhibitor sets a threshold for the onset of DNA replication. *Nature* 414, 514-521.
46. Durocher, D., Taylor, I.A., Sarbassova, D., Haire, L.F., Westcott, S.L., Jackson, S.P., Smerdon, S.J., and Yaffe, M.B. (2000). The molecular basis of FHA domain:phosphopeptide binding specificity and implications for phospho-dependent signaling mechanisms. *Mol Cell* 6, 1169-1182.

47. Verdecia, M.A., Bowman, M.E., Lu, K.P., Hunter, T., and Noel, J.P. (2000). Structural basis for phosphoserine-proline recognition by group IV WW domains. *Nat Struct Biol* 7, 639-643.
48. Hoffmeister, A., Ropolo, A., Vasseur, S., Mallo, G.V., Bodeker, H., Ritz-Laser, B., Dressler, G.R., Vaccaro, M.I., Dagom, J.C., Moreno, S., and Iovanna, J.L. (2002). The HMG-I/Y-related protein p8 binds to p300 and Pax2 trans-activation domain-interacting protein to regulate the trans-activation activity of the Pax2A and Pax2B transcription factors on the glucagon gene promoter. *J Biol Chem* 277, 22314-22319.
49. Cho, Y.W., Hong, T., Hong, S., Guo, H., Yu, H., Kim, D., Guszczynski, T., Dressler, G.R., Copeland, T.D., Kalkum, M., and Ge, K. (2007). PTIP associates with MLL3- and MLL4-containing histone H3 lysine 4 methyltransferase complex. *J Biol Chem*.
50. Jowsey, P.A., Doherty, A.J., and Rouse, J. (2004). Human PTIP facilitates ATM-mediated activation of p53 and promotes cellular resistance to ionizing radiation. *J Biol Chem* 279, 55562-55569.
51. Kim, D., Wang, M., Cai, Q., Brooks, H., and Dressler, G.R. (2007). Pax transactivation-domain interacting protein is required for urine concentration and osmotolerance in collecting duct epithelia. *J Am Soc Nephrol* 18, 1458-1465.
52. Snouwaert, J.N., Gowen, L.C., Latour, A.M., Mohn, A.R., Xiao, A., DiBiase, L., and Koller, B.H. (1999). BRCA1 deficient embryonic stem cells display a decreased homologous recombination frequency and an increased frequency of non-homologous recombination that is corrected by expression of a brca1 transgene. *Oncogene* 18, 7900-7907.
53. Moynahan, M.E., Chiu, J.W., Koller, B.H., and Jasin, M. (1999). Brca1 controls homology-directed DNA repair. *Mol Cell* 4, 511-518.
54. Westermarck, U.K., Reyngold, M., Olshen, A.B., Baer, R., Jasin, M., and Moynahan, M.E. (2003). BARD1 participates with BRCA1 in homology-directed repair of chromosome breaks. *Mol Cell Biol* 23, 7926-7936.
55. Cantor, S., Drapkin, R., Zhang, F., Lin, Y., Han, J., Pamidi, S., and Livingston, D.M. (2004). The BRCA1-associated protein BACH1 is a DNA helicase targeted by clinically relevant inactivating mutations. *Proc Natl Acad Sci U S A* 101, 2357-2362.
56. Stucki, M., Clapperton, J.A., Mohammad, D., Yaffe, M.B., Smerdon, S.J., and Jackson, S.P. (2005). MDC1 directly binds phosphorylated histone H2AX to regulate cellular responses to DNA double-strand breaks. *Cell* 123, 1213-1226.

57. Liu, K., Lin, F.T., Ruppert, J.M., and Lin, W.C. (2003). Regulation of E2F1 by BRCT domain-containing protein TopBP1. *Mol Cell Biol* 23, 3287-3304.
58. Furuya, K., Poitelea, M., Guo, L., Caspari, T., and Carr, A.M. (2004). Chk1 activation requires Rad9 S/TQ-site phosphorylation to promote association with C-terminal BRCT domains of Rad4TOPBP1. *Genes Dev* 18, 1154-1164.
59. Glover, J.N., Williams, R.S., and Lee, M.S. (2004). Interactions between BRCT repeats and phosphoproteins: tangled up in two. *Trends Biochem Sci* 29, 579-585.
60. Li, J., Lee, G.I., Van Doren, S.R., and Walker, J.C. (2000). The FHA domain mediates phosphoprotein interactions. *J Cell Sci* 113 Pt 23, 4143-4149.
61. Schlegel, B.P., Starita, L.M., and Parvin, J.D. (2003). Overexpression of a protein fragment of RNA helicase A causes inhibition of endogenous BRCA1 function and defects in ploidy and cytokinesis in mammary epithelial cells. *Oncogene* 22, 983-991.
62. Otwinowski, Z. (1993). Oscillation data reduction program. In *Data Collection and Processing*, L. Sawyers, N. Isaacs and S. Bailey, eds. (Warrington, UK: SERC Daresbury Laboratory), pp. 56-62.
63. Collaborative Computational Project, N. (1994). The CCP4 suite: programs for protein crystallography. *Acta Crystallogr. D* 50, 760-763.
64. Jones, T.A., Zou, J.Y., Cowan, S.W., and Kjeldgaard (1991). Improved methods for binding protein models in electron density maps and the location of errors in these models. *Acta Crystallogr A* 47, 110-119.
65. Bateman, A., Birney, E., Durbin, R., Eddy, S.R., Finn, R.D., and Sonnhammer, E.L. (1999). Pfam 3.1: 1313 multiple alignments and profile HMMs match the majority of proteins. *Nucleic Acids Res* 27, 260-262.

# Appendix Two

## Natural-like Function in Artificial WW Domains

Adapted and Expanded From:

William P. Russ, Drew M. Lowery, Prashant Mishra,  
Michael B. Yaffe, and Rama Ranganathan.  
Natural-Like Function in Artificial WW Domains. *Nature* 437, 2005.

### Contributions:

Bill Russ designed and performed all experiments not described below and co-wrote the manuscript. Prashant Mishra helped Russ with WW domain cloning, expression, and purification. Mike designed the WW domain binding screen. Rama Ranganathan developed the SCA methodology, provided intellectual support to all portions of the project, and co-wrote the manuscript. I designed and executed the validation phase of the WW domain binding screen shown in Figure A2.2 and A2.3 and utilized in A2.4A, A2.5, and A2.6, wrote the methods section for this experiment, and designed the peptide array binding experiment shown in Figure A2.7.

## **Abstract**

Protein sequences evolve through random mutagenesis with selection for optimal fitness [1]. Cooperative folding into a stable tertiary structure is one aspect of fitness, but evolutionary selection ultimately operates on function, not on structure. In a previous paper [2], Ranganathan and colleagues proposed a model for the evolutionary constraint on a small protein interaction module (the WW domain) through application of the SCA, a statistical analysis of multiple sequence alignments [3, 4]. Construction of artificial protein sequences directed only by the SCA showed that the information extracted by this analysis is sufficient to engineer the WW fold at atomic resolution. Here, we demonstrate that these artificial WW sequences function like their natural counterparts, showing class-specific recognition of proline-containing target peptides [5-8]. Consistent with SCA predictions, a distributed network of residues mediates functional specificity in WW domains. The ability to recapitulate natural-like function in designed sequences shows that a relatively small quantity of sequence information is sufficient to specify the global energetics of amino acid interactions.

## Results and Discussion

The basic premise of the SCA is that in accord with the cooperative nature of amino acid interactions in determining protein stability and function, the evolutionary constraint on proteins should be a distributed (rather than intrinsic) property of amino acid positions. That is, the conservation of amino acids at one site should be the result of constraints on that site taken independently, and of the constraints arising through energetic interactions with other positions. For example, consider the SCA for an alignment of 292 members of the WW domain family (Figure A2.1). This small protein interaction module adopts a curved three-stranded  $\beta$ -sheet structure with a binding site for proline-containing peptides formed on the concave surface of the sheet (Figure A2.1A). The binding surface includes an X-Pro binding site (positions 19 and 30, shown in blue as CPK representation; Figure A2.1A) that recognizes the canonical proline in target peptides, and a specificity site formed by residues in  $\beta$  2 and the  $\beta$  2– $\beta$  3 loop (positions 21, 23 and 26, shown in yellow as CPK representation; Figure A2.1A) [9]. WW domains are classified into four groups based on target peptide sequence motifs: group I, PpxY [6]; group II, PPLP [7]; group III, PPR [5]; and group IV, pS/pT-P [8], where x stands for any amino acid. The SCA output for the WW family is a matrix of coupling values organized such that columns represent positions in the WW alignment, and rows represent sites where perturbations are introduced to interrogate evolutionary coupling [4] (Figure A2.1B). Thus, each pixel shows the coevolution score for one pair of WW sites. Hierarchical clustering of this matrix reveals a remarkably simple global organization of conserved evolutionary interactions between amino acids. WW positions fall into two main clusters, one that shows minimal coupling to other sites, and one that comprises eight positions (marked in red) related by strong mutual coevolution (Figure A2.1C).

Is the amino acid composition at sites plus the information in the SCA matrix all the sequence information required to specify the WW domain? The prior paper provides the first phase of this experimental test by showing that artificial sequences designed using only these parameters adopt a stable WW-like tertiary structure [2]. However, a key further test is the sufficiency of this information for specifying function. If the SCA matrix captures the fitness constraints on the WW family, then the artificial sequences

should show class-specific recognition of proline-containing sequences and binding affinities like those of natural WW domains.

In order to assess the function of our artificial generated sequences we had to design an oriented peptide library binding assay for measuring WW domain binding specificity. Four biotinylated degenerate peptide libraries were constructed, each oriented around one group-specific WW recognition motif (Table A2.1). For example, the group-I-oriented peptide library was biotin-Z-GMAxxxPPxYxxxAKKK, where Z is 6-aminohexanoic acid and x stands for any amino acid except cysteine (theoretical degeneracy of  $8.9 \times 10^8$  sequences). A fifth proline-oriented library was also made as a control for nonspecific binding (Table A2.1). At first we attempted to use these peptide libraries as probes in far western blots. The WW domains were run on SDS-PAGE, transferred to nitrocellulose, probed with the biotinylated peptide libraries, and detected with avidin-HRP. After confirming similar amounts of proteins were run by coomassie stain (Figure A2.2A) the WW domains were probed with the five peptide libraries (Figure A2.2B). Very clear binding was seen with the positive controls for PPxY binding, Yap1 and Yap2, along with fairly robust binding to N35 and the designed WW domains CP11 and CP43 to the PPxY library (Figure A2.2B). However, very little if any binding was seen to any of the other peptide libraries suggesting that this assay only works for tightly binding sequences. Further tweaking of the system through optimization of washing and biotin binding reagents did not improve the results of the assay, and no signal was ever seen for the other libraries including the pSP library with a Pin1 WW domain construct.

Failure of the far western approach for screening of WW domain binding motifs suggested that a more quantitative method was required, so we turned to a 96 well plate ELISA assay. In this assay the biotinylated peptide libraries were bound to streptavidin coated 96 well plates, the WW domains were incubated in the plates, and the WW domains that remained bound after extensive washing detected by GST-HRP since the WW domains were all produced as GST fusion proteins in bacteria. To quantify the binding the amount of horse radish peroxidase (HRP) present was determined by incubation with 3,3',5,5'-tetramethylbenzidine liquid substrate system for five minutes

(which was found to give the optimal signal to noise ratio). The reaction was stopped by the addition of sulfuric acid, and the absorbance measured at 450 nm which is the peak absorbance wavelength for the product after HRP mediated cleavage. Typical results are shown in Figure A2.3A with a picture of the plate shown in Figure A2.3B. The background seen with GST against each of the libraries was relatively low, but the background seen with each individual protein against no peptide or the Pro only peptide varied widely. However, after subtracting this background specific signals were seen as expected for the various WW domains indicated. Both the Yap and Taz WW domains gave specific PPxY binding as expected. FBP11A very specifically binds the PPLP library, which is as expected. Pin1 has very high background, but the only signal above background was seen with pSP, which is the expected binding motif. CP11, CP43, and N39 all bind PPxY as expected, but also have some background with the Pro only library perhaps due to the existence of a fraction of the PPxY motif in this library. Additionally CP43 bind pSP and N39 binds PPR. Further optimization of this protocol gave consistent results and thus it was adopted for use against the full panel of natural and designed WW domains.

For a group I domain (Nedd4.3, or N39 by the numbering system in the accompanying paper [2]) the peptide library assay confirms specific interaction with the PPxY-containing sequences [10] (Figure A2.4A). Interestingly, CC43, an artificial WW domain created through SCA-based protein design [2], also specifically interacts with the PPxY peptide library (Figure A2.4B), suggesting that CC43 functions as a group I WW domain. To confirm these results independently, we carried out phage-display and fluorescence-based quantitative binding assays for N39 and CC43. Consistent with the peptide library screens, both N39 and CC43 selectively isolate PPxY-containing sequences from a random 12-mer phage display library (Figure A2.4C,D). In addition, both of these domains show similar binding affinities to a model group I peptide (N39, dissociation constant ( $K_d$ ) =  $11.2 \pm 1.2 \mu\text{M}$ ; CC43,  $K_d = 1.7 \pm 0.1 \mu\text{M}$ ; mean  $\pm$  s.d.; Figure A2.4E). Taken together, these data validate the oriented peptide library assay for classification of WW domain specificity, and demonstrate that one artificial WW domain, CC43, displays group I-specific binding.



Figure 6.5 summarizes the results of peptide library screening for 27 randomly chosen natural and ten natively folded artificial WW domains [2]. The Pin1 WW domain was added to the list of natural domains tested because it is the best-characterized member of the group IV specificity class [11]. The data are shown in clustered matrix format, with each row showing the binding for one domain to all five oriented peptide libraries normalized between the minimum (white) and the maximum (black) observed signal to allow comparison of specificity profiles. Group I WW domains fell into two distinct subclusters (I and Im (marginal group I)) that significantly differed in the degree of specificity for the PPxY motif library (Figure A2.6). Group III domains bound to the PPR-oriented peptide library as expected but also showed binding to the PPxY library and weak binding to PPLP and proline-alone libraries. The binding to the PPxY library may simply reflect the fact that this library contains a non-trivial fraction of PPRY sequences. Nevertheless, the overall profiles show that group III domains display far more relaxed specificity than group I domains (Figure A2.6). A similar ambiguity in the binding specificity of group III domains has been reported previously [12]. Finally, a minor fraction of the total natural sequences tested (2 out of 28) bound to pSP- and PPLP-oriented libraries, and were scored as group IV and group II, respectively.

Artificial (CC) WW domains are functionally indistinguishable from natural WW sequences (Figure A2.5). Of the ten artificial domains studied, six displayed group I specificity (one is Im) and four showed group III specificity, numbers that approximately reflect the distribution of these sequences in our MSA and in prior samplings of WW specificity [13, 14]. Quantitative binding isotherms measured for all group I artificial sequences show a range of binding affinities typical for natural WW domains (Figure A2.5, rightmost column). To probe further the similarity between natural and designed WW sequences, we carried out a saturation mutagenesis study of the group I and group III peptide ligands. In this experiment, every position of the target peptide is replaced individually to each of the 20 amino acids, and the effect on binding is measured by detecting protein hybridization to the array of peptide variants [14]. Figure A2.7 shows these data for two natural WW domains (N39, group I [10], and N31, group III [5, 14]), and two artificial domains (CC43, group I, and CC20, group III), demonstrating that the

designed sequences show a pattern of sensitivity to ligand mutagenesis similar to that for natural sequences. Thus, the amino acid composition at sites plus the information contained in the SCA matrix encodes the sequence rules for quantitatively specifying function in the WW domain.

No artificial sequences with group II or group IV specificity were identified. However, the paucity of group II and group IV sequences in our alignment of natural WW domains and the relatively small number of artificial domains tested so far probably account for the lack of these specificity classes. These classes may emerge from larger-scale design of artificial WW sequences.

Given these results, can we infer which positions constitute the sequence determinants for WW binding specificity? The eight positions comprising the primary cluster of coevolving residues in the WW family (Figure A2.1C) are highlighted in yellow in Figure A2.5. Sequences experimentally found to display group I binding specificity, whether natural or designed, strictly conserve a specific sequence motif in the coevolving cluster (<sup>3</sup>L<sup>4</sup>P<sup>6</sup>G<sup>8</sup>E<sup>21</sup>I/V<sup>22</sup>D/N<sup>23</sup>H<sup>28</sup>T). In contrast, the average sequence identity in non-cluster positions is barely different for group I sequences in comparison with all WW sequences:  $40.9 \pm 2.9\%$  within group I sequences and  $35 \pm 3.9\%$  overall (mean  $\pm$  s.d.). These results strongly suggest that this network of mutually evolving residues is the major determinant of group I binding specificity. In accord with this conclusion, marginal group I domains or the weakly specific group III domains display considerable variation within this cluster. A larger study of designed sequences may help to distil the minimal sequence profiles of these and other WW groups.

The spatial organization of the network residues provides an unexpectedly distributed picture of binding specificity in the WW domain. Rather than being restricted to the ligand-binding surface, the eight network residues are organized into a physically contiguous network linking the primary specificity determining pocket (positions 21, 23 and 28) with residues on the opposite side (3 and 4) through a few intervening residues (6, 8 and 22) (Figure A2.8). The coevolution of these positions predicts that some residues act at long range in mediating peptide binding, and the network amino acids act

cooperatively in determining the binding free energy. Previous mutagenesis studies already suggest that network residues at or close to the peptide binding surface (8, 21, 23 and 28) mediate binding specificity [15-18], and structural work in the dystrophin WW domain provides a mechanistic understanding for the contribution of these residues in group I domains [19]. To test more of the network for contribution to peptide binding, and to test the prediction of cooperative action, we carried out thermodynamic double mutant cycle analysis [20, 21] to measure the energetic coupling between mutations at binding-site position 28 and positions 3, 8 and 23 in the Nedd4.3 WW domain. In the mutant cycle method, the effect of one mutation on the equilibrium dissociation constant for peptide binding is measured in two conditions: (1) the wild-type background ( $X1 = K_d^{M1}/K_d^{WT}$ ), and (2) in the background of a second mutation ( $X2 = K_d^{M1,M2}/K_d^{M2}$ ) (Figure A2.8B). The ratio of these effects gives the coupling parameter  $\beta$ , a measure of the degree of interaction between the two mutations. If the two mutations are thermodynamically independent, the effect of the first mutation is the same in conditions 1 and 2, and  $\beta = 1$ . If  $\beta \neq 1$ , then the two mutations act cooperatively.

Consistent with earlier studies [17, 19], the E8A, H23A and T28A mutations all affected binding of a PPxY-containing peptide (Figure A2.8C). However, L3A also had a significant effect ( $5.15 \pm 0.99$  fold; mean  $\pm$  s.d.), although located on the opposite surface from the peptide-binding site. In addition, mutant cycle analyses for the T28A mutation with each of the three other mutations show  $\beta$  values that significantly differ from unity (Figure A2.8C; see also Figure A2.9). Specifically, the effects of mutations at 3, 8 and 23 are either diminished (L3A and H23A) or abrogated (E8A) in the background of T28A (Figure A2.9). Thus T28A is thermodynamically coupled to mutations at 3, 8 and 23. These results support the model that a distributed and cooperative network of residues predicted by the SCA contributes to peptide recognition in the WW domain.

It is perhaps surprising that all folded artificial WW domains could be classified into a known functional group. The SCA emphasizes the deeply conserved couplings between sequence positions in a protein family while down-weighting or even ignoring less conserved couplings. These weak couplings typically arise from small clades of more recently diverged sequences in the MSA, which are expected to contain many positional

correlations yet to be relaxed through variation. If these recent branchings of the phylogenetic tree also hold important information about the physical chemistry of specific binding in extant proteins, we might have expected many folded but functionally undifferentiated WW domains in SCA-based design. The data here suggest that at least as defined by *in vitro* assays, information specifying binding specificity is captured in positional interactions that are in the deep evolutionary record. Future studies of functional complementation *in vivo* will help further to address the completeness of the SCA-based sequence information in specifying natural-like proteins.

Compared with the current field of protein design, the SCA-based protein design takes a completely different but complementary approach to understanding the design of natural proteins. Using atomistic energy functions that approximate the physical forces between atoms, several groups have now achieved spectacular successes in the re-design of natural folds [22-24], including WW domains [25], and even in the *de novo* construction of artificial folds [26, 27]. These successes demonstrate the accuracy of the scoring functions used, but important unsolved issues remain. The basic design principle in atomistic protein design is optimization of a target potential function that produces sequences with deep thermodynamic minima in the native state and structures with high thermal stabilities [22, 27]. However, natural proteins are thought to have native states with shallow energy minima, resulting in marginally stable but dynamic folds that are often capable of supporting more than one conformation. In a purely statistical and mechanism-free way, SCA-based protein design produces sequences that show the same marginal stability of natural proteins and function like natural proteins. It may be interesting to combine the mechanistic description of energetics from atomistic design with the sparse and distributed architecture of amino acid interactions in SCA to understand better the design of evolved proteins. Ultimately having a better understanding of how folding relates to function in WW domains will allow the design of more potent or novel action inhibitors which may at a minimum be useful in treatment of Pin1 overexpressing breast cancers [28].

## **Experimental Procedures**

### **Statistical coupling analysis**

SCA was conducted as previously described [3, 4] on an alignment of 292 WW domain sequences, updated from the original alignment of 120 sequences in the accompanying paper using the March 2004 release of the non-redundant database. SCA results are essentially identical for the two alignments. Sequences were collected using PSI-BLAST (*e*-scores <0.001) and aligned using ClustalW [29] followed by manual adjustment. The alignment is available from our laboratory website (<http://www.hhmi.swmed.edu/Labs/rr>), and the code is available upon request.

### **Oriented peptide library assay**

Five biotinylated degenerate peptide libraries were synthesized using N- $\alpha$ -Fmoc protected amino acids and standard BOP/HOBt coupling chemistry. The libraries were constructed to present either a proline-only control (biotin-Z-GMAxxxxPxxxxAKKK) or the four different characteristic WW domain binding motifs: group-I-oriented (biotin-Z-GMAxxxPPxYxxxAKKK), group-II-oriented (biotin-Z-GMAxxxPPLPxxxAKKK), group-III-oriented (biotin-Z-GMAxxxPPRxxxAKKK) and group-IV-oriented (biotin-Z-GMAxxxxpSPxxxxAKKK), where Z is 6-aminohexanoic acid, pS is phosphoserine, and x denotes all amino acids except cysteine. In the original assay design these peptide libraries were used as probes for WW domains in a far western blot. WW domains purified from bacteria were run on SDS-PAGE, transferred to nitrocellulose, probed with the biotinylated peptide libraries, and detected using avidin-HRP (Sigma). To visualize the signal ECL (Enhanced chemiluminescence – Perkin Elmer) was used and the nitrocellulose exposed to Biomax film (Kodak). Subsequently a different assay was used as described below. Peptide libraries were immobilized onto pre-washed streptavidin-coated 96-well plates (10  $\mu$ g per well) in phosphate-buffered saline plus 0.5% Tween-20 (PBST) at 4 °C for 1 h. Wells were washed in PBST and incubated with GST-WW

domains (0.5  $\mu$ g) for 2 h, washed, and detected by ELISA using a horseradish peroxidase-conjugated anti-GST antibody (Amersham) at 1:5,000 dilution for 1 h at 4 °C followed by reaction with 3,3',5,5'-tetramethylbenzidine liquid substrate system (Sigma) for 5 min. Absorbance was monitored at 450 nm.

### **Phage display**

Phage display was carried out using a commercial random 12-mer library (PhD Phage Display kit, NEB) per protocols supplied by the manufacturer. Phage isolates were sequenced after three rounds of amplification and nonspecific elution with glycine-HCl, pH 2.2.

### **Binding assays**

Tryptophan fluorescence-based peptide binding assays were conducted on a PTI spectrofluorimeter, monitoring fluorescence emission at 340 nm (excitation at 295 nm). Group I peptide, EYPPYPPPPYPSG (Tufts Protein Chemistry Facility), was purified using reverse-phase high-performance liquid chromatography. Binding assays were conducted at 4 °C in buffer A (100 mM TrisHCL, pH 8.0, 100 mM NaCl) with 1  $\mu$ M WW domain. WW domains were cloned into the pHIS8-3 vector (provided by J. P. Noel), expressed and purified as described [2]. The assay follows the fraction of protein bound to peptide by the normalized fluorescence quenching of the Trp residue in the X-Pro binding pocket. Isothermal titration calorimetry measurements were made using a MicroCal VP-ITC calorimeter in buffer A at 4 °C, starting with 50–200  $\mu$ M WW domain in the sample cell and titrating 0.5–3 mM of the group I peptide. Data were fit using MicroCal Origin software provided by the manufacturer, using a one-site binding model. The marginal stability of WW domains required correction of apparent dissociation constants to account for the fraction of folded protein at the assay temperature. Assuming a two-state folding reaction, the correction applied was  $K_d = K_{d,app} \left( \frac{K_f}{1+K_f} \right)$ , where  $K_f$  is the equilibrium constant for the folding reaction. For each protein assayed,  $K_f$  was calculated using thermal denaturation studies carried out as in the accompanying paper [2], and assuming a previously reported value for the change in heat capacity for the unfolding

reaction[30].  $K_f$  values were: wild type, 38.8; L3A, 1.65; E8A, 15.7; H23A, 22.7; T28A, 32.0; L3A/T28A, 1.25; E8A/T28A, 8.54; H23A/T28A, 21.5.

### **Protein hybridization assay**

Protein hybridization assays were performed as described [14]. Arrays of all single amino acid substitutions for a group I peptide (GTPPPPYTVG) and a group III peptide (PPGPPPRGPPP) were synthesized on membranes by the M.I.T. Biopolymers Laboratory. Membranes were washed in PBS plus 0.1% Tween-20 (PBST), blocked for 2 h at room temperature in PBST plus 5% non-fat dry milk, washed, and incubated at 4 °C overnight with 10–400  $\mu\text{g ml}^{-1}$  of purified GST–WW domains. Membranes were washed, treated with horseradish peroxidase-conjugated anti-GST antibodies (Sigma) in PBST plus 5% non-fat dry milk at 4 °C for 2 h, washed again, and bound WW domains were detected using the ECL kit (Amersham).

**Figure A2.1**

**(A)** The peptide-binding surface of the WW domain contains two structurally defined pockets: the X-Pro binding site (in blue) and a specificity site (in yellow). Shown is the Nedd4.3 WW domain (Protein Data Bank 1I5H) bound to a group I peptide (in green) [31].

**(B)** A matrix of coevolution scores between all WW positions (columns) and 12 moderately conserved positions (rows) in an alignment of 292 WW domains. The colour scale ranges from blue (no coevolution) to red (maximal coevolution). Checked boxes mark the trivial self-correlation of sites in the SCA method.

**(C)** Hierarchical clustering shows that a single group of eight positions (marked in red) share a pattern of strong mutual coevolution.

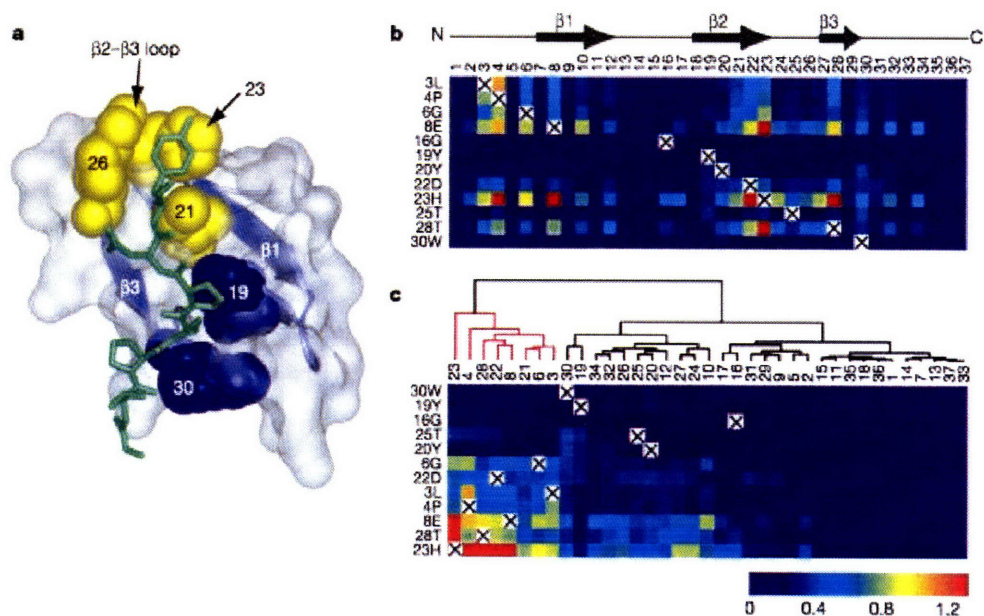




**Figure A2.2**

(A) Coomassie blue stained gel of the indicated WW domains purified from bacteria indicate approximately equal loading.

(B) WW domains detected by far western with the indicated biotinylated peptide library.

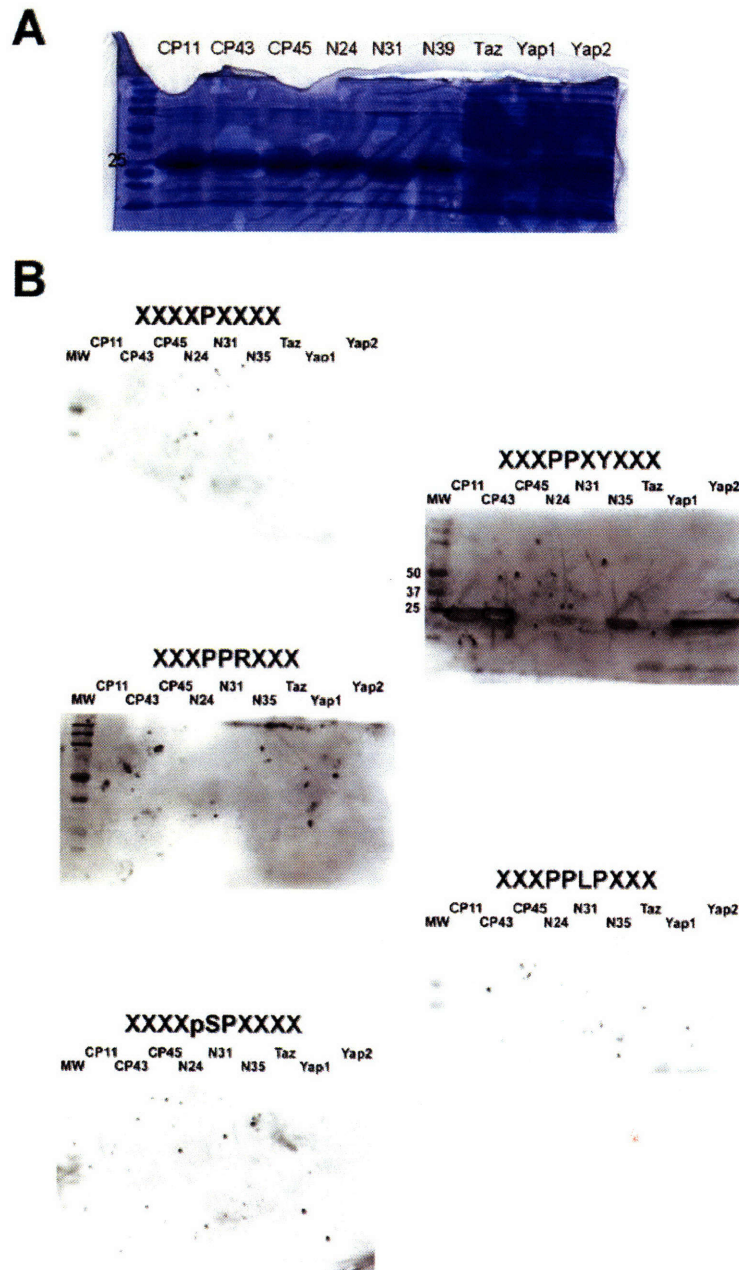


**Figure A2.3**

**(A)** Values of absorbance readings at 405nm of the plate shown in part B that indicate the amount of binding of the WW domains listed across the top to the biotinylated peptide libraries listed across the right. Well lanes and columns are also noted for convenience.

**(B)** Scan of 96 well plate after ELISA assay to determine binding between the WW domains and biotinylated peptide libraries indicated in part A.

**A.**

	None 1	Yap1 2	Yap1 3	Yap2 4	FBP11 5	FBP30 6	Pin1 7	Taz 8	CP11 9	CP43 10	N39 11	GST 12	
<b>B</b>	0	.0502	.1617	.0751	.1640	.3112	.9701	.1599	.2683	.2071	.4618	.0784	<b>None</b>
<b>C</b>	.0406	.0576	.0841	.0562	.2142	.3422	1.0126	.3861	.5042	.8376	.7066	.1630	<b>P</b>
<b>D</b>	.0204	.5418	.5137	.5598	.1914	.4008	.8084	.5504	.6719	.8367	.8312	.1807	<b>PPXY</b>
<b>E</b>	.0684	.0739	.1205	.0914	.1871	.2289	.8468	.2408	.2174	.2093	.7241	.0781	<b>PPR</b>
<b>F</b>	.1489	.1183	.0867	.0479	.5945	.4357	.8575	.1841	.1618	.2181	.4622	.1150	<b>PPLP</b>
<b>G</b>	.0160	.0758	.1237	.0488	.1595	.3350	1.4280	.0696	.1400	.4314	.4863	.0383	<b>pSP</b>

**B.**



**Figure A2.4**

**(A,B)** Oriented peptide library screening (see Methods) of binding specificity for N39, a natural domain with group I (PPxY) specificity **(A)**, or CC43, an artificial WW domain showing 37% average and 68% top-hit identity to natural WW domains in the MSA **(B)**. Binding is reported as fold above background in the absence of target peptides.

**(C,D)** Phage display analysis of binding specificity for N39 and CC43 WW domains; both domains select PPxY-containing sequences from a random 12-mer peptide library.

**(E)** Binding isotherms for N39 ( $K_d = 11.2 \pm 1.2 \mu\text{M}$ ) and CC43 ( $K_d = 1.7 \pm 0.1 \mu\text{M}$ ), assayed by Trp fluorescence quenching using a model group I peptide (EYPPYPPPPYPSG). Error bars represent standard deviation from at least four independent assays.

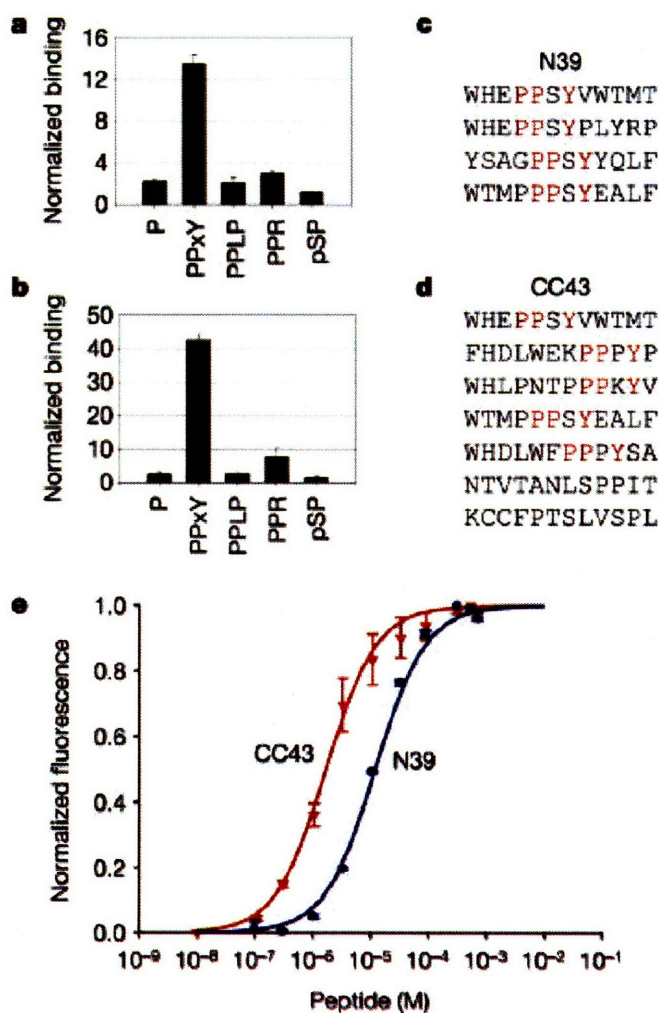




**Figure A2.5**

The matrix shows the results of oriented peptide library assays, clustered to reveal the similarities in binding specificity for different domains. The colour scale ranges from white (minimum signal) to black (maximum signal) for each domain. Class assignments for domains are shown at the right. Dissociation constants for selected group I domains were either measured by fluorescence binding assay (N39 and all artificial sequences) or were derived from literature references. Sequences are aligned per the MSA, and positions corresponding to the cluster of eight coevolving residues (Figure A2.1C) are highlighted in yellow. SCA-based designed sequences are shown in bold. Measurements are mean  $\pm$  s.d.

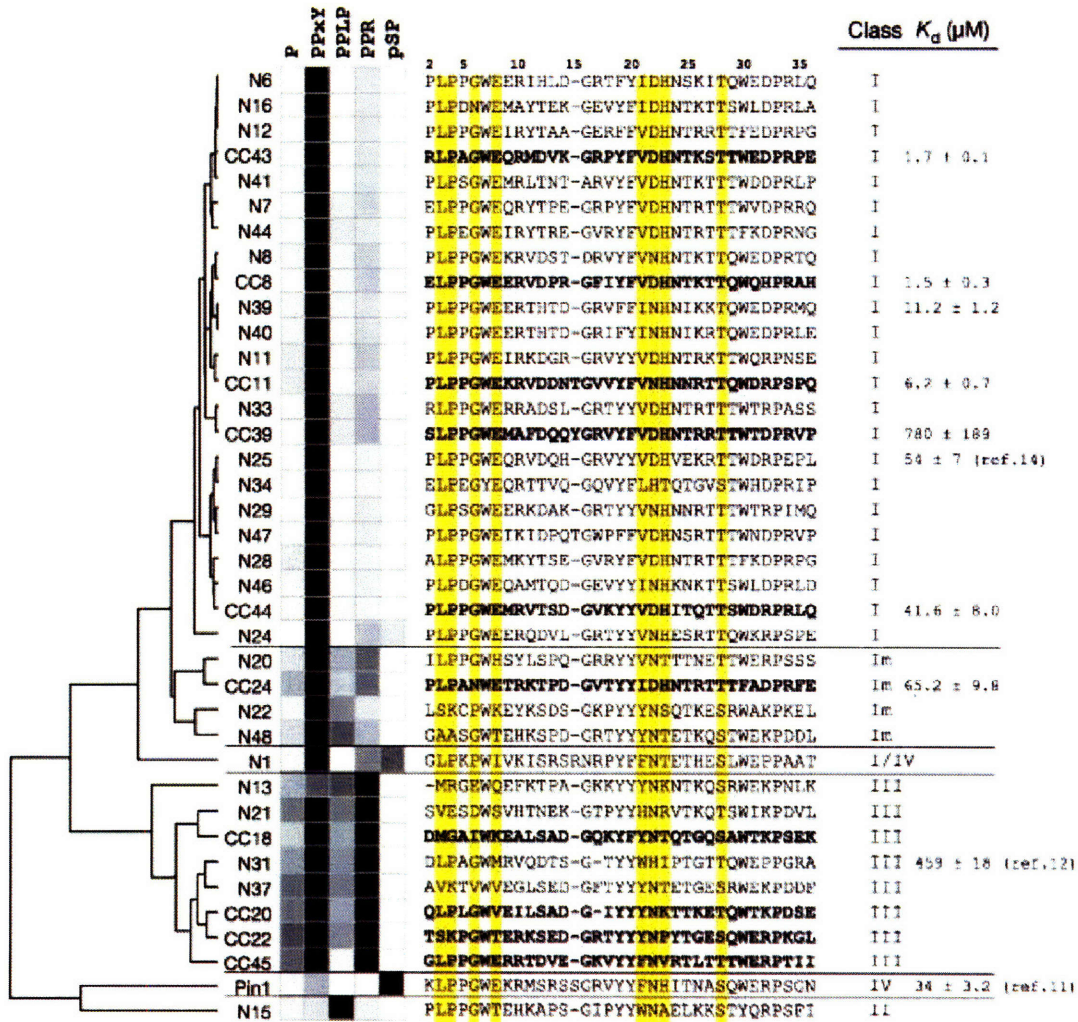


## Figure A2.6

**(A)** Binding specificity assays determined by the oriented peptide library assay for 28 natural WW domains. Binding is measured by ELISA using an HRP-assay, and the data are reported as fold above background binding in the absence of peptide substrate.

Peptide libraries are as described in the Figure A2.4 legend. Error bars show the standard deviation of 3-4 independent measurements.

**(B)** As in **A** for 10 artificial WW domains designed using the SCA matrix [2].

Figure A2.6 Continued

A

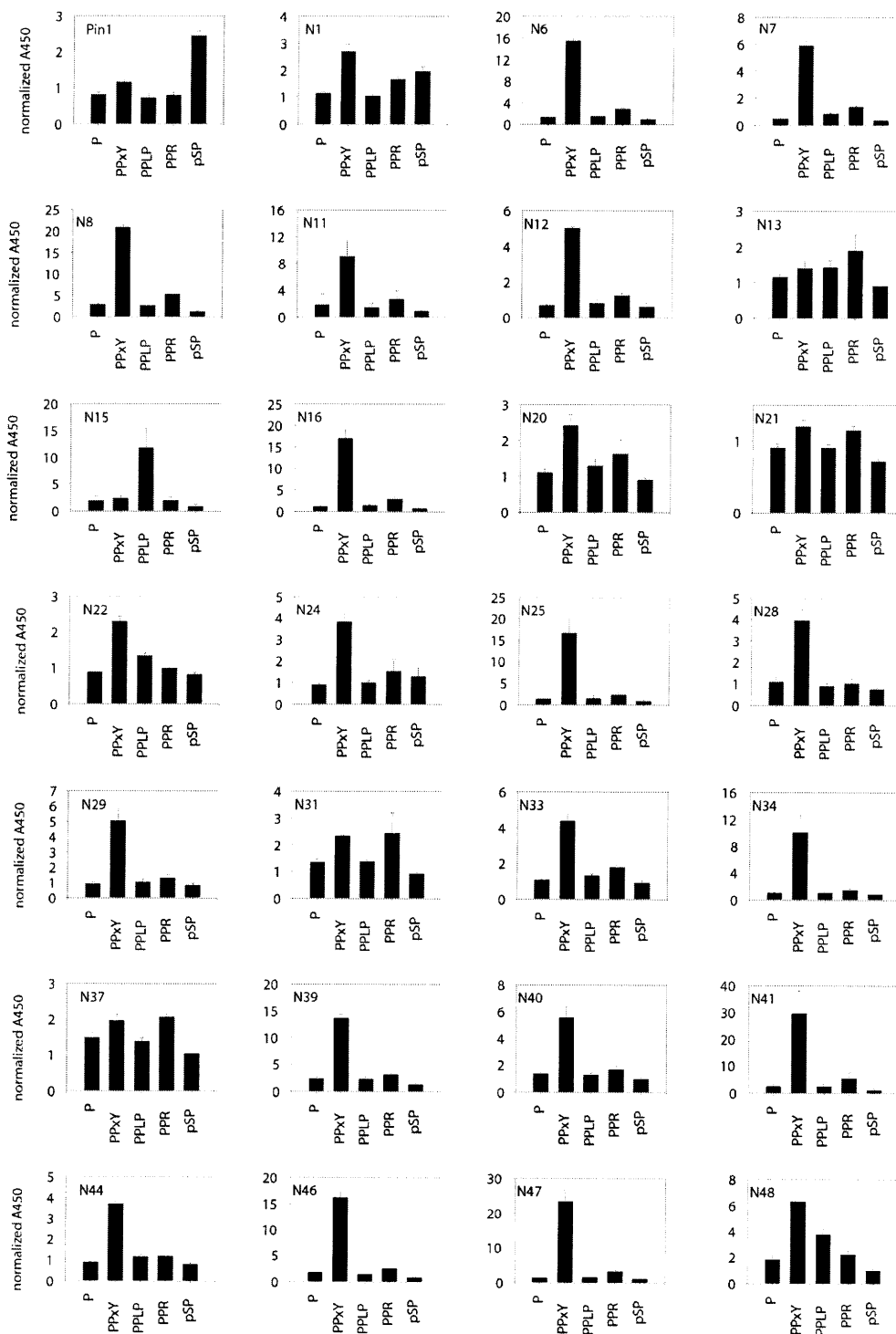
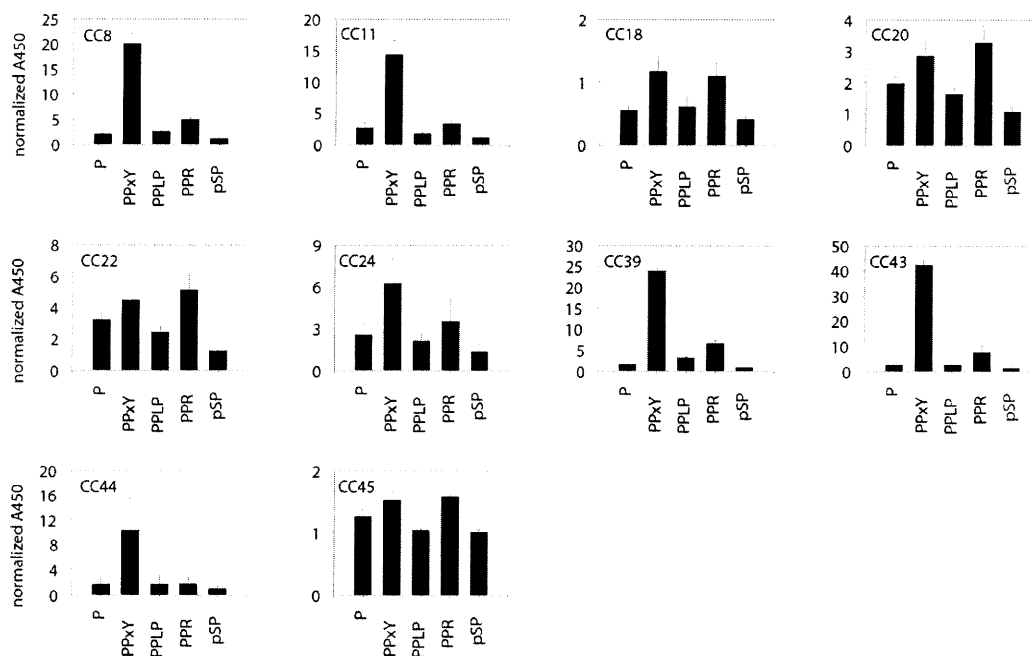


Figure A2.6 Continued

B



### Figure A2.7

Saturation mutagenesis of the peptide ligands for the two major functional classes of WW domains identified.

(A) A natural group I (Nedd4.3) WW domain was assayed for binding to an array of immobilized peptides representing all possible amino acid substitutions to a canonical group I peptide. The wild-type peptide sequence is given at the left of the blot, and each row represents the binding to peptides where that position is mutated to every amino acid as marked.

(B) A natural group III (FE65.1) WW domain assayed as in A using a canonical group III peptide.

(C) As in (A) with the group I artificial WW domain CC43. The artificial domain shows the same pattern of sensitivity to mutation of ligand positions as the natural domain.

(D) As in (B) with a group III artificial WW domain CC20. The artificial domain shows the same pattern of sensitivity to mutation of ligand positions as the natural domain.

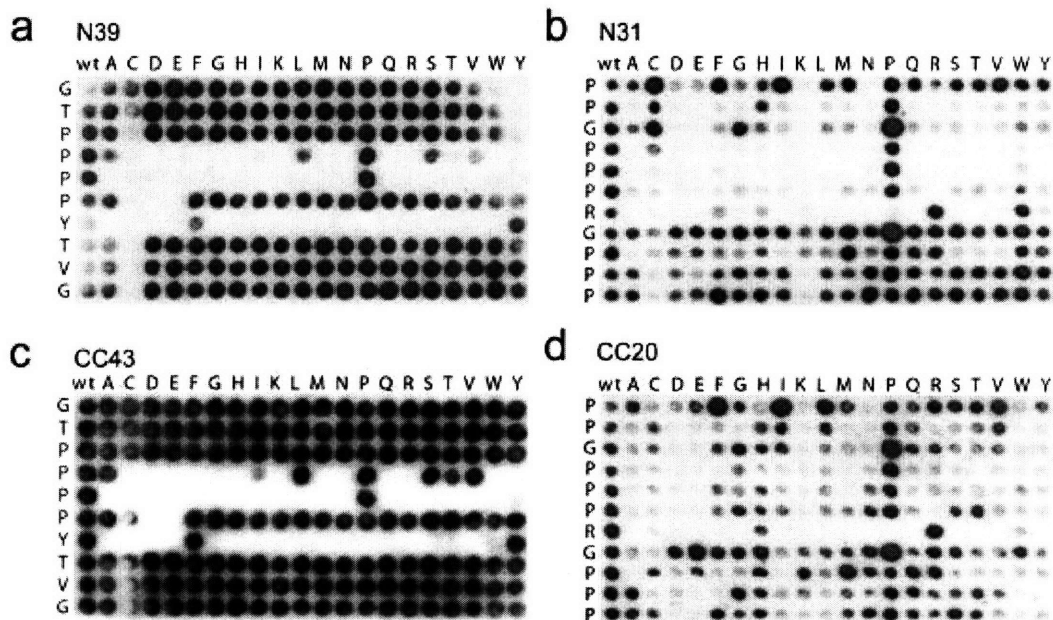




**Figure A2.8**

(A) The cluster of eight coevolving residues (Figure A2.1C) mapped on the Nedd4.3 WW domain structure (in red). The cluster forms a connected network that links binding site residues with the opposite side through a few intervening positions.

(B) The thermodynamic mutant cycle formalism. The fold effect of one mutation (M1) on an equilibrium constant is calculated in the wild-type background (X1) or in the background of the second mutation (X2). The coupling parameter  $\Omega$  is the ratio of these fold effects (X1/X2); that is, the degree to which the effect of one mutation depends on the second.

(C) Mutant cycle analysis of selected coevolving positions. Residues are shown in the same orientation as in A (right), with distances between  $\beta$ -carbons of residues indicated. Single mutations at all sites affect peptide binding (fold effect relative to wild type in parentheses), and mutant cycle analysis demonstrates energetic coupling ( $\Omega > 1$ ) between position 28 and positions 3, 8 and 23. Measurements are mean  $\pm$  s.d.

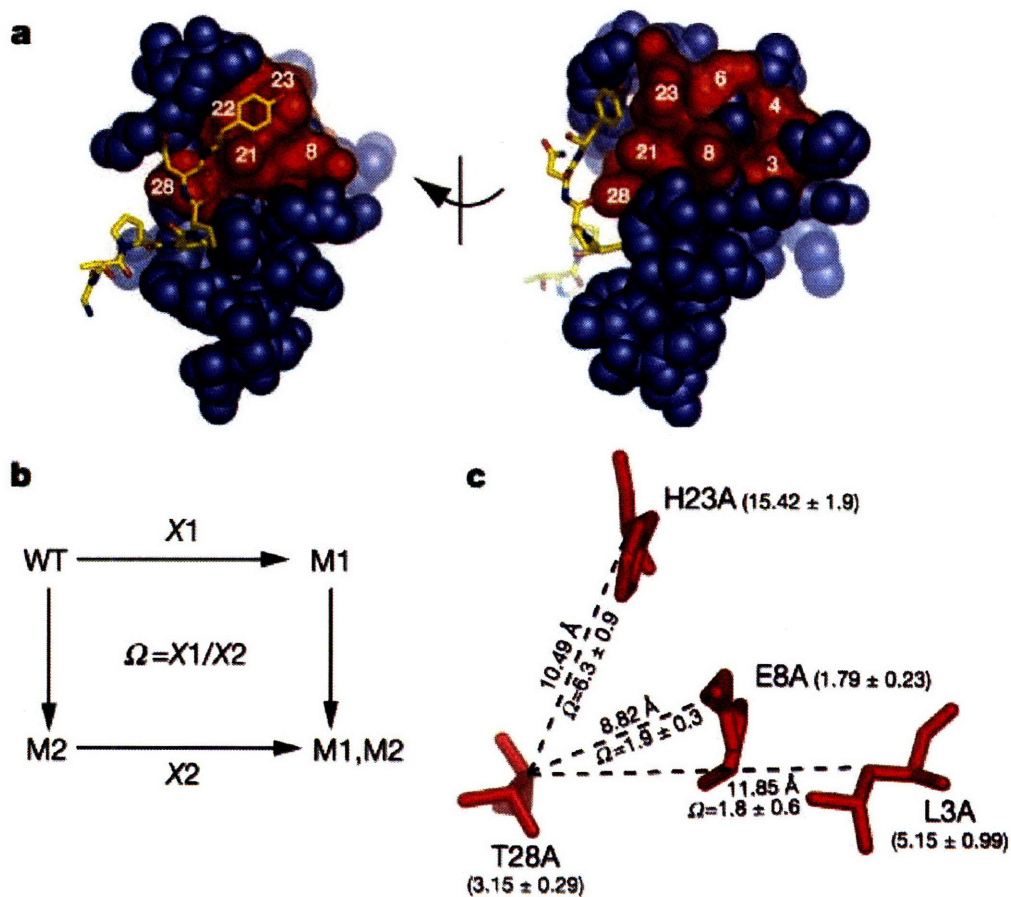


**Figure A2.9**

Thermodynamic double mutant cycles [20, 21] in the WW domain Nedd4.3 (N39), measuring the energetic coupling between the T28A mutant and mutants at three other sites within the network of co-evolving residues (L3A, E8A, and H23A). The thermodynamic mutant cycle formalism is shown in Figure A2.6B. Briefly, each corner of the box contains the equilibrium dissociation constant for a group I peptide (EYPPYPPPPYPSG) and either wild-type, single mutant, or double mutant WW proteins, measured through isothermal titration calorimetry. Values represent the mean and standard deviation of at least three measurements, reported in units of  $\mu\text{M}$ .  $\Omega$  is the coupling parameter as described in the text.

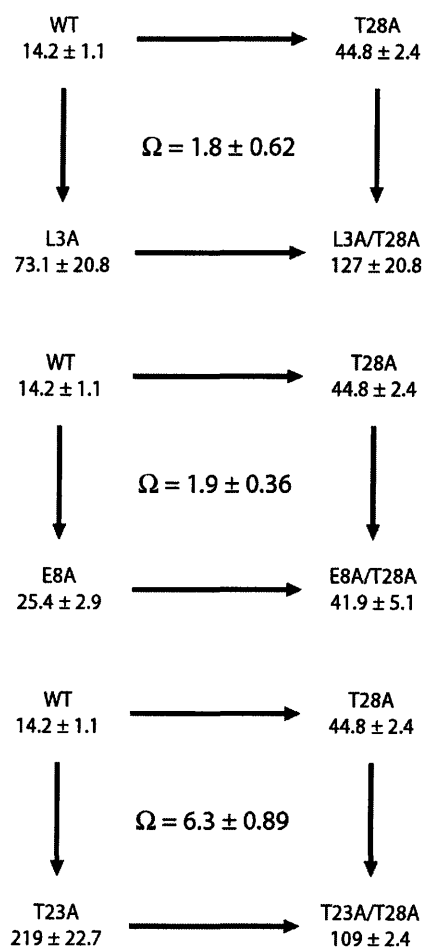


**Table A2.1: The Peptide Libraries**

<b>Orientation</b>	<b>Library Name</b>	<b>Peptide Library Sequence</b>
proline-only control	P	biotin-Z-GMAxxxxPxxxxAKKK
group-I-oriented	PPxY	biotin-Z-GMAxxxPPxYxxxAKKK
group-II-oriented	PPR	biotin-Z-GMAxxxPPLPxxxAKKK
group-III-oriented	PPLP	biotin-Z-GMAxxxPPRxxxAKKK
group-IV-oriented	pSP	biotin-Z-GMAxxxxpSPxxxxAKKK

## References

1. Voigt, C.A., Kauffman, S., and Wang, Z.G. (2000). Rational evolutionary design: the theory of in vitro protein evolution. *Adv Protein Chem* 55, 79-160.
2. Socolich, M., Lockless, S.W., Russ, W.P., Lee, H., Gardner, K.H., and Ranganathan, R. (2005). Evolutionary information for specifying a protein fold. *Nature* 437, 512-518.
3. Lockless, S.W., and Ranganathan, R. (1999). Evolutionarily conserved pathways of energetic connectivity in protein families. *Science* 286, 295-299.
4. Suel, G.M., Lockless, S.W., Wall, M.A., and Ranganathan, R. (2003). Evolutionarily conserved networks of residues mediate allosteric communication in proteins. *Nat Struct Biol* 10, 59-69.
5. Bedford, M.T., Sarbassova, D., Xu, J., Leder, P., and Yaffe, M.B. (2000). A novel pro-Arg motif recognized by WW domains. *J Biol Chem* 275, 10359-10369.
6. Chen, H.I., and Sudol, M. (1995). The WW domain of Yes-associated protein binds a proline-rich ligand that differs from the consensus established for Src homology 3-binding modules. *Proc Natl Acad Sci U S A* 92, 7819-7823.
7. Ermekova, K.S., Zambrano, N., Linn, H., Minopoli, G., Gertler, F., Russo, T., and Sudol, M. (1997). The WW domain of neural protein FE65 interacts with proline-rich motifs in Mena, the mammalian homolog of *Drosophila* enabled. *J Biol Chem* 272, 32869-32877.
8. Lu, P.J., Zhou, X.Z., Shen, M., and Lu, K.P. (1999). Function of WW domains as phosphoserine- or phosphothreonine-binding modules. *Science* 283, 1325-1328.
9. Zarrinpar, A., and Lim, W.A. (2000). Converging on proline: the mechanism of WW domain peptide recognition. *Nat Struct Biol* 7, 611-613.
10. Kanelis, V., Rotin, D., and Forman-Kay, J.D. (2001). Solution structure of a Nedd4 WW domain-ENaC peptide complex. *Nat Struct Biol* 8, 407-412.
11. Verdecia, M.A., Bowman, M.E., Lu, K.P., Hunter, T., and Noel, J.P. (2000). Structural basis for phosphoserine-proline recognition by group IV WW domains. *Nat Struct Biol* 7, 639-643.
12. Kato, Y., Nagata, K., Takahashi, M., Lian, L., Herrero, J.J., Sudol, M., and Tanokura, M. (2004). Common mechanism of ligand recognition by group II/III WW domains: redefining their functional classification. *J Biol Chem* 279, 31833-31841.

13. Hu, H., Columbus, J., Zhang, Y., Wu, D., Lian, L., Yang, S., Goodwin, J., Luczak, C., Carter, M., Chen, L., James, M., Davis, R., Sudol, M., Rodwell, J., and Herrero, J.J. (2004). A map of WW domain family interactions. *Proteomics* 4, 643-655.
14. Otte, L., Wiedemann, U., Schlegel, B., Pires, J.R., Beyermann, M., Schmieder, P., Krause, G., Volkmer-Engert, R., Schneider-Mergener, J., and Oschkinat, H. (2003). WW domain sequence activity relationships identified using ligand recognition propensities of 42 WW domains. *Protein Sci* 12, 491-500.
15. Chen, H.I., Einbond, A., Kwak, S.J., Linn, H., Koepf, E., Peterson, S., Kelly, J.W., and Sudol, M. (1997). Characterization of the WW domain of human yes-associated protein and its polyproline-containing ligands. *J Biol Chem* 272, 17070-17077.
16. Espanel, X., and Sudol, M. (1999). A single point mutation in a group I WW domain shifts its specificity to that of group II WW domains. *J Biol Chem* 274, 17284-17289.
17. Kasanov, J., Pirozzi, G., Uveges, A.J., and Kay, B.K. (2001). Characterizing Class I WW domains defines key specificity determinants and generates mutant domains with novel specificities. *Chem Biol* 8, 231-241.
18. Toepert, F., Pires, J.R., Landgraf, C., Oschkinat, H., and Schneider-Mergener, J. (2001). Synthesis of an Array Comprising 837 Variants of the hYAP WW Protein Domain This work was supported by the DFG (INK 16/B1-1), by the Fonds der Chemischen Industrie, and by the Universitätsklinikum Charite Berlin. *Angew Chem Int Ed Engl* 40, 897-900.
19. Huang, X., Poy, F., Zhang, R., Joachimiak, A., Sudol, M., and Eck, M.J. (2000). Structure of a WW domain containing fragment of dystrophin in complex with beta-dystroglycan. *Nat Struct Biol* 7, 634-638.
20. Carter, P.J., Winter, G., Wilkinson, A.J., and Fersht, A.R. (1984). The use of double mutants to detect structural changes in the active site of the tyrosyl-tRNA synthetase (*Bacillus stearothermophilus*). *Cell* 38, 835-840.
21. Hidalgo, P., and MacKinnon, R. (1995). Revealing the architecture of a K<sup>+</sup> channel pore through mutant cycles with a peptide inhibitor. *Science* 268, 307-310.
22. Dahiyat, B.I., and Mayo, S.L. (1997). De novo protein design: fully automated sequence selection. *Science* 278, 82-87.
23. Dwyer, M.A., Looger, L.L., and Hellinga, H.W. (2004). Computational design of a biologically active enzyme. *Science* 304, 1967-1971.

24. Kortemme, T., Joachimiak, L.A., Bullock, A.N., Schuler, A.D., Stoddard, B.L., and Baker, D. (2004). Computational redesign of protein-protein interaction specificity. *Nat Struct Mol Biol* *11*, 371-379.
25. Kraemer-Pecore, C.M., Lecomte, J.T., and Desjarlais, J.R. (2003). A de novo redesign of the WW domain. *Protein Sci* *12*, 2194-2205.
26. Harbury, P.B., Plecs, J.J., Tidor, B., Alber, T., and Kim, P.S. (1998). High-resolution protein design with backbone freedom. *Science* *282*, 1462-1467.
27. Kuhlman, B., Dantas, G., Ireton, G.C., Varani, G., Stoddard, B.L., and Baker, D. (2003). Design of a novel globular protein fold with atomic-level accuracy. *Science* *302*, 1364-1368.
28. Wulf, G.M., Ryo, A., Wulf, G.G., Lee, S.W., Niu, T., Petkova, V., and Lu, K.P. (2001). Pin1 is overexpressed in breast cancer and cooperates with Ras signaling in increasing the transcriptional activity of c-Jun towards cyclin D1. *Embo J* *20*, 3459-3472.
29. Thompson, J.D., Higgins, D.G., and Gibson, T.J. (1994). CLUSTAL W: improving the sensitivity of progressive multiple sequence alignment through sequence weighting, position-specific gap penalties and weight matrix choice. *Nucleic Acids Res* *22*, 4673-4680.
30. Ferguson, N., Johnson, C.M., Macias, M., Oschkinat, H., and Fersht, A. (2001). Ultrafast folding of WW domains without structured aromatic clusters in the denatured state. *Proc Natl Acad Sci U S A* *98*, 13002-13007.
31. Delano, W.L. (2002). The PyMOL Molecular Graphics System. <http://www.pymol.org>